Glycogen Synthase Kinase 3β Interaction Protein Is a Novel A-Kinase Anchoring Protein That Integrates PKA and GSK3β Signalling

DISSERTATION

zur Erlangung des akademischen Grades des

Doktors der Naturwissenschaften (Dr. rer. nat.)

eingereicht im Fachbereich Biologie, Chemie, Pharmazie

der Freien Universität Berlin

vorgelegt von

Philipp Skroblin

aus Mülheim an der Ruhr

Berlin, 2011

Diese Arbeit wurde von Juli 2007 bis April 2011
am Leibniz-Institut für Molekulare Pharmakologie in Berlin
unter der Leitung von Priv.-Doz. Dr. Enno Klußmann angefertigt.

Dissertation eingereicht am: 20. 04. 2011

Tag der Disputation: 21.06.2011

1. Gutachter: PD Dr. Enno Klußmann
2. Gutachter: Prof. Dr. Michael Krauß

Freie Universität Berlin, 2011

Selbstständigkeitserklärung

Hiermit erkläre ich, dass ich die vorliegende Arbeit selbstständig und nur unter Verwendung der angegebenen Literatur und Hilfsmittel angefertigt habe. Des Weiteren versichere ich, dass die vorliegende Arbeit nie Gegenstand eines früheren Promotionsverfahrens war. Die dem Verfahren zugrunde liegende Promotionsordnung ist mir bekannt.

Berlin, den 20.04.2011

Philipp Skroblin

Table of Contents

I. Abbreviations

Amino acids are abbreviated in one- or three-letter code.

2D	two-dimensional
3D	three-dimensional
8-AHA	8-(6-aminohexylamino-)
aa	amino acid
AC	adenylyl cyclase
ac	autocorrelation
AKAP	A-kinase anchoring protein
AMP	adenosine-5'-monophosphate
APC	adenomatosis polyposis coli
ATP	adenosine-5'-triphosphate
BP	band pass
BSA	bovine serum albumin
C	catalytic PKA subunit
cAMP	cyclic adenosine-3',5'-monophosphate
cc	cross correlation
CFP	cyan fluorescent protein
cGMP	cyclic guanosine-3',5'-monophosphate
CNB	cyclic nucleotide binding (domain)
CNG	cyclic nucleotide-gated
Cre	catalyses recombination
D/D	docking and dimerisation
DMEM	Dulbecco's modified eagle medium
DMSO	dimethyl sulphoxide
DNA	deoxyribonucleic acid
DTT	dithiothreitol
DUF	domain of unknown function
EDTA	ethylenediaminetetraacetic acid
EF	emission filter
EGTA	ethylene glycol tetraacetic acid
ELISA	enzyme-linked immunosorbent assay
Epac	exchange protein activated by cAMP

ES	embryonic stem
EtOH	ethanol
FBS	foetal bovine serum
FCS	fluorescence correlation spectroscopy
FCCS	fluorescence cross correlation spectroscopy
floxed	flanked by loxP
FLP	Flippase recombination enzyme
FMP	Leibniz-Institut für Molekulare Pharmakologie
flrted	flanked by FRT
FRT	FLP recombination target
Fw	forward (primer)
GDP	guanosine-5'-diphosphate
GEF	guanine nucleotide exchange factor
GFP	green fluorescent protein
GID	GSK3 interaction domain
GSK3	glycogen synthase kinase 3
GSKIP	GSK3β interaction protein
G protein	GTP-binding protein
GTP	guanosine-5'-triphosphate
HGNC	HUGO Gene Nomenclature Committee
HRP	horseradish peroxidase
HSQC	heteronuclear single quantum coherence
HSV-tk	herpes simplex virus thymidine kinase
HUGO	human genome organisation
IgG	immunoglobulin G
IP	immunoprecipitation
JNK	c-Jun N-terminal kinase
KO	knockout
LEF	lymphoid enhancer factor
LIF	leukaemia inhibitory factor
loxP	locus of crossing-over P1
LP	long pass
LSM	laser scanning microscope
LRP	low density lipoprotein receptor-related protein

MAP2	microtubule-associated protein 2
MAPK	mitogen-activated protein kinase
MBS	main beam splitter
MEF	murine embryonic fibroblast
neo	neomycin resistance gene cassette
NLS	nuclear localisation signal
NES	nuclear export signal
NMR	nuclear magnetic resonance
PAC	bacteriophage P1-derived artificial chromosome
PAGE	polyacrylamide gel electrophoresis
PBS	phosphate buffered saline
PCR	polymerase chain reaction
PDE	phosphodiesterase
PGE	prostaglandin E
pI	isoelectric point
PKA	protein kinase A
PKB	protein kinase B
PKC	protein kinase C
PKG	protein kinase G
PMSF	phenylmethylsulphonyl fluoride
PP	protein phosphatase
PVDF	polyvinylidene fluoride
R	regulatory PKA subunit
RIIBD	RII-binding domain
Rev	reverse (primer)
RNA	ribonucleic acid
rpm	revolutions per minute
RT	room temperature
sAC	soluble adenylyl cyclase
SBR	scaffold binding region
SDS	sodium dodecylsulfate
SPR	surface plasmon resonance
TAE	Tris/acetate/EDTA buffer
TBS	Tris buffered saline

TBST	TBS with Tween 20
TCF	T-cell factor
Tris	Tris(hydroxymethyl)-aminomethane
UV	ultraviolet
WT	wild-type
YFP	yellow fluorescent protein

II. Table of figures

1. Introduction

Extracellular stimuli as diverse as hormones, growth factors, cytokines, sensory inputs or pathogens trigger intracellular signal transduction events to elicit specific responses. In general, such signal transduction comprises receptors that recognise the extracellular signal and transduce it to the interior of the cell. On the intracellular side, signalling often involves the generation of second messengers, e.g. inositol trisphosphate, diacylglycerol, Ca^{2+}, cyclic adenosine monophosphate (cAMP), cyclic guanosine monophosphate (cGMP), or phosphatidylinositols, which modulate effector proteins and thereby evoke a cellular response [1]. The multitude of extracellular signals and their respective receptors is in contrast to the very limited number of intracellular second messenger systems which raises the question how specificity of signalling pathways is achieved. For example, two hormones, each binding to specific receptors, can both induce the generation of the same second messenger but result in completely different cellular effects. This is made possible by a tight spatial and temporal regulation of all constituents of the involved signalling cascades [2]. An important contribution to this regulation is made by scaffolding proteins, multivalent hubs which recruit specific components of a signalling pathway and thus allow a coordinated signal transduction [3;4]. Often these scaffolds contain proteins belonging to different signalling pathways and mediate the integration and cross-talk of these [5]. The following sections exemplify such compartmentalised signalling, describing the cAMP signalling pathway, its main effector (protein kinase A) and an important family of scaffolding proteins, A-kinase anchoring proteins (AKAPs) which regulate multiple aspects of cAMP-dependent signalling.

1.1 Cyclic adenosine monophosphate signalling

The second messenger cAMP [6] is generated by adenylyl cyclases (ACs) in response to the activation of certain G protein-coupled receptors (GPCRs, Fig. 1). Ligand binding to a GPCR induces conformational changes and causes the receptor to act as a guanine nucleotide exchange factor (GEF) for the associated heterotrimeric GTP-binding protein. Bound GDP is exchanged for GTP and the trimer dissociates into the GTP-bound G_α subunit and a $G_{\beta/\gamma}$ dimer. Both are attached to the plasma membrane by acylations and can modulate downstream effectors.

The intrinsic GTPase activity of the G_α subunit converts bound GTP to GDP which leads to the inactivation and reassembly of the heterotrimeric G proteins. These can thus be regarded as molecular switches. There are 27 different G_α subunits from four main families: $G_{\alpha s}$, $G_{\alpha i}$,

$G_{\alpha q}$ and $G_{\alpha 12/13}$. These families have distinct functions: $G_{\alpha s}$ (=stimulatory) activates ACs while $G_{\alpha i}$ (=inhibitory) inhibits ACs. G_q stimulates phospholipase C and $G_{\alpha 12/13}$ activates Src kinase and c-Jun N-terminal kinase (JNK). There are six different genes encoding G_β and 12 genes encoding G_γ subunits. The resulting proteins can assemble multiple different $G_{\beta/\gamma}$ dimers. These can modulate a wide range of target proteins such as ion channels, phospholipases, GPCRs, ACs, protein kinases and phosphatidylinositol-3-kinase γ. The high number of different α, β, and γ subunits that can assemble in different combinations allows the generation of a range of different heterotrimeric GTP-binding proteins which expands the variety of cellular effects initiated by GPCRs [7;8].

ACs convert ATP to the second messenger cAMP (Fig. 1). There are 10 human isoforms: Nine isoforms (AC1-AC9) are located in the plasma membrane and are activated by $G_{\alpha s}$. Depending on the isoform, they are additionally regulated by $G_{\alpha i}$ and $G_{\beta/\gamma}$ subunits of heterotrimeric G proteins as well as by protein kinases and Ca^{2+} [9-11]. The tenth isoform, soluble AC (sAC), differs significantly from the other isoforms: It is localised in the cytosol and it is not subject to regulation by G proteins but it is directly activated by bicarbonate [12]. AC1-8, and to a lesser extent also AC9, are activated by the plant diterpene forskolin. This is often taken advantage of in experiments to investigate cAMP signalling pathways, especially when the involved GPCRs are not known or no ligands are available [13].

The second messenger cAMP is freely diffusible within the cell and can activate several downstream effectors. Among these are cyclic nucleotide-gated (CNG) ion channels, which have increased open probability when cAMP is bound, and a family of guanine nucleotide exchange factors termed exchange proteins activated by cAMP (Epac, Fig. 1). There are two human Epac proteins (Epac-1 and -2) [14]. The binding of cAMP to Epac induces a conformational change that activates and exposes the GEF domain. Epac can activate the small monomeric GTP-binding proteins Rap-1 and Rap-2 which in turn suppress the activity of another GTP-binding protein, Ras. Ras is involved in mitogen-activated protein kinase (MAPK) pathways which often induce proliferation [15]. The cAMP effector protein kinase A, a serine-threonine kinase that is activated by cAMP, is discussed in the following chapter.

The termination of cAMP signalling is accomplished by phosphodiesterases (PDEs). PDEs hydrolyse the phosphodiester bond of the cyclic nucleotides cAMP and cGMP, thereby converting them to AMP and GMP, respectively. The PDE superfamily is subdivided into 11

families (PDE1-PDE11). PDE4, 7 and 8 are cAMP-selective whereas PDE5, 6 and 9 degrade only cGMP. PDE1, 2, 3, 10 and 11 can process both cAMP and cGMP [16-18].

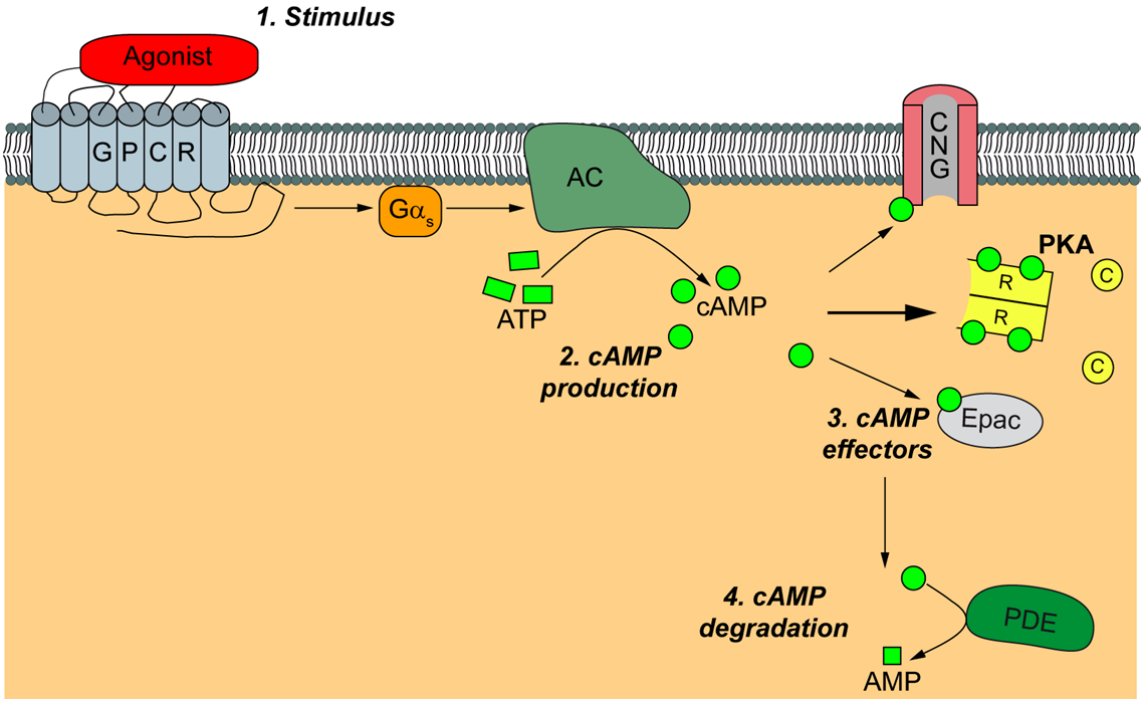

Fig. 1 The cAMP signalling pathway. 1. Agonist binding to a subset of G protein-coupled receptors (GPCR) activates $G\alpha_s$ proteins. 2. $G\alpha_s$ stimulates adenylyl cyclases (AC) to convert ATP into cAMP. 3. Different effector proteins, most importantly PKA but also exchange proteins activated by cAMP (Epac) and in certain cell types cyclic nucleotide gated channels (CNG) are activated by cAMP. 4. Specific phosphodiesterases (PDE) terminate cAMP signalling by hydrolysing the phosphodiester bond in cAMP, thereby generating AMP.

1.1.1 Protein Kinase A (PKA)

The cAMP-dependent protein kinase, originally abbreviated cAPK, now referred to as protein kinase A (PKA) [19;20] is a serine/threonine protein kinase that belongs to the AGC kinase (cAMP-dependent protein kinase A, cGMP-dependent protein kinase G, and phospholipid-dependent protein kinase C) family [21].

In its inactive state, PKA consists of a dimer of regulatory (R) subunits and two catalytic (C) subunits. In this holoenzyme, each C subunit is bound to one R subunit and thereby inhibited. The activation of PKA is triggered by the binding of two cAMP molecules to each R subunit. This binding induces a conformational change in the R subunits which lowers their affinity towards the C subunits. The C subunits are released and can phosphorylate nearby substrates. PKA substrate proteins usually contain the consensus sequence (R-R-X-S/T, Fig. 2) [22;23].

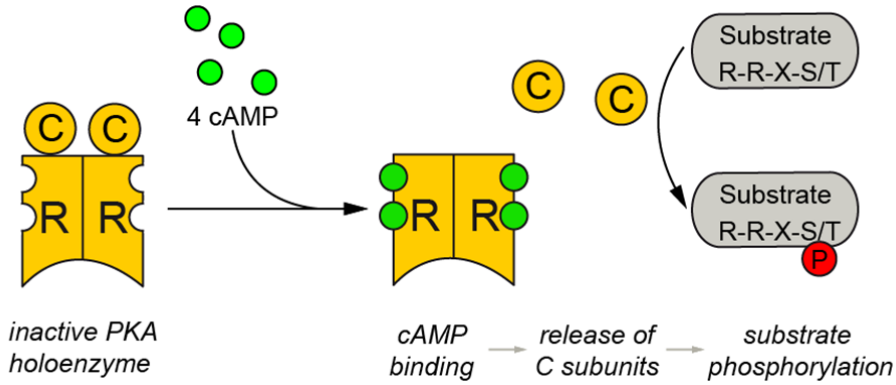

Fig. 2 The activation of PKA by cAMP. The PKA holoenzyme consists of a dimer of regulatory (R) subunits and two catalytic (C) subunits. In the absence of cAMP, each C subunit is bound and inhibited by one R subunit. The binding of two molecules of cAMP to an R subunit induces a conformational change, causing the release of an active C subunit. Activated PKA can phosphorylate serine or threonine residues, preferably in substrate proteins containing the sequence (R-R-X-S/T).

In mammals, there are three genes encoding the different catalytic subunit isoforms, Cα [24], Cβ [25;26] and Cγ [27]. The four isoforms of regulatory subunits are encoded by four distinct genes: RIα, RIβ, RIIα, RIIβ. PKA is classified as type I or type II based on the type of R subunits present in the holoenyzme (RI or RII). In general, R subunits form homodimers (e.g. RIIα/RIIα) but RIα/RIβ heterodimers have also been reported [28;29]. Type I PKA is mostly located in the cytoplasm, but there are a few RI-binding AKAPs that target type I PKA to specific cellular compartments [30-32]. The expression pattern of RIα is ubiquitous while RIβ is mainly found in the central nervous system [33]. The majority of type II PKA is anchored to subcellular structures by AKAPs [31;34-36]. RIIα expression is ubiquitous, whereas RIIβ expression is mostly confined to the brain, neuroendocrine, reproductive and adipose tissues [37].

Multiple different PKA holoenzymes can be formed from regulatory and catalytic subunit isoforms. Apparently, all C subunits can associate with any R subunit dimer [37]. This diversity is further enhanced by the combination of different splice variants. These are known to exist in the case of Cα (two splice variants), Cβ (six splice variants) and RIα (two splice variants [38-40]. The different properties of the components of various PKA holoenzymes, e.g. with respect to cAMP sensitivity and interaction with AKAPs, enhance the specificity of cAMP/PKA signalling [37]. In addition to the regulation of PKA by AKAPs, several proteins interact with PKA C subunits, thereby controlling their localisation or activity [32]. For example, the A-kinase interacting protein (AKIP1) binds C subunits in the nucleus and facilitates the PKA phosphorylation of nuclear substrates [41;42].

PKA R subunits consist of three major domains: an N-terminal dimerisation and docking (D/D) domain and two cyclic nucleotide binding (CNB) domains. The D/D domain is connected to the first CNB domain by an unstructured linker region. This linker contains an inhibitor sequence that occupies the catalytic site of the bound C subunit in the PKA holoenzyme. In RI subunits, this sequence is a pseudosubstrate while it is a PKA substrate in RII subunits. The D/D domains of two R subunit monomers form a four-helix-bundle, thereby achieving the dimerisation of R subunits and providing the docking site for AKAPs (Fig. 3) [20].

The catalytic centre of C subunits is located in the kinase core, which is conserved in all members of the protein kinase superfamily [20]. In addition to this core, PKA C subunits comprise an N- and a C-terminal tail. The N-tail can be modified posttranslationally, which affects the localisation of C subunits [20;43-45], whereas the C-tail interacts with regulatory proteins [20;46].

Many other AGC kinases contain canonical protein-protein or protein-lipid interaction domains that control their localisation. These, however, are absent from PKA which explains the important role AKAPs play in controlling the localisation of PKA [21].

1.1.2 A-kinase anchoring proteins (AKAPs)

PKA is recruited to intracellular locales by AKAPs, a family of scaffolding proteins comprising over 40 members. AKAPs were discovered as contaminants of isolated RII subunits [47]. The AKAP family was expanded by using radioactively labelled RII subunits as probes in far-western blotting assays (RII overlays) [48]. The characteristic property of all AKAPs is the presence of a PKA-binding domain, also named RII-binding domain (RIIBD) because most AKAPs mainly anchor RII subunits. The RIIBD consists of an amphipathic α-helix of 14 to 18 amino acids. The hydrophobic face of this helix binds to a hydrophobic groove formed by the four-helix bundle of a PKA R subunit D/D domain dimer (Fig. 3).

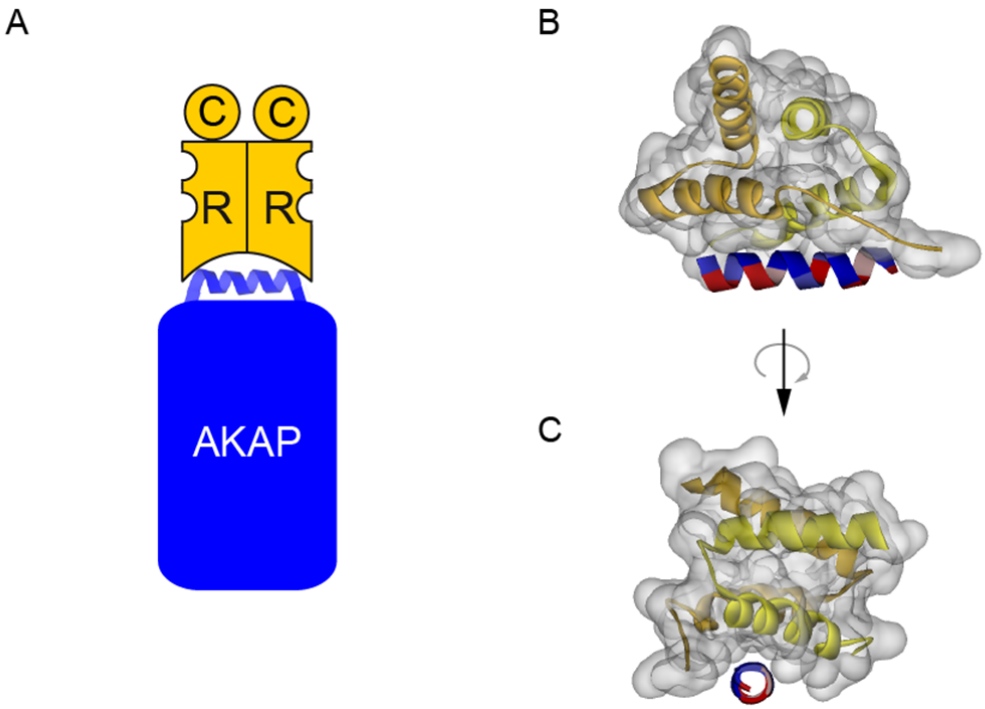

Fig. 3 The AKAP-PKA interaction. A. Schematic representation of an AKAP (blue) in complex with a PKA holoenzyme (yellow). The amphipathic helix (RIIBD) of an AKAP binds to the R subunit dimer. R, regulatory subunit, C, catalytic subunit. **B. and C.** Crystal structure of a D-AKAP2 peptide in complex with the D/D domain dimer of RIIα (PDB: 2HWN) [49]. The two RIIα D/D domain protomers are shown in orange and yellow, respectively. The surface of the D/D domain dimer is illustrated in transparent grey. Amino acids of the D-AKAP2 peptide are coloured according to their polarity (blue: hydrophobic, red: polar). The hydrophobic face of the AKAP helix binds to a hydrophobic groove formed by both N-terminal helices of the D/D domain dimer. **B.** Visual axis perpendicular to helix axis. **C.** Visual axis identical to helix axis. Adapted from Skroblin *et al*. [32].

The activity of PKA often requires tight local control to allow the selective phosphorylation of substrates. Consequently, AKAPs tether PKA to most organelles (e.g. the plasma membrane, the cytoskeleton, mitochondria, the Golgi apparatus, the nucleus or vesicular structures) into close proximity of its substrates (Fig. 4, Fig. 5) [35]. This is achieved by a targeting domain within an AKAP that interacts with organelle-specific proteins or lipids and thereby controls the localisation of the respective AKAP-PKA complex.

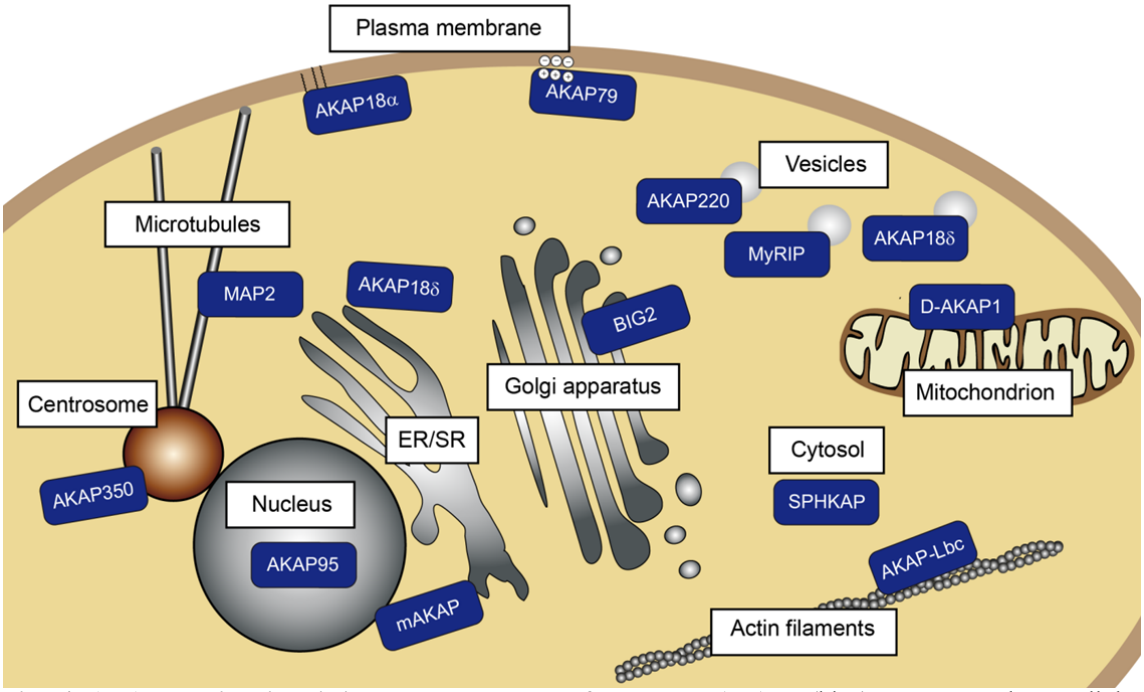

Fig. 4 AKAPs reside in distinct compartments of the cell. AKAPs (blue) are targeted to cellular compartments/organelles (white boxes). The AKAPs' specific localisation is achieved by interactions with proteins or lipids of the target compartment.

AKAPs do not only control the localisation of PKA but also its activity by interacting with components of the cAMP signalling machinery such as GPCRs [50], ACs [51], Epac [52] or PDEs [17;53] (Fig. 5). They also function as integrators of cellular signalling by binding other signalling proteins (Fig. 5) [32;35;36] including protein phosphatases [54;55] or protein kinases such as Akt/protein kinase B (PKB) [52] protein kinase C (PKC), protein kinase D, protein kinase N [35], extracellular-signal regulated kinase (ERK) 1/2 [56] or glycogen synthase kinase 3 β (GSK3β) [54;57;58]. The signalling proteins within these multi-protein complexes formed by AKAPs often regulate each other, e.g. by phosphorylation or dephosphorylation, or they affect downstream proteins in a concerted fashion. Some AKAPs also bind to and regulate ion channels. AKAP18α, for instance, binds to and mediates the PKA-dependent phosphorylation of the L-type Ca^{2+} channel which affects Ca^{2+} fluxes and Ca^{2+}-dependent signalling pathways [59].

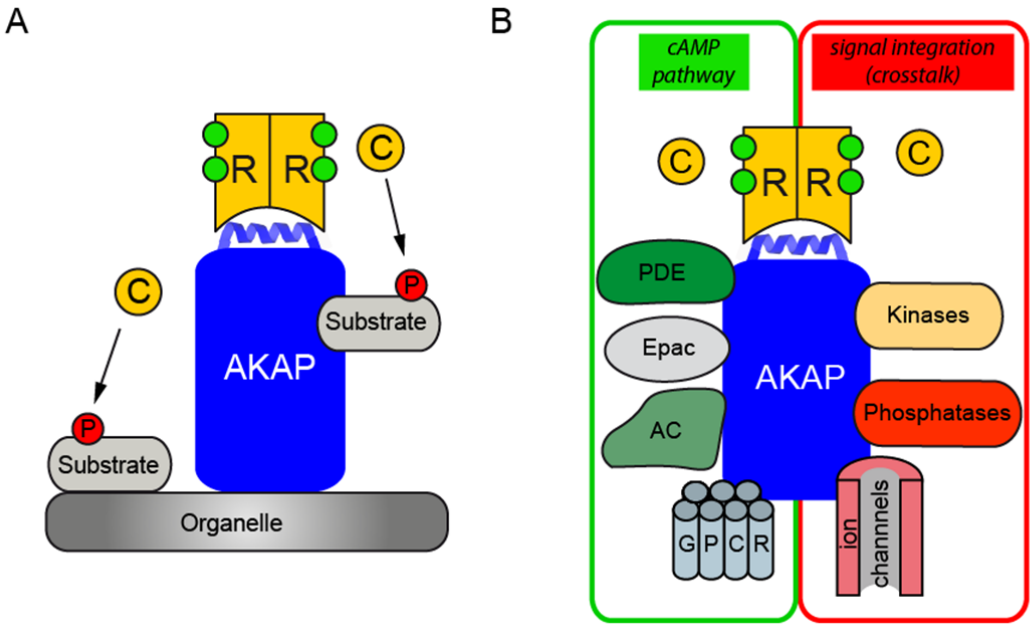

Fig. 5 AKAPs are signalling hubs. A. AKAPs localise PKA to specific compartments and facilitate the phosphorylation (P) of nearby substrate proteins by PKA. **B.** AKAPs can interact with components of the cAMP pathway (green box), thus contributing to the regulation of incoming signals (GPCR), cAMP synthesis (AC), cAMP effectors (PKA, Epac) and cAMP degradation (PDE). By binding further signalling proteins (red box), AKAPs serve as platforms for the integration of different signalling pathways. Adapted from Skroblin *et al*. [32].

Based on their specificity for the different R subunit isoforms of PKA, AKAPs can be subdivided into three groups: RI-specific, RII-specific or dual-specific [60]. In contrast to the canonical AKAPs, which employ an amphipathic helix to bind to the D/D domain of PKA R subunits, proteins that interact with R subunits via alternative binding sites and mechanisms can be classified as non-canonical AKAPs [32;61]. In the following, all AKAPs referred to are canonical AKAPs unless indicated otherwise.

In the original AKAP nomenclature, an AKAP's name was derived from its apparent molecular weight determined by SDS gel electrophoresis. For example, AKAP79 migrates at 79 kDa in SDS-PAGE. This system can be confusing because AKAPs with different molecular weight-derived names can be splice variants of the same gene (e.g. AKAP350 and AKAP450) or orthologues from different species (e.g. bovine AKAP75, human AKAP79, murine AKAP150).

Therefore, a new nomenclature was introduced by the human genome organisation nomenclature committee (HGNC), renaming AKAPs with running numbers from AKAP1 to AKAP14. However, the original molecular weight-derived names are still used more commonly. Proteins which were described before their AKAP function was discovered often keep their original name (e.g. microtubule-associated protein 2, Yotiao). An overview of

AKAPs, their different splice variants and alternative names is given in recent reviews [31;32].

1.1.2.1 PKA anchoring disruptor peptides

AKAP-PKA interactions can be disrupted with peptides to reveal the contribution of anchored PKA to cellular processes. As mentioned above, the RIIBDs of different AKAPs and their interaction with PKA are conserved. Peptides derived from the RIIBD of an AKAP can bind to R subunits and effectively disrupt AKAP-PKA complexes. These disruptor peptides can also be used to clarify whether a peptide or protein interacts with R subunits in the fashion of a canonical AKAP: The binding of canonical AKAPs to R subunits is reduced in the presence of these disruptor peptides. Non-canonical AKAP-PKA interactions, in contrast, are generally not affected.

The first peptide demonstrated to be a PKA anchoring disruptor was Ht31, which comprises the RIIBD of AKAP-Lbc/AKAP13 [62]. Ht31 disrupts both RI- and RII-AKAP complexes *in vitro* [63] as well as in cell or animal systems [64]. Ht31 peptides bind RIIα with a nanomolar affinity [62]. As an alternative, peptides derived from the AKAP18δ, which display an even higher affinity, can be used (e.g. the modified peptide AKAP18δ-L314E, $K_D = 2.2 \pm 0.3$ nM) [65;66]. Variants of these peptides in which two hydrophobic amino acids of the RIIBD are substituted by proline lack the typical helical structure of an RIIBD and are consequently PKA-binding deficient. These proline peptides are used as controls to rule out unspecific effects on the experimental system. Further development of PKA anchoring disruptors also yielded RI- and RII-specific peptides which are based on D-AKAP10 or the synthetic peptide AKAP-*IS* [67]. A detailed review of different PKA anchoring disruptor peptides is given in [67].

1.1.2.2 An AKAP consensus motif

As individual AKAPs have distinct functions, display different protein-protein interactions as well as specific localisations and expression patterns, it is not surprising that they do not share any overall sequence similarity. The only part in which all canonical AKAPs are related is the RIIBD, especially the hydrophobic amino acids therein. These are located in conserved positions. Aligning the RIIBDs of known AKAPs yielded a consensus sequence representing the preferred hydrophobic amino acids. It was also taken into account that some AKAPs contain polar amino acids (Ser or Glu) in the N- or C-terminal conserved position. This led to the following consensus sequence: [(AVLISE)-X-X-(AVLIF)-(AVLI)-X-X-(AVLI)-

(AVLIF)-X-X-(AVLISE)], with amino acids in parentheses denoting alternatives of the amino acids in conserved positions of RIIBDs, and X standing for any amino acid. In addition, the isoelectric point (pI) of the RIIBDs of known AKAPs is in the range of 3.43 to 6.23 [58].
These prerequisites (the AKAP consensus sequence and the pI range) were used to search the SwissProt database for previously unidentified AKAPs. Sequences complying with these parameters were synthesised as peptide spots, and probed for RII binding by RII overlay. Roughly 800 RII-binding peptides were found. To test for a typical AKAP-like binding to the D/D domain of RII subunits, these peptides were subjected to another RII overlay in which the RII probe was either preincubated with the PKA anchoring disruptor peptide AKAP18δ-L314E, the RII-binding deficient AKAP18δ-PP or with no peptide. 10 peptides derived from established AKAPs as well as 27 peptides derived from AKAP candidates displayed reduced RII binding in the presence of AKAP18δ-L314E, indicating a canonical AKAP-like binding to the D/D domain. Of these 27 potential new AKAPs, glycogen synthase kinase 3β interaction protein (GSKIP) was further characterised with regard to its AKAP function [58;68;69]. As GSKIP's name implies, the first function that was identified for this protein is its interaction with glycogen synthase kinase 3β (GSK3β) [70]. Therefore, GSK3β, its characteristic properties, important associated protein-proteins interactions and pathways will be introduced in the next section, followed by a summary of the state of knowledge on GSKIP.

1.2 Glycogen Synthase Kinase 3β (GSK3β)

The glycogen synthase kinase 3 (GSK3) family of serine/threonine kinases was first discovered as a negative regulator of glycogen synthase, the key enzyme of glycogen synthesis [71]. GSK3 proteins are found in all eukaryotes. While fungi, plants and invertebrates only have one GSK3 isoform, there are two GSK3 isoforms encoded by distinct genes in vertebrates: GSK3α (51 kDa) and GSK3β (47 kDa) [72]. Both isoforms are ubiquitously expressed, with notably high levels in the brain [73]. GSK3α and GSK3β share high sequence identity in their kinase domains (>98%) but GSK3α contains an N-terminal cysteine-rich stretch that is not found in GSK3β. Despite their high similarity and overlapping functions, these isoforms are not fully redundant. This is suggested by the embryonic lethality of GSK3β knockout mice, indicating that the loss of GSK3β cannot be compensated by GSK3α [74]. GSK3β is involved in multiple signalling pathways, for instance regulating glycogen metabolism, insulin signalling, cell proliferation, neuronal function, oncogenesis

and embryonic development [75]. Accordingly, a role of GSK3β has been implicated in various diseases such as type 2 diabetes, cancer, Alzheimer's disease, Parkinson's disease, bipolar disorder or cardiac hypertrophy [76-78].

Two noticeable properties distinguish GSK3β from most other protein kinases: (A) Many GSK3β substrates require priming, i.e. pre-phosphorylation, by a different kinase. The priming phosphorylation site is located 4 amino acids C-terminal to the residue phosphorylated by GSK3β within the consensus site (S/T-X-X-X-S^P/T^P), with the GSK3β substrate residue underlined and ^{P} indicating the priming phosphorylation site (Fig. 6 A) [79]. (B) GSK3β is constitutively active in its basal state. The major mechanism to control its activity is an inhibitory phosphorylation of Ser9 by other kinases (Fig. 6 B). This phosphorylation turns the N-terminus into a GSK3 pseudosubstrate that binds to the phosphate recognition site (Arg96) which otherwise may bind the phosphate of primed substrates [80].

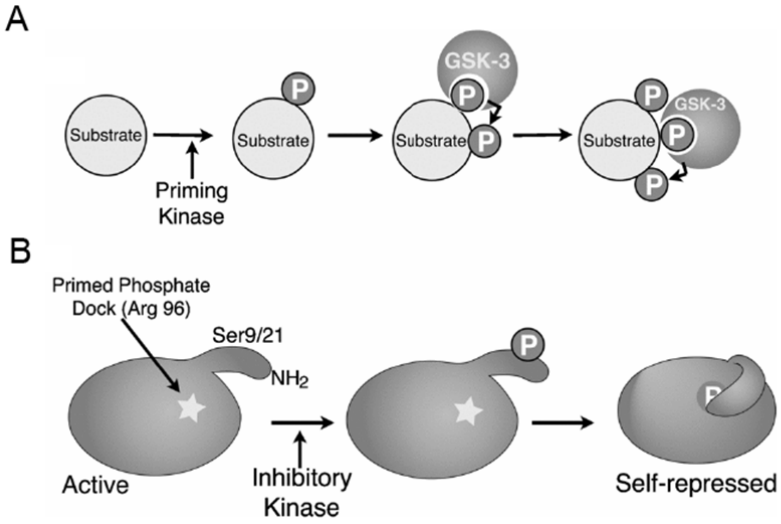

Fig. 6 Priming of GSK3 substrates and regulation of GSK3 by inhibitory phosphorylation. A. GSK3 preferentially phosphorylates substrates that are pre-phosphorylated by a priming kinase. In the case of the GSK3 substrate β-catenin, prephosphorylation on S45 primes it for sequential phosphorylation on Thr41, Ser37 and Ser33 by GSK3. **B.** GSK3α Ser21 and GSK3β Ser9 can be phosphorylated by protein kinases, and then function as primed pseudosubstrates that block the substrate binding pocket of GSK3, thereby preventing the phosphorylation of GSK3 substrates. Adopted from Patel *et al*. [81].

Protein kinases that have been shown to phosphorylate GSK3β Ser9 include PKA [82;83], Akt/PKB [84], p70 ribosomal S6 kinase (p70RSK) [85], p90 ribosomal S6 kinase (p90RSK/RSK1) [86], protein kinase G (PKG) [87], serum/glucocorticoid regulated kinase 1 (SGK1) [88], integrin-linked kinase (ILK) [89] and different PKC isoforms [90]. A PKA-mediated phosphorylation of Ser9 is induced in response to adrenaline [91], endothelin-1 (ET-1) [92], Wnt5a [93], parathyroid hormone (PTH) [94], prostaglandin E_2 (PGE_2) [95],

human chorionic gonadotropin (hGC) [54], corticotropin-releasing factor (CRF) [96], glucagon-like peptide-1 [97] and -2 (GLP-1/2) [98], and basic fibroblast growth factor (bFGF, Fig. 7) [99]. Due to the ubiquitous nature of PKA and GSK3β and their presence in multiple compartments, it is plausible that scaffolding proteins such as AKAPs form complexes containing PKA and GSK3β to facilitate this phosphorylation [32]. Consequently, it was demonstrated that PGE_2-induced phosphorylation of Ser9 requires an unidentified AKAP as it is abolished by the PKA-anchoring disruptor peptide Ht31 [100]. Also the phosphorylation of GSK3β triggered by hCG is dependent on an AKAP, namely microtubule-associated protein 2 D (MAP2D), which interacts with type II PKA and GSK3β [54]. Another AKAP which forms a complex with PKA and GSK3β and thus promotes Ser9 phosphorylation is AKAP220 [57]. In this case, however, an associated physiological stimulus or signalling pathway has so far not been identified. Because of the multiple signals causing the PKA-dependent phosphorylation of Ser9, it may well be that further AKAPs have the ability to bind GSK3β. An involvement of GSKIP in PKA-dependent phosphorylation is conceivable because it is an interaction partner of GSK3β and a supposed AKAP.

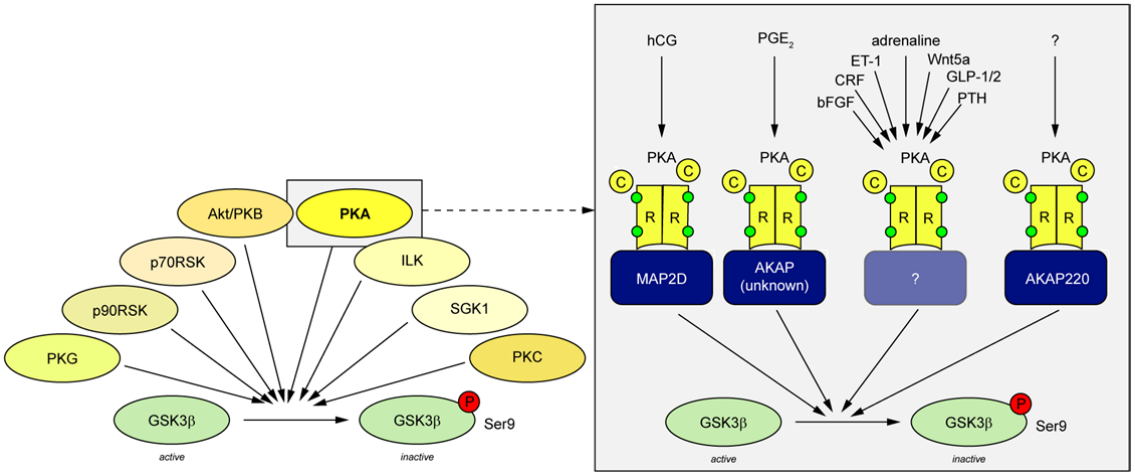

Fig. 7 The inhibitory phosphorylation of GSK3β on Ser 9. *Left panel*: Kinases known to phosphorylate GSK3β on Ser9 are illustrated. *Right panel*: the cAMP-elevating agents that lead to a phosphorylation of Ser9 by PKA and AKAPs involved in the control of this phosphorylation are shown. See text for abbreviations.

1.2.1 The canonical Wnt signalling pathway

The canonical Wnt signalling pathway, which is essential for embryonic development and plays a role in tumourigenesis, is a prime example for a role of GSK3 in signal transduction. In the absence of a Wnt signal, the cytosolic "destruction complex", consisting of GSK3, axin and the adenomatosis polyposis coli (APC) protein, causes the degradation of β-catenin and prevents its translocation into the nucleus. In this complex, both axin and APC interact with

β-catenin and allow its phosphorylation by GSK3. This phosphorylation induces the polyubiquitination and subsequent proteasomal degradation of β-catenin.

When a member of the Wnt family of secreted lipid-modified proteins binds to the LRP5/6 (low density lipoprotein receptor-related protein 5/6) and frizzled receptors, axin is recruited to this receptor complex. As a consequence, the destruction complex is inactivated, β-catenin can accumulate and enter the nucleus. There, β-catenin activates, together with TCF/Lef (T-cell factor/lymphoid enhancer factor) transcription factors, the transcription of Wnt target genes. The consequently regulated proteins can modify cell survival, proliferation, differentiation or migration (Fig. 8) [97].

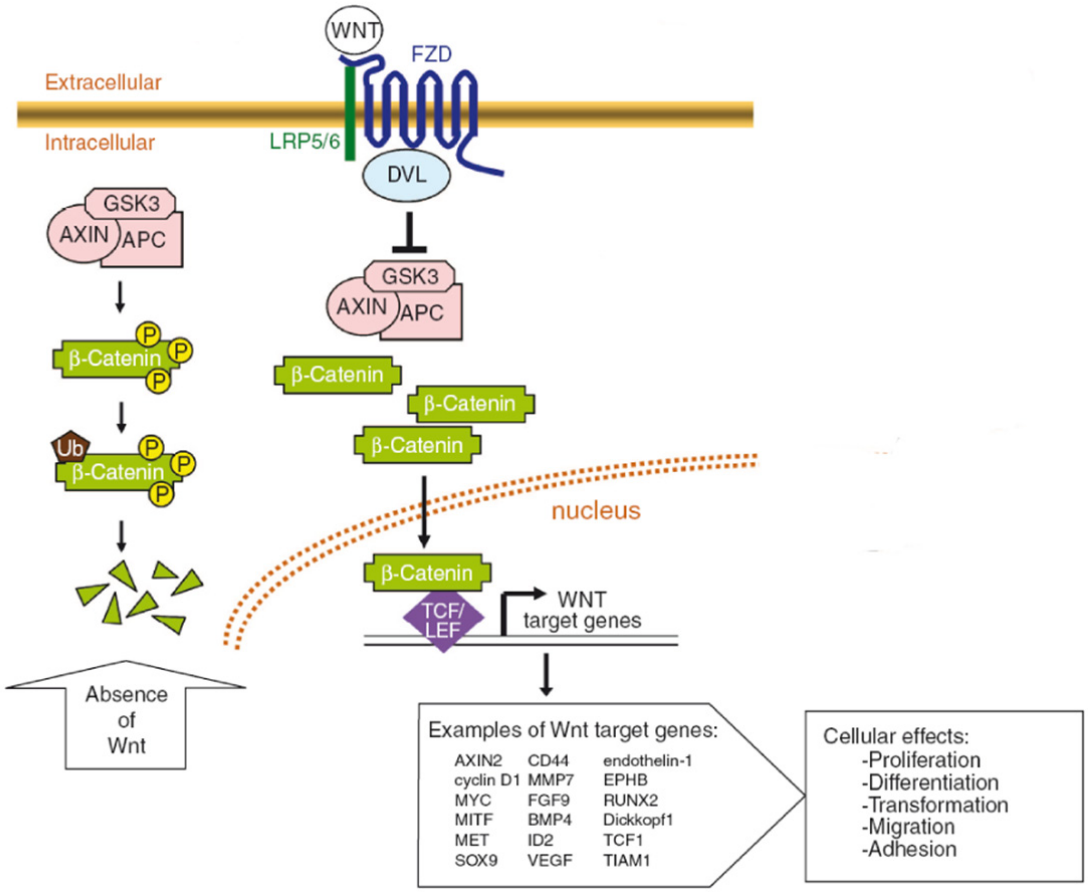

Fig. 8 The canonical Wnt signalling pathway. *Left panel:* In the absence of an extracellular Wnt signal, the destruction complex, containing GSK3, axin and APC, catalyses the phosphorylation of β-catenin which initiates its polyubiquitination (Ub) and proteasomal degradation. *Right panel:* When Wnt binds to its receptor, consisting of the LRP5/6 and Frizzled (FZD) co-receptors, the destruction complex is inhibited. β-catenin accumulates, enters the nucleus and, together with TCF/LEF, activates the transcription of Wnt target genes. Adapted from Chien *et al*. [101].

1.2.2 The GSK3β/axin interaction

The binding of axin to GSK3β holds the kinase in the destruction complex. The GSK3β interaction domain (GID) of axin is a sequence spanning 25 amino acids (corresponding to position 380 to 404 of mouse/human axin-1) [102]. A crystal structure of GSK3β with the GID of axin revealed the amino acids involved in this interaction [103]. The axin GID forms an amphipathic helix. On the hydrophobic face of this helix, four amino acids (Phe388, Leu392, Leu396 and Val 399) constitute a hydrophobic ridge that binds to a hydrophobic groove on the surface of GSK3β (Fig. 9). A single hydrogen bond between axin Arg395 and GSK3β Asp264 contributes to the interaction. The helical structure is essential for the GID. A helix-breaking Leu396Pro mutation completely abolishes the binding to GSK3β [104].

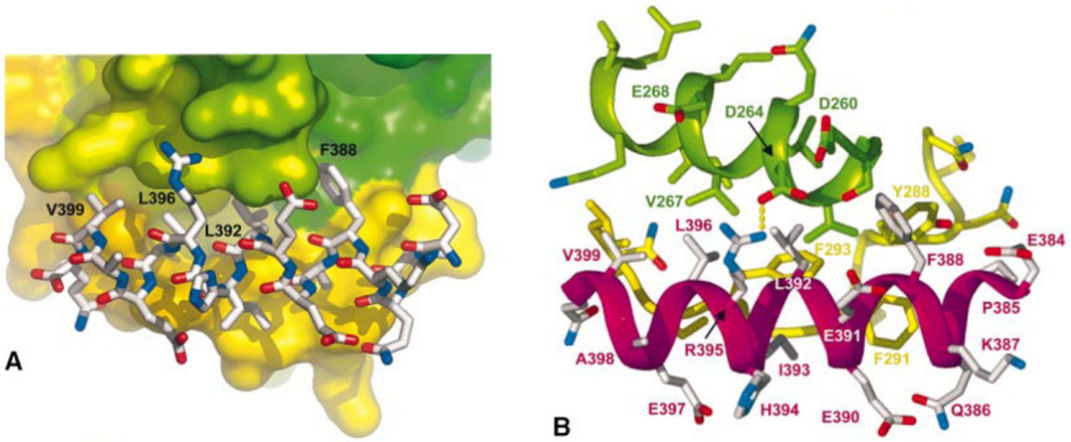

Fig. 9 Structural aspects of the Axin-GSK3β interaction. A. Axin residues Phe388, Leu392, Leu396 and Val399 form a hydrophobic helical `ridge' that packs into a hydrophobic groove formed between helix 262-273 (green surface) and the extended loop from 285-299 (yellow surface) in GSK3β. **B.** The axin (383-401) peptide (magenta and white) forms a single side chain hydrogen bond to GSK3β (green/yellow), from Arg395 to Asp264. Adapted from Dajani *et al*. [103].

1.3 GSKIP

GSKIP (GSK3β interaction protein) is also termed C14orf129/CN129 because the gene encoding human GSKIP is located on chromosome 14, open reading frame 129. Further alternative names are HSPC210 and MGC4945. Before any functional properties of GSKIP were known, its structure was resolved by NMR analysis (PDB ID: 1SGO, Northeast Structural Genomics Consortium 2004). Based on this structure, the protein can be divided into four parts (Fig. 10): an unfolded, flexible N-terminus (aa 1-32), an adjacent α-helix (aa 33-48), a central β-sheet domain (aa 49-115) and a second α-helix (aa 116-139).

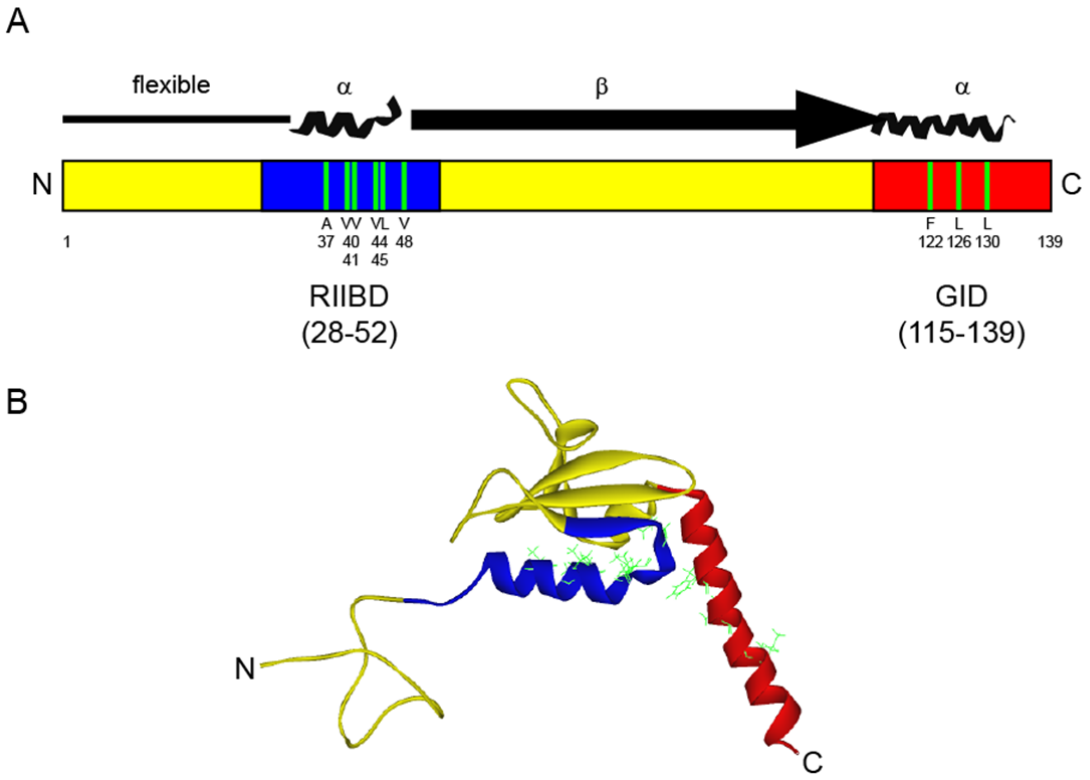

Fig. 10 The structure of GSKIP. A. Based on the NMR structure of GSKIP (PDB: 1SGO), GSKIP can be divided into four major parts, a flexible N-terminus (line), two α-helices (α) and a β-strand region (β, arrow). *Rectangular box:* the positions of functionally assigned regions are indicated, the RII-binding domain (RIIBD, blue) and the GSK3β interaction domain (GID, red). The positions of essential hydrophobic amino acids within these two interaction domains are indicated by green lines. **B.** The tertiary structure of GSKIP. The RIIBD, the GID and their important amino acids (stick models) are highlighted in the same colours as in A. N, N-terminus; C, C-terminus.

Chou *et al.* identified GSKIP in a yeast-two-hybrid screen for binding partners of GSK3β. Further experiments revealed that the C-terminus of GSKIP (aa 115-139) is necessary and sufficient for this interaction. The C-terminus of GSKIP shares homology with the GSK3β interaction domain (GID) of human axin-1 and -2 [70]. The helical structure with an amphipathic character, the four hydrophobic amino acids and the hydrogen-bond forming arginine are conserved between axin-1, axin-2 and GSKIP [70], indicating that all three proteins bind GSK3β through a similar mechanism and that this interaction is most likely mutually exclusive as they all bind to the same site on GSK3β. Accordingly, a mutation of GSKIP Leu130 to Pro, corresponding to axin Leu396Pro (see above), abrogates the ability to interact with GSK3β. In a further study, truncation and substitution mutations of GSK3β revealed that GSKIP and axin indeed bind to the same region of GSK3β, termed scaffold binding region I (SBRI). *In silico* docking of the C-terminus of GSKIP to the surface of GSK3β based on the structure of the GSK3β/axin complex (see above) suggested that the

conformations which GSK3β adopts when binding the GIDs of either axin or GSKIP are very similar [105].

Recombinant wild-type GSKIP but not the L130P mutant was found to interact with endogenous GSK3α and GSK3β [70]. Both interactions were confirmed in independent high-throughput screens for protein-protein interactions [106;107]. In addition to merely interacting with GSK3β *in vitro*, GSKIP and a peptide derived from its C-terminus (GSKIPtide, aa 115-139) inhibit GSK3β phosphorylation of unprimed substrates, such as axin, β-catenin and tau, *in vitro* [70]. An overexpression of GSKIP in HeLa cells decreased the phosphorylation of β-catenin, consequently increased its abundance and activated β-catenin-dependent transcription [70].

As mentioned above, GSKIP was also found to be a potential AKAP in a database search using the AKAP consensus sequence (1.1.2.2). The conserved hydrophobic residues of GSKIPs putative RIIBD are indicated in Fig. 10. Various peptide spot/RII overlay experiments confirmed the RII-binding capacity of this sequence and the necessity of the specified hydrophobic amino acids for RII binding [68]. The AKAP function was further consolidated by evidence that full-length GSKIP protein binds to RIIα in RII overlay assays and surface plasmon resonance measurements [58].

According to Chou *et al.*, GSKIP is expressed in a broad range of tissues [70]. This is confirmed by microarray data for human, mouse and rat GSKIP (http://biogps.gnf.org/gene/51527) [108-111]. Because similar amounts of GSKIP mRNA were detected in all tissues within a panel of 79 human tissues tested, it can be assumed that GSKIP is ubiquitously expressed [109].

The domain of unknown function 727 (DUF727, Pfam ID: 05303, InterPro accession IPR007967) was introduced based on sequence similarities of proteins from different species which are presumable GSKIP orthologues [112;113]. It corresponds to amino acids 32-139 of human GSKIP. Currently, there are 87 DUF727 proteins from diverse eukaryotic taxonomic groups (green plants, fungi, amoeba, invertebrate and vertebrate animals, Fig. 11).

Despite the available information on the structure, expression, evolution and protein-protein interactions of GSKIP, its physiological function remains unclear. One approach to elucidate the biological relevance of a protein is to disrupt the encoding gene in an animal model.

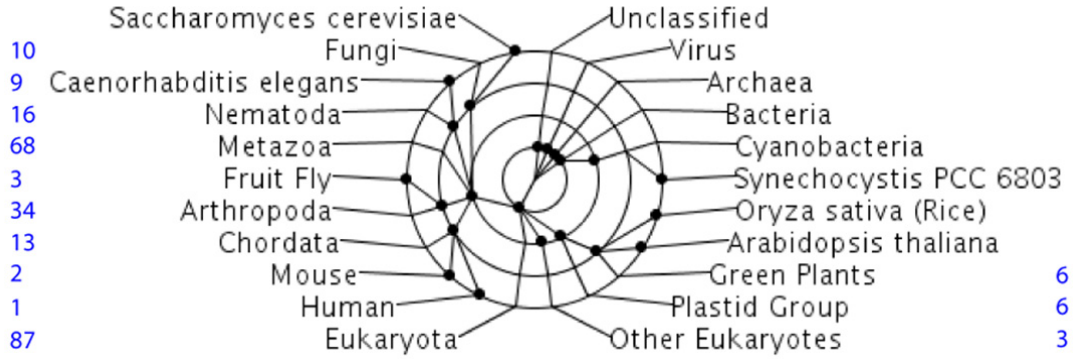

Fig. 11 Taxonomic distribution of DUF727 proteins. The numbers of DUF727 proteins from the respective taxonomic groups are shown in blue. The circles represent: first (inner) circle, domains (e.g. eukaryotes); second circle, kingdoms (e.g. metazoa); third circle phyla (e.g. chordata); fourth (outer) circle, species (e.g. human). Adapted from http://www.ebi.ac.uk/interpro/IEntry?ac=IPR007967 [113].

1.4 Conditional Gene Targeting

Model organisms are essential to our understanding of biological processes as they allow *in vivo* experiments in which biological molecules such as proteins can be investigated in their native environment. The mouse (*Mus musculus*) is especially important as a model animal due to its high physiological and genetic similarity with man. More than 99% of the identified mouse genes have human homologues (and vice versa) [114]. The benefits of mice in research were greatly increased with the introduction of targeted genetic modifications which was made possible by two methods established in the 1980s: the isolation of embryonic stem (ES) cells and their in vitro cultivation in an undifferentiated state [115;116] and the use of homologous recombination to integrate artificial DNA into eukaryotic chromosomes [117].

ES cells are derived from the inner cell mass of blastocyst-stage mouse embryos. They are undifferentiated and pluripotent, i.e. they are able to differentiate into any body cell type. ES cells can be injected into genetically different embryos. Such manipulated embryos can then be implanted into a surrogate mother. The resulting progeny are genetic chimeras; their cells descend either from the injected ES cells or from the acceptor blastocyst cells. If cells descending from the injected ES cells differentiate into gametes, their genetic information can be passed on to the next generation. This process is referred to as germline transmission [118]. The modified ES cells are generally from a mouse strain with a coat colour that is different from the recipient strain. Analysing the coat colour pattern of the resulting mice allows the identification of chimeric mice.

In order to introduce targeted genetic alterations, the genome of cultured ES cells can be modified by homologous recombination. This technique was used for the first time to inactivate the selectable hypoxanthine-guanine phospho-ribosyltransferase 1 (HPRT) locus in

ES cells. These recombinant ES cells were used to establish the first knockout mouse line, an animal model for the human Lesch Nyhan syndrome. This disease is caused by a deficiency of the enzyme hypoxanthine guanine phosphoribosyltransferase which is encoded by the HPRT locus [119;120]. Until today, knockout mouse strains for more than 3000 genes have been established [121].

In a conventional gene targeting/knockout approach, a part of the coding sequence of the target gene is replaced with a neomycin resistance cassette which allows the selection of recombinant ES cells and irreversibly disrupts the target gene. This may be useful to investigate systemic effects of a gene. But in several cases, the missing gene function can be compensated by other proteins and hamper the phenotypic analysis. The gene disruption is present in all cells and throughout the entire development of the animal. This may lead to embryonic or perinatal lethality and thus make experiments with adult knockout mice impossible [122]. Moreover, the genetic modification affects multiple different cell and tissue types, resulting in a complex phenotype in which it is difficult to distinguish a direct effect in a particular tissue from secondary effects caused by altered gene function in other tissues [123]. Some of the drawbacks of conventional gene targeting can be overcome by conditional knockout strategies which employ site-specific recombination systems.

Site-specific recombination enzymes allow genetic modifications such as the deletion of a target gene in a tissue- or cell-type specific manner. The two recombinases which are used most frequently in mouse models are Cre (catalyses recombination) recombinase from the bacteriophage P1 [124] and FLP (Flippase recombination enzyme) recombinase from *Saccharomyces cerevisiae* [125]. They both belong to the integrase family of recombinases [126]. Cre catalyses the recombination of two specific recognition sites, termed loxP (locus of crossing-over P1). loxP sites consist of 34 bp and contain an asymmetric 8 bp core sequence which is flanked by two sets of palindromic 13 bp sequences (Fig. 12A). If two loxP sites located on the same DNA molecule have opposite orientations, Cre recombinase activity will result in the inversion of the sequence which is flanked by the loxP sites. If the loxP sites have the same orientation, Cre activity will lead to the excision of the flanked sequence and one of the loxP sites. This principle is exploited in conditional gene targeting. For a conditional knockout, a coding exon of the target gene is floxed (flanked by loxP sites). Since the loxP sites are integrated into intron regions of the gene, they are unlikely to affect the transcription of a gene. Only when Cre recombinase is expressed in a targeted cell, the floxed exon is excised which leads to the inactivation of the targeted gene. There is a broad range of mouse strains expressing Cre recombinase [121;127]. Mouse strains which express Cre recombinase

ubiquitously are termed Cre deleters and lead to a global recombination of floxed loci. In this case, the resulting genotype is equivalent to a conventional gene targeting strategy. But there are also strains in which the Cre gene is under the control of a cell type- or tissue-specific promoter. Breeding the Cre strain with the gene-targeted mice will then result in a locally confined, cell type- or tissue-specific knockout. There is also the possibility to gain temporal control over the genetic modification by using strains in which Cre is controlled by a drug-inducible promoter. Alternatively, a fusion of Cre with the ligand-binding domain of a steroid hormone is expressed. These fusion proteins are bound by heat-shock proteins that inactivate Cre. Addition of the hormone ligand releases the chaperone and renders Cre active. This strategy can also be cell-type specific by employing specific promoters for the expression of the Cre fusion. Inducible gene targeting has the advantage that the genetic modification can be initiated at a desired time point, which allows normal development of mice until they reach the adult age [121;127].

The function of FLP recombinase is analogous to Cre. The recognition sites of FLP are named FRT (FLP recognition target) and have the same architecture as loxP sites (34 bp total length, 13 bp palindromes, 8 bp core). The FLP/FRT system can be used in combination with the Cre/loxP system (dual recombinase strategy, Fig. 12C). In analogy to floxed sequences, DNA that is flanked by FRT sites is referred to as flrted. If, for example, Cre/loxP is used to establish the desired genetic manipulation, the neomycin resistance (neo) cassette, which is necessary for the selection of recombinant ES cells but not required in the knockout mice, can be flrted. By breeding with FLP deleter strains, the neo cassette can be removed without affecting the floxed sequence. This is advisable because the genomically integrated selection cassette can have various side effects such as an altered transcription of surrounding genes [128].

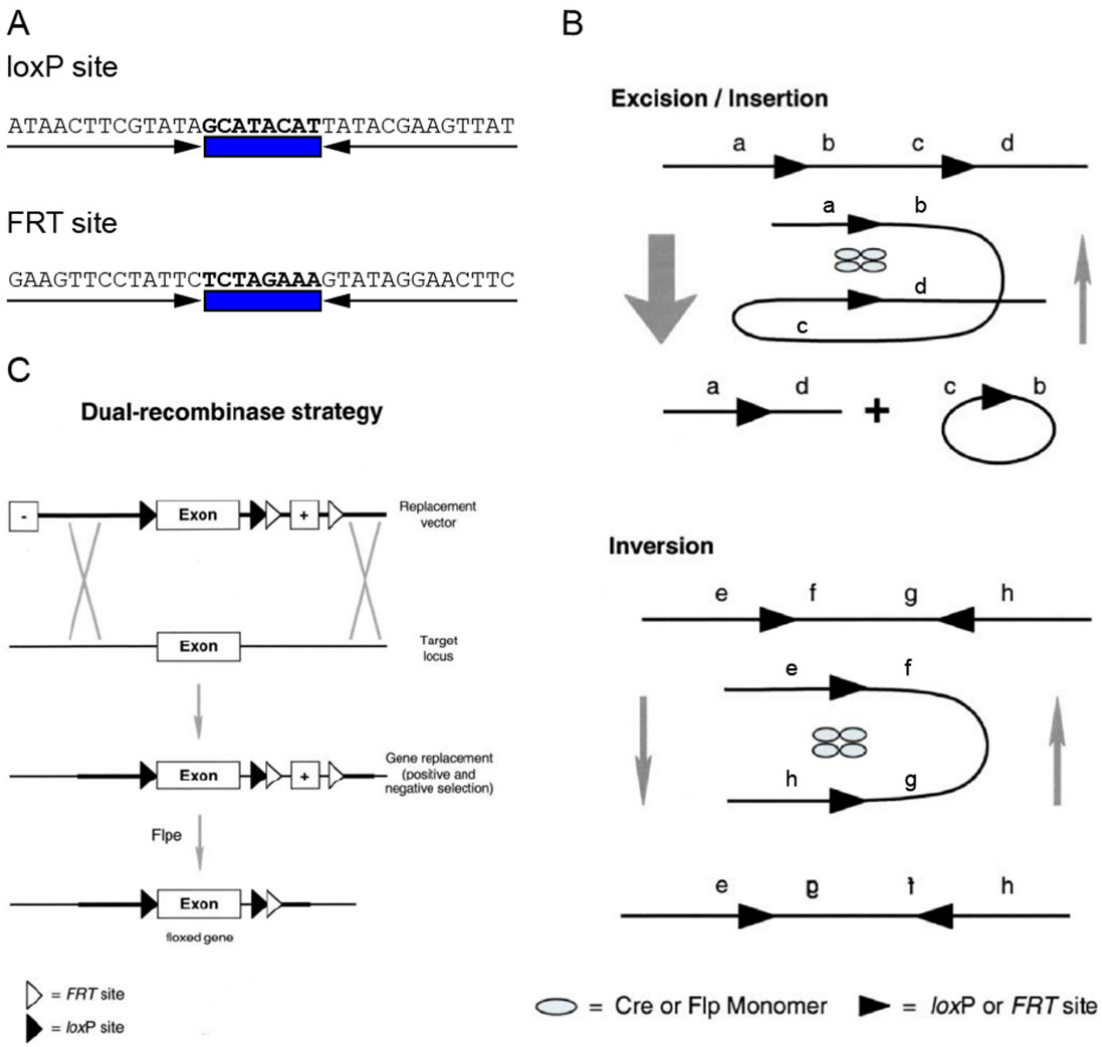

Fig. 12 The Cre/loxP and FLP/FRT system. A. The 34 bp loxP and FRT sites are displayed. The 13 bp palindrome sequences are indicated by arrows, the 8 bp core (bold) is indicated by a blue box. **B.** If recombinase recognition sites (triangles) on a DNA molecule have the same orientation, Cre- or FLP-mediated recombination causes the excision of the flanked sequence (b, c) and of one recognition site. If the recognition sites have opposite orientations, recombinase activity will invert the flanked sequence (f, g). **C.** Dual recombinase strategy for conditional gene targeting. In a targeting vector, an exon of interest is floxed and a positive selection marker (+) is flrted. The sequences upstream and downstream of the floxed/flrted region share homology with the target locus and allow homologous recombination. A negative selection (-) marker is located outside the homology region which allows the negative selection of non-homologous recombination events. After homologous recombination, the positive selection marker can be removed by FLP expression, resulting in a floxed exon and a single FRT site. The floxed exon can subsequently be eliminated by Cre recombinase. **B.** and **C.** Adapted from Branda *et al*. [128].

1.5 Aim of this thesis

A-kinase anchoring proteins (AKAPs) function as cellular signalling nodes by binding protein kinase A (PKA) and other signalling proteins. These AKAP-based complexes facilitate the temporal and spatial integration of cellular signalling. The highly conserved glycogen synthase kinase 3β interaction protein (GSKIP) has been shown to function as an AKAP *in vitro* and to bind glycogen synthase kinase 3β (GSK3β). GSK3β is regulated by other kinases, including PKA, through an inhibitory phosphorylation on serine-9. Thus the question arises whether GSKIP assembles a complex containing PKA and GSK3β and whether GSKIP facilitates the phosphorylation of GSK3β by PKA.

The major objectives of this thesis were: (1) The AKAP function of GSKIP was to be explored in live cells. (2) The potential complex formation of GSKIP with PKA and GSK3β and the relevance of such a complex for the PKA-dependent phosphorylation of GSK3β was to be elucidated. (3) It was to be determined to what extent GSKIP's interactions with PKA and GSK3β are conserved among GSKIP orthologues. (4) A mouse model for the conditional knockout of GSKIP was to be generated in order to develop a basis for clarifying the physiological role of GSKIP.

2. Material and Methods

2.1 Material

2.1.1 Equipment and Software

Equipment	Description	Supplier
Bruker Avance 600 MHz	NMR spectrometer	Bruker BioSpin GmbH (Rheinstetten, D)
GenePulser Xcell™	Electroporation system	Bio-Rad Laboratories GmbH (München, D)
GeniosPro	Microtitre plate reader	Tecan (Durham, USA)
LSM710-FCS	Confocal microscope	Carl Zeiss MicroImaging GmbH (Jena, D)
LumiImager™ F1	Gel documentation system	Roche Diagnostics (Mannheim, D)
Mastercycler gradient	Gradient Thermocycler	Eppendorf AG (Hamburg, D)
MiniProtean®	Polyacrylamide gel electrophoresis cell	Bio-Rad Laboratories GmbH (München, D)
PerfectBlue Mini L	Agarose gel electrophoresis chamber	PeqLab Biotechnologie GmbH (Erlangen, D)
Potter	Cell Homogeniser	Braun Biotech Int. GmbH (Melsungen, D)
Storm 830	Phosphorimager	GE Healthcare (München, D)
Trans Blot SD	Semi-Dry Western Blot module	Bio-Rad Laboratories GmbH (München, D)
Wallac 1410	Liquid scintillation counter	PerkinElmer (Rodgau, D)

Tab. 1 Equipment used for experimental procedures.

Software	Purpose	Supplier/URL
Clone Manager 5	DNA sequence analysis, cloning strategies	Sci-Ed Software (Cary, USA)
ClustalW	Sequence alignments	www.ebi.ac.uk/clustalw/
Discovery Studio 2.5	Molecular graphics	Accelrys Software Inc. (San Diego, USA)
Excel 2003	Spreadsheets	Microsoft (Redmond, USA)
GraphPad Prism 5.01	Statistical analysis	GraphPad Software (San Diego, USA)
Illustrator CS3	Graphics, drawing	Adobe Systems Inc (San Jose, USA)
ImageQuant v5.1	Autoradiography quantification	GE Healthcare (München, D)
LumiAnalyst 3.0	Densitometry, gel documentation	Roche Diagnostics (Mannheim, D)
Photoshop CS3	Image processing	Adobe Systems Inc. (San Jose, USA)
Powerpoint 2003	Presentations	Microsoft (Redmond, USA)
Pyrat V1.6 Build 109	Mouse husbandry management	Scionics Computer Innovation (Dresden, D)
Word 2003	Word processing	Microsoft (Redmond, USA)
ZEN	Confocal microscopy, image acquisition and analysis	Carl Zeiss MicroImaging GmbH (Jena, D)

Tab. 2 Software.

2.1.2 Antibodies

Antibody	Origin	Supplier, article number (#)
Primary antibodies		
Glyceraldehyde 3-phosphate dehydrogenase (GAPDH)	Rabbit, monoclonal	Cell Signaling Technology (Danvers, USA) #2118
Green fluorescent protein (GFP)	Rabbit, polyclonal	R. Schülein (FMP Berlin, D) [129]
GFP (JL-8)	Mouse, monoclonal	Clontech Inc. (Saint-Germain-en-Laye, F) #632380
GSK3β	Rabbit, monoclonal	Cell Signaling Technology (Danvers, USA) #9315
GSKIP (CN129)	Rabbit, polyclonal	Biogenes (Berlin, D) #8877*
Glutathione S-transferase (GST)	Rabbit, polyclonal	Millipore (Schwalbach, D) #AB3282
Lamin A/C	Goat, polyclonal	Santa Cruz Biotechnologies (Heidelberg, D) #sc-6215
c-Myc	Mouse, monoclonal	Calbiochem (Nottingham, UK) #OP10
Phospho-GSK3β (Ser9)	Rabbit, polyclonal	Cell Signaling Technology (Danvers, USA) #9336
PKA RIIα	Mouse, monoclonal	BD Biosciences (Heidelberg, D) #612243
β/γ-tubulin	Mouse, monoclonal	Calbiochem (Nottingham, UK) #CP06
Secondary antibodies		
Horseradish peroxidase (HRP)-anti-goat IgG	Donkey, polyclonal	Dianova (Hamburg, D) # 705-035-147
HRP-anti-mouse IgG	Donkey, polyclonal	Dianova (Hamburg, D) #715-035-151
HRP-anti-rabbit IgG F(ab')2	Donkey, polyclonal	Dianova (Hamburg, D) #711-036-152

Tab. 3 Antibodies. *, Using recombinant human full-length GSKIP [68], polyclonal antisera #8877 and #8878 were custom-generated in rabbits (Biogenes GmbH). GSKIP-specific antibodies were isolated from the antisera by affinity chromatography using GSKIP immobilised on thiopropyl sepharose 6B (GE Healthcare) as described previously [130].

2.1.3 Deoxyribonucleic acids

Vectors

pECFP-C1, pECFP-N1, pEGFP-N1, pEYFP-N1 (Clontech Inc., Saint-Germain-en-Laye, F). pmCherry-C1, pmCherry-N1 (C. Rutz, FMP, Berlin, D), pNEB193 (New England Biolabs, Frankfurt a. M., D), pZero^{TM}-2 (Life Technologies, Darmstadt, D), pPNT-FRT3 (K. P. Knobeloch, FMP, Berlin, D).

Recombinant Plasmids

Plasmid	Sequence of interest	Source
pmCherry-C1-GSKIP	mCherry-GSKIP	Cloned for this work
pmCherry-C1-GSKIP-V41P/L45P	mCherry-GSKIP-V41P/L45P	Cloned for this work
pECFP-N1-GSKIP	GSKIP-CFP	C. Hundsrucker (FMP, Berlin, D) [58]
pECFP-N1-GSKIP-V41P/L45P	GSKIP-V41P/L45P-CFP	C. Hundsrucker (FMP, Berlin, D) [58]
pEGFP-N1-myc-GSKIP	myc-GSKIP (myc-GSKIP was inserted via EcoRI and NotI sites, replacing GFP)	V. Popara (FMP, Berlin, D)
pET28a(+)-GSKIP	His-GSKIP	V. Popara (FMP, Berlin, D)
pZero™-2-GSKIP	GSKIP genomic DNA (EcoRI fragment)	Cloned for this work
pPNT-FRT3-GSKIP	GSKIP genomic DNA (5' and 3' homology), neo and HSV-tk cassettes	Cloned for this work
pEGFP-N1-RIIα	RIIα-GFP	B. Edemir (FMP, Berlin, D)
pEYFP-N1-RIIα	RIIα-YFP	B. Edemir (FMP, Berlin, D)[130]
pECFP-N1-AKAP18α	AKAP18α-CFP	S. Großmann (FMP, Berlin, D)
pmCherry-N1-AKAP18α	AKAP18α-mCherry	Cloned for this work
pmCherry-C1-AKAP18δ	mCherry-AKAP18δ	Cloned for this work
pmCherry-N1-GFP	GFP-mCherry	C. Rutz (FMP, Berlin, D)
RZPDo839B1162-pdEYFP-C1amp (YFP-GSK3β)	YFP-GSK3β	Imagenes (Berlin, D)
pEGFP-N1-corticotropin releasing factor receptor 1 (CRF1R)	CRF1R-GFP	U. B. Kaupp (IBI research centre, Jülich, D)

Tab. 4 Recombinant plasmids.

Oligonucleotides

Oligonucleotides used for oligonucleotide cloning or as primers for PCR and sequencing were ordered from BioTeZ Berlin Buch GmbH (Berlin, D). The oligonucleotides were synthesised in a 10 nmol scale, dissolved in sterile *Aqua deion.* and stored in a freezer as 50 µM stock and 10 µM working solutions.

2.1.4 Chemicals and Buffers

Chemicals and reagents

All reagents were obtained from Sigma-Aldrich (Taufkirchen, D) or Carl Roth (Karlsruhe, D) unless indicated otherwise. Restriction enzymes, T4 DNA ligase and the respective reaction buffers were obtained from New England Biolabs (Frankfurt a.M., D). OptiTaq thermostable DNA polymerase, reaction buffer and dNTPs for polymerase chain reaction (PCR) were purchased from Roboklon (Berlin, D). Water (referred to as *Aqua deion.*) was purified by the Milli-Q Plus system (Millipore, Schwalbach, D) to ≤ 10µS/cm at room temperature (RT) in the institute.

Buffers and solutions

All buffers and solutions were prepared with *Aqua deion*.

Buffer/solution	Composition
Blocking buffer (Protein overlay)	1× TBS-T; 3% BSA
Blocking buffer (RII overlay)	1× PBS; 5% non-fat dry milk; 0.1% BSA; 0.02% NaN_3
Blocking buffer (Western Blot)	1× TBS-T; 3% BSA
Coating buffer Enyzme-linked immunosorbent assay, ELISA)	1× PBS; 1 mM benzamidine; 0.5 mM PMSF; 3.2 µg/ml Trypsin inhibitor type I-S; 1.4 µg/ml Aprotinin; 1 mM DTT
Blocking buffer (ELISA)	1× Coating buffer (ELISA); 0.3% non-fat dry milk; 0.05% Tween-20
Denhardt's solution (100 ×)	2% BSA; 2% Ficoll; 2% Polyvynilpyrrolidone
ES cell lysis buffer	50 mM Tris-HCl; 100 mM EDTA;100 mM NaCl; 1% sodium dodecyl sulfate (SDS); 400 µg/ml Proteinase K
Fractionation buffer	250 mM sucrose; 20 mM HEPES, pH 7.4; 10 mM KCl;1.5 mM $MgCl_2$; 1 mM EDTA; 1 mM EGTA; 1 mM DTT
Homogenisation buffer	250 mM sucrose; 3 mM imidazole
Lysogeny broth (LB) medium	1% peptone; 0.5% yeast extract; 86 mM NaCl For LB agar plates, 15 g agar/l was used
RII overlay reaction buffer	25 mM KH_2PO_4;10 mM $MgCl_2$;10 µM cAMP; 0.5 mM DTT
Phosphate-buffered saline (PBS)	137 mM NaCl; 2.7 mM KCl; 1.5 mM KH_2PO4; 8.1 mM Na_2HPO_4, pH 7.4
Pre-hybridisation solution (Southern Blot)	5× SSC; 0.5% SDS; 5× Denhardt's solution; 100 µg/ml salmon sperm DNA, denatured
RIPA buffer	50 mM Tris-HCl, pH 7.4; 150 mM NaCl; 1% Triton-X 100; 1% sodium deoxycholate; 0.1% SDS; 1 mM EDTA
Saline-sodium citrate (SSC) buffer (20x)	3 M NaCl; 0.3 M sodium citrate, pH 7.0
SDS-polyacrylamide gel electrophoresis (PAGE) running buffer	25 mM Tris; 192 mM glycine; 0.1% SDS
Semi-dry transfer buffer (Western Blot)	48 mM Tris; 39 mM glycine; 1.3 mM SDS; 20% (v/v) methanol
Separating gel buffer (SDS-PAGE)	0.625 M Tris-HCl, pH 6.8
Stacking gel buffer (SDS-PAGE)	0.75 M Tris-HCl, pH 8.8
Standard Church Buffer	500 mM KH_2PO_4; 1 mM EDTA; 1% BSA; 7% SDS
Transfection buffer (ES cells)	1× PBS; 10 mM HEPES
Transfer buffer (Southern Blot)	0.4N NaOH
Tris-acetate-EDTA (TAE) buffer	40 mM Tris; 1 mM EDTA; 1.14% (v/v) glacial acetic acid
Tris-buffered saline (TBS)	10 mM Tris-HCl, pH 7.4; 150 mM NaCl
TBS + Tween (TBS-T)	1× TBS; 0.05% Tween-20
Tris-EDTA (TE) buffer	10 mM Tris-HCl, pH 8.0; 1 mM EDTA
Wash buffer I	2× SSC; 0.2% SDS
Wash buffer II	0.2× SSC; 0.2% SDS
Washing buffer (ELISA)	1× PBS; 0.05% Tween-20

Tab. 5 Buffer and solutions.

2.1.5 Medium for *E. coli*

Lysogeny broth (LB) medium

1% (w/v) peptone, 0.5% (w/v) yeast extract, 86 mM NaCl. For LB agar plates, 15 g agar/l was used. For antibiotic selection of *E. coli*, LB medium was supplemented with 100 µg/ml ampicillin or 30 µg/ml kanamycin, respectively.

2.1.6 Cell culture media for eukaryotic cells

Feeder medium

DMEM, 10% FBS, 0.2 mM glutamine, 0.2 mM non-essential amino acids, 0.1 mM β-mercaptoethanol, 100 U/ml penicillin, 100 µg/ml streptomycin sulfate.

ES cell medium

DMEM, 15% FBS, 0.2 mM glutamine, 0.2 mM non-essential amino acids, 0.1 mM β-mercaptoethanol, nucleoside solution (6 ml/500 ml medium) 100 U/ml penicillin, 100 µg/ml streptomycin sulfate, Leukaemia inhibitory factor (LIF, 2000 U/ml).

Freezing medium

ES cell medium containing 50% FBS and 10% DMSO.

2.1.7 Bacterial strains and eukaryotic cells

Bacterial strain	Genotype	Supplier
E. coli Top10	F- mcrA Δ(mrr-hsdRMS-mcrBC) φ80lacZΔM15 ΔlacX74 nupG recA1 araD139 Δ(ara-leu)7697 galE15 galK16 rpsL(Str^R) endA1 λ^-	Life Technologies (Darmstadt, D)
E. coli 294-Cre	endA thiA hsdR17 supE44 lacZ::cI857-Cre	Gene Bridges GmbH (Heidelberg, D)

Tab. 6 Bacterial strains.

Eukaryotic cell type	Description	Supplier
HEK293	human embryonal kidney line; transformed by adenovirus type 5 (Ad 5), DSMZ #: ACC 305	Deutsche Sammlung von Mikroorganismen und Zellkulturen GmbH (DSMZ, Braunschweig, D) [131]
SH-SY5Y	clonal subline of the neuroepithelioma cell line SK-N-SH, metastatic neuroblastoma, DSMZ #: ACC 209	DSMZ [132]
E14	Murine embryonic stem cells, strain 129/ola	[133]
Murine Embryonic fibroblasts	Isolated from embryos at day 13.5	[134]

Tab. 7 Eukaryotic cell lines and primary cells.

2.1.8 Animals

Strain	Remarks	Supplier
Wistar Hannover Rats		Charles River GmbH (Sulzfeld, D)
Mouse strains		
C57/Bl6	Standard wild-type mouse strain	Charles River GmbH (Sulzfeld, D)
FLPe deleter	Expression of FLPe recombinase	AG C. Birchmeier (MDC, Berlin, D) [135;136]
Cre deleter	Expression of Cre recombinase	AG T. Jentsch (MDC, Berlin, D) [137]

Tab. 8 Rat and mouse strains.

2.1.9 Genomic mouse DNA library

The mouse genomic DNA bacteriophage P1 artificial chromosome (PAC) library RPCI-21 [138] was obtained from the Deutsches Ressourcenzentrum für Genomforschung GmbH (RZPD, Berlin, D). The library had been generated as follows: Female 129S6/SvEvTac mouse spleen genomic DNA (partially MboI digested) was cloned into the BamHI sites of the vector pPAC4. PAC clones were transformed into *E. coli* and gridded onto nylon hybridisation membranes. The library has an average insert size of 137 kb.

2.2 Methods

2.2.1 Isolation and purification of DNA

2.2.1.1 Plasmid purification

Plasmid DNA amplified in *E. coli* was purified in a small scale with the Nucleospin® Plasmid QuickPure kit (Macherey-Nagel, Düren, D) or in a large scale with the NuceloBond® Xtra Midi kit (Macherey-Nagel, Düren, D) according to the manufacturer's instructions.

2.2.1.2 Purification of PCR products and DNA fragments from agarose gels

PCR products and DNA fragments separated by agarose gel electrophoresis were purified with the NucleoSpin® Extract II kit (Macherey-Nagel) according to the manufacturer's instructions.

2.2.1.3 P1 artificial chromosome (PAC) purification

PAC DNA amplified in *E. coli* was purified using the QIAGEN Large-Construct kit (Qiagen, Hilden, D) according to the manufacturer's instructions.

2.2.1.4 Isolation of genomic DNA from embryonic stem cells

For the isolation of genomic DNA, ES cells were cultured in 24-well plates.
When the cells had reached confluence, the medium was removed and the cells were lysed by adding 500 µl ES cell lysis buffer and incubating (3 h, 56 °C). 500 µl isopropanol was added to the lysate and the plate was placed on a shaker for 10 min to precipitate the DNA. The DNA precipitate was removed with a pipette tip and redissolved in 200 µl TE buffer at 56 °C overnight (O/N).

2.2.1.5 Isolation of genomic DNA from mouse biopsies

Genomic mouse DNA was isolated from mouse biopsies (tail tips or ear punches) with the Tissue DNA purification kit (Roboklon, Berlin, D).

2.2.2 Analysis and modification of DNA

2.2.2.1 Polymerase chain reaction

The polymerase chain reaction (PCR) is a method for the *in vitro* amplification of DNA sequences. The DNA fragment to be amplified is determined by a pair of specific synthetic oligonucleotide primers. The forward (Fw) primer is identical to the 5' end of the forward strand; the reverse (Rev) primer is identical to the 5' end of the complementary reverse strand of the required product. The primers anneal to a denatured single-stranded DNA template and are extended in 5'→3' direction by a DNA polymerase. The newly synthesised template/product double strands are denatured by heating the sample. Usually 25-35 cycles (denaturing, annealing, extension) are performed. As the synthesised strands also serve as templates in the next cycles, the desired product is amplified exponentially. Here, PCR was employed for cloning purposes and for the genotyping of genomic mouse DNA. The following tables show the composition of a typical PCR reaction and the cycling protocol. PCR products were analysed by agarose gel electrophoresis and, if necessary, excised from the gel, purified and ligated into a vector. The oligonucleotide primer sequences are shown in Appendix A.

Component	Final concentration
Template DNA	50-200 ng
10× Buffer C (Roboklon, contains 15 mM $MgCl_2$)	1× (1.5 mM $MgCl_2$)
dNTP mix (Roboklon, 5 mM each)	0.2 mM
FW primer (10 µM)	0.44 µM
Rev primer (10 µM)	0.44 µM
OptiTaq Polymerase (Roboklon, 5 U/µl)	0.5 U
H_2O	*ad* 15 µl

Tab. 9 PCR reaction composition.

	Step		Temperature	Time
	1	Initial Denaturation	94 °C	3-5 min
34×	2	Denaturation	94 °C	15-30 sec
	3	Annealing	50-68 °C	30 sec
	4	Elongation	72 °C	1 min/kb
	5	Final elongation	72 °C	5 min
	6	Cooling	4 °C	∞

Tab. 10 PCR protocol. The annealing temperature was optimised for each primer pair. The elongation time was adjusted according to the product length. Steps 2-4 were performed 35 times before proceeding to the final elongation step.

2.2.2.2 Restriction enzyme digestion of DNA

The site-specific digestion of DNA for analytical and cloning purposes was carried out using restriction endonucleases and buffers supplied by New England Biolabs (Frankfurt a. M., D) according to the manufacturer's instructions. The resulting DNA fragments were analysed by agarose gel electrophoresis.

2.2.2.3 Agarose gel electrophoresis of DNA fragments

Horizontal agarose gel electrophoresis was employed to separate DNA molecules according to their size for analytical and preparative purposes. Depending on the size of the DNA fragments, 0.6-1.5% (w/v) agarose gels were used. The agarose was dissolved in TAE buffer by boiling in the microwave. After cooling to approx. 60 °C, the DNA stain Redsafe (Intron Biotechnology, Seongnam, Korea) was added in a dilution of 1:50,000 and gels were cast. Samples were loaded in 1× DNA sample buffer (Bioline, Luckenwalde, D) into the wells. Gels were run at 100 V for 30-45 min in TAE buffer. The separated DNA was visualised with a LumiImager™ F1 using a 520 nm filter.

2.2.2.4 DNA ligation

For cloning purposes, DNA fragments (PCR or restriction products) were integrated into target vectors by enzymatic DNA ligation. The ligation of blunt or sticky end DNA fragments was performed using T4 DNA ligase (New England Biolabs) in a 10 µl reaction volume containing 0.5 µl T4 DNA ligase and 1 µl 10× T4 DNA ligase reaction buffer. Generally, a molar vector-insert ratio of 1:3 was used. The ligation reaction was incubated for 30 minutes at room temperature and used for the subsequent transformation into *E. coli*.

2.2.2.5 Electroporation of *E. coli*

For the transformation of recombinant plasmid DNA by electroporation, electrocompetent cells of the *E. coli* strain Top10 were used. 40 µl of bacterial suspension were gently mixed with 1 µl plasmid DNA and transferred to GenePulser cuvettes (gap 0.1 cm, Bio-Rad) pre-chilled on ice. The cells were electroporated with a GenePulser Xcell™, immediately resuspended in 1 ml LB medium and incubated in a thermomixer (37 °C, 300 rpm) to allow the expression of the plasmid-conveyed antibiotic resistance. The cells were streaked on LB agar plates containing the appropriate antibiotic and grown in an incubator (37 °C, O/N). Single clones were transferred to LB containing the appropriate antibiotic, amplified and plasmid DNA was isolated and analysed by restriction/gel electrophoresis and DNA sequencing.

2.2.2.6 DNA sequencing

Cloned vectors and genomic DNA fragments were verified by DNA sequencing. The Value Read Tube Service by Eurofins MWG Operon (Ebersberg, D) was utilised to sequence DNA.

2.2.3 DNA hybridisation techniques

Here, DNA hybridisation techniques were used for the identification of specific DNA sequences. The use of sequence-specific, labelled oligonucleotide probes which hybridise with target DNA in a sequence-specific fashion allows the identification of a sequence of interest within a mixture of DNA fragments or in lysed bacterial colonies without the need of prior DNA isolation or amplification.

2.2.3.1 Generation of radioactive hybridisation probes

Sequence-specific radioactive probes used for the Southern Blots, PAC library screening and colony hybridisation were generated with the Amersham Rediprime™ II DNA Labeling System (GE Healthcare, München, D). For the PAC library screening and colony

hybridisation, rat GSKIP cDNA was used as a template. For Southern Blots, a sequence located downstream of the 3' homology region of the GSKIP genomic DNA EcoRI fragment was excised using XhoI and BamHI (3' XhoI/BamHI probe, Fig. 30).

100 ng template DNA in 50 µl H2O was denatured by boiling for 5 min and then placed on ice (5 min). 45 µl of the single-stranded template DNA were pipetted into a Rediprime tube (containing dATP, dGTP, dTTP, exonuclease free Klenow enzyme and random primers), mixed and 5 µl [α-^{32}P]dCTP (Hartmann Analytic, Braunschweig, D) were added. The reaction mix was incubated (10 min, 37 °C). Excess radioactive nucleotides were removed by purifying the DNA with the GeneMatrix PCR / DNA Clean-Up DNA Purification Kit (Roboklon, Berlin, D) according to the manufacturer's instructions.

2.2.3.2 Colony Hybridisation

Colony hybridisation allows the detection of a DNA sequence of interest in a high number of *E. coli* colonies in a parallel approach. For this purpose, bacterial colonies were transferred to nylon membranes and their DNA fixed to these membranes.

In detail, *E. coli* were plated on agar plates containing a selection antibiotic and grown overnight (37 °C). Single colonies were picked with a sterile pipette tip, streaked on a nylon membrane marked with a numbered grid placed on a fresh agar plate, and then streaked on the corresponding position on a replica agar plate. After incubating both plates (O/N, 37 °C), the membrane was incubated in denaturing solution (5 min, RT) to lyse the bacteria and denature the DNA which would then bind to the positively charged membrane. After neutralisation in neutralising solution (5 min, RT) and two wash steps in 2× SSC, the membrane was pre-hybridised in Standard Church Buffer (1 h, 63 °C). Then the radioactive denatured probe (rat GSKIP cDNA, 2.2.3.1) was added and hybridised (O/N, 63 °C). The membrane was washed three times with wash buffer II (20 min, 63 °C). A Phosphorimager screen was exposed to the membrane for four hours and signals were recorded with a Phosphorimager. Clones containing the sequence of interest were picked from the replica plate and amplified for the isolation of DNA.

2.2.3.3 Southern Blot

Southern Blotting, named after its inventor Edwin Southern, is a method for the detection of specific sequences in DNA samples [139]. It involves the transfer of DNA from an agarose gel to a membrane and the subsequent hybridisation with a labelled DNA probe complementary to the sequence of interest. Since the binding of the probe is sequence-specific, only DNA fragments containing the desired sequence are visualised.

Genomic DNA was digested with EcoRI overnight and separated on a 0.6% agarose gel at 70V. The Southern Blot transfer was assembled as follows (from bottom to top): three layers of Whatman paper placed on a glass bridge with their ends soaking in a reservoir filled with transfer buffer, the gel, the nylon membrane (adjusted to gel size), three layers of Whatman paper, a stack of paper towels, a glass plate and a weight on the glass plate. The area of the Whatman paper surrounding the gel was covered with Parafilm to ensure that the capillary flow had to pass the gel. After the capillary transfer (O/N, RT), the membrane was rinsed with 2× SSC to remove the sodium hydroxide and used for hybridisation.

To prevent unspecific binding of the GSKIP 3' hybridisation probe, the membrane was pre-hybridised (blocked) with 5 ml pre-hybridisation solution (6 h, 63 °C). Then the radioactively labelled, purified and denatured probe was added and hybridised (O/N, 63 °C). In order to remove unspecific signals, the membrane was washed with once wash buffer I (20 min, 63 °C, low stringency) and then twice with wash buffer II (20 min, 63 °C, higher stringency). A Phosphorimager screen was exposed to the membrane overnight and signals were recorded with a Phosphorimager.

2.2.4 Biochemical methods

2.2.4.1 Peptide synthesis

Peptides derived from the RII-binding domains of AKAPs or the GSK3β-interaction domain (GID) of GSKIP (GSKIPtide) were synthesised by the Peptide Synthesis group (Dr. Michael Beyermann, FMP) as described [140] (for sequences see Appendix 2). Protein-derived peptides were named after the substitution compared with the corresponding position in the full-length protein, e.g. the peptide GSKIPTide-L130P comprises amino acid residues 115-139 of GSKIP with a leucine to proline substitution at the position corresponding to leucine 130 in GSKIP. For cell-based experiments, peptides were N-terminally coupled to stearic acid to render them membrane-permeable. The identity of peptides was verified by mass spectrometry (MS). HPLC analysis (220 nm) was employed to ensure that peptide purities were > 90%.

Peptide arrays were produced by Angelika Ehrlich (FMP) by automatic SPOT-synthesis on Whatman 50 cellulose membranes using Fmoc (fluoren-9-ylmethoxycarbonyl) chemistry in an AutoSpot-Robot ASS 222 (Intavis Bioanalytical Instruments AG, Köln, D) as described previously [53;141;142]. Control spots (approx. 50 nmol of peptide per spot) excised from the cellulose membrane were analysed by MALDI-TOF (matrix-assisted laser-desorption ionisation-time-of-flight)-MS and HPLC.

2.2.4.2 Protein overlay of GSK3β on peptide arrays

The interaction of GSK3β with potential or established GSK3β-binding proteins was assayed using peptide spots derived from the GSK3β-binding proteins which were incubated with recombinant GST-tagged GSK3β protein. To determine the binding of GSK3β protein to peptide spots, peptide arrays were briefly equilibrated in EtOH, washed in TBS-T and blocked in blocking buffer (3% BSA in TBS-T, 1 h, RT). The membranes were then incubated with 1 µg/ml GST-GSK3β or GST (negative control) in blocking buffer (O/N, 4 °C). When indicated, GSK3β was preincubated with the peptides GSKIPtide or GSKIPtide-L130P (10 µM each, 10 min, 4 °C). Excess protein was removed by washing three times with TBS-T before primary anti-GST antibody was added (1:1000 in blocking buffer, 1 h, RT). After another washing step (3× in TBS-T) and incubation with secondary horseradish peroxidase (HRP)-coupled anti-rabbit antibody (1:5000 in blocking buffer, 1 h, RT), ECL reagent (Lumi Light, Roche) was added to the membranes and chemiluminescence was visualised with the LumiImager F1.

2.2.4.3 Cell homogenisation and lysis

For the isolation and detection of proteins and protein complexes (2.2.4.4-2.2.4.7), cells or tissues were homogenised mechanically in homogenisation buffer supplemented with protease inhibitors (1 mM benzamidine, 0.5 mM phenylmethanesulfonyl fluoride, 3.2 µg/ml trypsin inhibitor I-S, 1.4 µg/ml aprotinin) and phosphatase inhibitors (50mM NaF and 100 µM Na_3VO_4) using a Potter homogeniser. The cells were disrupted with 10 strokes at 1200 rpm. Nuclei and debris were removed by centrifugation (3,000 × g, 15 min, 4 °C). The homogenate was used as an input for cAMP agarose pull-down or immunoprecipitation experiments or it was prepared for SDS-PAGE by adding Roti®-Load sample buffer (Carl Roth, Karlsruhe, D) and heating (95 °C, 5 min).

Cell or tissue lysis was achieved in RIPA buffer supplemented with protease inhibitors and phosphatase inhibitors. Insoluble debris was removed by centrifugation (15,000 × g, 4 °C, 15 min) and the resulting lysate was used for the same downstream applications as homogenates (see above).

2.2.4.4 Preparation of nuclear, membrane and cytosolic fractions

SH-SY5Y cell homogenates were fractionated into nuclear, membrane and cytosolic fractions by differential centrifugation in order to determine the intracellular distribution of endogenous GSKIP. SH-SY5Y cells were homogenised (2.2.4.3) in 500 µl fractionation buffer

supplemented with protease and phosphatase inhibitors per 100 mm cell culture dish and centrifuged (10 min, 4 °C, 700 × g). This yielded a nuclear pellet which was washed with fractionation buffer, centrifuged again, and resuspended in RIPA buffer. The supernatant was centrifuged (100,000 × g, 4 °C, 60 min). The pellet contained the particulate/membrane and the supernatant the cytosolic fraction. Samples of each fraction were analysed by Western Blotting.

2.2.4.5 cAMP agarose pull-downs

PKA R subunits are generally among the most abundant cAMP-binding proteins of mammalian cells. Therefore, agarose beads with surface-bound cAMP derivatives are suitable for the enrichment of R subunits and associated proteins from cell/tissue lysates or homogenates.

40 µl 8-AHA-cAMP-agarose slurry (Biolog, Bremen, D) were added to 1.8 ml lysate or homogenate (protein concentration 1 mg/ml) and rotated (3 h, 4 °C). As a negative control, the lysate/homogenate was pre-incubated with an excess of cAMP (50 mM) for 30 min before beads were added. The cAMP in solution blocks the cAMP binding sites of proteins and prevents their binding to the cAMP on the beads. The beads were then gently centrifuged (1000 × g, 4 °C, 2 min) and washed four timed with 500 µl of the respective lysis or homogenisation buffer. After the final washing step, the wash buffer was removed completely and protein were eluted from the beads by adding 40 µl 4× Roti®-Load sample buffer (Carl Roth, Karlsruhe, D) and heating (95 °C, 5 min). The eluate was subjected to SDS-PAGE and subsequent Western Blot detection of RII subunits and other proteins.

2.2.4.6 Immunoprecipitation

Specific proteins were isolated from cell lysates or homogenates by incubation with a suitable antibody followed precipitation of the antibody/antigen complex via IgG-binding Protein-A-sepharose. 30 µl of a Protein-A-sepharose suspension (70 mg/ml) were incubated with an immunoprecipitation antibody (3 µl) and 1.8 ml lysate or homogenate (4 °C; O/N). The subsequent washing and elution of immunoprecipitated proteins was performed as described in 2.2.4.5. The proteins were analysed by Western Blotting or RII overlay.

2.2.4.7 Western Blotting

Protein samples were heated (5 min, 95 °C) in 1× Roti®-Load sample buffer (Carl Roth, Karlsruhe, D), separated by SDS-PAGE and subsequently transferred to polyvinylidene fluoride (PVDF) membranes using the Trans Blot SD system (Bio-Rad). Membranes were

blocked in blocking buffer (1% BSA in TBS-T) for one hour at room temperature, followed by incubation with primary antibodies (in blocking buffer, O/N, 4 °C). Thereafter, membranes were washed with TBS-T (3×10 min) and incubated with secondary HRP-coupled antibodies, followed by a further washing step (TBS-T, 3×10 min). Finally, an ECL reaction was carried out using the Immobilon® Western Chemiluminescent HRP substrate (Millipore). ECL signals were visualised with the Lumi Imager F1 and the LumiAnalyst software was used for densitometric analysis.

2.2.4.8 RII overlay

The RII overlay, established by Lohmann *et al.* [48], can be used to assay the binding of PKA RII subunits to proteins immobilised on Western Blot membranes or to peptide spot arrays. Here, a modified version of this assay was employed using ^{32}P-labelled RIIα subunit probes [143;144]: Membranes were equilibrated in EtOH, washed with PBS and blocked in blocking buffer (3h, RT). Recombinant human RIIα subunits (2.5 µg) were radiolabelled through phosphorylation catalysed by purified bovine catalytic subunits of PKA (207 U ≙ 3.12 µg) and 0.1 µM [γ] ^{32}P-ATP (6000 Ci/mmol) in 500 µl reaction buffer. After 10 min incubation at room temperature, the final ATP concentration was set to 10 µM by addition of non-radioactive ATP. Following 50 min incubation on ice and addition of 70 µl dextran blue (10 mg/ml), the reaction was stopped by removal of cAMP and the separation of radiolabelled RIIα via gel filtration (Sephadex G-50, medium; Pharmacia Fine Chemicals). RIIα subunits coelute with the dextran blue fraction. The total activity of the dextran blue fraction was measured and specific activity was calculated in cpm (counts per minute; Liquid scintillation counter Wallac 1410). The membranes were incubated overnight with radiolabelled RII subunits in blocking buffer (specific activity of RII subunits = (1.4 ± 0.3) × 108 cpm/µg of protein per ml of hybridisation solution), washed with blocking buffer (4 times, 10 min) and twice with PBS. Signals were detected by autoradiography (Phosphorimager Storm 830) and analysed with the ImageQuant software.

2.2.4.9 Enzyme-linked immunosorbent assay

Enzyme-linked immunosorbent assays (ELISA) were carried out by Frank Christian to monitor the complex formation of RIIα, GSKIP and GSK3β in vitro. ELISAs were performed in 384-well clear or white flat bottom polystyrene high bind microplates (Corning B.V., Schiphol-Rijk, NL). The plates were coated by incubation with 20 µl/well RIIα (50 nM; prepared as described in [63]) in coating buffer for 1 h at room temperature (RT). After

removal of the coating buffer, blocking buffer was added (100 µl, 1 h, RT). Monitoring of interactions of RIIα with GSKIP and/or GSK3β was conducted in newly added blocking buffer (20 µl/well, 1 h, RT). Protein concentrations are indicated in the legend to Fig. 20. Non-bound protein was removed by washing 3 times with 100 µl washing buffer. Monoclonal anti-polyhistidine HRP-conjugated antibody (Sigma; 1:8000 in blocking buffer, 1 h, RT) was used to detect bound His-GSKIP. Bound GSK3β was detected by incubation with rabbit anti-GSK3β antibody (1:1500 in blocking buffer) and HRP-conjugated anti-rabbit IgG (1:3000, 1 h, RT). A washing step was performed after each antibody incubation. The HRP reaction was started by addition of 3,3',5,5'-tetramethylbenzidine (TMB) ELISA substrate solution (Sigma) and stopped after 30 min by addition of HCl (1 M; 20 µl/well). The coloured reaction product was quantified in a GeniosPro plate reader by measuring $A_{450\ nm}$ with 10 flashes/well. Based on a one-site-binding model, curves were fitted and K_D values were calculated using Prism.

2.2.4.10 Nuclear magnetic resonance (NMR) measurements

NMR experiments were performed and analysed in collaboration with Mangesh Joshi and Bernd Reif (Solid-state NMR group, FMP, Berlin, D). ^{1}H-^{15}N heteronuclear single quantum coherence (HSQC) measurements [145] were carried out to determine amino acids of GSKIP involved in the interaction with RII. For that, isotopically enriched GSKIP was expressed in the *E. coli* strain BL21-DE3 with ^{15}N-NH_4Cl as a nitrogen source. ^{1}H,^{15}N correlation experiments with ^{15}N-GSKIP in the presence or absence of the unlabelled D/D domain of RIIα (aa 1-44) were recorded using a HSQC programme employing WATERGATE for solvent suppression [146]. A Bruker 600 MHz Avance spectrometer equipped with a triple channel cyroprobe was used to measure NMR. The sample temperature was set to 30 °C and the typical protein concentration was in the order of 0.1 mM. In the direct dimension, the acquisition time was restricted to 150 ms. A total of 256 increments was recorded in the indirect dimension.

2.2.5 Mammalian cell culture

2.2.5.1 Cultivation of mammalian cell lines

HEK293 cells were maintained in Dulbecco's modified Eagle's medium (DMEM) supplemented with 10% foetal bovine serum (FBS), 100 units/ml penicillin G and 100 µg/ml streptomycin sulfate. For confocal microscopy of HEK293 cells, 30 mm glass coverslips were

coated with 500 µl poly-L-lysine (0.1 mg/ml) and incubated for 30 min (RT). The solution was aspirated and the coverslips were air-dried for one hour before seeding the cells.
SH-SY5Y cells were maintained in DMEM/Ham's F-12 (1:1) supplemented with 10% FBS, 1% non-essential amino acids, 100 units/ml penicillin G and 100 µg/ml streptomycin sulfate.

2.2.5.2 Transient transfection of HEK293 cells

The synthesis of proteins with fluorescence or affinity tags was achieved by transient lipid-mediated transfection of HEK293 cells with plasmid DNA containing the respective coding sequence. Lipofectamine™ 2000 (Life Technologies, Darmstadt, D) was used as a transfection agent. 24 h before transfection, the cells were seeded in antibiotic-free DMEM/FBS: 1.5×10^5 cells per 30 mm coverslip in 6-well plates or 4×10^6 cells per 100 mm dish. For the transfection, Lipofectamine™ 2000 (2 µl/µg plasmid DNA) was diluted in serum-free DMEM and incubated for five min. Plasmid DNA (0.5 µg/30 mm coverslip, 6 µg/100 mm dish) in serum-free DMEM was added to the transfection reagent. This transfection mix was incubated for 30 min (RT) to allow the formation of DNA/lipid complexes and then added to the cells. 24 hours after the transfection, the cells were used for further analysis.

2.2.6 Embryonic stem (ES) cells

Murine ES cells are derived from the inner cell mass of blastocyst stage embryos. ES cells are pluripotent, i.e. they have the ability to contribute to any cell type in a mouse embryo, including the germline [147]. This allows the propagation of genetic modifications, to which ES cells can be subjected in cell culture, *in vivo*. Here, ES cells were transfected with the targeting vector for the conditional gene targeting of GSKIP and recombinant ES cells were injected into mouse embryos which gave rise to conditionally targeted mice.
For the preservation of their pluripotency, it is essential to maintain ES cells in an undifferentiated state until they are injected into an embryo. This requires stringent ES cell culture conditions. ES cells are grown on a layer of feeder cells, usually murine embryonic fibroblasts (MEFs), which provide a suitable extracellular matrix and growth factors for the attachment and proliferation of ES cells.

2.2.6.1 Cultivation of murine embryonic fibroblasts

MEFs were prepared as described previously [134] and cultivated as follows: 1×10^6 cells per 100 mm dish were seeded in 6 ml feeder medium and grown to confluence for three to four days (1×10^6 cells per dish). Confluent MEFs were split at a ratio of 1:4 to 1:5 and were

passaged up to five times. MEFs used as feeder cells for the culture of ES cells contained a neomycin resistance cassette in order to survive the antibiotic selection of the ES cells.

2.2.6.2 Inactivation of murine embryonic fibroblasts

MEFs used as a feeder layer for ES cells were mitotically inactivated using mitomycin C to prevent them from overgrowing the ES cells. High concentrations of the cytotoxic agent mitomycin C induce DNA cross-linking and thereby apoptosis. At lower concentrations, the cells remain viable but they cannot undergo mitosis and therefore no longer divide. The ideal concentration of mitomycin C for the inhibition of MEF cell division is 10 µg/ml. Cell culture dishes containing a confluent layer of MEFs were treated with 10 µg/ml mitomycin C for three hours at 37 °C. The cells were then washed three times with PBS, detached with Trypsin/EDTA, resuspended in feeder medium at a concentration of $2\text{-}3\times10^6$ cells/ml and plated on gelatine-coated cell culture dish as follows:

Vessel	Cell suspension (ml)
100 mm	10
60 mm	3.3
6-well	1.25/well
24-well	0.2/well
96-well	0.05/well

Tab. 11 Seeding of MEFs

Inactivated MEFs were used for up to 4 days. After the MEFs had properly attached (12 hours), ES cells were seeded on the feeder layer.

2.2.6.3 Cultivation of ES cells

Undifferentiated ES cells form distinct colonies, in which cell borders are barely recognisable. Single cells display a large nucleus with pigmented nucleoli. ES cells were maintained at 37 °C and 5% CO_2. In order to prevent a differentiation of the cells, parameters such as cell density, pH value need to be kept constant which requires a daily change of the ES cell medium. Murine Leukaemia inhibitory factor (LIF) was added to the medium as an essential supplement for the maintenance of the pluripotent state of the cells.

ES cells were seeded at 1×10^6 cells per gelatinised 100 mm dish (with feeder layer) and cultured for two to three days. At this point, single colonies should be clearly separated from each other. The cells were split by washing with PBS, followed by incubation with 2 ml Trypsin/EDTA (5 min, 37 °C). The Trypsin was inactivated with 6 ml feeder medium and the

cells were centrifuged (560 × g, 5 min). The supernatant was discarded; the ES cell pellet was resuspended in ES cell medium and plated.

2.2.6.4 Electroporation of ES cells

The GSKIP targeting vector was linearised with NotI and purified by Phenol/chloroform extraction followed by a precipitation with 100% EtOH and two washing steps with 70% EtOH. The DNA was dried under a sterile hood and dissolved in sterile PBS.

1×10^6 ES cells were seeded on a 100 mm dish and cultured for two days. The medium was changed 2 hours prior to electroporation to increase the amount of cells being in S-phase at the time of transfection. The cells were trypsinised (as described in 2.2.6.3), resuspended in transfection buffer and centrifuged again. 1×10^7 cells were resuspended in 800 µl transfection buffer with 25 µg targeting vector DNA (1 µg/µl in PBS). The cells were transferred to an electroporation cuvette, electroporated (250 µF, 400 V) and chilled on ice for 20 min. The transfected cells from one cuvette were plated on three 100 mm dishes.

2.2.6.5 Selection of recombinant ES cells

24 h after electroporation, the ES cells were selected with G418 (280 µg/ml). G418 blocks the elongation step of translation. It can be inactivated by an aminoglycoside 3‘-phosphotransferase which is encoded by the neomycin resistance cassette of the target vector. Therefore, only recombinant cells with an integrated target vector survive G418 selection. Two days later, the negative selection of the remaining cells was performed using ganciclovir (2 µg/ml), a guanine analogue. The HSV-tk cassette, which conveys sensitivity to ganciclovir, is located outside the homology region of the target vector. Thus ganciclovir is only toxic in cells which have undergone non-homologous recombination and integrated non-homologous parts of the target vector.

After this double selection, surviving clones were screened with a stereo microscope. Undifferentiated colonies were picked with a sterile 200 µl micropipette tip and transferred to 96-well plates (round bottom) containing 30 µl Trypsin/EDTA per well. After filling each well with an individual clone, the plate was incubated for 5 min at 37 °C. Subsequently, 200 µl ES cell medium were added, the cells were singularised with an 8-channel pipette and transferred to a flat bottom 96-well plate with a feeder layer. After one to three days, depending on the cell shape and density, the cells were again split and divided onto two flat bottom 96-well plates. The cells on one plate containing freezing medium were frozen; the cells on the other plate were grown further for the isolation of genomic DNA. After three days, the cells were transferred to gelatinised 24-well plates and cultured for another three

days to increase the amount of genomic DNA. Genomic DNA was isolated as described in 2.2.1.4.

2.2.6.6 Freezing and thawing of ES cells

When cells are frozen a cooling rate of 1 °C/min should not be exceeded to prevent damage to the cells. Therefore, cells in vials were frozen in freezing containers ("Mr. Frosty" Nalgene) which are filled with isopropanol and adjusted to the ideal cooling rate of 1 °C/min. Cells in multi well plates were frozen in Styrofoam boxes.

Large amounts of cells were trypsinised, resuspended in medium, centrifuged, transferred to cryovials with freezing medium (10% DMSO, 50% FBS in ES cell medium) and frozen in freezing containers to -80 °C. Long-term storage of the vials was accomplished in liquid nitrogen.

For the freezing in multi well plates, cells were trypsinised and directly resuspended in freezing medium. The plates were put in a styrofoam box and placed in an ultra-deep freezer (-80 °C).

When thawing the cells, the toxic DMSO needs to be removed as quickly as possible. Vials containing frozen cells were thawed in a water bath (37 °C) and transferred into centrifuge tubes containing 10 ml medium. The cells were centrifuged, resuspended in fresh medium and plated. Cells in multi well plates were thawed by adding prewarmed medium to the wells, centrifuged, resuspended in fresh medium and seeded in a new multi well plate.

2.2.6.7 Injection of ES cells into mouse embryos

By injection of recombinant ES cells into embryos and the subsequent development of mice from these, the genetic modifications applied to ES cells were transferred from cell culture into an *in vivo* animal model. The Laser-assisted microinjection of recombinant ES cells into morula-stage embryos was performed at the Max Planck Institute of Molecular Cell Biology and Genetics (Dresden, Germany) in the transgenic core facility (TCF, head: Ronald Naumann) as previously described [148].

2.2.7 Microscopic methods

Live cell confocal laser scanning microscopy was performed to monitor the intracellular localisation of specific proteins and to measure the complex formation of proteins by fluorescence cross correlation spectroscopy. All microscopic measurements were carried out with an LSM710-FCS microscope using HEK293 cells which had previously been transiently transfected with constructs encoding fluorescent fusion proteins.

2.2.7.1 Live cell microscopy

24 h after transfection of HEK293 cells, 30 mm coverslips (2.2.5.2) were placed in a custom-made cuvette (B. Wiesner, FMP, Berlin, D) and the cells were covered with PBS. The cuvette was then mounted on the microscope. Images were recorded with the settings given in Tab. 12.

Fluorophores	CFP (A) YFP (B)
Objective	PlanNeofluar 40×/1.3 Oil
Excitation wavelength	A: 458 nm B: 514 nm
Beam splitters	MBS: 458/514 (A, B)
Filters	EF: BP 462-510 (A) EF: BP 516-701 (B)
Scanning mode	FRAME

Tab. 12 Microscope settings for confocal microscopy. MBS, main beam splitter; EF, emission filter; BP, band pass.

2.2.7.2 Fluorescence cross correlation spectroscopy (FCCS)

Fluorescence correlation spectroscopy (FCS) is a highly sensitive optical analysis method which measures fluctuations of fluorescence intensity within the confocal volume [149]. This allows the determination of the molecular mobility and concentration of a fluorescent molecule. When two spectrally different fluorophores are measured in an experiment, a trace is obtained for each fluorophore (fluorescence intensity as a function of time F(t)). Each peak of a trace represents a fluorescent molecule passing through the confocal volume. Since a particle molecule requires a certain time to diffuse through the confocal volume, photons from the same molecule can be measured at consecutive time points. The fluorescence intensities are therefore temporally correlated (autocorrelation). The autocorrelation function $G(\tau)$ provides information on the diffusion constant and concentration of the fluorophore. The traces of two fluorophores can also be correlated to each other. This is referred to as cross-correlation. If a cross-correlation is observed, it can be assumed that both fluorophores co-diffuse within the confocal volume. Fluorescence cross correlation spectroscopy (FCCS) can thus be used to determine the interaction of two molecules [150]. As an optical method, FCCS can be employed to monitor diffusion processes in live cells without disrupting cellular structures [151]. The fluorophores used for FCCS should have minimal overlapping spectra in order to prevent a cross-talk. Here, EGFP and mCherry were used as fluorescence tags to track the diffusion of proteins in live cells. Cell transfection and preparation for microscopy was performed as described above (2.2.7.1). For measurements, the laser was focussed on a region of the plasma membrane or the cytosol, depending on the localisation of the

fluorescent fusion proteins. The microscope settings are given in Tab. 1. Ten FCS traces, which were recorded for a duration of 4 seconds each, were averaged and regarded as one measurement (N = 1). For each sample, a minimum of 5 measurements, each in a different cell, was performed.

Fluorophores	GFP (A) mCherry (B)
Objective	C-Apochromat 40×/1.20 W Korr M27
Excitation wavelength	A: 488 nm B: 561 nm
Beam splitters	MBS: 488/561 (A, B) DBS: NFT 565 (A, B)
Filters	EF: BP 505-550 (A) EF: LP 580 (B)
Correlator binning	0.20 µs

Tab. 13 Microscope settings for fluorescence correlation microscopy. MBS, main beam splitter; DBS, dichroic beam splitter; NFT, neutral filter; EF, emission filter; BP, band pass; LP, long pass.

The obtained data for membrane proteins were fitted by the Zen Software using the following equation for two-dimensional (2D) diffusion of 1 component. For cytosolic proteins, a three-dimensional (3D) diffusion of 1 component was assumed. The analytical functions of the two models take the following form:

$$G(\tau) = 1 + G_t + G_d$$

with: G_t - the function for the triplet state
G_d - the function for the translation process

$$G_t(\tau) = 1 + \frac{T_t \times e^{-\tau/\tau_t}}{1 - T_t}$$

with: T_t - triplet fraction
τ_t - triplet relaxation time

$$G_d(\tau) = \frac{\Phi}{\left[1 + \left(\frac{\tau}{\tau_d}\right)^{\alpha}\right] \times \left[\left(1 + \left(\frac{\tau}{\tau_d}\right)^{\alpha} \times \frac{1}{S}\right)^{0.5}\right]^{e_d}}$$

with: Φ - fractional intensity
f - fraction of molecules
η - molecular brightness
τ_d - diffusional correlation time
S - structural parameter
ω_z - axial focus radius
ω_r - lateral focus radius
α - anomaly parameter
c - concentration
N - total number molecules
L_A - Avogadro number
and: e_d = 0 (2D) or 1 (3D)

In order to have descriptive and comparable values for the cross correlation of different samples, the autocorrelation (ac) with the lower amplitude within a sample (either GFP or mCherry) was set to 100% and the respective cross-correlation (cc) was expressed as a relative percentage.

2.2.8 Animal keeping and breeding

Mice maintained according to recommendations of the Federation of European Laboratory Animal Science Associations (FELASA). They were housed in a specific-pathogen-free environment in the animal facilities of the Max-Delbrück-Centrum (MDC, Berlin, D) with food and water provided *ad libitum* in air conditioned rooms at 22-23 °C with a standard 12 h light/dark cycle. 20 days after birth, mice were weaned and ear-punched for numbering and identification. Young female and male mice were placed in separate cages. For breeding, one male was placed in a cage with one or two appropriate female mice. All procedures were in accordance with ethical guidelines laid down by the local governing body and approved by the Landesamt für Gesundheit und Soziales (LAGeSo), Berlin.

3. Results

This thesis is based on previous studies of the protein GSKIP in which interactions with GSK3β [70;106] and RII subunits of PKA [68;69] were identified. In addition, initial information about the expression pattern, cellular localisation and evolutionary conservation of GSKIP had been obtained [70]. During the work for this doctoral thesis, these previous results were expanded: The interaction of GSKIP with GSK3β was confirmed (3.1), followed by an analysis of the tissue (3.2) and intracellular (3.3) distribution of GSKIP. Thereafter, GSKIP's AKAP function, which had been demonstrated *in vitro*, was analysed structurally and verified in live cells (3.4).

In further sections, the formation of a GSKIP-PKA-GSK3β complex (3.5) and the involvement of GSKIP in the phosphorylation of GSK3β were investigated (3.6). Moreover, it was explored to what extent the evolutionary conservation of the GSKIP sequence comprised a functional conservation of GSKIP's protein-protein interactions (3.7). Apart from GSKIP, the interactions of further proteins (AKAP220, MAP2D, SMYD2) with GSK3β were analysed (3.8). This chapter is concluded with a database analysis of GSKIP expression in cancer (3.9) and a description of the GSKIP knockout mouse model (3.10).

3.1 The GSKIP-GSK3β interaction

The interaction of GSK3β with GSKIP was originally described in two independent studies [70;106]. Here, in order to confirm this interaction, Co-IPs of GSKIP and GSK3β labelled with different tags were performed (myc-GSKIP, YFP-GSK3β). The IP of myc-GSKIP was performed using an anti-GSKIP antibody which had previously been generated in our group using full-length recombinant GSKIP as an antigen. For this experiment, HEK293 cells transiently expressing myc-GSKIP and YFP-GSK3β or myc-GSKIP and CFP as a negative control were used. The expression of the respective recombinant proteins was detected by Western Blotting (Fig. 13, lanes 1, 2).

YFP-GSK3β was precipitated with an anti-GFP antibody and a co-precipitation of myc-GSKIP was observed (Fig. 13, lane 3). When an anti-GSKIP antibody was used for the IP, myc-GSKIP was clearly enriched and YFP-GSK3β was detected (Fig. 13, lane 5). An interaction of myc-GSKIP with the fluorescent protein tag was excluded as an IP of CFP with anti-GFP did not result in Co-IP of myc-GSKIP (Fig. 13, lane 6). A non-specific rabbit IgG used as a negative control precipitated neither YFP-GSK3β nor CFP nor GSKIP (Fig. 13,

lanes 4, 7). In this experiment, GSKIP and GSK3β were successfully co-precipitated in IPs of either GSKIP or GSK3β (via the YFP tag) which confirmed their interaction and demonstrated the suitability of the applied constructs and antibodies.

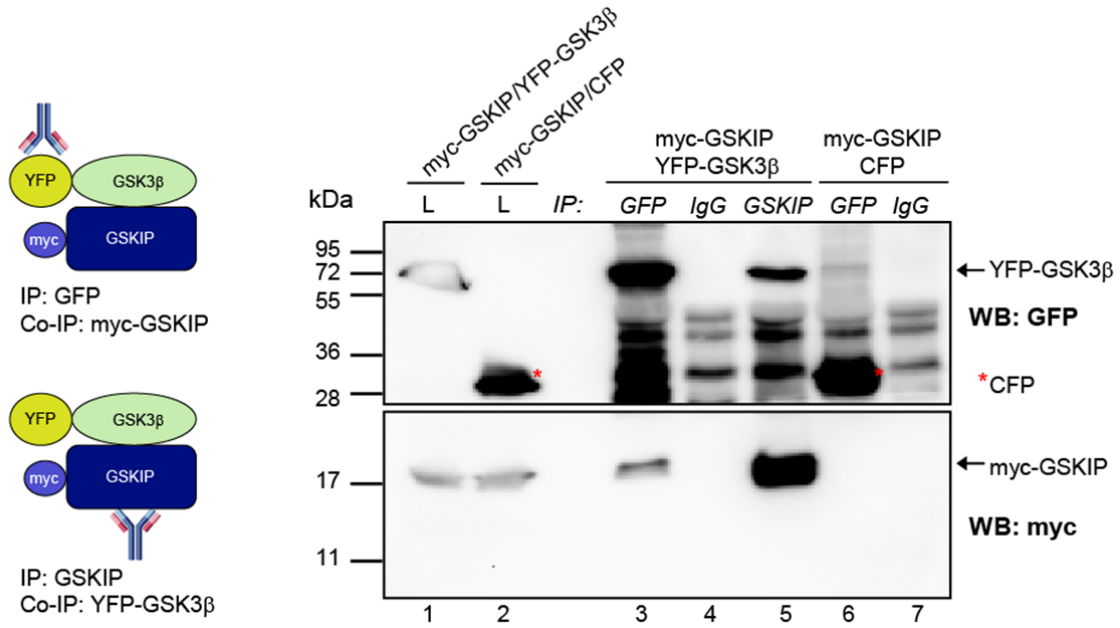

Fig. 13 Co-immunoprecipitation of GSKIP and GSK3β. *Left panel*: schematic illustration of the Co-IPs of YFP-GSK3β and myc-GSKIP. *Right panel*: myc-GSKIP in combination with YFP-GSK3β or CFP was transiently expressed in HEK293 cells as indicated at the top. Cells were lysed (L) and proteins were precipitated (IP) using the rabbit antibodies indicated in italics (IgG, non-related rabbit IgG). Proteins were detected by Western Blotting with anti-GFP (YFP-GSK3β, CFP) and anti-myc (GSKIP). Myc-GSKIP was detected in the IP of YFP-GSK3β and *vice versa*.

Because GSK3β is expressed ubiquitously, it was investigated whether this is also the case for its interaction partner GSKIP.

3.2 GSKIP is a ubiquitously expressed protein

So far, no information on the *in vivo* abundance of GSKIP had been available. The only previous evidence for endogenous GSKIP protein was delivered by a high throughput screen for protein-protein interactions in which endogenous GSKIP from HEK293 cells was identified by mass spectrometry in IPs of GSK3β [106]. In order to analyse the protein abundance of GSKIP, various rat organ lysates were subjected to SDS-PAGE/Western Blotting and probed with the anti-GSKIP antibody.

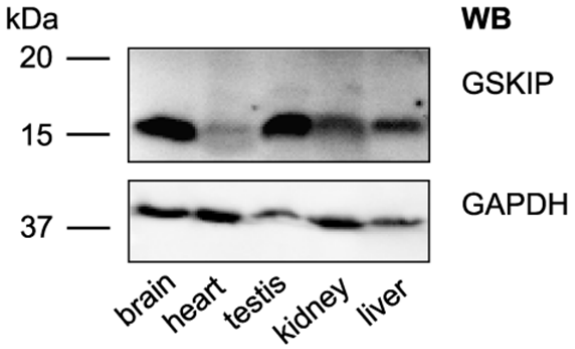

Fig. 14 GSKIP protein is present in various rat organs. Lysates obtained from the indicated rat organs were subjected to Western blot analysis with an anti-GSKIP antibody. GAPDH was detected as a loading control (150 µg total protein per lane). This research was originally published in [58].

GSKIP protein was found in all organs tested (Fig. 14, brain, heart, testis, kidney, liver). The highest abundance was observed in brain and testis. Together with previous analyses on the transcriptional level, this result suggests that GSKIP is a ubiquitously expressed protein: Chou *et al.* reported the expression of GSKIP mRNA in various human organs (heart, brain, placenta, lung, liver, skeletal muscle, kidney, pancreas) as detected by Northern Blot [70]. In addition, microarray data for human, mouse and rat GSKIP indicated a ubiquitous expression since comparable levels of GSKIP transcripts were found in a panel of different tissues (e.g. 79 human tissues) [108-111]. After detecting endogenous GSKIP in a range of organs, its intracellular localisation was investigated.

3.3 GSKIP is a cytosolic protein

Since AKAPs are found in most organelles [32], and GSK3β is localised mostly in the cytosol, but also present in the plasma membrane, nucleus and mitochondria [152;153], GSKIP may be localised in various cellular compartments. Chou *et al*. reported that recombinant HA-GSKIP is localised in the cytosol of HeLa cells [70] but in a further study conducted with GFP-GSKIP in SH-SY5Y cells, GSKIP was distributed evenly throughout the cytosol and the nucleus [154]. Such inconsistent results can be caused by modifications of the protein or by the detection method. Therefore, software prediction tools were employed here to gather information about potential targeting motifs within GSKIP and to predict possible localisations of GSKIP (Tab. 14).

Integral membrane proteins and luminal proteins of the ER, the Golgi apparatus, vesicular organelles as well as secreted proteins contain specific targeting sequences that direct them to the secretory pathway. These sequences are signal peptides in the case of secreted and luminal proteins. Integral membrane proteins can either contain a signal peptide or a signal anchor

sequence. Several secreted proteins do not take the canonical route via ER/Golgi and are termed non-classical secreted proteins [155].

The prediction tools SignalP 3.0 and SecretomeP 2.0 did not find any signal peptide, signal anchor sequence or characteristics of a non-classically secreted protein in the GSKIP sequence (Tab. 14). Thus, a targeting of GSKIP via the classical or a non-classical secretory pathway is not likely. Consistently, no transmembrane helix was predicted to be present in GSKIP (Tab. 14, TMHMM). This result was expected because GSKIP contains only two amphipathic helices but transmembrane helices are generally hydrophobic. No nuclear localisation signal (NLS) was identified in GSKIP but one potential nuclear export signal (NES) was identified around Leu80 (Tab. 14, PredictNLS/NetNES). This residue is however located in the core of GSKIP and it is therefore questionable whether it is indeed part of a functional NES. The absence of specific targeting motifs within human GSKIP argues for a cytoplasmic localisation of GSKIP which is supported with high confidence by several software tools that estimate the cellular localisation of proteins using different approaches (Tab. 14).

Prediction tool	Result	References
SignalP 3.0 [Signal peptide and signal anchor]	Prediction: Non-secretory protein Signal peptide probability: 0.000 Signal anchor probability: 0.000	[156]
SecretomeP 2.0 [non-classical protein secretion]	NN-score: 0.452 Non-classically secreted proteins should obtain an NN-score exceeding the normal threshold of 0.5, but not at the same time be predicted to contain a signal peptide.	[157]
TMHMM 2.0 [transmembrane helices]	Number of predicted TMHs [transmembrane helices]: 0	[158]
PredictNLS Online [nuclear localisation signals]	This protein does not contain a nuclear localization signal	[159]
NetNES 1.1 [nuclear export signals]	[Nuclear export signal predicted for Leu80, see Appendix C for details]	[160]
pTarget [cellular localisation]	Localization: cytoplasm, Confidence: 87.6 %	[161]
YLoc [cellular localisation]	Predicted Location: Cytoplasm Probability: 94.28 % Confidence: Strong (0.80) The most important reason for making this prediction is the small length of longest very hydrophobic region. 30% of the proteins from the cytoplasm have a similar attribute, whereas only about 0% of the proteins from the plasma membrane show this property. Moreover, the protein has a very negatively charged N-terminus. 42% of the proteins from the cytoplasm have a similar attribute, whereas only about 1% of the proteins from the extracellular space and mitochondrion show this property. There are more properties that support the predicted location.	[162;163]
SherLoc2 [cellular localisation]	Predicted Location: **cytoplasmic: 0.98;** nuclear: 0.01; peroxisomal: 0.0; Golgi apparatus: 0.0; mitochondrial: 0.0; extracellular: 0.0; plasma membrane: 0.0; lysosomal: 0.0; ER: 0.0	[164]
MultiLoc2-HighRes [cellular localisation]	Predicted Location: **cytoplasmic: 0.72;** peroxisomal: 0.1; nuclear: 0.09; mitochondrial: 0.06; extracellular: 0.01; plasma membrane: 0.01; Golgi apparatus: 0.01; ER: 0.0; lysosomal: 0.0	[165]

Tab. 14 Bioinformatic prediction of the localisation of GSKIP. The sequence of human GSKIP was analysed with the indicated bioinformatics programmes. The original output was placed in the column "result", additional remarks are given in square brackets.

After the *in silico* prediction, the distribution of GSKIP protein tagged with CFP was monitored in HEK293 cells. The interaction of GSKIP with PKA RII subunits could have an effect on its localisation. This was tested by including the PKA-binding deficient mutant GSKIP-V41P/L45P as a CFP fusion protein. CFP-AKAP18α was used to allow the comparison with a protein localised in the plasma membrane. In order to monitor the anticipated colocalisation with PKA RIIα, the CFP-tagged GSKIP and AKAP18α constructs were co-transfected with YFP-RIIα (Fig. 15 A).

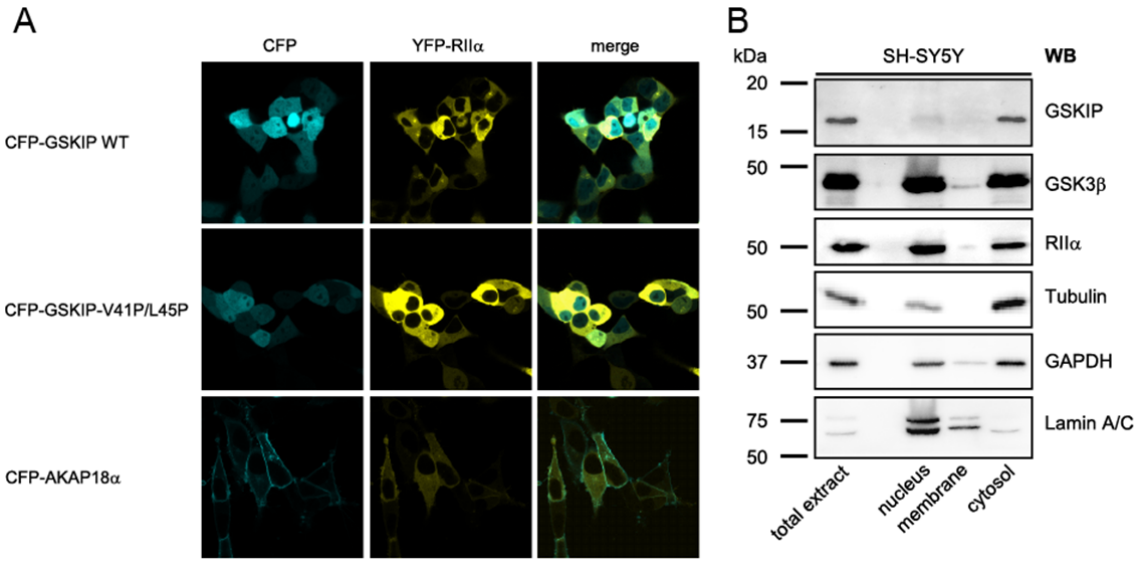

Fig. 15 The cellular localisation of GSKIP. A. HEK293 cells were transiently transfected to express YFP-RIIα and fusions of CFP with wild-type GSKIP (CFP-GSKIP WT), GSKIP-V41P/L45P or AKAP18α. Both CFP-GSKIP WT and CFP-GSKIP-V41P/L45P were localised in the nucleus and the cytosol. **B.** Subcellular fractions (nucleus, membrane, cytosol) were obtained from SH-SY5Y cells. 10 µg of total protein/lane were analysed by Western blotting with antibodies directed against the indicated proteins. GSKIP was detected in the cytosolic fraction. This research was originally published in Hundsrucker *et al*. [58].

CFP-GSKIP was evenly distributed throughout the cell; it was detected in the cytosol and the nucleus (Fig. 15 A, upper panel, cyan). YFP-RIIα colocalised with GSKIP in the cytosol but it was not visible in the nucleus (Fig. 15 A, upper panel, yellow). The same pattern was observed for GSKIPV41P/L45P, indicating that the mutation does not influence the location of GSKIP (Fig. 15 A, middle panel). As expected, AKAP18α was predominantly present in the plasma membrane and was able to recruit a portion of YFP-RIIα to the plasma membrane although most of YFP-RIIα remained in the cytosol (Fig. 15 A, lower panel).

Fusions with fluorescence proteins can affect a protein's properties, especially its localisation. Therefore, the localisation of endogenous GSKIP and its interaction partners GSK3β and RIIα was analysed by cell fractionation of SH-SY5Y cells (Fig. 15 B). Nuclear, membrane and cytosolic fractions were obtained by differential centrifugation (2.2.4.4) and analysed by Western Blotting (Fig. 15 B). The enrichment of nuclei was verified by detection of the nuclear marker Lamin A/C. Both RIIα and GSK3β were detected in the nuclear fraction. Small amounts of RIIα and GSK3β were also found in the membrane fraction. GSKIP was only detected in the cytosolic fraction, along with RIIα, GSK3β and the cytosolic markers GAPDH and tubulin. Minor amounts of the latter two proteins were also present in the nuclear fraction, indicating an impurity in the nuclear fraction, possibly due to intact cells sedimented together with the nuclei.

In summary, this fractionation experiment revealed that wild-type GSKIP is a cytosolic protein. This conclusion is supported by the previous study of Chou *et al*. showing immunofluorescence microscopic detection of HA-GSKIP only in the cytosol [70]. RIIα and GSK3β were found in the nucleus, membrane and cytosolic fraction. The nuclear localisation observed with CFP-GSKIP (Fig. 15 A) and GFP-GSKIP [154] is thus probably an artefact caused by the fluorescent protein moieties. Indeed, GFP can enter the nucleus, even when expressed as a homo-oligomeric fusion protein [166], and could facilitate the nuclear localisation of the smaller GSKIP as part of GFP-GSKIP fusion protein. After demonstrating the presence of endogenous GSKIP in rat organs and SH-SY5Y cells and establishing its cytosolic localisation, its putative AKAP function was validated.

3.4 The AKAP function of GSKIP

After the identification of an AKAP consensus sequence within GSKIP, its ability to bind PKA RIIα subunits was confirmed by RII overlay of GSKIP peptide spots [68]. Following SPR resonance experiments revealed that full-length GSKIP binds RIIα with a higher affinity (K_D = 5 nM) than RIIβ (K_D = 43 nM) but no binding to RIα or RIβ subunits was observed [69]. This indicates that not only the peptide derived from the AKAP consensus sequence of GSKIP but also the full-length protein is capable of binding RII subunits. This binding was completely blocked in the presence of the PKA anchoring disruptor peptides AKAP18δ-L314E and Ht31. Proline-containing derivatives of these peptides had no effect [68;69]. The selectivity for RII over RI classifies GSKIP as an RII-specific AKAP and the susceptibility of the GSKIP-RII interaction to PKA anchoring disruptor peptides indicates a canonical AKAP-PKA interaction. In an effort to confirm the involvement of the identified GSKIP RIIBD in binding the PKA RIIα D/D domain dimer, NMR measurements were performed.

3.4.1 Structural aspects of the GSKIP-RIIα interaction

In order to determine residues of GSKIP involved in the interaction with RII, ^{1}H-^{15}N heteronuclear single quantum coherence (HSQC) spectra of ^{15}N-labelled GSKIP in the absence or presence of the D/D domain of RIIα (aa 1-44, unlabelled) were recorded (Fig. 16). NMR experiments were performed and analysed in collaboration with Mangesh Joshi and Bernd Reif (Solid-state NMR group, FMP, Berlin, D). Changes in the NMR signals of a GSKIP residue in the presence of the D/D domain are most likely to occur when the residue is either involved in the interaction, situated near the binding site or affected by conformational changes caused by the interaction [145]. The hydrophobic residues of the RIIBD were

expected to be engaged in the interaction with the D/D domain. Indeed, signal attenuation in the presence of the D/D domain was observed for six hydrophobic residues within the RIIBD (Leu35, Val41, Leu45, Phe46, Ala47, Met51). This is indicating that the hydrophobic face of the RIIBD helix binds to the D/D domain dimer.

In addition, decreased NMR signals were observed for residues located in the β-sheet region (Ala64, Asn67, Lys71, Leu80, Thr81, His104, Asp112, Leu114) and amino acids localised in the C-terminal helix of GSKIP (Phe122, Gly123, Ala125). Most of these residues are in close proximity to the RIIBD. They could possibly contribute to the interaction with the D/D or be affected by conformational changes caused by D/D binding. In summary, ^{1}H-^{15}N HSQC NMR experiments underlined the importance of hydrophobic residues within the RIIBD of GSKIP and revealed further residues being involved in or affected by the interaction with the D/D domain of PKA RIIα.

Most experiments concerning the AKAP function of GSKIP had been performed using peptide spots or recombinant GSKIP protein purified from *E. coli*. However, posttranslational modifications often affect a protein's conformation and its interactions. These modifications applied to proteins in bacteria often differ from eukaryotic cells. Thus, full-length GSKIP was produced in eukaryotic cells and tested for RII binding.

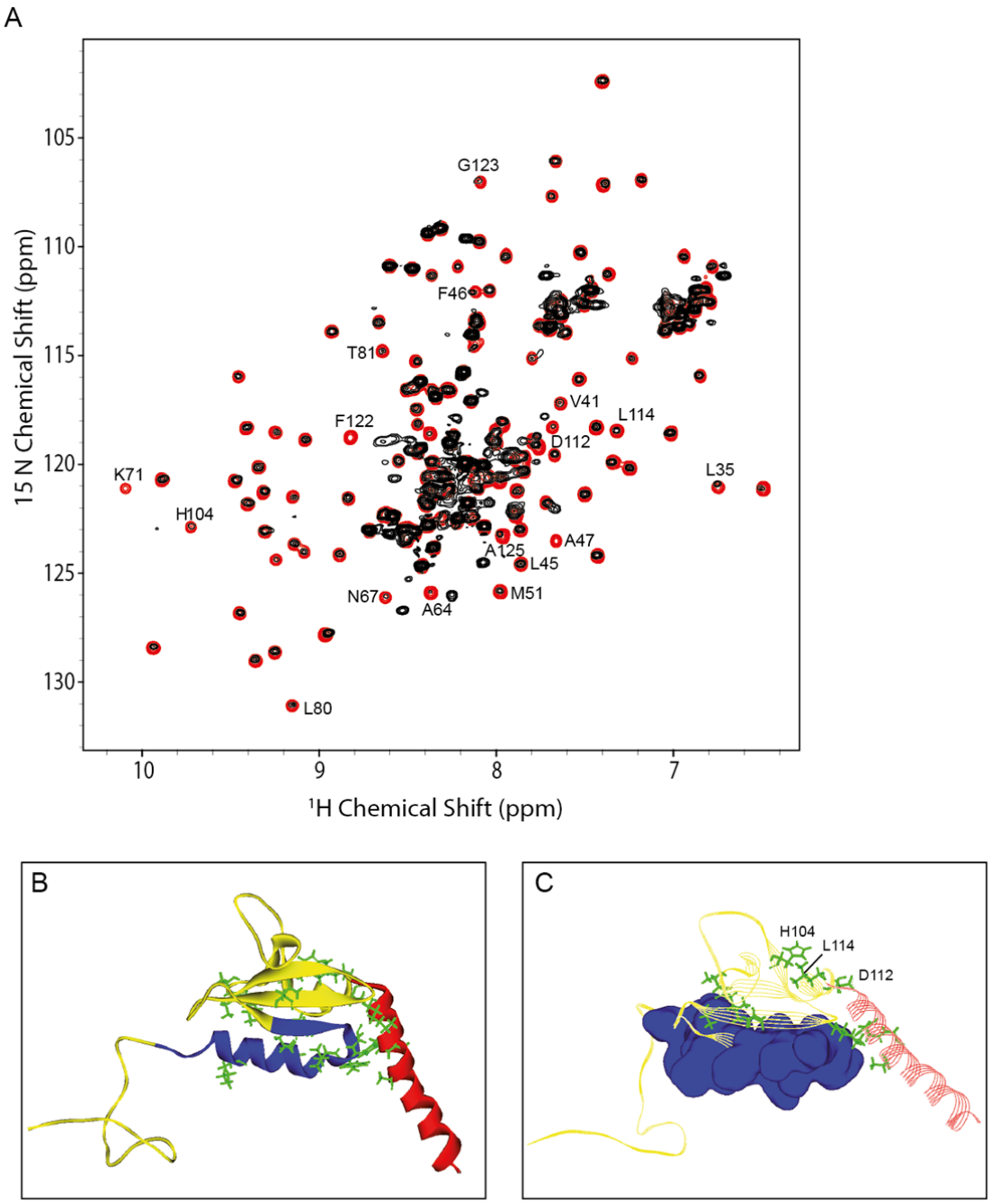

Fig. 16 Mapping the GSKIP-RIIα interaction by ^{1}H-^{15}N HSQC NMR. A. ^{1}H-^{15}N heteronuclear single quantum coherence spectra of GSKIP in the absence (red) or presence of the RIIα D/D domain (black) at 1:0.5 ratio are shown. Residues for which a signal attenuation was observed in the presence of the D/D domain are indicated. **B.** The residues identified in **A.** were visualised as green stick models in the NMR structure of GSKIP PDB: 1SGO). The tertiary structure is shown in yellow and the RIIBD (aa 28-52, blue) and the GID (aa 115-139, red) are highlighted. **C.** The surface of the RIIBD is illustrated in blue. With the exception of His104, Asp112 and Leu114, all amino acids showing signal attenuation are in close proximity to the RIIBD. This research was originally published in Hundsrucker *et al*. [58].

3.4.2 GSKIP expressed in eukaryotic cells binds RII subunits

An RII overlay (2.2.4.8) was performed to confirm the binding of GSKIP to RIIα. CFP-GSKIP was transiently expressed in HEK293 cells. The cells were lysed and CFP-GSKIP was immunoprecipitated using the rabbit anti-GSKIP antibody. IPs were subjected to SDS-PAGE, transfer to PVDF membranes and RII overlay assay. A similar experiment had been carried out before but yielded additional signals apart from the one observed in the molecular weight range of CFP-GSKIP [66]. Therefore, the experiment was repeated to validate the capability of GSKIP to bind RII subunits.

Western Blots using an anti-GFP antibody indicated that similar amounts of CFP-GSKIP (wild-type) and CFP-GSKIP-V41P/L45P but no CFP were immunoprecipitated with the GSKIP antibody (Fig. 17, lower left). No GSKIP was detected in the negative control (preimmune serum, Fig. 17, lower middle). In the RII overlay assay, a specific autoradiography signal was only observed for the WT but not for GSKIP-V41P/L45P (Fig. 17, upper left panel). This demonstrates that WT GSKIP expressed in eukaryotic cells can interact with RIIα subunits. This interaction is abolished by the insertion of two proline residues into the RIIBD of GSKIP (GSKIP-V41P/L45P, Fig. 17, upper left panel). This disruption of the RIIBD's helical structure has the same effect on other AKAPs such as Ht31 [167] and AKAP18δ [130]. Preincubation of the RIIα probe with the PKA anchoring disruptor peptide AKAP18δ-L314E (1.1.2.1) prevented RIIα from binding to GSKIP. This confirms that GSKIP binds to the D/D domain of RII subunits and is, therefore, a canonical AKAP.

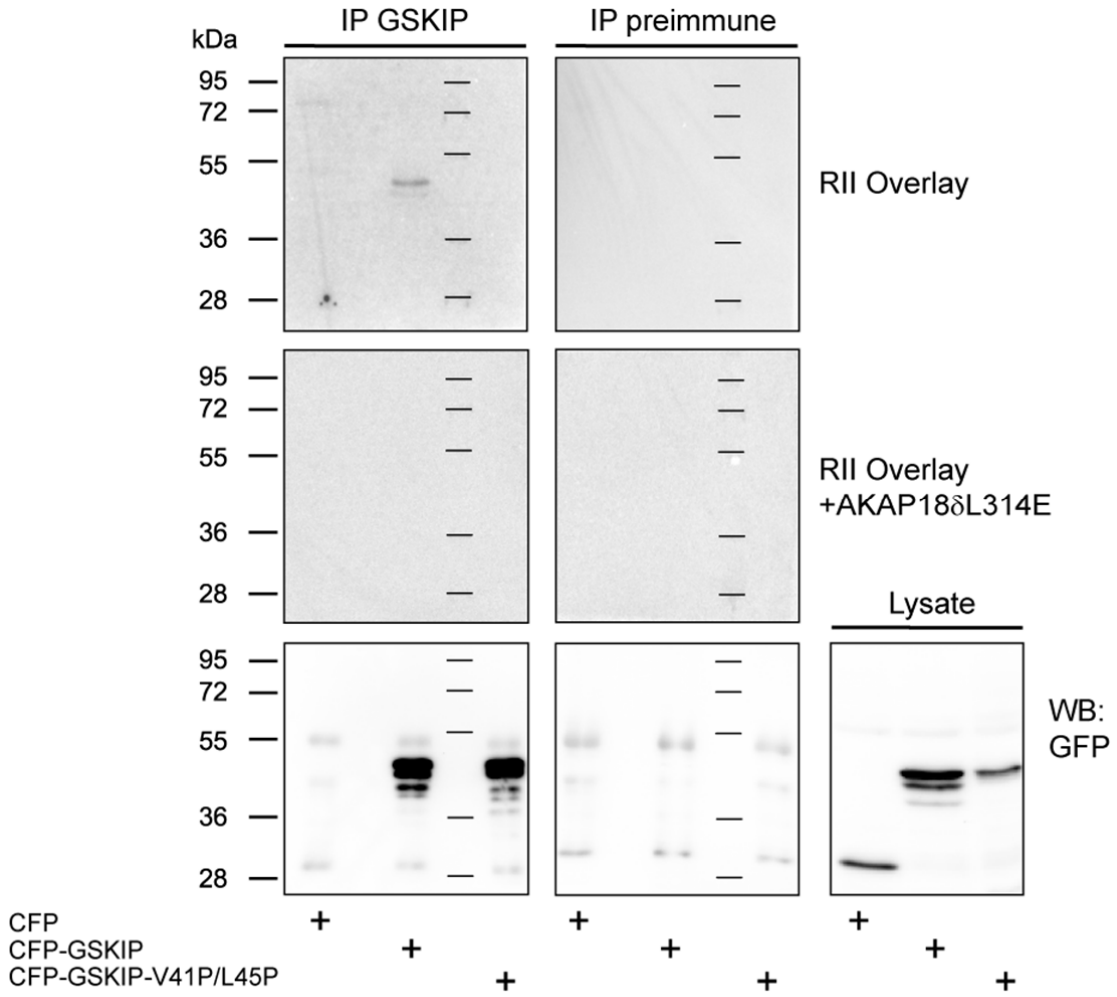

Fig. 17 Immunoprecipitated GSKIP binds RIIα. HEK293 cells were transiently expressing the proteins indicated at the bottom. GSKIP was precipitated with an anti-GSKIP antibody (IP GSKIP) or the corresponding preimmune serum (IP preimmune) as a negative control. The presence of the proteins in the cell lysate and in the IPs was detected by Western Blotting with a mouse anti-GFP antibody which also detects CFP [129]. The immunoprecipitated proteins were probed for RII binding in an RII overlay assay. CFP-GSKIP but not CFP-GSKIP-V41/L45P yielded a signal indicating RII binding. When the probe was preincubated with the PKA anchoring disruptor peptide AKAP18δ-L314E, the binding to GSKIP was blocked. This research was originally published in Hundsrucker *et al*. [58].

In order to clarify whether GSKIP interacts with PKA in live cells, cAMP agarose pull-down experiments were performed. Using modified cAMP coupled to agarose beads (8-AHA-cAMP-agarose), cAMP-binding proteins can be isolated from cell extracts. Interaction partners of the precipitated cAMP-binding proteins can be detected via Western Blotting. Because of the relatively low abundance of GSKIP in different cell lines tested, this experiment was first carried out using HEK293 cells transiently expressing myc-tagged GSKIP. The cells were homogenised and cAMP-binding proteins were precipitated using 8-AHA-cAMP-agarose. As a negative control, homogenates were pre-incubated with an excess of cAMP in solution (50 mM) in order to occupy cAMP-binding sites of proteins and thus prevent their binding to the 8-AHA-cAMP-agarose beads (Fig. 18A).

RIIα was detectable in homogenates (H) from both untransfected cells and cells expressing myc-GSKIP. RIIα was enriched in cAMP agarose pull-downs (PD, Fig. 18 A, upper panel). In the homogenate (H) of myc-GSKIP expressing cells, two bands were detected with the GSKIP antibody (approx. 17 and 18 kDa). The lower band was also observed in untransfected cells and is most likely endogenous GSKIP. The upper, higher intensity band corresponds to myc-GSKIP. As expected, myc-GSKIP was co-precipitated in cAMP-agarose pull-downs (PD) from myc-GSKIP expressing cells (Fig. 18A, lower panel). No protein was detected with the GSKIP antibody in the pull-down from untransfected cells. In the negative control containing 50 mM cAMP (Fig. 18A, (-), upper panel), no RIIα was detected. A small amount of myc-GSKIP was precipitated in the negative control but the signal was very weak and could have been caused by residual protein binding unspecifically to the beads (Fig. 18A, (-), lower panel). Endogenous GSKIP was not detected in the PDs from either untransfected or myc-GSKIP expressing cells, probably due its low abundance in comparison to myc-GSKIP.

After detecting recombinant GSKIP, it was tested whether endogenous GSKIP can also be co-precipitated in cAMP agarose pull-down experiments. For this purpose, SH-SY5Y cells were used because they express a higher amount of GSKIP protein than HEK293 cells. RIIα and GSKIP were detected in SH-SY5Y homogenates (Fig. 18B, left lane). In the cAMP agarose pull-down (PD), a strong signal for RIIα and a co-precipitation of GSKIP was observed. In the negative control (-), no RIIα and merely a faint band representing GSKIP were present. This shows that endogenous GSKIP is co-precipitated in cAMP agarose pull-downs from SH-SY5Y cell homogenates which affirms the AKAP function of GSKIP.

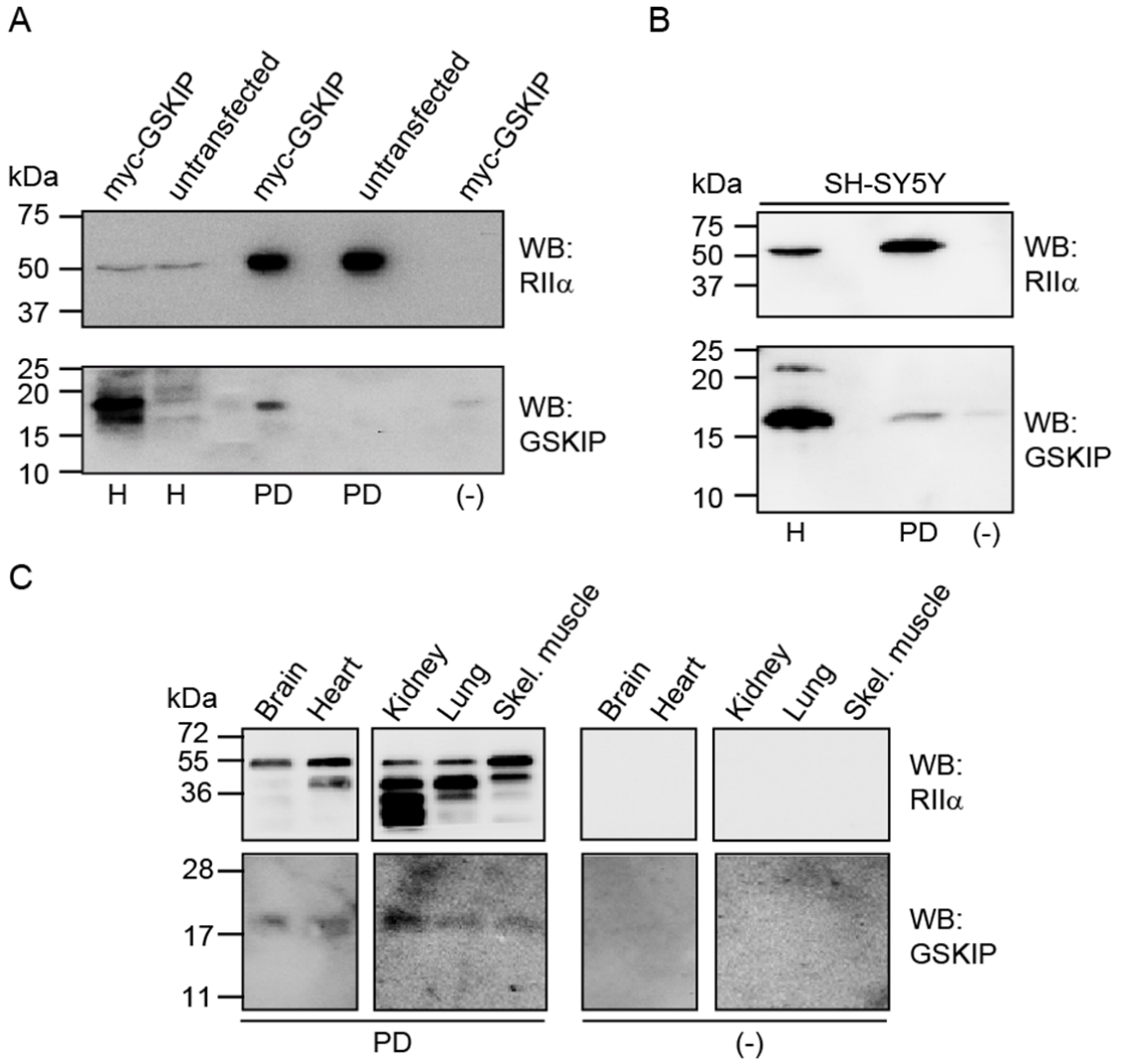

Fig. 18 Detection of GSKIP in cAMP agarose pull-downs. Cyclic AMP-binding proteins were precipitated from cell homogenates or organ lysates using 8-AHA-cAMP-agarose (2.2.4.5). The presence of RIIα and GSKIP was detected by Western blotting (WB). H, homogenate; PD, cAMP agarose pull-down; (-), negative control: PD performed in the presence of 50 mM cAMP; Skel., Skeletal. **A.** Homogenates from untransfected HEK293 cells or from HEK293 cells transiently expressing myc-GSKIP cells were subjected to cAMP agarose pull-down. myc-GSKIP was clearly detected in the pull-down from transfected cells but not from untransfected cells. In the negative control (-), only a neglectable amount of myc-GSKIP was detected. **B.** SH-SY5Y cell homogenate was used for a cAMP agarose pull-down. Endogenous GSKIP was present in the homogenate (H) and in the pull-down (PD). A minor amount of GSKIP was also detected in the negative control (-). **C.** GSKIP was detected in cAMP agarose pull-downs from various rat organ lysates (as indicated). No GSKIP was found in the respective negative controls (-). **C.** This research was originally published in Hundsrucker *et al*. [58].

Since cell lines are normally either derived from cancer cells (e.g. SH-SY5Y) or artificially immortalised (e.g. HEK293), their proteome and interactome do not necessarily reflect the normal physiological situation [168;169]. Therefore, rat tissue lysates were used as the input for the cAMP agarose pull-down (Fig. 18C). Like in the previous cell-line-based experiments, both RIIα and GSKIP were detected in the cAMP agarose pull-down from rat brain, heart, kidney, lung and skeletal muscle lysates (Fig. 18C, PD). Neither GSKIP nor RIIα were found

in the negative control (Fig. 18C, PD). For RIIα, not only the full-length protein (55 kDa) but also additional bands were visible, especially in pull-downs from kidney and lung lysates. Since these organs are known to contain high levels of proteases [170], these bands were probably caused by proteolytic degradation of RIIα protein in spite of the presence of protease inhibitors in the lysis buffer.

In summary, Cyclic AMP agarose pull-down experiments demonstrated the interaction of GSKIP and RII subunits extracted from live cells. GSKIP was detected as a co-precipitated protein in cAMP agarose pull-downs, either as an overexpressed protein (myc-GSKIP in HEK293 cells) or as an endogenous protein (SH-SY5Y, rat organs). This strongly supports but does not ultimately prove that they interact in live cells because the disruption of cellular structures as well as buffer conditions which deviate from the native cellular milieu can theoretically cause non-physiological protein-protein interactions to form. Therefore, it was investigated whether GSKIP and RIIα are associated in intact, live cells.

3.4.3 GSKIP and RIIα interact in live cells

Fluorescence cross correlation spectroscopy (FCCS) is a non-invasive optical single-molecule method. It can be used to monitor the co-diffusion of fluorescently labelled molecules in live cells. Here, FCCS was employed to measure to what extent GSKIP and RIIα form complexes in cells. The experiment described here is the first approach to monitor AKAP-PKA interactions by this method. Therefore, as positive controls for AKAP-RIIα interactions, AKAP18α and AKAP18δ were used because they are high-affinity AKAPs which are known to co-localise with RIIα in cells when fused to fluorescent proteins [171;172]. The FCCS experiments were carried out in HEK293 cells transiently expressing fusion proteins of the abovementioned AKAPs with the red fluorescent protein mCherry and an RIIα construct with a C-terminal GFP tag. The results are summarised in Fig. 19.

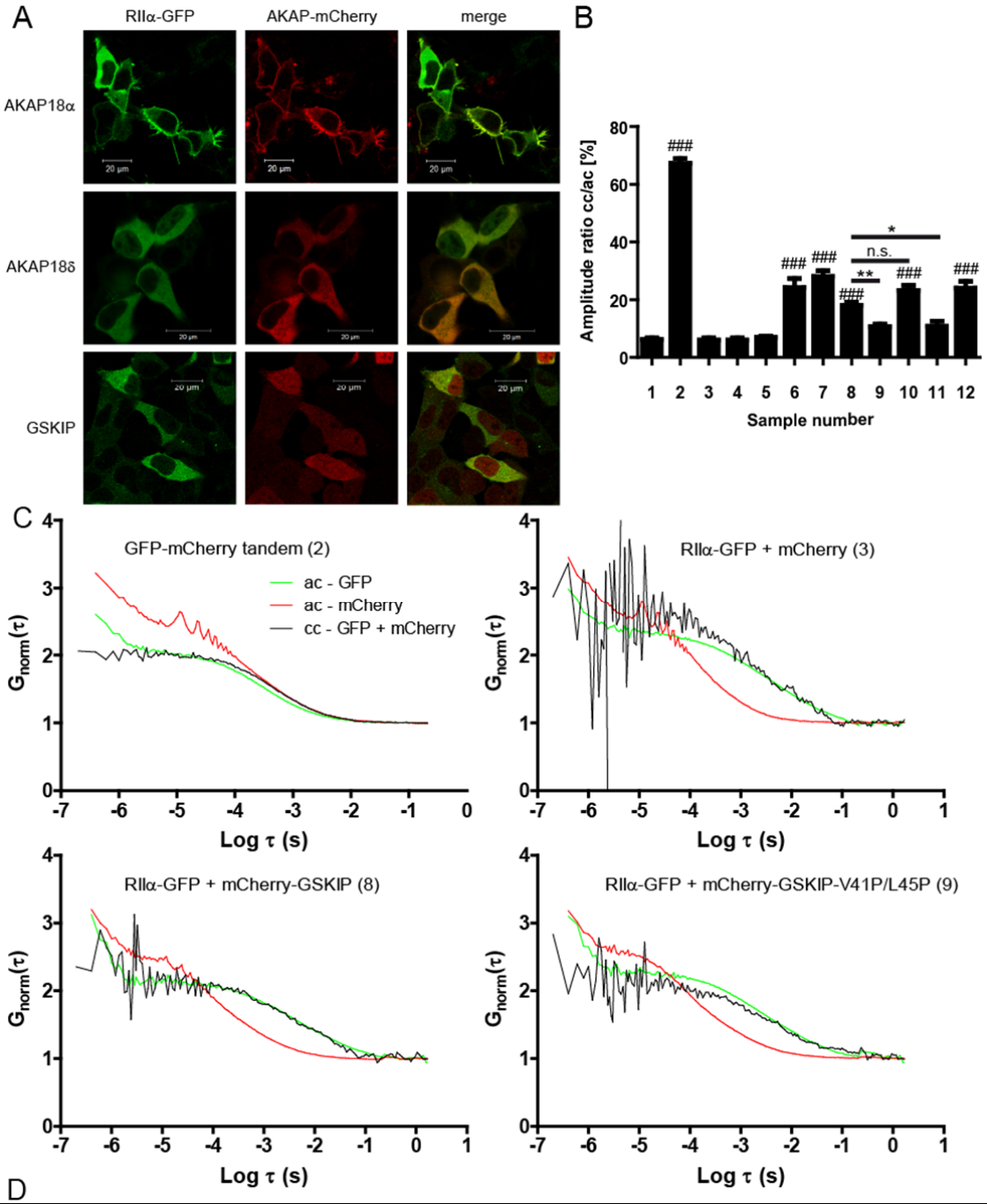

D

No.	Proteins		Mean cc/ac (%)	N	SEM
1	GFP	+ mCherry	6.24	24	0.53
2	GFP-mCherry (Tandem)		67.33	11	1.55
3	RIIα-GFP	+ mCherry	6.01	10	0.73
4	GFP	+ mCherry-GSKIP	6.58	8	0.73
5	CRF1R-GFP	+ AKAP18α-mCherry	6.99	12	0.40
6	RIIα-GFP	+ AKAP18α-mCherry	24.25	5	3.14
7	RIIα-GFP	+ mCherry-AKAP18δ	28.09	7	1.92
8	RIIα-GFP	+ mCherry-GSKIP	18.04	8	1.11
9	RIIα-GFP	+ mCherry-GSKIP-V41P/L45P	10.60	13	0.87
10	RIIα-GFP	+ mCherry-GSKIP + DMSO	23.25	8	1.70
11	RIIα-GFP	+ mCherry-GSKIP + S-Ht31	10.86	10	1.70
12	RIIα-GFP	+ mCherry-GSKIP + S-Ht31-P	24.03	10	2.34

Fig. 19 FCCS analysis of GSKIP and RIIα in live cells. HEK293 cells were transiently transfected to express the indicated combinations of fluorescent fusion proteins. **A.** Confocal laser-scanning microscope images of RIIα-GFP with the indicated AKAPs expressed as mCherry fusion proteins. **B.** FCS traces for GFP and mCherry were recorded as described in 2.2.7.2. Auto- (ac) and cross-correlations (cc) were calculated and the amplitude ratio of cc/ac for each sample is shown (means +/- SEM). The proteins expressed in the respective samples are shown in D. Significantly different from negative control (1): ###, $p < 0.001$. Significant differences between indicated samples: *, $p < 0.05$; **, $p > 0.01$. n.s., not significant. **C.** The normalised FCS traces of samples 2, 3, 8 and 9 are shown. τ, correlation time; $G_{norm}(\tau)$ correlation function. **D.** Table showing the recombinant proteins expressed, additional treatment of the cells (samples 10-12) and the values (Mean, N, SEM) illustrated in **B**.

Fig. 19A shows confocal microscopic images of HEK293 cells expressing fluorescent fusion proteins used for FCCS analyses. AKAP18α was localised in the plasma membrane whereas AKAP18δ and GSKIP exhibited a cytosolic localisation. GSKIP was additionally observed in the nucleus. RIIα was present in the cytosol and, in the presence of AKAP18α, additionally at the plasma membrane. The observed localisations of the AKAPs and RIIα were in accordance with previous experiments (Fig. 15) [171;172]. As expected, the fluorescent proteins GFP and mCherry were evenly distributed across the cytosol and the nucleus [173]. This localisation was not affected by any of the co-expressed proteins (data not shown). FCCS measurements were performed and auto- and cross-correlations were calculated as described in 2.2.7.2. For FCCS analyses of AKAP18α (samples 5 and 6), the laser was focused at the plasma membrane. For all other measurements, a region in the cytosol was focused. As examples, the normalised FCS traces of samples 2, 3, 8 and 9 are shown in Fig. 19C. For the positive control containing the GFP-mCherry fusion protein (sample 2), the cross-correlation curve (black) is almost congruent with the GFP auto correlation curve (green). Due to the covalent fusion of the fluorophores, the cross-correlation curve was very stable and showed hardly any fluctuations which consequently resulted in a high ratio of cross-correlation to auto-correlation (67.33%, Fig. 19D). This value can be regarded as the maximum for this experimental setting because the two fluorophores are fused in one molecule and thereby always co-diffuse. The deviation to the theoretical maximum of 100% can be explained by bleaching of the fluorophores during the experiment.

Several control experiments were performed to rule out interactions of the fluorescent protein moieties with each other or with a protein of interest. In the negative control containing RIIα-GFP and mCherry (sample 3), there were strong fluctuations of the cross-correlation curve and the correlation function dropped below one, which indicates that there was no cross-correlation between GFP and mCherry (Fig. 19C). Nevertheless, a minor amount of cross-correlation (6.01%) was observed for this sample due to the incomplete spectral separation and the resulting cross-talk of both fluorescence channels. Comparable values were obtained for the other negative controls comprising combinations GFP/mCherry (6.24%),

GFP/mCherry-GSKIP (6.58%) and CRF1R-GFP/AKAP18α-mCherry (6.99%). From this, it can be concluded that the fluorescence proteins mCherry and GFP did not interact with each other or with RIIα or GSKIP, respectively. The combination of CRF1R and AKAP18α served as a negative control for non-interacting membrane proteins.

In the samples comprising RIIα-GFP in combination with mCherry-GSKIP (8) or mCherry-GSKIP-V41P/L45P (9), a cross-correlation was observed (Fig. 19 C). In the case of mCherry-GSKIP-V41P/L45P, the amplitude of the cross-correlation curve was lower, indicating a decreased pair formation compared to wild-type GSKIP. For the high-affinity AKAPs, AKAP18α and AKAP18δ, values of 24 and 28% pair formation with RIIα were calculated. The value for GSKIP (18.04%) was lower but significantly different from all negative controls (Fig. 19B). In contrast, the V41P/L45P mutant of GSKIP exhibited a clearly decreased cross-correlation with RIIα (10.6%). This value did not differ significantly from any of the negative control, implying that GSKIP and RIIα interact in live cells and that a helical structure within the RIIBD of GSKIP is necessary for this interaction. These results are in line with SPR experiments showing the direct interaction of GSKIP with RIIα in vitro, which is weaker than the AKAP18δ-RIIα interaction and which is abolished in GSKIP-V41P/L45P [58].

The lack of a significant pair formation of GSKIP-V41P/L45P and RIIα indicates a canonical AKAP function of GSKIP. In order to confirm this, the cells were pre-treated with the stearate-coupled PKA anchoring disruptor peptide S-Ht31 which markedly decreased the cross-correlation of GSKIP and RIIα (10.86%). Cells pre-treated with the solvent used for the peptide (DMSO, final concentration 1% v/v) displayed a slight but insignificant increase in the cross-correlation of GSKIP and RIIα (23.25%). The double-proline substituted peptide S-Ht31-P, which does not bind to PKA, had no effect on the cross-correlation of GSKIP and RIIα (24.03%).

In summary, the interaction of the AKAPs AKAP18α, AKAP18δ and GSKIP with PKA RIIα subunits was demonstrated in live cells by FCCS. The interaction of GSKIP with RIIα was drastically reduced by expressing a proline-containing GSKIP mutant or by the PKA anchoring disruptor peptide S-Ht31. This strongly supports the canonical AKAP function of GSKIP. An overview comprising all experiments that were performed to explore the AKAP function of GSKIP is given in Tab. 15.

Method	System	GSKIP	PKA R subunits	Sensitive to PKA anchoring disruptor peptides	Result	Ref.
Bioinformatic prediction	*In silico*	Human GSKIP sequence (SwissProt database)	-	Not applicable	GSKIP contains an AKAP consensus sequence	[58;68]
RII overlay	*In vitro*	Peptide spots	Recombinant, ^{32}P-labelled RIIα	Yes	RIIα binds to peptide derived from putative GSKIP RIIBD	[58;68]
SPR	*In vitro*	Recombinant, His-tagged	Recombinant RIα, RIβ, RIIα, RIIβ	Yes	RIIα and RIIβ bind to GSKIP protein, no binding of RIα or RIβ	[58;69]
RII overlay	*In vitro*	Recombinant, CFP-tagged, immunoprecipitated from HEK293 lysate	Recombinant, ^{32}P-labelled RIIα	Yes	GSKIP mutation V41P/L45P abolishes RII-binding	Fig. 17 [58;68]
^{1}H-^{15}N HSQC NMR	*In vitro*	Recombinant, tag-free	Recombinant D/D domain of RIIα	Not tested	GSKIP interacts with the D/D domain of RIIα	Fig. 16 [58]
ELISA	*In vitro*	Recombinant, His-tagged	Recombinant RIIα	Not tested	Detection of an RIIα-GSKIP-GSK3β complex	Fig. 20 [58]
FCCS	Cell culture	Recombinant, mCherry-tagged in HEK293 cells	Recombinant, GFP-tagged RIIα	Yes	RIIα and GSKIP interact in live cells	Fig. 19
cAMP pull-down	Cell culture	Recombinant myc-tagged GSKIP in HEK293 cells	Endogenous	Not tested	Endogenous RIIα/recombinant GSKIP complex from cell line	Fig. 18
cAMP pull-down	Cell culture	Endogenous GSKIP from SH-SY5Y cells	Endogenous	Not tested	Endogenous RIIα-GSKIP complex from cell line	Fig. 18
cAMP pull-down	*In vivo (rat organs)*	Endogenous	Endogenous	Not tested	Endogenous RIIα-GSKIP complex from rat organs	Fig. 18 [58]

Tab. 15 Evidence for the AKAP function of GSKIP. An overview of the different methods by which the AKAP function of GSKIP was characterised. The utilised GSKIP and RII peptides/proteins are indicated. Ref., Reference.

3.5 The PKA RIIα-GSKIP-GSK3β complex

Two regions within GSKIP are involved in the interactions with PKA RII (aa 28-52) and GSK3β (aa 115-139). This raises the question whether GSKIP can simultaneously interact with PKA and GSK3β. ELISA experiments were performed to assay a potential complex formation of GSKIP with RIIα and GSK3β *in vitro*. ELISA plates were coated with GSKIP and then incubated with increasing concentrations of GST-GSK3β to quantitatively investigate their interaction in the ELISA system. To assay a trimeric complex formation, plates were coated with RIIα and incubated with increasing concentrations of GST-GSK3β in the presence or absence of GSKIP (Fig. 20).

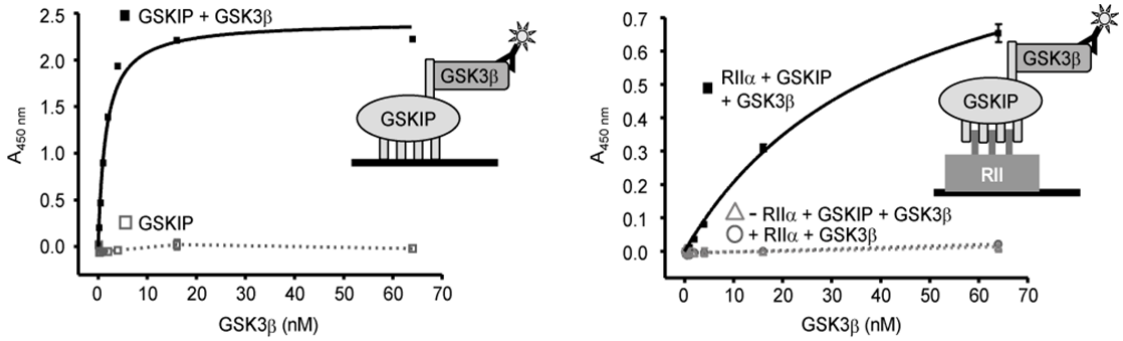

Fig. 20 GSKIP forms a ternary complex with PKA RIIα and GSK3β *in vitro*. *Left panel*: microtitre plates were coated with His-GSKIP (500 nM) and incubated with GST-GSK3β (0.25-64 nM, ■) in blocking buffer or with blocking buffer alone (□). GSK3β was detected with an anti-GSK3β and a secondary HRP-conjugated antibody and an HRP-catalysed reaction with a chromogenic substrate. *Right panel*: His-GSKIP (500 nM) was added together with increasing concentrations of GST-GSK3β (0.25-64 nM) to wells of microtitre plates coated with blocking buffer (△) or RIIα (50 nM, ■). To exclude direct binding to RIIα, GST-GSK3β (0.25-64 nM) was added to RIIα-coated wells in the absence of GSKIP (○). The detection was carried out as above. The result is representative for three independent experiments. This research was originally published in Hundsrucker *et al*. [58].

As expected, GSK3β bound to GSKIP-coated plates in a concentration-dependent manner (Fig. 20 left panel, filled squares) and no binding of GSK3β to plates blocked with blocking buffer alone was observed (Fig. 20 left panel, open squares). The K_D for the GSKIP-GSK3β interaction calculated from this experiment is 1.6 ± 0.2 nM. This indicates a high-affinity interaction.

When plates were coated with RIIα and incubated with GSKIP and GSK3β, binding of GSK3β was detected which indicates the presence of a ternary complex consisting of GSKIP, RIIα and GSK3β (Fig. 20 right panel, filled squares). A direct interaction of RIIα and GSK3β could be excluded because GSK3β did not bind to RIIα-coated plates in the absence of GSKIP (Fig. 20 right panel, open circles). The K_D for the RIIα-GSKIP-GSK3β interaction is

43 ± 5 nM. This affinity shows that the complex forms readily *in vitro* and potentially also *in vivo*.

If a complex of GSKIP, PKA and GSK3β exists *in vivo*, the question arises what functional significance it may have. The AKAP-PKA-GSK3β complexes formed by AKAP220 [57] and MAP2D [54] mediate the inhibitory phosphorylation of GSK3β on Ser9 by PKA. This could also be the case for the GSKIP complex.

3.6 GSKIP controls the phosphorylation of GSK3β by PKA

Multiple stimuli induce the phosphorylation of GSK3β by PKA (1.2). It is not known whether GSKIP is required for mediating the phosphorylation triggered by any of these hormones. If this is the case, a relevant cell type may be difficult to determine because GSKIP, PKA and GSK3β are all ubiquitously expressed proteins. Therefore, forskolin, an activator of ACs [13], was used to raise cAMP levels in HEK293 cells, causing a global activation of PKA. In order to determine the effect of GSKIP on the phosphorylation of GSK3β, the cells were either expressing CFP-GSKIP or CFP alone as a control. Western blot analyses were performed to assay the phosphorylation of GSK3β (Fig. 21). The phospho-specific GSK3β antibody detected endogenous phosphorylated GSK3β (47 kDa) and GSK3α (51 kDa). In untreated HEK293 cells, the phosphorylation of GSK3β was approximately twofold higher in cells transfected with CFP-GSKIP than in CFP-expressing cells (Fig. 21A). Forskolin significantly increased GSK3β phosphorylation. Again, the level of phospho-GSK3β was higher in CFP-GSKIP-expressing cells (Fig. 21A). When cells were incubated with the PKA inhibitor H89 prior to forskolin treatment, the forskolin-induced and GSKIP-dependent raise in p-GSK3β was blocked, indicating an involvement of PKA (Fig. 21A).

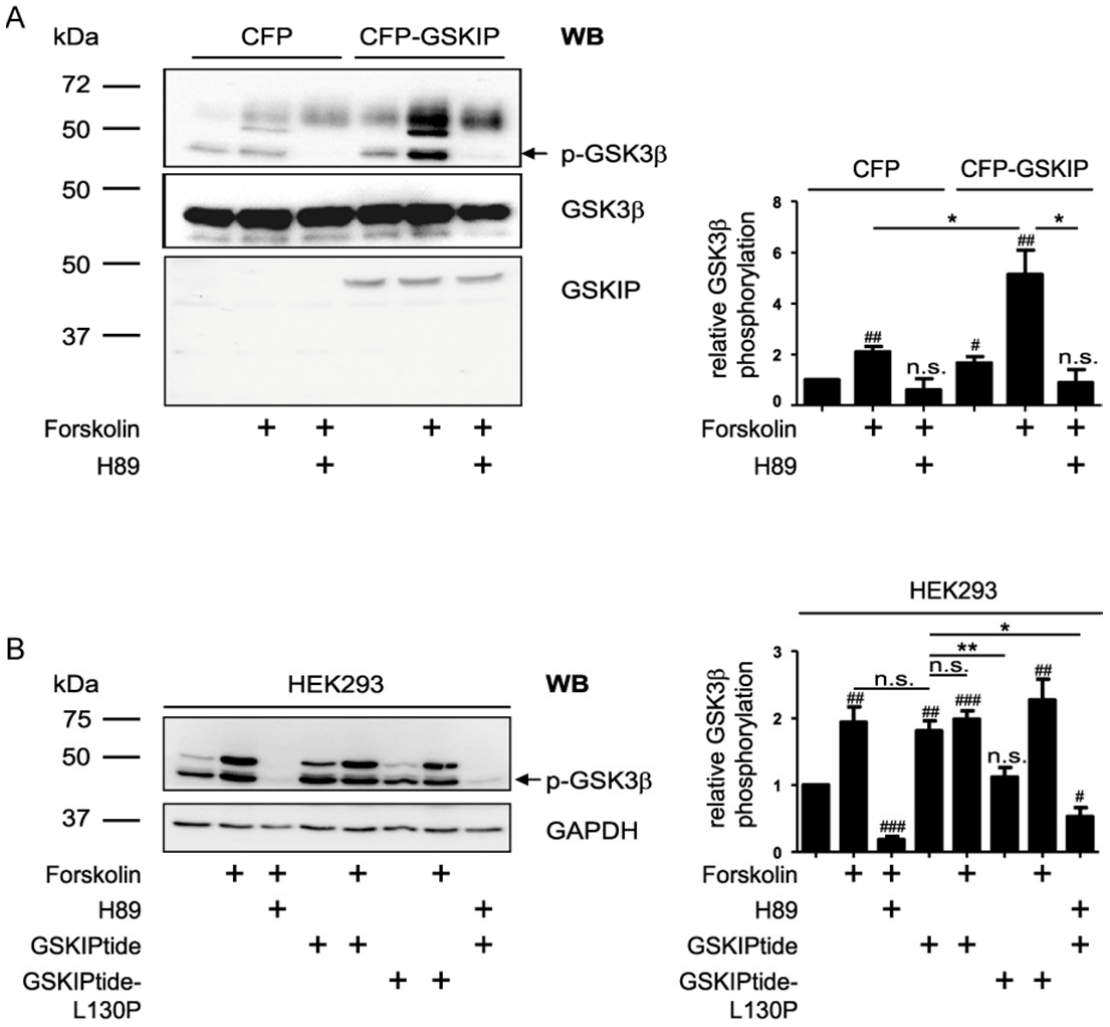

Fig. 21 GSKIP and GSKIPtide increase the phosphorylation of GSK3β on Ser9. A. HEK293 cells transiently expressing CFP or CFP-GSKIP were left untreated or incubated with forskolin (20 µM, 30 min) in the presence or absence of the PKA inhibitor H89 (30 µM, 30 min prior to forskolin treatment). Cells were lysed, and CFP-GSKIP, phospho-GSK3β and total GSK3β were detected by Western blotting. *Right panel*: Western Blot signals were analysed densitometrically and the ratio of p-GSK3β to GSK3β was calculated ($n \geq 5$ independent experiments for each experimental condition, mean ± S.E.). **B.** HEK293 cells were treated with forskolin or H89/forskolin as in A. and, in addition, with stearate-coupled GSKIPtide which disrupts the GSKIP-GSK3β interaction or with the inactive control peptide GSKIPtide-L130P (100 µM, 30 min). Lysed cells were subjected to Western blotting with detection of phospho-GSK3β and GAPDH (loading control). **A.** and **B.** Significantly different from untreated control: #, $p < 0.05$; ##, $p < 0.01$; ###, $p < 0.001$. Significant differences between groups connected by lines: *, $p < 0.05$; **, $p > 0.01$. n.s., not significant. This research was originally published in Hundsrucker *et al*. [58].

To determine whether the AKAP function of GSKIP is involved in this, non-transfected HEK293 cells were incubated with a peptide derived from the C-terminus of human GSKIP (aa 115-139), GSKIPtide [70], which is equivalent to the GID of GSKIP. GSKIPtide binds to GSK3β and it is likely to compete with GSKIP protein for GSK3β binding and thus displace GSK3β from GSKIP and associated PKA. In cells treated with GSKIPtide, the level of phospho-GSK3β was doubled in comparison to untreated cells and similar to forskolin-treated cells (Fig. 21B). The combination of GSKIPtide and forskolin did not increase GSK3β

phosphorylation further (Fig. 21B, lane 5). A preincubation with H89 prevented both forskolin- and GSKIPtide- induced GSK3β phosphorylation (Fig. 21B). The GSK3β-binding deficient GSKIPtide-L130P did not have any effect on the cells, both basal and forskolin-induced GSK3β phosphorylation were comparable to cells with no peptide treatment (Fig. 21B).

On the whole, both full-length GSKIP and the peptide GSKIPtide increase the PKA-dependent phosphorylation of GSK3β to a similar degree. When PKA is activated by forskolin, only GSKIP but not GSKIPtide facilitates a further increase in GSK3β phosphorylation. This suggests that, in a resting state, the interaction of GSKIP (or GSKIPtide) with GSK3β is sufficient to induce a basal phosphorylation of GSK3β. In contrast to GSKIPtide, GSKIP contains an RIIBD and is able to recruit PKA. This implies that the AKAP function of GSKIP is required for an increased GSK3β phosphorylation after PKA activation. Having established a functional connection between the protein-protein interactions of GSKIP, it was investigated whether these are conserved in orthologues of GSKIP.

3.7 The conservation of GSKIP and its protein-protein interactions

The major part of GSKIP, which is represented in DUF727, is evolutionarily conserved. Both known protein-protein interaction domains of GSKIP, the RIIBD and the GID, are part of DUF727. It was, therefore, tested whether the ability to interact with RIIα and GSK3β has also been conserved in DUF727 proteins from different invertebrate and vertebrate species. For this purpose, sequences of DUF727 proteins corresponding to the human GSKIP RIIBD and GID, respectively, were synthesised as peptide spots. Overlay techniques were employed to test the ability of these peptides to bind PKA RIIα and GSK3β, respectively.

3.7.1 The RII-binding domain of GSKIP is conserved in vertebrates

To probe for RII binding, peptide spots comprising the potential RIIBDs from DUF727 proteins were subjected to RII overlay assays. To verify a canonical AKAP-like binding to the D/D domain, RIIα subunits were preincubated with the PKA anchoring disruptor peptide AKAP18δ-L314E. The conservation of the amino acids in the RIIBD of vertebrate GSKIP orthologues is very high. The hydrophobic residues in the AKAP consensus sequence and the residues between them are identical, with the exception of the variant of human GSKIP (F46→S) which is based on an alternative cDNA sequence [174]. All tested peptides derived from vertebrate GSKIP orthologues showed RII binding in the RII overlay assay (Fig. 22,

upper panel). As expected for canonical AKAPs, this binding was blocked by preincubation of RIIα with AKAP18δ-L314E. A decreased binding was observed for spots 4, 6, 8, and 10. These deviate from human GSKIP in one to three positions in the C-terminus of the sequence (Fig. 22).

Spot	Species	Prot.-ID	Position	Sequence
1	*H. sapiens*	Q9POR6	(28-52)	TDMKDMRLEAEAVVNDVLFAVNNMF
2	*H. sapiens(var)*	Q9POR6	(28-52)	TDMKDMRLEAEAVVNDVLSAVNNMF
3	*R. norvegicus*	Q5PPI3	(28-52)	TDMKDMQLEAEAVVNDVLFAVNNMF
4	*B. taurus*	Q0P5A3	(74-98)	TDMKDMRLEAEAVVNDVLFAVNTMF
5	*C. familiaris*	XP_873500	(28-52)	ADMKDMKLEAEAVVNDVLFAVNNMF
6	*M. musculus*	Q3TBR1	(33-57)	ADMKDMQLEAEAVVNDVLFAVNHMF
7	*G. gallus*	Q5ZMC6	(28-52)	TDVKDMRLEAEAVVNDVLFAVSNMF
8	*T. nigroviridis*	Q4RLX4	(24-48)	GDMKDMRLEAEAVVNDVLFAVSQMH
9	*X. laevis*	Q6IRM4	(26-50)	TEGKDMSLEAEAIVNDVLFAVGNMF
10	*D. rerio*	Q7ZWI4	(23-47)	GEVKDMRLEAEAVVNDVLFAVSDMH

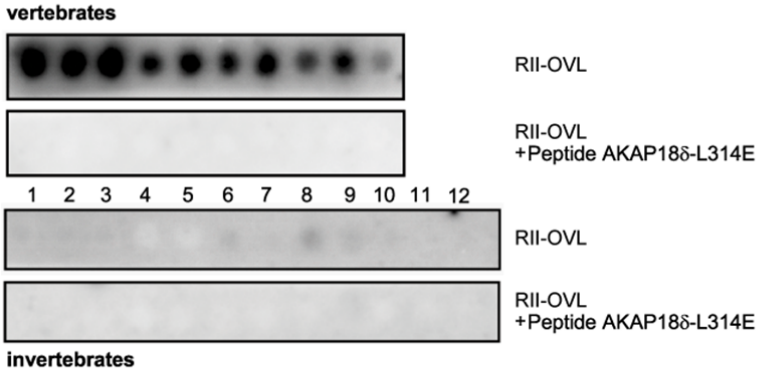

Spot	Species	Prot.-ID	Position	Sequence
1	*C. elegans*	Q9XWX6	(78-102)	GGESSLELEAIAAVHELSFAVQSIS
2	*C. elegans*	Q9XWX7	(151-175)	GGESSLELEAIAAVHELSFAVQSIS
3	*C. briggsae*	Q61TP3	(78-102)	GGESSLELEAIAAVHELSFAVSSIS
4	*C. elegans*	Q9XU41	(137-161)	DDVGPLELEAIAAVHELAHEVQDIS
5	*C. briggsae*	Q628G9	(135-159)	DDVGPLELEAIAAVHELAHEVEDIS
6	*C. briggsae*	Q620Y2	(36- 60)	AEKTGLEETAMAAVREHAFAVNLIG
7	*C. elegans*	Q22757	(37- 61)	VEKSTLEEEAMAAVRENAFAVNLIG
8	*D. melanogaster*	Q9VNV2	(13- 37)	EQAFNCEDEANAIINDVKAHVAEIC
9	*S. japonicum*	Q5DES9	(21- 45)	ENVKLCSVEAKAAIAEVGFGVKEIC
10	*A. gambiae*	Q7QL76	(14- 38)	ANIIDWAQEAESVIRDIAEHVKEAS
11	*A. gambiae*	Q5TRP4	(14- 38)	ANIIDWAQEAESVIRDIAEHVKEAS
12	*D. melanogaster*	Q9V8F3	(8- 32)	ENDFHALREAQRMVDSCQDFADHLI

Fig. 22 The RIIBD of GSKIP is conserved among vertebrates. Peptides corresponding to the RIIBD of human GSKIP from the indicated species were synthesised as peptide spots and subjected to RII overlay (RII-OVL) in the absence or presence of the PKA anchoring disruptor peptide AKAP18δ-L314E (10 µM). Signals were detected by autoradiography. The result is representative for three independent experiments. Amino acids matching the AKAP consensus sequence (1.1.2) are highlighted in grey. This research was originally published in Hundsrucker *et al*. [58].

In contrast, for none of the investigated invertebrate orthologues, a clear binding of RIIα was observed Fig. 22, lower panel). Only four of the invertebrate peptides fully comply with the consensus sequence (# 4, 5, 10, 11) and these also have pI values in the range of typical

RIIBDs and are predicted to form α-helices. Nonetheless, no RII binding was observed with these peptides for unknown reasons.

In summary, the data suggest that the highly conserved vertebrate orthologues of GSKIP are AKAPs whereas invertebrate orthologues are not. This experiment was performed at an early stage of this thesis when the DUF727 only comprised the proteins shown in Fig. 22. Out of 62 invertebrate DUF727 proteins which were not tested for RII binding here, only two (*Nematostella vectensis* A7SRB6/ *Culex quinquefasciatus* B0XA92) contain an AKAP consensus sequence. Thus, it is not likely that an AKAP function is a general feature of invertebrate DUF727 proteins.

3.7.2 The interaction of GSKIP with GSK3β is conserved from fungi to man

Besides the RIIBD, DUF727 also spans the C-terminus of human GSKIP, which harbours the GID (1.3). Therefore, it was tested whether orthologues of GKSIP are potential interaction partners of GSK3β. The interaction of human GSKIP with GSK3β has been discovered in previous studies [70;105] and confirmed in this thesis (3.1 and 3.5). In addition, one DUF727 protein from *C. elegans* (Q22757) was found to interact with *C. elegans* GSK3 (UniProt ID: Q9U2Q9) in a yeast two-hybrid screen approach to map the interactome of *C. elegans* [175]. This raises the question whether GSK3 binding is a conserved feature of DUF727 proteins. To investigate this, peptide spots derived from DUF727 proteins, corresponding to the GID of human GSKIP, were incubated with purified human GST-GSK3β protein. As positive controls, peptides derived from the GIDs of human axin-1 and -2 were included. Protein binding was detected with an anti-GST antibody. To exclude binding of the GST tag to the peptide spots, recombinant GST was used as a negative control. Here, more peptides were analysed than in the RII overlay (3.7.1) because these experiments were carried out at a later point at which the DUF727 comprised more proteins.

All 13 vertebrate peptides (11 GSKIP orthologues plus human axin-1 and-2) bound GSK3β (Fig. 23, upper right panel). When the leucine corresponding to Leu130 in human GSKIP was substituted to proline, binding was abolished completely, underlining the importance of a helical structure for the interaction with GSK3β. This is in accordance with previous studies showing that a mutation of this position in axin or human GSKIP abrogates the interaction with GSK3β [70;105;176;177].

The sequences of 38 invertebrate DUF727 proteins were also analysed. One of them did not share any homology with the GID of human GSKIP (*C. briggsae* A8WMZ1). Nine did have homologous sequences but did not contain the hydrophobic amino acids necessary for the

interaction with GSK3β (F-X-X-X-L-X-X-X-L), which explains why these sequences did not bind GSK3β in the spot-overlay assay (Fig. 23, spots 42-50). The remaining 28 proteins with homologous sequences contained the GSK3β-binding FLL-motif and 27 of the 28 derived peptides displayed GSK3β binding as did both peptides derived from fungal DUF727 proteins (Fig. 23, lower right panel). In summary, 50 peptides derived from 10 vertebrate, 21 invertebrate and 2 fungal species were assayed for GSK3β binding. For each of these species, with the single exception of *Culex quinquefasciatus* (Southern house mosquito), at least one GSK3β-binding peptide was identified.

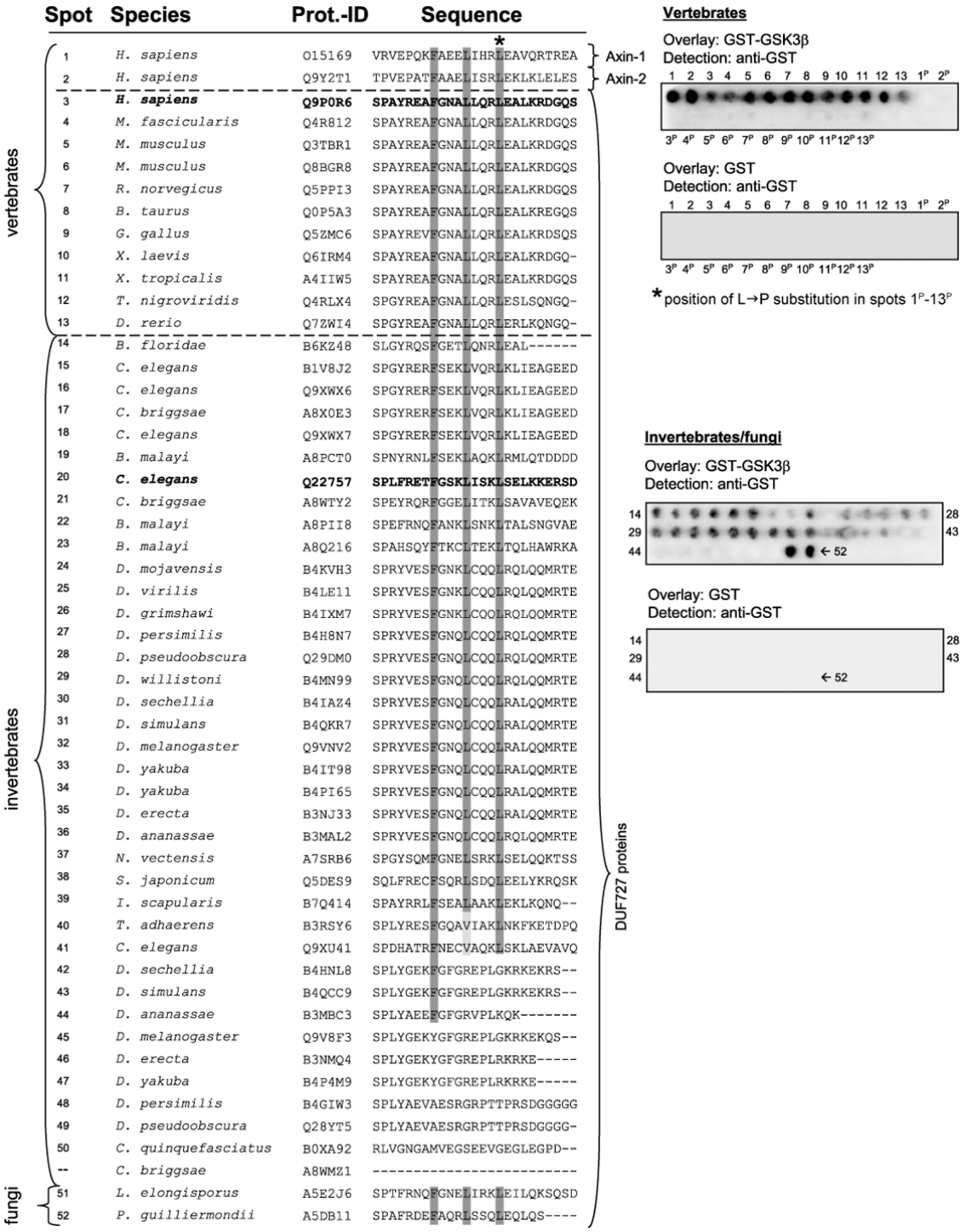

Fig. 23 The GSK3β-interaction domain of GSKIP is conserved throughout evolution. Peptides corresponding to the GSK3β interaction domain (GID) of human GSKIP derived from the indicated DUF727 proteins were synthesised as peptide spots and incubated with GST-GSK3β or GST as a negative control. Protein binding to the spots was determined with an primary anti-GST and a secondary HRP-labelled antibody, followed by an ECL reaction. The asterisk indicates the position of the L→P substitution in spots 1^P-13^P. The amino acids essential for GSK3β binding are highlighted in dark grey (identical to axin-1) or light grey (similar to axin-1). Human GSKIP and *C. elegans* Q22757 for which an interaction with GSK3β had been demonstrated before are shown in bold [70;106;175]. This research was originally published in Hundsrucker *et al*. [58].

As an example for an invertebrate DUF727 protein, the entire sequence of *Drosophila* Q9VNV2 was synthesised as overlapping peptide spots and tested for binding of GSK3β in the presence of GSKIPtide or its GSK3β-binding deficient variant GSKIPtide-L130P. The aim of this experiment was to confirm that the Q9VNV2-derived peptide with a sequence homologous to the GID of human GSKIP actually represents the part of the Q9VNV2 protein with the highest affinity for GSK3β. In addition, the binding site for GSKIP on the GSK3β probe was blocked with the peptide GSKIPtide to find out whether the Q9VNV2-derived peptides bind to the same site on GSK3β.

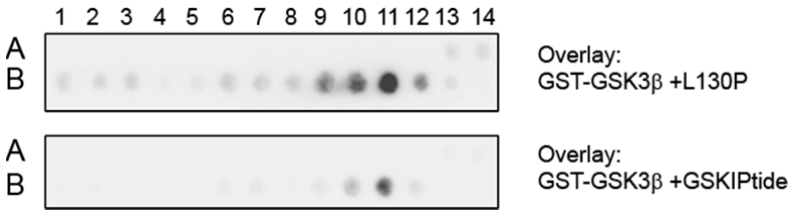

Fig. 24 Confirmation of the GSK3β-binding site of *Drosophila melanogaster* Q9VNV2. The entire sequence of the DUF727 protein Q9VNV2 was synthesised as overlapping peptide spots. These were incubated with GST-GSK3β preincubated with the peptide GSKIPtide (10 µM) or its GSK3-binding deficient variant GSKIPtide-L130P as indicated. Protein binding to the spots was determined with an anti-GST antibody and a secondary HRP-labelled antibody, followed by an ECL reaction. The consecutive spots with the highest signal (B9-B11) contain the previously identified GID (B10 = spot 32 in Fig. 23). Binding of GSK3β to the spots was decreased by GSKIPtide. Peptide sequences are shown in Appendix B.

High signal intensity, indicating a binding of GSK3β, was observed for one region of Q9VNV2, represented by the peptides B9-B11 (Fig. 24, upper panel). Notably, these were the only spots which contain the FLL motif. Spot B10 is identical to spot 32 from the previous experiment (Fig. 23). The binding of GSK3β was clearly reduced when it was preincubated with GSKIPtide (Fig. 24, lower panel). These results suggest that the previously identified sequence, which is homologous to the GID of human GSKIP, is the region with the highest affinity for GSK3β within Q9VNV2 and that it binds to the same site on GSK3β as the binding is inhibited by GSKIPtide.

3.8 Characterisation of further protein interactions of GSK3β

3.8.1 AKAP220 interacts with GSK3β in an axin- and GSKIP-like fashion

The existence of different GSK3β-interacting AKAPs (AKAP220, MAP2 and GSKIP) raises the question whether their modes of binding to GSK3β are similar and thus mutually exclusive or whether the individual AKAPs employ different sequences that bind distinct regions of GSK3β, thereby allowing simultaneous interaction of different AKAPs with one molecule of GSK3β. Furthermore, the binding of axin to GSK3β is homologous to the

binding mode of GSKIP (Fig. 23). Therefore, the interaction of a protein with GSK3β in a GSKIP-like fashion would exclude simultaneous binding of axin to GSK3β.

The region of AKAP220 necessary for the interaction with GSK3β has roughly been mapped to amino acids 1017-1316 of human AKAP220 [57]. Therefore, peptides covering amino acids 1017-1316 of human AKAP220 (25mers, shift 5) were spot-synthesised to determine the involved amino acids (Fig. 25). The incubation with GST-GSK3β and the negative control GST as well as the preincubation with GSKIPtide were performed as above (Fig. 24).

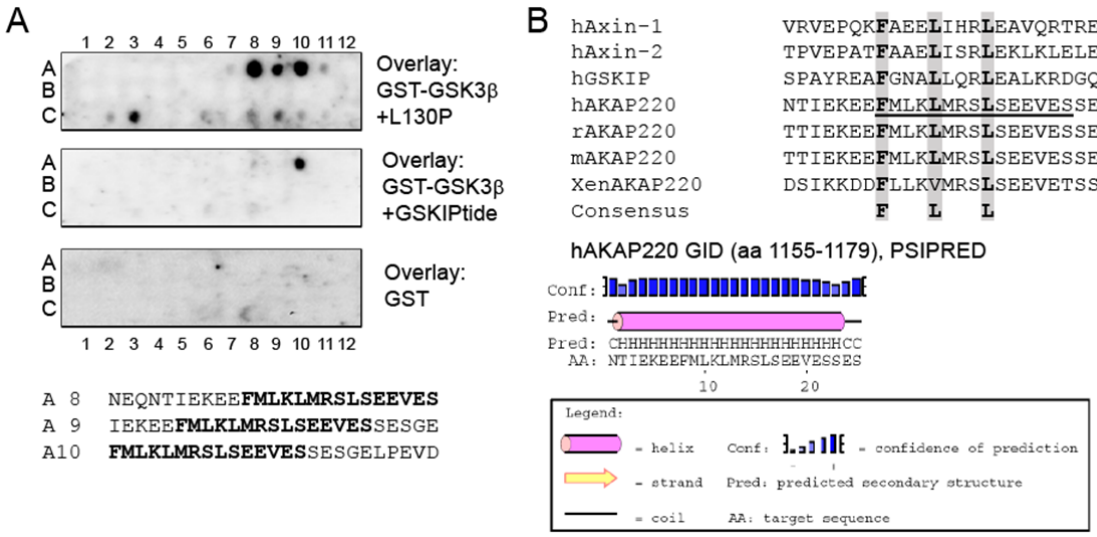

Fig. 25 Mapping the GSK3β-binding domain of AKAP220. A. *Upper panel:* The part of human AKAP220 (aa 1017-1316) that was previously shown to bind GSK3β directly [57] was synthesised as overlapping peptide spots. Incubation with proteins and detection was carried out as above (Fig. 24). Strong binding of GSK3β to spots A8-A10 (aa 1152-1186) was observed. This binding was drastically reduced in the presence of GSKIPtide. No binding of GST (negative control) to any of the spots was observed. *Lower panel:* The sequence of spots A8-A10 is shown with the amino acids, the amino acids common to these spots (1162-1176) are indicated in bold. **B.** *Upper panel:* Alignment of the GSK3-interaction domains of axin-1, -2 and GSKIP with corresponding sequences of AKAP220 orthologues (human, rat, mouse, *Xenopus*). The sequence found in spots A8-A10 (underlined) contains the conserved hydrophobic residues of the GIDs of axin and GSKIP (bold, highlighted in grey). These are also conserved in the orthologues of AKAP220, with the exception of a Val instead of a Leu in the central hydrophobic position of *Xenopus* AKAP220. *Lower panel:* Secondary structure prediction of the presumptive GID of human AKAP220 using PSIPRED [178] shows a high probability to form an α-helix.

When the experiment was carried out with the inactive peptide GSKIPtide-L130P, several consecutive peptides in the examined part of AKAP220 bound GSK3β protein (Fig. 25A, spots A7-A11, aa 1147-1191). The sequence that is common to the three spots with the highest intensity in this region (A8-A10) is **F**MLK**L**MRS**L**SEEVES, containing the motif (**F**-X-X-X-**L**-X-X-X-**L**) found in the GIDs of axin and GSKIP. This motif is predicted to form an α-helix (Fig. 25B). In the presence of GSKIPtide, the binding of GSK3β to these spots was drastically reduced (Fig. 25A, middle panel), indicating that GSKIP/GSKIPtide and AKAP220 bind to the same region on GSK3β. In the negative control (overlay with GST, Fig.

25A, lower panel), no signal was detected. This suggests that neither the GST tag nor the antibodies bound to the peptide spots unspecifically.

In summary, the part of AKAP220 which binds GSK3β could be narrowed down to amino acids 1155-1179. This sequence features an FLL motif, an α-helical structure, and competition with GSKIPtide for GSK3β binding. These are the known characteristics of an axin- and GSKIP-like GID. Thus it is very likely that axin, GSKIP and AKAP220 bind to the same site on GSK3β and thereby control distinct pools of GSK3β. In addition to GSKIP and AKAP220, MAP2D is the third AKAP known to bind GSK3β [54]. The next experiment was carried out in order to characterise the interaction of MAP2D and GSK3β.

3.8.2 The MAP2D-GSK3β interaction

Microtubule-associated protein 2 (MAP2) is a protein that binds microtubules and controls microtubule dynamics. MAP2 is regulated through phosphorylation by multiple kinases including PKA and GSK3β [179]. There are three human (MAP2A-C) and four rat (MAP2A-D) splice variants of MAP2 [180]. All MAP2 isoforms are AKAPs [181;182] and MAP2D also interacts with GSK3β [54]. Because molecular details of the interaction between MAP2D and GSK3β were not known, the entire sequence of rat MAP2D was synthesised as overlapping peptide spots. These were incubated with GST-GSK3β in the presence of the peptides GSKIPtide or GSKIPtide-L130P or with GST as a negative control (Fig. 26).

In the presence of the GSK3-binding deficient control peptide GSKIPtide-L130P, several spots bound GSK3β (Fig. 26, upper left panel). The strongest signal was detected for spot J6, which represents the 25 C-terminal amino acids of MAP2D. The signal intensity of this spot was drastically reduced when the GSK3β probe was preincubated with GSKIPtide (Fig. 26, upper middle panel). For spot J5, no binding was detected. J5 lacks the 3 C-terminal amino acids of MAP2D “QGL”. The negative control (GST) did not bind to any of the MAP2D spots (Fig. 26, upper right panel).

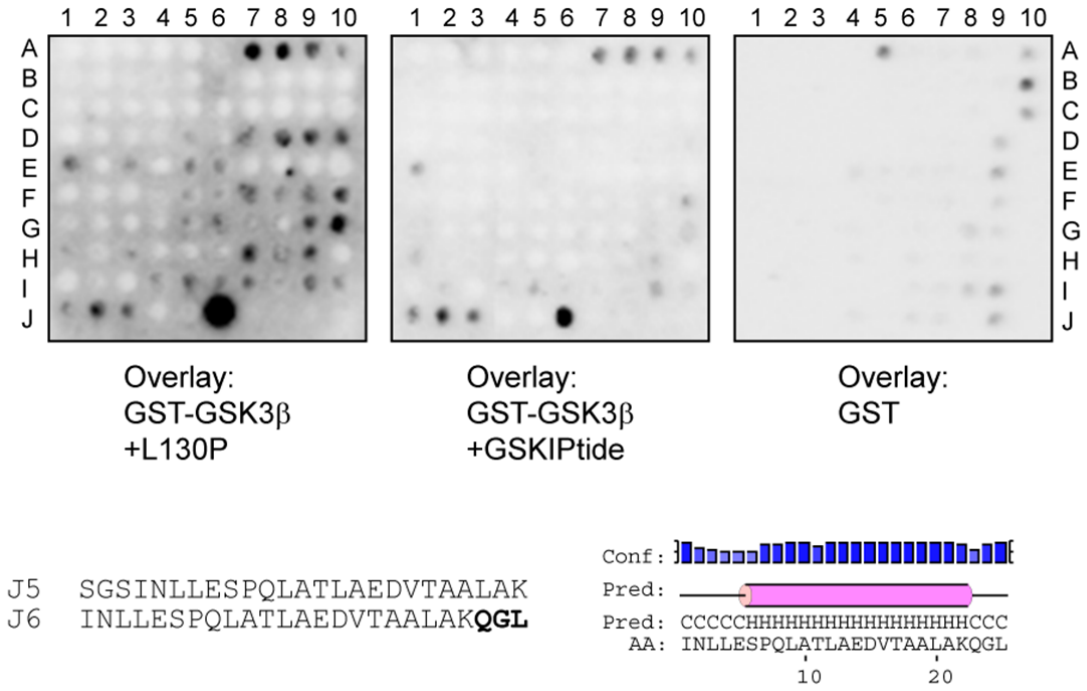

Fig. 26 Mapping the GSK3β-binding domain of MAP2D. *Upper panel*: The entire sequence of rat MAP2D which was previously shown to interact with GSK3β [54] was synthesised as overlapping peptide spots. Incubation with proteins/peptides and detection were carried out as above (Fig. 24). GSK3β bound strongly to spot J6. This binding was reduced in the presence of GSKIPtide. No clear binding of GST (negative control) to any of the spots was observed. *Lower panel*: The amino acid sequence of spots J5 and J6 is shown; amino acids not present in J5 indicated in bold. Secondary structure prediction of the presumptive GID of rat MAP2D (spot J6) using PSIPRED [178] shows a high probability to form an α-helix. The legend for the PSIPRED image is shown in Fig. 25.

This experiment suggests that the C-terminus of MAP2D is involved in an interaction with GSK3β. It is predicted to adopt a helical structure (Fig. 26, lower panel) but it does not share any sequence similarity with the GIDs of GSKIP, axin and AKAP220. Nevertheless, the binding of GSK3β to this sequence is inhibited by GSKIPtide, implying that MAP2D might bind to the same site on GSK3β as GSKIP, axin and AKAP220. Peptide spot overlay experiments helped to understand the interactions of AKAP220 and MAP2D with GSK3β. Thus they were also applied to a potential interaction partner of GSK3β, namely SMYD2.

3.8.3 SMYD2 – A potential interaction partner of GSK3β and GSKIP

The high throughput screen in which the interaction between GSKIP and GSK3β was found independently of the results by Chou *et al.* also yielded an interaction of GSK3β with SMYD2 (SET and MYND domain-containing protein 2) [106]. SMYD2 was identified as a prey protein in an IP of GSK3β and vice versa. It is noteworthy that interactions of SMYD2 with GSKIP, axin-1 and AKAP220 were also identified in this study. These three interaction partners of GSK3β, namely GSKIP, axin-1 and AKAP220 were identified as prey proteins in

IPs of SMYD2 (bait). There are different explanations for these results: (A) SMYD2 could interact directly with GSK3β as well as with GSKIP, axin-1 and AKAP220, (B) SMYD2 could interact with GSK3β directly and GSKIP, axin-1 and AKAP220 were co-precipitated due to their ability to bind GSK3β, (C) SMYD2 could interact with GSKIP, axin-1 and AKAP220 directly, causing co-precipitation of GSK3β.

A potential direct interaction of SMYD2 with GSK3β was investigated using a GSK3β overlay over SMYD2 peptide spots (25mers, shift 5). The GSK3β probe was preincubated with GSKIPtide or GSKIPtide-L130P to determine whether the peptides derived from SMYD2 would bind to the same site on GSK3β as GSKIP/GSKIPtide.

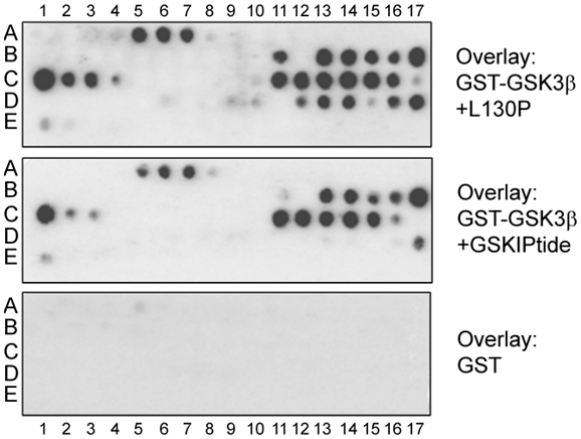

Fig. 27 Mapping the GSK3β-binding domain of SMYD2. The entire sequence of human SMYD2 was synthesised as overlapping peptide spots. Binding of GST-GSK3β to the spots was assayed as above (Fig. 24). Binding of GSK3β was shown for several spots; the ones with the highest signal intensity were B17-C1 and C11-C15. Only for spots D12-A17, GSKIPtide caused a clear signal reduction. No binding of GST (negative control) to any of the spots was observed.

Several SMYD2 peptide spots exhibited binding of GSK3β (Fig. 27, upper panel). The highest signal intensity was obtained for the spots B17 and C1, the sequence that is common to these spots is "SLVVLFAQVNSNGFTIEDEE". A second potential binding region spans the spots C11 to C15. These spots share the sequence "IDLLY". The binding of GSK3β to both groups (B17-C1, C11-15) is not affected by GSKIPtide (Fig. 27, middle panel), indicating that SMYD2 could bind to a site on GSK3β that is different from the one axin-1 and GSKIP bind to. In addition to the abovementioned sequences, weaker binding of GSK3β was observed for spots A5-A8, B11, B13-B16 and D12-D17. The signals of the latter spots were clearly inhibited in the presence of GSKIPtide, implying a "GSKIP-like" binding to GSK3β. However, a relevance of this sequence (D12-17) for the binding of GSK3β is unlikely because of the relatively low signal intensity. In the negative control using GST as a

probe, no signal was detected (Fig. 27, lower panel). Hence unspecific binding of the GST tag or the antibodies to any of the spots could be excluded.

3.9 GSKIP expression is downregulated in glioma

Since there were no indications for a pathway- or cell type-specific function of GSKIP, gene expression databases were searched for data on GSKIP with the goal of gaining insight into its physiological or pathophysiological function.

The Oncomine database contains microarray data on gene expression in cancer [183]. Oncomine version 4.3 was screened for altered expression of GSKIP in cancer vs. normal tissue. The threshold was set to a minimum 1.5 fold change in expression with a minimum P value of 0.01 and the prerequisite that GSKIP belongs to the top 5% of differentially expressed genes. For an over-expression of GSKIP in cancer, no datasets were identified that meet these criteria. On the other hand, 8 data pairs comparing normal and cancer tissue from 4 different datasets showed a decreased expression of GSKIP in cancer complying with the abovementioned settings. Fig. 28 shows the types of cancer samples in which GSKIP was downregulated [184-187].

GSKIP was found to be among the top 5% downregulated genes in 8 out of 102 analyses. 6 out of these 8 were classified gliomas. Gliomas arise from glial cells and are named according to a cell type they resemble histologically (e.g. astrocytoma, oligodendroglioma). In addition, GSKIP downregulation was shown in 2 adenocarcinomas of the colon and the pancreatic duct, respectively. When less stringent threshold values were set (top 10% downregulated genes), GSKIP downregulation was even observed in 9 out of 18 glioma analyses (data not shown). With the aim of gaining insight into its physiological and pathophysiological functions, a GSKIP knockout mouse model was developed.

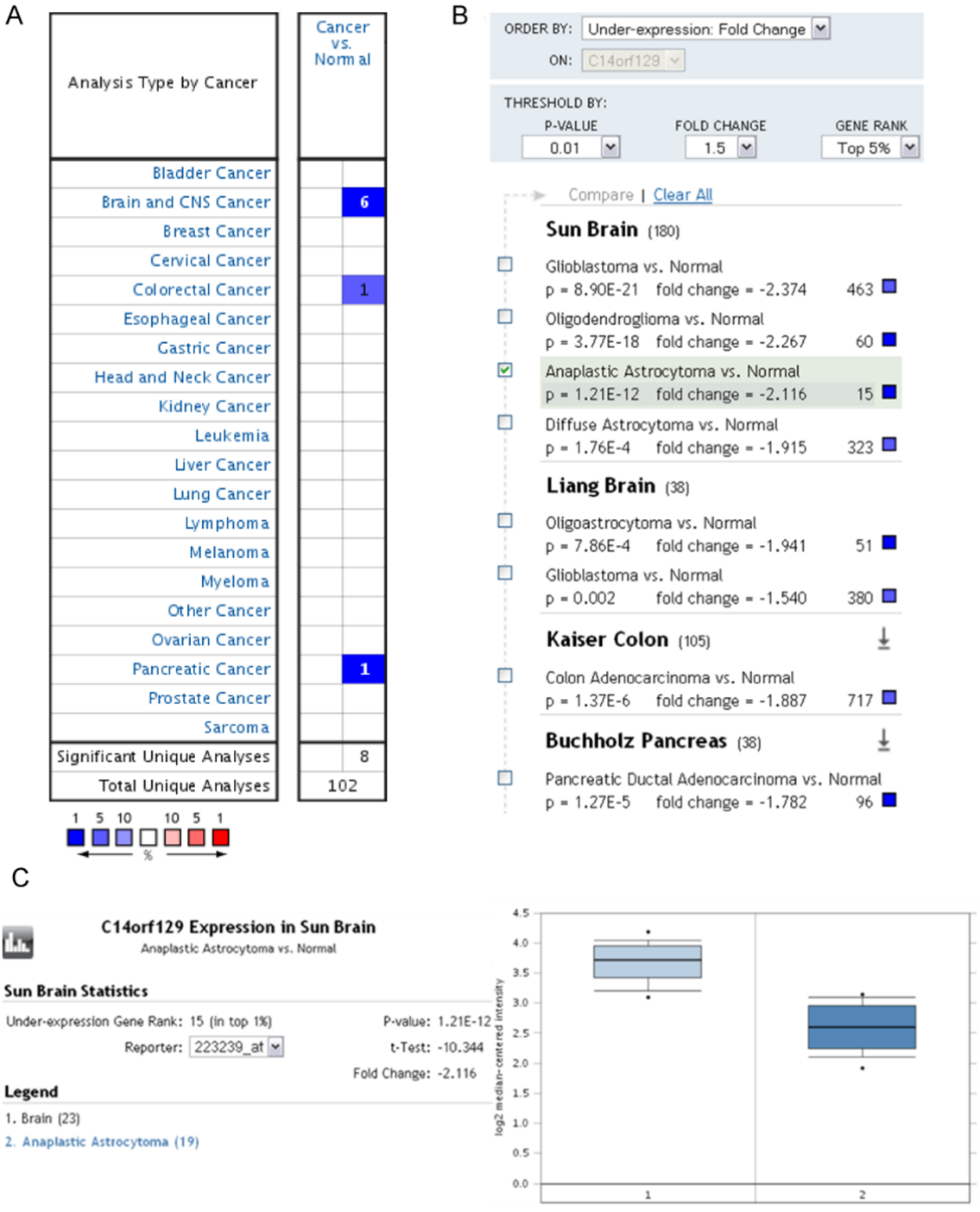

Fig. 28 Reduced expression of GSKIP (C14orf129) in various cancers. A. The Oncomine database was searched for cancer samples with altered expression of GSKIP. The cell colour is determined by the best gene rank percentile for the analyses within the cell. The colour code (bottom) indicates whether GSKIP belongs to the top 1%, 5% or 10% of up- (red) or downregulated (blue) genes. No cancer samples over-expressing GSKIP were found. 8 analyses in which GSKIP was found to be downregulated are shown in B. **B.** The threshold values are stated at the top. The analyses from different data sets (bold, total sample numbers in parentheses) are given with the respective p values, fold changes and gene rank (left of blue boxes). **C.** As an example, the data for normal brain (1) vs. anaplastic astrocytoma (2) are depicted. All panels are original outputs from www.oncomine.org [183] using datasets from [184-187].

3.10 The GSKIP knockout mouse model

The high degree of evolutionary conservation and the ubiquitous expression pattern point to an important physiological role of GSKIP. Here, it was demonstrated that the AKAP function of GSKIP facilitates the phosphorylation of GSK3β by PKA. But so far, this result could not be brought into a physiological context. For the exploration of GSKIP's function *in vivo*, a conditional gene targeting approach was chosen in order to deplete GSKIP in a mouse model.

3.10.1 Structure of the GSKIP gene

The gene encoding human GSKIP (HGNC symbol: C14orf129) is located on chromosome 14, region q32.2. The transcript spans 24 kb and consists of 4 exons. Exons 1 and 2 are non-coding, exon 3 and 4 are coding. No splice variants for human GSKIP have been reported. The major part of the human chromosome 14q arm has homology with mouse chromosome 12 [114]. In line, the mouse GSKIP gene (HGNC symbol: 4933433P14Rik) is located on chromosome 12, region E. The transcript spans 18 kb and contains 3 exons. In the GSKIP gene, there are two alternative start codons, suggesting that two isoforms of GSKIP (with 139 and 144 amino acids, respectively) could be translated (Fig. 29). The 139 amino acid-isoform is considered the canonical isoform because for other species (*Homo sapiens*, *Rattus norvegicus*, *Bos taurus*, *Gallus gallus*, *Xenopus laevis*) only this isoform has been described [188]. For the existence of the potential 144 amino acid-isoform, there is no experimental evidence but it cannot be excluded that such an isoform of GSKIP exists in mice. Therefore, it had to be taken into consideration for the GSKIP targeting strategy.

3.10.2 GSKIP gene targeting strategy

When applying a conditional gene targeting strategy based on the Cre/loxP system, an essential coding exon of the gene of interest is selected to be flanked by loxP sites to allow the Cre-mediated removal of this exon [189]. Two important prerequisites for the selection of the targeted exon were that the introduction of the loxP sites must not affect the GSKIP transcript and that removal of the floxed sequence must result in non-functional mRNA.

The start codon for the canonical GSKIP isoform is located in exon 2. Therefore, a targeting of exon 1 was excluded because the resulting mRNA would still include the entire coding sequence for GSKIP. A deletion of exon 3 would result in a truncated mRNA that misses the codons for the 53 C-terminal amino acids of GSKIP. The corresponding protein might retain some of its biological functions such as PKA anchoring. Consequently, only exon 2 is suitable for gene targeting. The theoretical effects of a deletion of exon 2 on the mRNA sequence

(shown as cDNA) and the resulting GSKIP protein are shown in Fig. 29. After deletion of exon 2, no functional GSKIP is expected to be synthesised. For the shorter canonical isoform, the loss of the start codon prevents protein synthesis. For the potential longer isoform, which employs the alternative start codon located in exon 1, the five N-terminal amino acids are encoded correctly. But the loss of exon 2 causes a frameshift and in this case the amino acids encoded by exon 3 do not correspond to wild-type GSKIP or any other mouse protein. Therefore, it can be assumed that the deletion of exon 2 completely abolishes the biological function of GSKIP.

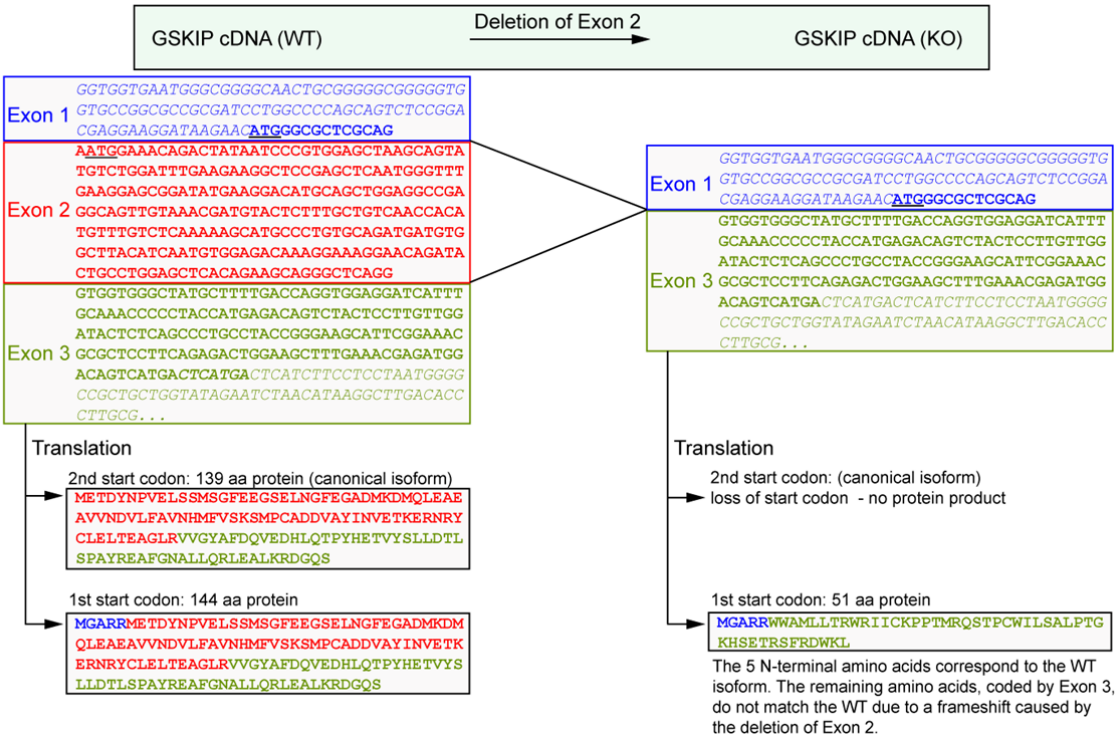

Fig. 29 Anticipated effects of the deletion of exon 2 on the sequence of GSKIP. *Left side*: The cDNA sequence of wild-type (WT) GSKIP encoded by exons 1 (blue), 2 (red) and 3 (green) is shown. Coding nucleotides are indicated in bold. The two possible start codons are underlined. On the bottom, the corresponding amino acids of the GSKIP protein are labelled according to the coding exons. *Right side*: The cDNA and GSKIP protein after deletion of exon 2. For the canonical isoform, the loss of the start codon would result in no protein product. Due to its start codon located in exon 1, the longer isoform would retain the 5 N-terminal amino acids encoded by exon 1 but the deletion of exon 2 causes a frameshift and an amino acid sequence which resembles no wild-type mouse protein.

In consequence, the central aspect of the targeting strategy was floxing exon 2 of the GSKIP gene. The neomycin resistance cassette required for the selection of recombinant embryonic stem (ES) cells was flanked by FRT sites (flrted) and integrated downstream of the floxed sequence. The targeting vector comprised two homology regions, both approximately 3.5 kb long, surrounding the neo cassette (Fig. 30). These regions which are homologous to the wild-type GSKIP locus were required for site-specific recombination, i.e. integration of the

targeting vector into the genome of ES cells. All parts of the targeting vector located outside the homology regions were not supposed to be integrated into the GSKIP allele. In order to eliminate ES cell which had undergone non-homologous recombination, an HSV-tk cassette was located in the targeting vector downstream of the 3' homology region. The HSV-tk cassette confers sensitivity to ganciclovir which was used for the negative selection of ES cells. For the identification of targeted ES cells, genomic DNA was screened by Southern blotting. Homologous recombination can only be verified using an external probe binding within the targeted gene but outside the homology regions [189]. For this, an XhoI/BamHI fragment from GSKIP genomic DNA was used as a template for a 3' Southern Blot probe (Fig. 30).

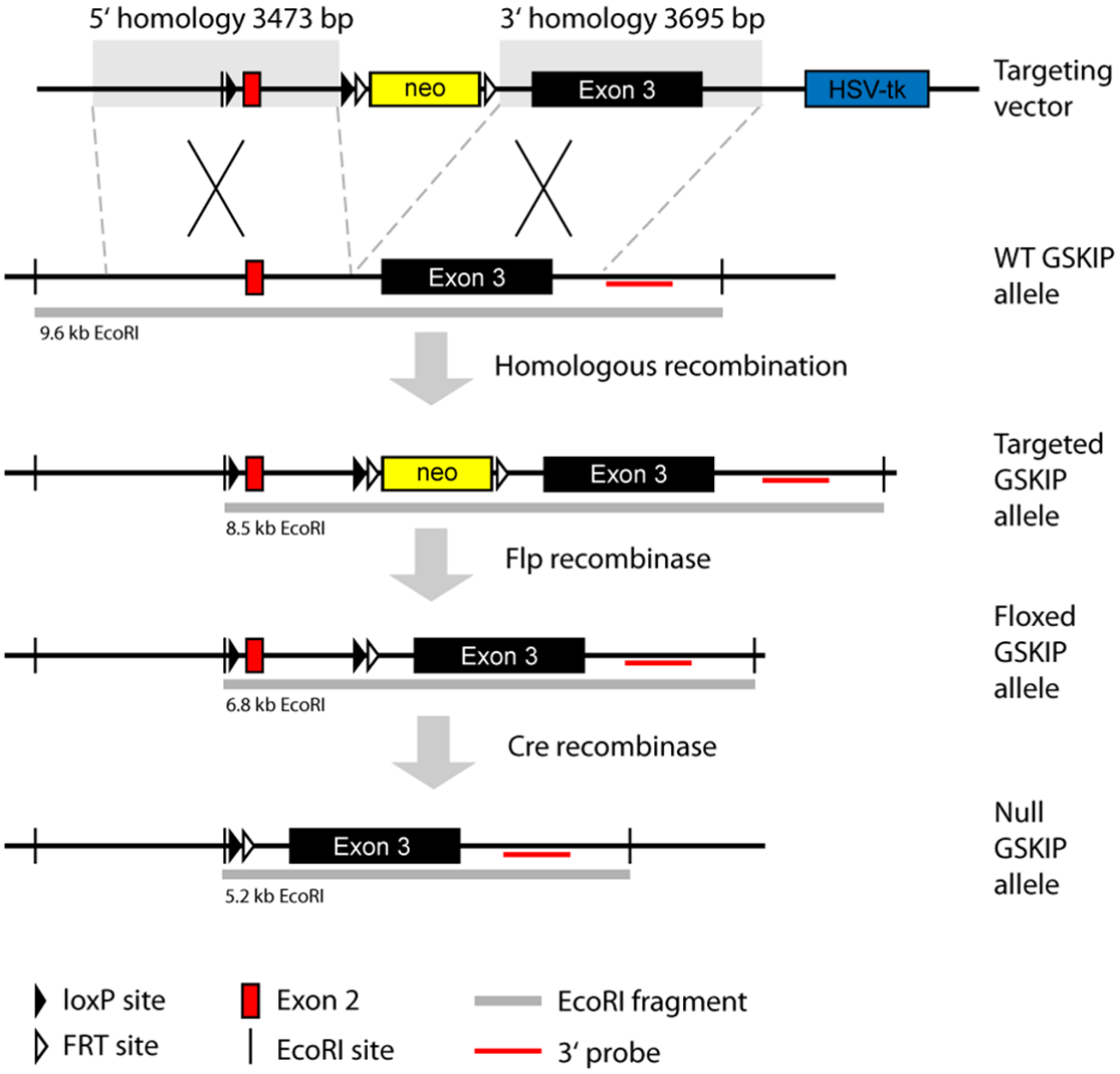

Fig. 30 Targeting strategy for the conditional knockout of GSKIP. After homologous recombination with the targeting vector, exon 2 (red box) of the GSKIP gene was replaced with a floxed exon 2 and a flrted neomycin resistance cassette (neo) was introduced between exons 2 and 3. Mice carrying a targeted GSKIP allele were bred to FLP recombinase-expressing mice to remove the neo cassette. The deletion of exon 2 was subsequently achieved by mating floxed mice with a Cre recombinase expressing strain. The position of the 3' probe (XhoI/BamHI fragment) is indicated.

In the following sections, the single steps towards a knockout of GSKIP in mice are described in detail.

3.10.3 Isolation of GSKIP genomic DNA

A PAC library of the mouse strain 129S6/SvEvTac (RPCI-21) [138] was screened for GSKIP genomic DNA. Rat GSKIP cDNA was used as a template to generate a hybridisation probe with the Rediprime labeling kit (2.2.3.1). Hybridisation of the PAC library with the GSKIP probe yielded two PAC clones (RPCIP711D02345Q3 and RPCIP711L13558Q6) containing GSKIP genomic DNA. Stab cultures of the PAC clones were ordered from the RZPD (Deutsches Ressourcenzentrum für Genomforschung GmbH). Single colonies of these clones were streaked on kanamycin agar plates, transferred to nylon membranes and the insert was verified by hybridisation with the rat GSKIP probe. A hybridisation signal was observed for both clones (Fig. 31A). Clone D02345Q3 was amplified in LB medium and the PAC DNA was isolated using a QIAGEN large construct kit. Since the clones of the PAC library have an average insert size of 137 kb, the PAC DNA was subcloned to allow better handling (shotgun cloning). For this, PAC DNA was digested with EcoRI and ligated with the vector pZero^{TM}-2 (Fig. 31B). After electroporation into *E. coli* Top10 and plating on Kanamycin agar, subclones were screened by colony hybridisation with the rat GSKIP probe. 5 out of 135 clones (# 32, 63, 75, 98, 123) hybridised with the probe (Fig. 31C). These clones were propagated in LB medium supplemented with kanamycin. Their plasmid DNA was amplified and isolated by Mini Prep (2.2.1.1) and thereafter digested with EcoRI. All clones contained a fragment corresponding to the vector pZero^{TM}-2 (3.3 kb). In clones 32, 63, 75 and 98 but not in 123 a 9.6 kb EcoRI fragment was detected. These clones were sequenced using SP6 and T7 sequencing primers, revealing that the 9.6 kb insert contained the coding region of the GSKIP gene. The DNA isolated from clone 75 (pZero^{TM}-2-GSKIP) was used as a template for the generation of the GSKIP target vector.

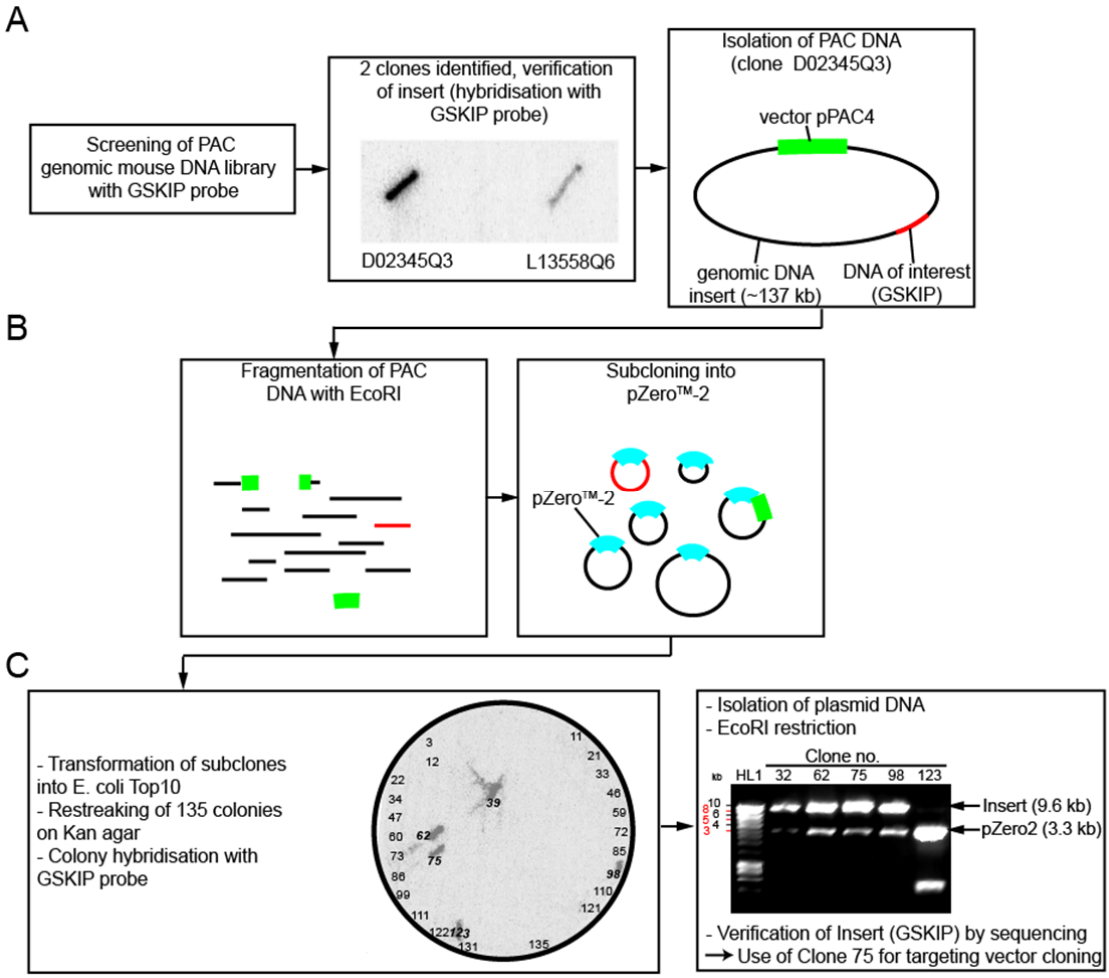

Fig. 31 Workflow for the identification and isolation of GSKIP genomic DNA. See text for details**. A.** Identification and isolation of PAC DNA. **B.** Subcloning (shotgun cloning) of PAC DNA. **C.** Identification of subclones containing a GSKIP genomic insert. Circle: Hybridisation membrane containing 135 clones (the first and last clone within each row is indicated). Clones hybridising with the GSKIP probe are shown in bold (39, 62, 75, 98, 123). HL1, Hyperladder I.

3.10.4 Targeting vector design and cloning

As mentioned above, a targeting vector was designed in which exon 2 of the GSKIP gene is floxed. As starting material, the genomic DNA of PAC subclone 75 (pZero™-2-GSKIP, 3.10.2) was used. The vector pPNT-FRT3 was used as the backbone for cloning the targeting vector. It contains a single loxP site upstream of a flrted neo cassette which is followed by an HSV-tk cassette (Fig. 30). A KpnI restriction fragment comprising exon 2 and the surrounding sequence was used as 5' homology region (Fig. 32). As 3' homology region, a KpnI/XhoI fragment comprising exon 3 was utilised.

The 5' loxP site was inserted into the 5' homology region upstream of exon 2 by oligonucleotide cloning. The complementary oligonucleotides CN129-AclI-Fw and CN129-AclI-Rev were annealed (see Appendix A for sequences) and digested with AclI. The plasmid pZero™-2-GSKIP was opened with AclI and the oligonucleotide was ligated into the AclI site

of the 5‘ homology region (Fig. 32). This introduced the 5’ loxP site and an EcoRI restriction site in the 5’ homology region which allowed the identification of successful integration of the oligonucleotide. In addition, the artificial EcoRI site was helpful for the detection of recombinant ES cells by Southern blotting (Fig. 30 and Fig. 34). The 5’ homology region was excised via KpnI restriction and ligated into the single KpnI site of pPNT-FRT3 which is located directly upstream of the 3’ loxP site. This cloning step integrated the 5’ homology region into the targeting vector and resulted in a floxed exon 2.

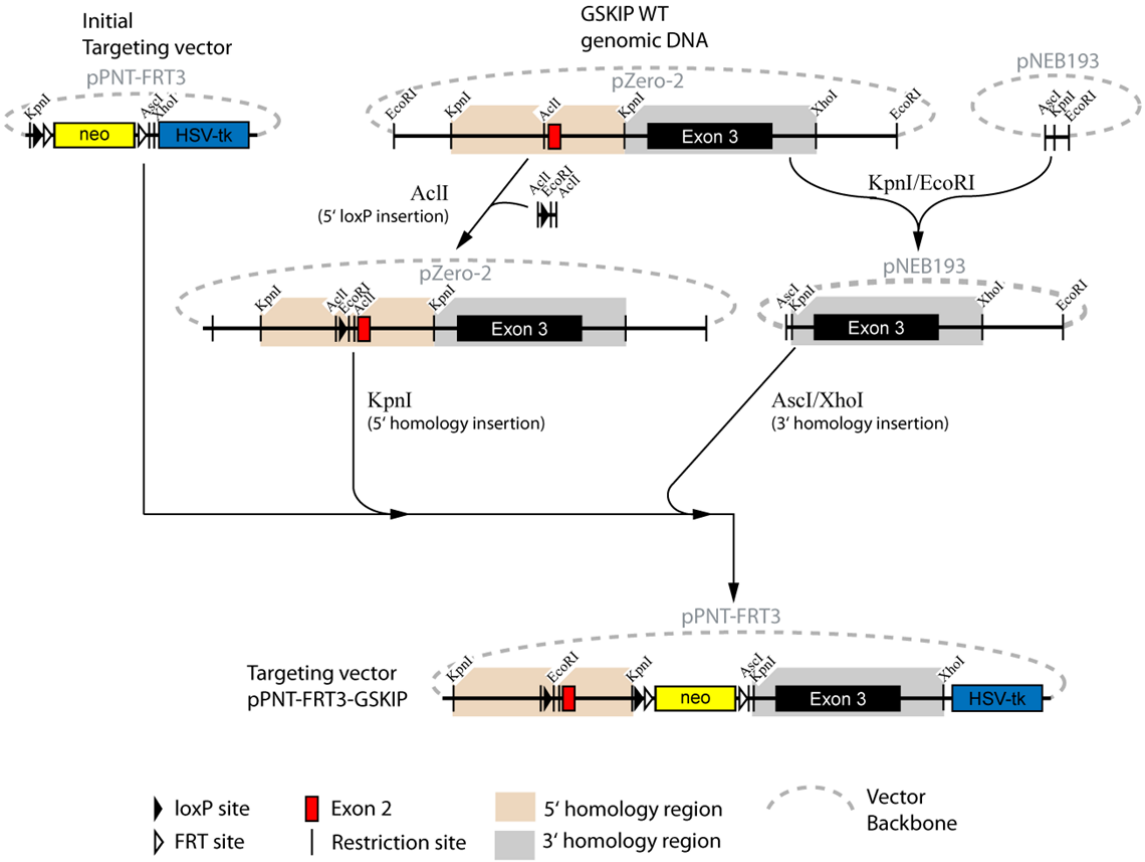

Fig. 32 Cloning scheme for the targeting vector pPNT-FRT3-GSKIP. A loxP site was inserted into the AclI site upstream of GSKIP exon 2 by oligonucleotide cloning. The 5’ and 3’ homology regions were cloned into pPNT-FRT3 via the indicated restriction sites. The 3’ homology region was intermediately cloned into pNEB193 to attach an AscI site and then finally inserted into the targeting vector as an AscI/XhoI fragment. The sequence of pPNT-FRT3-GSKIP is shown in Appendix D.

The KpnI/XhoI fragment containing exon 3 was designated as the 3’ homology region. Because the restriction sites were not completely compatible with the insertion site on pPNT-FRT3, the 3’ homology region was intermediately cloned into the vector pNEB193 to attach an AscI restriction site. For this, a KpnI/EcoRI fragment was excised from pZero^{TM}-2-GSKIP and ligated into the intermediate vector pNEB193. The 3’ homology was then excised as an AscI/XhoI fragment from pNEB193 and ligated into pPNT-FRT3, which already contained the 5’ homology region, via AscI and XhoI sites. This positioned the 3’ homology region

downstream of the neomycin cassette and upstream of the HSV-tk cassette. The correct assembly of the finalised targeting vector pPNT-FRT3-GSKIP was ascertained by analytical restriction digestion and sequencing. The restriction sites employed for the insertion of the homology regions, the GSKIP coding sequence, the loxP and the FRT sites were found to have exactly the anticipated sequence. The full sequence of the targeting vector pPNT-FRT3-GSKIP is shown in Appendix D. The next step was to test for the ability of Cre to recombine the loxP sites of the targeting vector.

3.10.5 Validation of the loxP sites in *E. coli*

After verifying the sequence of the targeting vector, the functionality of its loxP sites was assessed. For this, the *E. coli* strain 294-Cre which expresses Cre recombinase [190] was transformed with the targeting vector. Transformed clones were selected on Ampicillin agar, amplified in LB medium and plasmid DNA was isolated. The Cre-mediated recombination of the target vector's loxP sites was verified by restriction of the plasmid DNA.

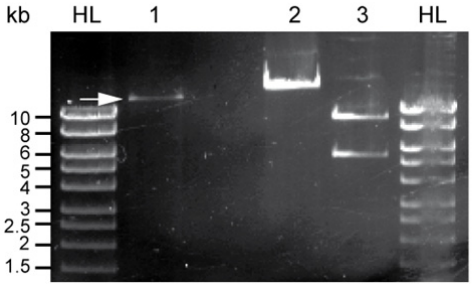

Construct (strain)	Enzymes	Fragments (kb)
1: pPNT-FRT3-GSKIP (294-Cre)	XhoI/SalI	12.9
2: pPNT-FRT3-GSKIP (Top10)	XhoI	14.5
3: pPNT-FRT3-GSKIP (Top10)	XhoI/SalI	9 and 5.5

Fig. 33 Cre-mediated recombination in *E. coli* 294-Cre. The GSKIP targeting vector (pPNT-FRT3-GSKIP) was transformed into the Cre recombinase-expressing *E. coli* strain 294-Cre. The subsequently isolated plasmid DNA was digested with XhoI and SalI (1). For comparison, pPNT-FRT3-GSKIP plasmid DNA isolated from *E. coli* Top10 was digested with XhoI alone (2) or XhoI and SalI (3). The presence of Cre caused a complete removal of the 1.6 kb fragment located between the two loxP sites, causing the size difference between the fragments seen in (1, white arrow) and (2). Because the SalI site was removed by Cre-mediated recombination, only one fragment was observed in (1) as opposed to (3). HL, Hyperladder I.

The floxed region on the target vector comprises 1.6 kb. Hence, this was the size difference expected for target vector DNA isolated from the standard cloning strain Top10 and the Cre-expressing strain 294-Cre. The only SalI restriction site of the target vector is located between the loxP sites and was therefore used as a marker for the specific recombination of this sequence. An XhoI/SalI double digest yielded two fragments of the targeting vector (Fig. 33, lane 3), but only one fragment after Cre recombination, i.e. removal of the floxed sequence and thereby the SalI site. The calculated size of this single restriction fragment is 12.9 kb (Fig. 33 lane 1) and it was evidently smaller than the linearised target vector (14.5 kb, Fig. 33 lane 2). This result clearly indicates that the loxP sites of the target vector are correctly recognised by Cre recombinase and that the sequence flanked by these loxP sites is removed specifically.

In conclusion, sequence analysis and testing the Cre-catalysed recombination of the target vector ensured its correctness and suitability for its transfer into murine ES cells by electroporation.

3.10.6 Electroporation and selection of murine ES cells

The GSKIP targeting vector was incorporated into murine embryonic stem (ES) cells by electroporation (2.2.6.4). The transfected ES cells were selected for the integration of the neomycin cassette of the targeting vector with G418 (positive selection). A subsequent negative selection with ganciclovir was conducted to eliminate cells which had undergone non-homologous recombination and integrated the HSV-tk cassette, which confers sensitivity to ganciclovir. After the double selection, clones were selected and propagated for DNA isolation.

3.10.7 Identification of recombinant ES cells

The selected clones were checked for site-specific recombination, i.e. integration of the modified DNA into the GSKIP locus, by Southern blotting. For that, genomic DNA was digested with EcoRI and subjected to 0.6% w/v agarose gel electrophoresis with subsequent transfer to nylon membranes. The membranes were hybridised with the 3' XhoI/BamHI probe (Fig. 30). In DNA isolated from WT ES cells, a 9.6 kb fragment is specifically recognised (Fig. 31C). The recombinant fragment has a size of 8.5 kb. Because of the rare occurrence of site-specific recombination events only heterozygous ES cells but no homozygous clones with two recombinant alleles were expected.

Three positive clones with heterozygous site-specific integration of the recombinant DNA out of 480 clones, selected after double selection with G418/ganciclovir, were identified. These were in positions G6 and H3 on plate III (Fig. 34A, upper panel) and C11 on plate V (Fig. 34A, lower panel). Frozen stocks of these clones were thawed and the cells were propagated for DNA isolation. The clones were re-checked with the same Southern blotting procedure to confirm the specific recombination and to ensure that the correct clones were thawed and amplified. As a further control, the essential features (loxP sites, FRT sites and GSKIP-coding sequences) of the introduced DNA were verified by sequencing. For this, the 5' homology region was amplified by PCR.

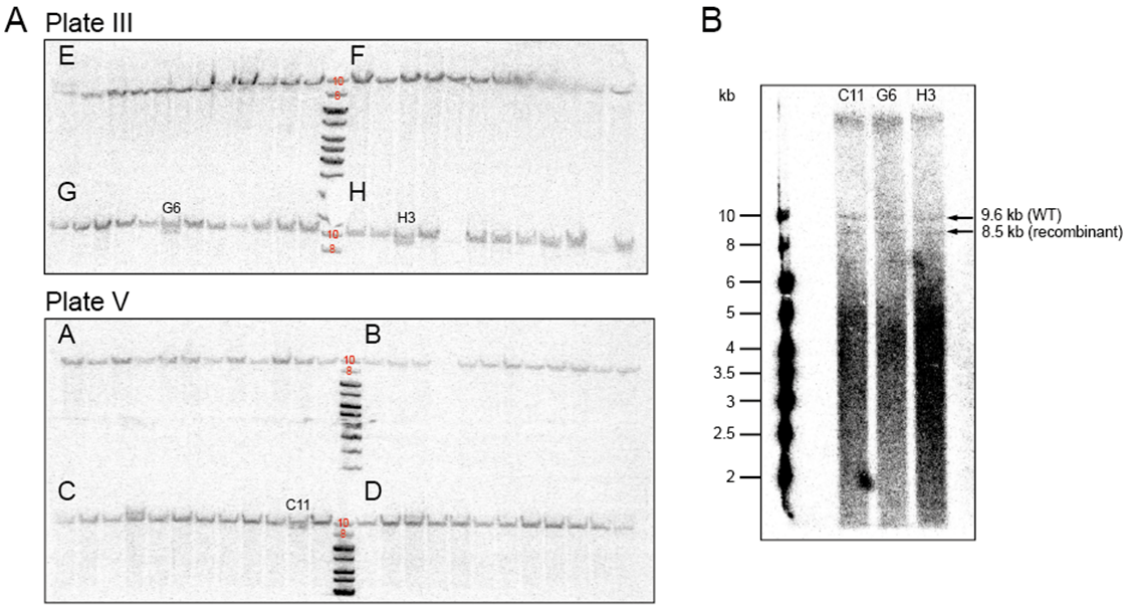

Fig. 34 Identification of recombinant ES cell clones by Southern Blotting. A. Genomic DNA was isolated from 480 selected ES cell clones and digested with EcoRI. EcoRI fragments were separated by agarose gel electrophoresis, transferred to nylon membranes and hybridised with the 3' XhoI/BamHI probe which labels a 9.6 kb WT and a 8.5 kb recombinant fragment. Here, membranes with samples from plate III (rows E-H) and plate V (rows A-D) are shown. The 8.5 kb fragment was detected together with the WT fragment in 3 clones (G6, H3 and C11). The 10 and 8 kb bands of the DNA marker (Fermentas GeneRuler™ 1 kb DNA ladder) are indicated by red numbers. **B.** Frozen stocks of clones G6, H3 and C11 were thawed, expanded and subjected to the same Southern Blot procedure as in A. to confirm the site-specific recombination and to exclude any mix-up of clones.

The forward primer was designed to bind upstream of the 5' homology region to confirm the correct integration of the target vector DNA. The reverse primer was set in the neomycin cassette. Thus the resulting 4 kb PCR product contained the entire 5' homology region, both loxP sites, exon 2 of the GSKIP gene and the 5' FRT site. A similar approach was used for the 3' homology region (forward primer in the 3' region of the neomycin cassette and reverse primer downstream of the 3' homology integration site) but no specific PCR product was obtained. Therefore, a shorter PCR product was used based on the same forward primer but a reverse primer binding to the non-coding region of exon 3. The resulting 1 kb PCR product contained the 5' FRT site and the coding sequence of exon 3. Both PCR products of each ES cell clone (G6, H3 and C11) were cloned into appropriate vectors and transfected into *E. coli* Top10 to amplify the DNA. The resulting plasmid DNA of the 5' homology and the 3' homology PCR product was sequenced. In all three clones, the correct insertion site of the 5' homology arm was confirmed and no mutations were found in the loxP sites, FRT sites, exon 2 and the coding region of exon 3. Thus it was verified that the integration of the target vector DNA occurred site-specifically and a normal transcription of the targeted GSKIP gene resulting in a wild-type mRNA could be assumed. The functionality of the loxP sites was assured as they were identical to the loxP sites of the target vector which had successfully

been recombined by Cre expressed in *E. coli*. Therefore, the selected ES cell clones (G6, H3 and C11) were suitable for morula injection, the next step of the conditional targeting strategy.

3.10.8 Injection of ES cells into morulas

The laser-assisted injection of recombinant ES cells into morula-stage embryos and the following implantation into foster mothers was performed at the Max Planck Institute of Molecular Cell Biology and Genetics (Dresden, Germany) in the transgenic core facility (TCF, head: Ronald Naumann). Frozen stocks of the ES cell clones G6, H3 and C11 were sent to the TCF where the cells were thawed and cultured. Clone H3 displayed the best morphology in cell culture and was injected into morula-stage embryos (strain C57BL/6). The ES-cell containing morulas were implanted into foster mothers and the litters were selected according their coat colour. Chimeric mice were required for the propagation of the targeted genetic modification. These Chimera had black- and agouti-coloured patches of fur because cells from the recipient morula (black coat colour, C57BL/6 genetic background) and from the injected ES cells (agouti coat colour, 129 genetic background) contributed to their development.

3.10.9 Genotyping of targeted mice

In order to ascertain the germline transmission of the targeted GSKIP allele, chimeric males were bred with black-coloured females (C57BL/6). Spermatozoa descending from the recombinant ES cells result in agouti-coloured offspring. Because the gene-targeting event affected only one allele of the GSKIP gene (heterozygous), the agouti-coloured litters could have inherited a wild-type or a targeted GSKIP allele from the chimeric male. Therefore, the presence of the 5' loxP site was verified by PCR to ensure germline transmission of the targeted GSKIP allele. For this, a primer pair was designed to bind upstream (FW primer) and downstream (rev primer) of the 5' loxP site. For WT GSKIP alleles, the amplified sequence is 325 bp long. Due to the insertion of the loxP site, the PCR product based on the recombinant (targeted) allele is 371 bp long. Mice in which both PCR products were specifically amplified were thus classified as heterozygously targeted and used for further breeding. As controls for both genotypes, genomic DNA isolated from the recombinant ES cell clone H3 and from WT ES cells was used (Fig. 35).

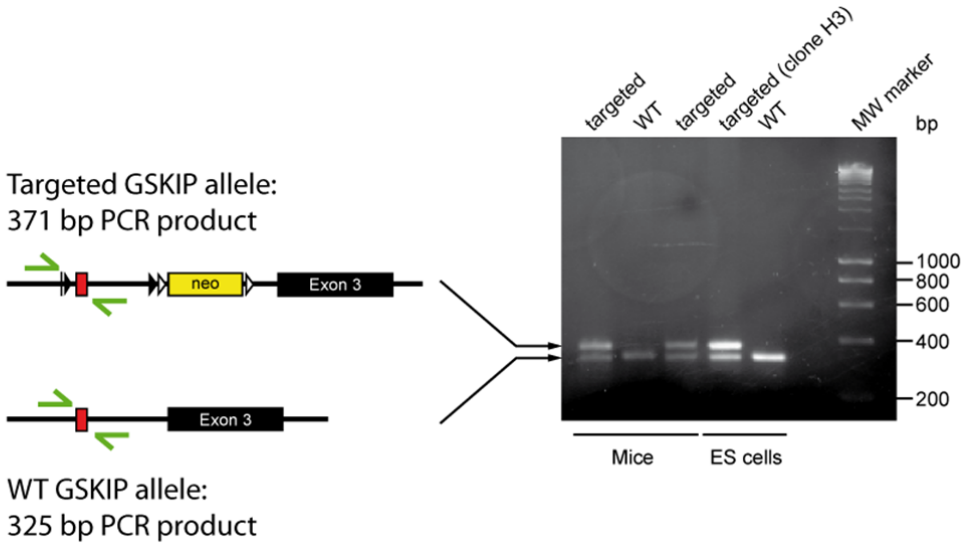

Fig. 35 PCR for the identification of heterozygously targeted mice. Genomic DNA from agouti-coloured offspring of a chimeric male (descendant from ES cell clone H3) bred with C57BL/6 females was used as a template for PCR. The primers (green arrows) and their binding sites on the targeted and WT GSKIP alleles are shown schematically. A 325 bp-PCR product was obtained from WT GSKIP alleles and a 371 bp-PCR product from targeted, recombinant GSKIP alleles. As controls, genomic DNA from targeted ES cells (clone H3) and WT ES cells was used. MW, molecular weight.

3.10.10 Removal of the neomycin cassette

The targeted GSKIP allele in the ES cells and the resulting mice contained a neomycin resistance cassette that was essential for the selection of recombinant ES cells but it was no longer required in the mice. Also, the neomycin cassette could lead to unforeseeable biological effects, either caused through expression of the neomycin phosphotransferase or by altered expression of other genes such as GSKIP or neighbouring genes [191;192]. Such effects could impede a phenotypic analysis of GSKIP null mice and lead to false conclusions about the function of GSKIP. Therefore, mice carrying a targeted GSKIP allele were mated with FLP deleter mice, a strain that constitutively expresses the FLP recombinase. In animals of the daughter generation, FLP catalysed the recombination of the FRT sites within the targeted allele and thereby the excision of the encompassed neo cassette.

The flrted region and one of the FRT sites were excised by FLP-mediated recombination. The length of the removed sequence is 1669 bp. The expression of FLP recombinase and excision of this fragment were verified by PCR and mice carrying a floxed allele (Fig. 30) were used for further breeding.

3.10.11 Conditional knockout of GSKIP

After the removal of the neo cassette by FLP-catalysed recombination, floxed mice were crossed with a Cre deleter strain which expresses the Cre recombinase constitutively and ubiquitously. The resulting offspring were genotyped by PCR (Fig. 36). The presence of a Cre

allele was tested for using primers which amplify a specific product from the Cre coding sequence but not from WT mice. A combination of two PCRs was used to identify the genotype of the GSKIP allele. In a PCR with primers binding upstream of the 5' loxP site and downstream of the 3' loxP site, three different products for floxed, WT and null GSKIP alleles were amplified (Fig. 36, upper panel). The WT and null GSKIP alleles could be identified simultaneously. Although floxed and WT alleles resulted in PCR products of different length, they were difficult to distinguish. Therefore, the PCR for the amplification of the 5' loxP site (Fig. 35) was additionally employed, allowing a clear distinction: This 5' loxP PCR yielded a short (325 bp) PCR product for a WT GSKIP allele and a longer product (371 bp) for a floxed allele. Since the binding site for the reverse primer is located within the floxed region, no PCR product was obtained for a null (KO) GSKIP allele (Fig. 36, middle panel).

This is the first evidence for the *in vivo* deletion of exon 2 of a GSKIP allele in a mouse model. The PCR product amplified from the null allele corresponded exactly to the expected size indicating that Cre-mediated recombination occurred specifically between the loxP sites inserted upstream and downstream of GSKIP exon 2. GSKIP+/- mice were viable, fertile and exhibited no overt phenotype.

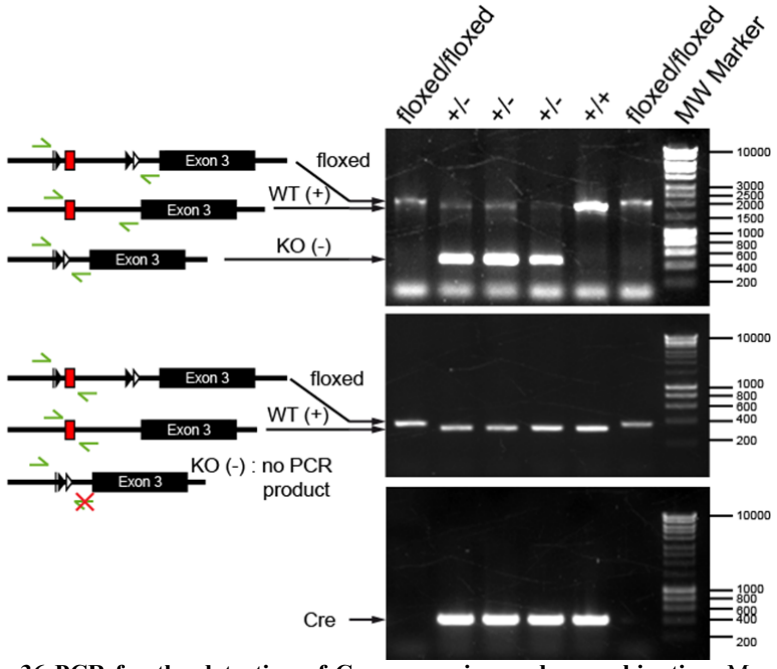

Fig. 36 PCR for the detection of Cre expression and recombination. Mouse genomic DNA was used as a template for PCR reactions. The primers (green arrows) and their binding sites on the floxed, WT (+) and null/KO (-) GSKIP alleles are shown schematically. The genotype of both GSKIP alleles is indicated above the images showing the PCR products. MW, molecular weight.

Female and male GSKIP$^{+/-}$ mice were mated in order to obtain homozygous GSKIP$^{-/-}$ mice. Theoretically a ratio of 1:2:1 (+/+ : +/- : -/-) was expected for the F1 generation.

Genotype	number of animals	%	ratio
$GSKIP^{+/+}$	27	29.7	1
$GSKIP^{+/-}$	64	70.3	2.37
$GSKIP^{-/-}$	0	0	0
total	91	100	

Tab. 16 Genotyping the offspring of $GSKIP^{+/-}$ × $GSKIP^{+/-}$ breedings.

In a total of 91 genotyped mice, no $GSKIP^{-/-}$ animal was identified (Tab. 16). This points to an embryonic lethality of the homozygous GSKIP knockout. Future experiments will aim at identifying the cause of this lethality. In addition, tissue-specific and inducible expression of Cre (1.4) is going to be utilised in order to achieve a homozygous knockout of GSKIP in adult mice.

4. Discussion

4.1 GSKIP is a ubiquitously expressed protein

Here, endogenous GSKIP was detected for the first time by Western blotting in different rat organ lysates (brain, kidney, liver, heart, testis, skeletal muscle, Fig. 14) as well as in SH-SY5Y cells (Fig. 18). The detection of endogenous GSKIP has previously only been described once, in a high-throughput screen for protein-protein interactions, identifying GSKIP as a prey protein in IPs of GSK3β and SMYD2 by mass spectrometry [106]. The Western Blot detection of GSKIP is in line with the data on GSKIP mRNA expression yielded by Northern blotting [70] and microarray analysis [108-111], suggesting that GSKIP is a ubiquitously expressed protein. Its abundance is highest in brain and testis (Fig. 14). This may be explained by the high levels of GSK3α and GSK3β in these tissues [193] which require appropriate levels of scaffolding proteins such as GSKIP. Notably, also AKAP220 and MAP2D are most abundant in brain and reproductive tissues. It is conceivable that distinct AKAPs form complexes with PKA and GSK3β in different cellular compartments: GSKIP in the cytosol, MAP2D on microtubules and AKAP220 on vesicles [180;194]. Since GSKIP is expressed to a similar extent in all tissues, it appears to carry out vital functions. This is also supported by the high level of conservation of GSKIP orthologues.

4.2 GSKIP is a cytosolic protein

Bioinformatic prediction tools and cell fractionation experiments (3.3) speak for a cytosolic localisation of endogenous GSKIP. This result is in agreement with previous immunofluorescence experiments performed with HA-tagged GSKIP [70]. Only fusion proteins of GSKIP with CFP, GFP or mCherry show an additional nuclear localisation but this effect is probably an artefact as it can be attributed to the properties of the fluorescent proteins. Given that GFP and related proteins are approximately twice the size of GSKIP and known to enter the nucleus [166], it is conceivable that they cause a partial nuclear localisation of the GSKIP fusion proteins.

In live-cell imaging (Fig. 15 and Fig. 19) of HEK293 cells and immunofluorescence microscopy [70] of HeLa cells, GSKIP showed an even distribution throughout the entire cytosol and no accumulation on cytoskeletal structures. An exclusively cytosolic localisation is rather exceptional for an AKAP because most AKAPs are tightly associated with distinct cellular organelles [31;35]. As a cytosolic protein, GSKIP could have the function of

restricting the activity of cytosolic GSK3β (4.4) or of establishing cytosolic kinase-substrate scaffolds containing PKA and/or GSK3β.

4.3 The AKAP function of GSKIP

The binding of RII subunits to peptide spots representing the RIIBD of GSKIP (aa 28-52) and to the full-length GSKIP protein *in vitro* suggested that GSKIP is an AKAP [58;68;69]. In this thesis, several methods were used to examine the AKAP function of GSKIP, especially in live cells. The different approaches that were employed to validate the interaction of GSKIP with PKA R subunits are summarised in Tab. 15. Due to the combination of various methods showing an interaction of GSKIP with RII subunits, it was concluded that GSKIP is indeed an AKAP [58].

Structural aspects of the GSKIP/RIIα interaction

Several crystal structures of peptides derived from the RIIBDs of AKAPs in complex with D/D domain dimers of PKA yielded insight into the interactions of the AKAP-PKA interface [49;195;196]. As these peptides represent only short fragments of AKAPs, no information on the overall protein structure has been obtained. The only available 3D structure of a full-length AKAP is the NMR structure of free, unbound GSKIP (PDB: 1SGO, Fig. 10). But to date, there is no structural information on an AKAP protein in complex with R subunits. Hence several aspects of AKAP-PKA interactions remain unclear: (A) It is not known what conformational changes within an AKAP are required to expose the hydrophobic face of the amphipathic helix for PKA binding. Such conformational changes could affect other protein-protein interactions of an AKAP or have an influence on the PKA-binding affinity or kinetics. In the structure of GSKIP (Fig. 10), the polar residues of the amphipathic RIIBD helix are located on the surface of the protein whereas the hydrophobic residues required for PKA binding are buried in the core of the protein. As solvent-exposed hydrophobic amino acids are usually energetically unfavourable it can be assumed that this is also the case for other AKAPs. In consequence, R subunit binding would require conformational rearrangements within an AKAP. (B) Due to the structure of the AKAP peptide-D/D domain interaction sites [49;195;196] it is likely that other parts of an AKAP come into direct contact with the surface of the D/D domain dimer. This might contribute to the binding energy and would partially explain differences in the affinity of different AKAPs for PKA R subunits.

In order to confirm the AKAP function of GSKIP and to obtain information on the structural aspects of the GSKIP-RII interaction, ^{1}H-^{15}N HSQC NMR spectra of ^{15}N-labelled GSKIP in

the presence or absence of unlabelled D/D domain dimers of RIIα were recorded. An attenuation of signals corresponding to amino acids of the RIIBD was observed in the presence of the D/D domain which suggests binding of the D/D domain dimer to the RIIBD. This experiment confirmed that the D/D domain of RIIα is sufficient for an interaction with GSKIP, which supports the canonical AKAP function of GSKIP (see below). Signals assigned to residues of GSKIP located outside of the RIIBD were also decreased in the presence of the D/D domain. Most of these residues are located close to the RIIBD in the NMR structure of free GSKIP. Thus it is likely that their signal attenuation in the presence of the D/D domain is caused by conformational changes within GSKIP or by an involvement of these residues in the interaction with the D/D domain.

FCCS as a tool to study AKAP-PKA complexes

Only a very limited number of methods allow the detection of protein complexes in live cells without disrupting cellular structures. Förster resonance energy transfer (FRET) is often used to determine the interaction of two proteins in live cells [197]. FRET was employed to investigate the interaction of GSKIP and RIIα in live cells but no significant FRET signal was detected (data not shown). A disadvantage of FRET is that signals depend on the dipole orientation of the involved fluorophores. When the dipoles are oriented perpendicular to each other, the FRET efficiency is reduced. Consequently, there may be false negative results in which no FRET is observed although the investigated molecules actually interact [198]. As other results clearly supported a direct interaction of GSKIP and RIIα (Tab. 15), fluorescence cross correlation spectroscopy (FCCS) was used as an alternative to FRET to monitor the complex formation between GSKIP and RIIα in HEK293 cells. Unlike FRET, FCCS does not depend on the dipole orientation of the fluorophores. Park *et al*. already demonstrated that FCCS can be used to measure the complex formation of PKA R and C subunits and the induction of the PKA holoenzyme dissociation by cAMP [199]. The RIIβ subunit used for these experiments had a C-terminal GFP tag, like the RIIα used here. This suggests that the RIIα construct is functional regarding PKA holoenzyme formation. While the GFP was fused to the C-terminus of RIIα, the D/D domain involved in AKAP binding is N-terminally localised. Therefore, it is very unlikely that the GFP moiety had an effect on the AKAP-PKA interaction.

The FCCS experiments show that RIIα and GSKIP form a complex in live HEK293 cells (Fig. 19). FCCS reflects the co-diffusion of two proteins but it does not strictly prove a direct

interaction. In the case of RIIα and GSKIP, the complex formation was reduced by the PKA anchoring disruptor peptide Ht31 and by expressing the mutant GSKIP-V41P/L45P, which has been shown to be RII-binding deficient (Fig. 17). These results suggest a direct binding of GSKIP to RIIα in the fashion of a canonical AKAP. Nevertheless, data obtained by FCCS should generally be complemented with other results showing the direct interaction of the proteins of interest. In the case of GSKIP and RIIα, this has been demonstrated using various *in vitro* approaches (Tab. 15).

For FCCS and other fluorescence-based methods, fluorescent probes are required. Here, fusions of the proteins of interest with fluorescent proteins were used. Several controls were included to ensure that the fluorescent proteins do not interfere with or contribute to the complex formation of GSKIP and RIIα: GFP and mCherry did neither interact with each other nor with GSKIP or RIIα, respectively (Fig. 19). These controls argue against an effect of the fluorescent proteins on the interaction of GSKIP with RIIα. It is therefore likely that this interaction occurs not only between the fluorescent fusion proteins but also between the endogenous proteins which is supported by cAMP agarose pull-down experiments (Fig. 18). In this thesis, FCCS was used for the first time as a tool to monitor AKAP-PKA interactions in live cells. The approach was successfully applied to membrane-bound (AKAP18α) and cytosolic AKAPs (AKAP18δ, GSKIP). Also, the effect of mutations or the influence of PKA anchoring disruptor peptides on the AKAP-PKA interaction can be investigated by FCCS.

GSKIP is a canonical RII-specific AKAP

Different criteria can be used to classify AKAPs. The mode of interaction with PKA and the structural motifs involved therein determine whether an AKAP is canonical, i.e. forming an amphipathic helix that docks into the hydrophobic groove formed by the D/D domain dimer of R subunits [32]. Non-canonical AKAPs employ different motifs to interact with R subunits. If the binding site of a non-canonical AKAP on R subunits is different from the binding site of canonical AKAPs, its binding to PKA is not sensitive to PKA anchoring disruptor peptides such as Ht31 or AKAP18δ-L314E [61;200]. All lines of evidence support the classification of GSKIP as a canonical AKAP: The presence of an AKAP consensus sequence, the susceptibility of the GSKIP-RII interaction to PKA anchoring disruptor peptides and the loss of RII binding upon proline insertion into the RIIBD (Tab. 15). Furthermore, GSKIP binds to full-length RII subunits and D/D domains (3.4.1). Canonical AKAPs can further be divided into RI-, RII- or dual specific AKAPs. Most AKAPs are RII-

specific. Dual-specific or RI-specific AKAPs contain, in addition to the typical amphipathic helix, a second region that binds to RI subunits. This sequence, termed RI-specifier region (RISR), is located N-terminal of the amphipathic helix and contains two consecutive basic residues (Lys or Arg) [60]. GSKIP does not contain any basic amino acids in the N-terminus (aa 1-27). There are two basic residues in the N-terminal part of the RIIBD but these are not directly adjacent. Therefore, GSKIP does not contain a canonical RISR. Accordingly, GSKIP did not bind RI subunits in SPR measurements [69] and can be regarded as an RII-specific AKAP. So far, no AKAP is known to interact exclusively with either RIIα or RIIβ subunits. Also GSKIP was found to bind both RIIα and RIIβ subunits [69].

4.4 GSKIP links the PKA and GSK3β pathways

Two distinct α-helices of GSKIP are involved in the binding of PKA RII subunits (aa 28-52) and GSK3β (aa 115–139). These sites are not overlapping, which theoretically allows a simultaneous interaction of GSKIP with both proteins. Complex formation of GSKIP with both PKA and GSK3β *in vitro* was investigated in an ELISA-based approach. The experiments confirmed that the interaction of GSKIP and GSK3β is direct, with a high affinity (K_D = 1.6 ± 0.2 nM). This value is approximately 1000-fold lower than the affinity of the GSKIPtide-GSK3β interaction (K_D = 2.7 μM) determined by SPR by Chou *et al*. [70]. This might result from the different methods used for the affinity determination, which are not directly comparable. For the SPR-based affinity determination, chip-coupled GSKIPtide was used. Steric hindrance or interactions of the peptide with the chip surface may have interfered with the binding of GSK3β. In addition, other regions of GSKIP than the C-terminal helix could be involved in the interaction with GSK3β and thus increase the affinity compared to GSKIPtide. Further experiments, directly comparing the binding of GSKIPtide, full-length and truncated GSKIP to GSK3β would be required to elucidate the reason for their different binding affinities.

ELISA experiments with GSK3β and surface-bound RIIα excluded a direct interaction of the two proteins. A complex was only formed when GSKIP was added. The K_D value for the binding of GSK3β to RIIα-bound GSKIP is 43 nM ± 5 nM (Fig. 20). The affinity in the nanomolar range indicates that this complex is readily formed *in vitro*. However, *in vivo* so far only the binary interactions of GSKIP with RIIα (Tab. 15) and GSK3β [70] have been demonstrated. Conceivable biological functions of a PKA-GSKIP-GSK3β complex would

include (1) facilitating simultaneous access of PKA and GSK3β to common substrates and/or (2) mediating the inhibitory phosphorylation of GSK3β on Ser9 by PKA:

(1) As mentioned in the introduction, substrate proteins often need to be pre-phosphorylated (primed) by another kinase to enable the phosphorylation by GSK3β (Fig. 6A). PKA is one of the known priming kinases for GSK3β substrates. In some cases, these phosphorylations are known to be coordinated by scaffolding proteins which bind PKA, GSK3β and a common substrate [32]. It is possible that GSKIP also assembles such a complex by interacting with a PKA-primed GSK3β substrate.

(2) A potential influence of GSKIP on GSK3β phosphorylation was tested in two experimental settings in HEK293 cells. Cells were either transfected with CFP-GSKIP or treated with GSKIPtide, a peptide that comprises the C-terminus of GSKIP (aa 115-139) which is equivalent to the GID (Fig. 10). The peptide GSKIPtide increases the level of PKA-dependent GSK3β phosphorylation in unstimulated cells (Fig. 21). It is unlikely that this is caused by the recruitment of other kinases to GSK3β because GSKIPtide consists only of the GID of GSKIP. Therefore, GSK3β phosphorylation is probably stimulated by GSKIPtide through different means. There are different possible mechanisms for GSKIPtide-induced phosphorylation of GSK3β: (A) Binding of GSKIPtide could alter the conformation of GSK3β, thereby making Ser9 more accessible to phosphorylation by other kinases such as PKA or PKB (Fig. 37A). (B) GSKIPtide could interfere with a protein complex that counteracts Ser9 phosphorylation. Indeed, the GSK3β scaffold protein axin interacts with the protein phosphatase PP2A [201;202]. PP2A has been shown to dephosphorylate Ser9 on GSK3β [203;204]. GSKIPtide and axin bind to the same site on GSK3β. GSKIPtide might displace an axin-PP2A complex from GSK3β, thereby prevent dephosphorylation of Ser9 by PP2A and in consequence increase the level of p-GSK3β (Fig. 37B). (C) The third model involves an autoregulation of GSK3β. Chou *et al*. reported that both GSKIP and GSKIPtide inhibit GSK3β in the absence of other kinases, i.e. independently of Ser9 phosphorylation [70]. Yet, in cell-based assays, an increase in Ser9 phosphorylation is observed in the presence of GSKIPtide or overexpressed GSKIP. Similar observations have been made with the GSK3β inhibitor lithium. It inhibits GSK3β activity *in vitro* and increases levels of p-GSK3β in cells [176] as well as in mice *in vivo* [205]. This augmented GSK3β phosphorylation is not caused by activation of Ser9-phosphorylating kinases but by the inhibition of GSK3β dephosphorylation [176]. When GSK3β is active, it phosphorylates IPP-2, an inhibitor of protein phosphatase 1 (PP1). PP1 is thus activated and can dephosphorylate

p-GSK3β on Ser9. When GSK3β is inhibited by lithium, however, IPP-2 can block PP1 activity and p-GSK3β can accumulate [176]. This system can be regarded as an activity switch for GSK3β: active GSK3β stimulates GSK3β Ser9 dephosphorylation by PP1 and an inhibition of GSK3β leads to PP1 inhibition and consequently an accumulation of p-GSK3β. GSKIPtide and GSKIP could, like lithium, augment GSK3β phosphorylation by preventing the activation of PP1 through GSK3β (Fig. 37C). These potential mechanisms for GSKIPtide-induced Ser9 phosphorylation need to be validated in future experiments, for instance by investigating the amount of GSK3β complexed with axin or the phosphorylation status of IPP-2 in the presence and absence of GSKIPtide.

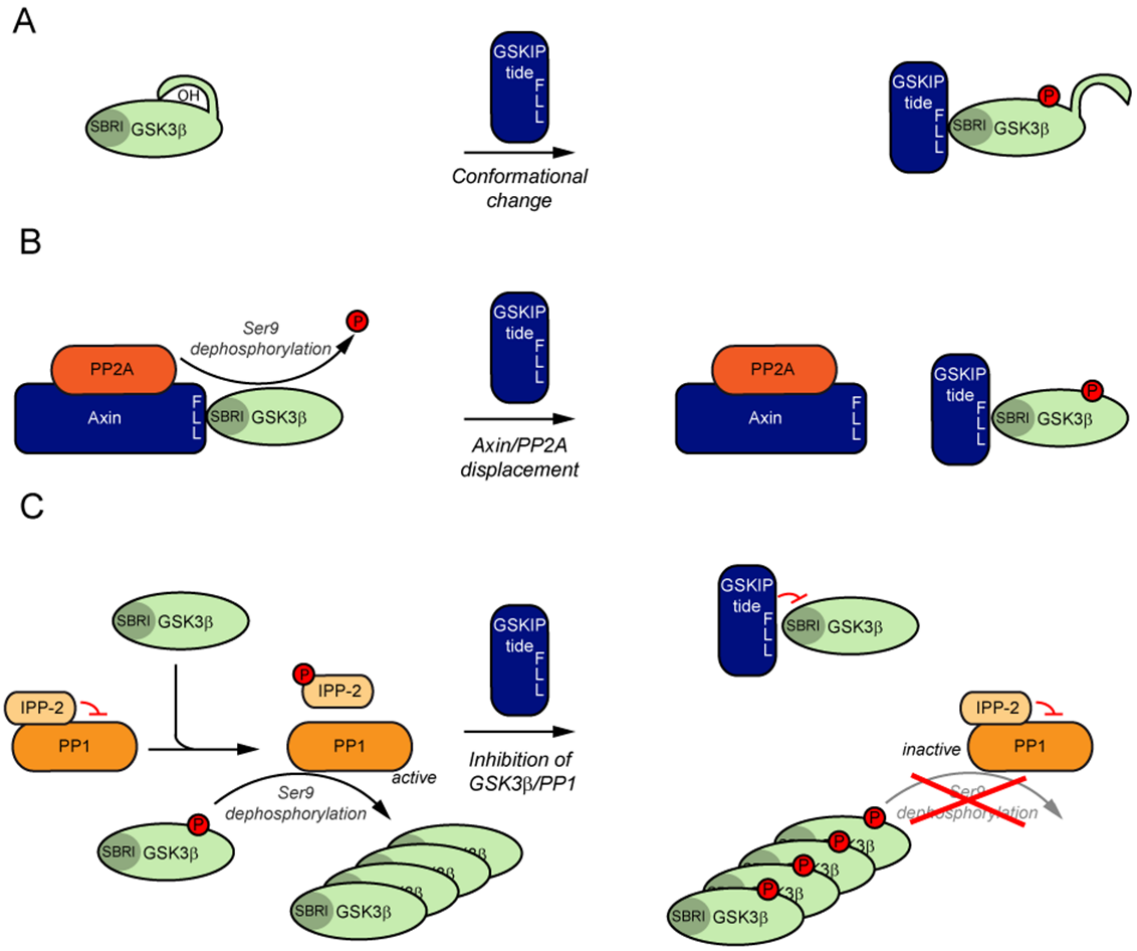

Fig. 37 Potential mechanisms of GSKIPtide-induced phosphorylation of GSK3β. See text for details **A.** Binding of GSKIPtide could cause a conformational change within GSK3β that facilitates the phosphorylation of Ser9. **B.** GSKIPtide could displace an axin/PP2A complex from GSK3β, resulting in reduced dephosphorylation of Ser9. **C.** Active GSK3β phosphorylates IPP-2, an inhibitor of PP1, which leads to an activation of PP1. Active PP1 dephosphorylates GSK3β molecules. When GSKIPtide inhibits GSK3β, the activation of PP1 might be blocked, causing an accumulation of phospho-GSK3β.

While GSKIPtide doubles the phosphorylation of GSK3β in HEK293 cells in a basal state (Fig. 21), the global activation of PKA by forskolin does not lead to a further increase in

GSK3β phosphorylation in GSKIPtide-treated cells. The expression of CFP-GSKIP increases the basal phosphorylation of GSK3β to a similar extent as GSKIPtide. However, in this setting an activation of PKA by forskolin causes a further rise of p-GSK3β levels. The AKAP function of GSKIP and thereby the recruitment of PKA into the proximity of GSK3β most likely accounts for this difference between the effects of GSKIPtide and GSKIP protein. In conclusion, the current data point to a dual mode of GSK3β inhibition by GSKIP: In resting cells, GSKIP (or GSKIPtide) interacts with GSK3β and inhibits its activity [70] which also induces partial phosphorylation of Ser9 (Fig. 37). When cAMP production is stimulated, a further elevation of GSK3β phosphorylation is induced by GSKIP and the associated PKA but not by GSKIPtide. The physiological function of the GSKIP complex and the related phosphorylation of GSK3β is not known. There are, however, multiple physiological stimuli which cause a PKA-dependent phosphorylation of Ser9 (Fig. 7). For most of these signals it is not known whether an AKAP is required for the Ser9 phosphorylation. It is conceivable that GSKIP is involved in one of these processes. For the exploration of the physiological functions of GSKIP, the GSKIP knockout mouse model will be an essential tool (4.8).

4.5 Conservation of GSKIP – Evolutionary aspects

GSK3 proteins are found in all eukaryotes, and even orthologues from distant species such as humans and *Dictyostelium* share over 80% similarity within their kinase domains [72]. There is a number of scaffolding and regulatory proteins for GSK3, among these Frequently rearranged in T-cell lymphomas/GSK3-binding protein (FRAT/GBP) [206], AKAP220 [57], and most prominently axin [207]. While orthologues of these proteins exist in different metazoan species, no universal GSK3-interacting protein is known to occur in all eukaryotes. Peptide spot overlay experiments indicate that GSKIP orthologues/DUF727 proteins from a broad range of invertebrate and vertebrate metazoans and two fungi have the potential to interact with GSK3 (Fig. 23). This is supported by data showing an interaction of a DUF727 protein from *C. elegans* with *C. elegans* GSK3 [172]. Moreover, the observation that human axin interacts with a GSK3 protein from the fission yeast *Schizosaccharomyces pombe* suggests that the ability of GSK3 to interact with axin and GSKIP has been conserved throughout eukaryote evolution [208]. Tab. 17 summarises the occurrence of the abovementioned GSK3-binding proteins in different species.

Orthologues of FRAT/GBP and AKAP220 are only known in vertebrates, whereas axin is found in *C. elegans*, *D. melanogaster* and in vertebrates. This is plausible because axin is a central protein in the Wnt signalling pathway which is essential for the development of all

metazoans [209;210]. Since GSKIP orthologues have conserved the ability to bind GSK3 from fungi to man, they can be regarded as the evolutionarily oldest group of GSK3-binding proteins known to date. This, in turn, indicates that GSKIP plays an important role in fungal/metazoan cellular function.

Taxonomic group	Species	GSKIP/DUF727	Axin	FRAT/GBP	AKAP220
Mammal	*H. sapiens*	+	+	+	+
Amphibian	*X. laevis*	+	+	+	+
Fish	*D. rerio*	+	+	+	-
Insect	*D. melanogaster*	+	+	-	-
Nematode	*C. elegans*	+	+	-	-
Amoeba	*D. discoideum*	+	-	-	-
Fungi	*L. elongisporus*	+	-	-	-
	P. guilliermondii	+	-	-	-

Tab. 17 Evolutionary conservation of GSK3-binding proteins. The existence of known orthologues of the given GSK3-binding proteins in different species is indicated by (+). (-): no orthologue of the indicated protein is known in the respective species. Data were obtained from the UniProtKB and Pfam entries Pf05303 (DUF727), Pf08833 (axin), and Pf05350 (FRAT) [112;188].

Unlike the interaction with GSK3β, the AKAP function of GSKIP was only found in vertebrates. Invertebrate-derived peptides homologous to the RIIBD of human GSKIP did not bind PKA RIIα (Fig. 22). Out of the total of 87 DUF727 proteins (Interpro entry IPR007967), all 13 vertebrate proteins contain a sequence which is homologous to the RIIBD of human GSKIP and complies with the AKAP consensus sequence in every position (Fig. 22). Only six out of the remaining 74 DUF727 proteins meet this prerequisite for canonical AKAPs. Peptides derived from four of these proteins were tested in the RII overlay (Fig. 22). The remaining two AKAP consensus sequence-containing proteins (*Nematostella vectensis* A7SRB6/*Culex quinquefasciatus* B0XA92) have not been tested for RII binding since they had not yet been included in the list of DUF727 proteins at the time the experiments were performed.

The current data argue against but do not ultimately exclude an AKAP function of non-vertebrate GSKIP orthologues as the RII overlay assay was carried out with human RIIα protein as a probe. We have previously demonstrated that a database search of *Drosophila* proteins based on the AKAP pattern in combination with an RII overlay assay of the resulting peptide spots identified both PKA-binding domains of *Drosophila* AKAP550 (unpublished data), showing that the use of a human RII probe is suitable for the detection of invertebrate AKAPs. However, the D/D domain of human RIIα is only 47% identical to the homologous *Drosophila* sequence. As a consequence, unidentified invertebrate AKAPs might bind invertebrate but not human PKA R subunits and thus evade detection in the RII overlay with a human RII probe.

Our data show that the interaction with GSK3 is generally conserved among GSKIP proteins whereas RII binding was only found in vertebrates, implying that GSKIP gained the AKAP function during vertebrate evolution. This is in accordance with the concept that vertebrates express a higher number of AKAPs than invertebrates in order to establish the tightly regulated and compartmentalised signalling pathways necessary to maintain highly differentiated cellular architectures and complex physiological processes [32].

4.6 Axin and AKAPs assemble distinct GSK3β complexes

Using peptide spots and a GSK3β overlay technique, the interactions of the AKAPs AKAP220 (3.8.1) and MAP2D (3.8.2) with GSK3β were characterised. The identified GSK3β-binding sequences were compared to those of the established GSK3β interaction partners axin and GSKIP. In addition, SMYD2 was tested for a potential direct interaction with GSK3β using the same approach (3.8.3). SMYD2 was previously shown to interact with GSK3β, GSKIP, axin-1 and AKAP220 [106] but it was not known whether these interactions are direct.

These experiments showed that AKAP220 contains a helical FLL motif which is similar to the GIDs of axin and GSKIP. GSKIPtide blocks the binding of GSK3β to this motif, suggesting that AKAP220 also binds to the SBRI of GSK3β, the binding site of axin and GSKIP/GSKIPtide (1.3). The consensus motif (F-X-X-X-L-X-X-X-L) may, in combination with a high probability to form an α-helix, help to identify axin-like GSK3β-binding sequences within a candidate protein. In contrast, MAP2D does not contain an FLL motif. Nevertheless, a peptide derived from the C-terminus of MAP2D was found to bind GSK3β (Fig. 26). GSKIPtide reduced this binding. It is therefore likely that MAP2D and the FLL-containing proteins (axin, GSKIP, AKAP220) bind to identical or at least overlapping sites on the surface of GSK3β.

Peptide spot array-based overlay techniques are helpful tools to map protein-protein interactions and to determine the involvement of single amino acids. There are, however, limitations of this technology: While continuous binding sites (such as RIIBDs of AKAPs or the GIDs of axin and GSKIP) can often be identified, discontinuous binding sites are generally difficult to detect. In addition, peptide spots may bind proteins via electrostatic or hydrophobic interactions which do not occur between the full-length proteins due to steric or conformational conditions. This can result in false positives. Therefore, the GSK3β-binding sites of AKAP220 and MAP2D need to be confirmed on the protein level, e.g. by Co-IPs or

by pull-down experiments using recombinant proteins. In this context, it will be interesting to examine whether AKAP220, MAP2D, GSKIP and axin compete for GSK3β binding which is suggested by the experiments with GSKIPtide (Fig. 38).

As axin, GSKIP, AKAP220 and MAP2D presumably interact with GSK3β in a mutually exclusive fashion, it can be assumed that they all assemble distinct pools of GSK3β, possibly with different functions (Fig. 38). While the role of the axin/GSK3β interaction within the canonical Wnt signalling pathway is well established, the physiological function of the complexes formed by GSKIP, AKAP220 and MAP2D are not clear. Since GSKIP, AKAP220 and MAP2D have been shown to mediate the inhibitory phosphorylation of GSK3β [54;57;58], they could serve as reservoirs or buffers that maintain defined pools of GSK3β in an inactive state. The inhibition of GSK3β mediated by GSKIP, AKAP220 and MAP2D could be modified by specific signalling events. This might be important for a tightly controlled phosphorylation of GSK3β substrates.

The 25 C-terminal amino acids of MAP2D, identified here as a putative GID, are identical in all mammalian MAP2 isoforms (MAP2A-C). This suggests that the other isoforms of MAP2 may also interact with GSK3β. Based on sequence similarities, the MAP2/tau family of proteins was defined. It comprises the microtubule-binding proteins MAP2A-D, tau and MAP4 [211]. The C-terminal amino acids of tau and MAP2 are highly similar: 17 of 25 amino acids within the C-terminus of tau are identical to the MAP2 C-terminus. In contrast, the C-terminal 25 amino acids of MAP4 do not share homology with MAP2 and tau. Given that the C-terminus of MAP2D is likely to engage GSK3β in a direct protein-protein interaction (Fig. 26), this interaction is also conceivable for the C-termini of other MAP2 isoforms or tau due to the identical or highly similar sequence, respectively. Since both MAP2 and tau are GSK3β substrates [179;212], a direct interaction of MAP2 and tau with GSK3β could facilitate their phosphorylation. A direct interaction is also required for the efficient phosphorylation of MAP2 by PKA: When the N-terminus of MAP2, which harbours the RIIBD, is deleted the phosphorylation by PKA is reduced [213]. The phosphorylation of tau by GSK3β is relevant for the development of Alzheimer's disease [214]. It is therefore important to understand the mechanisms underlying tau phosphorylation. In case the C-terminus of MAP2D is confirmed as a GSK3β-binding motif in further experiments, the C-termini of other MAP2 isoforms and tau could also be tested for GSK3β binding and a potential relevance for the phosphorylation of MAP/tau by GSK3β.

Protein overlays over spot-synthesised peptides derived from SMYD2 revealed that GSK3β is potentially a direct binding partner of SMYD2. A distinct binding site could not be determined because several peptides derived from SMYD2 were capable of binding GSK3β. A GSKIP- and axin-like binding of SMYD2 to GSK3β seems unlikely because peptides with the highest signal for GSK3β binding were not affected by GSKIPtide. This implies that these peptides bind to a different site of GSK3β than axin-1 and GSKIP. It is thus conceivable that SMYD2 binds to axin-1, AKAP220- or GSKIP-bound GSK3β. This in turn would explain how axin-1, AKAP220 and GSKIP were identified as prey proteins in IPs of SMYD2 (Fig. 38).

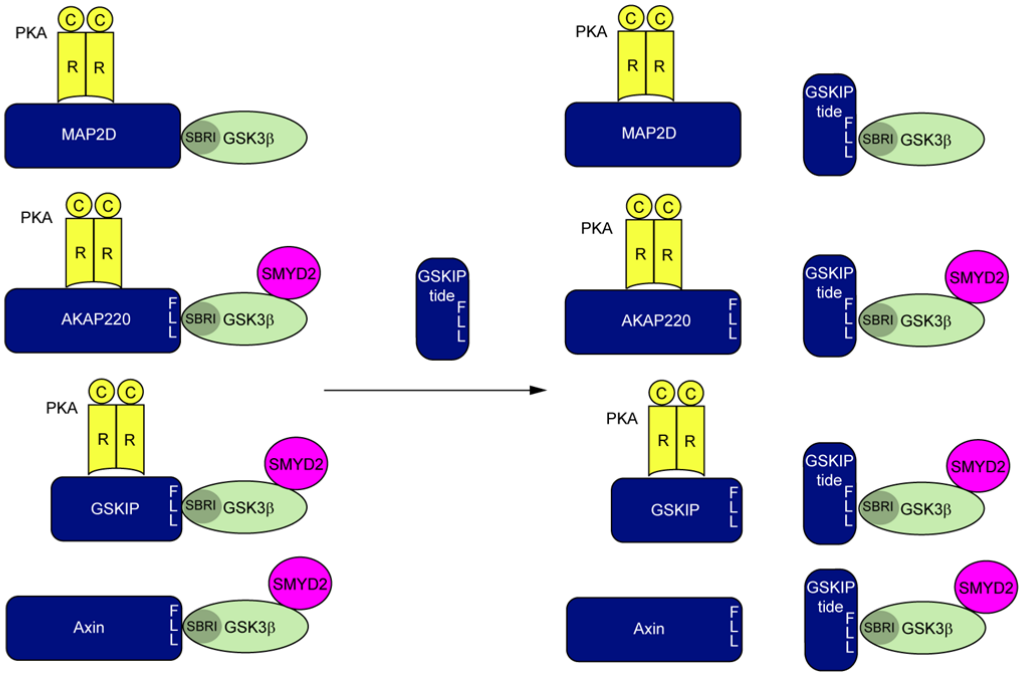

Fig. 38 Model for GSK3β-containing protein complexes. Axin and the AKAPs MAP2D, GSKIP and AKAP220 bind to the scaffold binding region I (SBRI) of GSK3β. AKAP220, GSKIP and axin contain an FLL motif that binds to GSK3β. The binding of MAP2D, AKAP220, GSKIP and axin to GSK3β is inhibited by the peptide GSKIPtide. SMYD2 presumably binds GSK3β directly and axin, AKAP220 and GSKIP indirectly via GSK3β. As indicated by peptide spot experiments (Fig. 27), the binding of SMYD2 to GSK3β is not affected by GSKIPtide.

Functionally, SMYD2 is a histone H3 methyltransferase and was also shown to methylate and thereby inactivate the tumour suppressor proteins p53 [215] and retinoblastoma-associated protein (Rb) [216]. GSK3β interacts with p53 directly [217], which could grant SMYD2 access to this substrate. But at this point, it can only be speculated whether a GSK3β-SMYD2 complex is of any relevance for the methylation of SMYD2 substrates such as p53. The occurrence of several SMYD2-derived GSK3β-binding peptides could either point to a discontinuous binding domain or to unspecific binding (see above). In order to obtain reliable

information on the SMYD2-GSK3β interaction, experiments using the full-length proteins will be required. If a direct interaction is verified, its relevance for the function of GSK3β or SMYD2 could be explored. In addition, the scaffolding proteins axin, AKAP220 and GSKIP, which were found in IPs of SMYD2 [106], might play a role in this context.

4.7 GSKIP – a tumour suppressor?

The expression of GSKIP is downregulated gliomas (3.9). This can be caused by various changes, such as altered abundance or regulation of transcription factors, by increased mRNA degradation, by genetic, epigenetic or by genomic alterations. The GSKIP locus is located on chromosome 14, in region 14q32.2. A deletion of this region and thereby a loss of one allele of GSKIP occurs in a subset of gliomas [218;219], accounting for a reduced gene dosage. It is not known whether a reduced amount of GSKIP plays any role in tumour development but there is evidence that GSK3α/β is deregulated in gliomas. The inhibition of GSK3α/β by LiCl, specific pharmacological inhibitors or siRNA-mediated knockdown reduces the migration of glioma cells [220]. GSK3β is not only important for migration of glioma cells, but also inhibits their differentiation and apoptosis [221]. This is underlined by data showing that an inhibition of GSK3β enhances the sensitivity of glioma cells towards chemotherapy and radiation [222] and reduces the proliferation of glioblastoma cells [223].

In the Oncomine database, no over-expression of GSK3β is found in glioma samples (data not shown). As GSKIP acts as an inhibitor of GSK3β, its reduced expression in gliomas could cause an increased activity of GSK3β, which in turn might contribute to its tumour-promoting properties. Thus GSKIP could be essential for normal cellular function by restricting the activity of GSK3β. Interestingly, a caffeine-induced elevation of cAMP levels in glioma cells leads to an increase in the PKA-dependent phosphorylation of GSK3β on Ser9 and results in increased apoptosis [224]. As an interaction partner of both PKA and GSK3β, GSKIP could potentially mediate this phosphorylation and thus exert a tumour-protective effect.

4.8 The GSKIP knockout mouse model

In this thesis, a conditional GSKIP knockout mouse model was established based on the Cre/loxP system.Various knockout and mutant mouse models were generated to study the function of AKAPs and anchored PKA signalling. In several cases, the complete ablation of an AKAP is lethal or causes infertility [32]. This was taken into account for the generation of the GSKIP knockout mouse strain and was one reason to decide for a conditional targeting strategy.

As alternatives to the knockout of the entire AKAP, the RIIBD has been deleted in mutant mouse models for several AKAPs like MAP2 [213], AKAP150 [225-227] and AKAP10 [228]. Such an approach allows investigating the consequences of a loss of PKA anchoring within an AKAP while not interfering with its other functions or protein-protein interactions.
Yet, in the case of GSKIP this was not feasible. In contrast to most other AKAPs, GSKIP is a very small protein and its RIIBD domain is located in the central part of the protein. It is involved in multiple intramolecular interactions with the β-sheet region (Fig. 10). Therefore, the deletion of the RIIBD of GSKIP would most likely cause a drastic change of the overall protein structure and reduced protein stability. Already for the insertion of two prolines into the RIIBD of GSKIP, which disrupts the helical structure of the RIIBD, a reduced abundance of GSKIP is observed (Fig. 17). In conclusion, only a targeting strategy that would result in a complete ablation of GSKIP was suitable to eliminate the AKAP function of GSKIP. In turn, this means that any phenotype observed in the GSKIP KO model cannot directly be ascribed to the AKAP function.
The following steps were carried out to construct a GSKIP knockout mouse model during this thesis: the isolation of genomic DNA containing the GSKIP coding sequence, the construction of the GSKIP targeting vector comprising a floxed exon 2 and a flrted neo cassette, the transfection of the vector into ES cells, the selection of homologous recombinant ES cells, the transfer of ES cells into mouse embryos, germline transmission of targeted ES cells, FLP-catalysed removal of the neo cassette and Cre-mediated removal of exon 2. All steps were validated with appropriate controls.
$GSKIP^{+/-}$ mice are viable, fertile and they display no overt phenotype. So far, no $GSKIP^{-/-}$ mice were born which points to embryonic lethality of the homozygous knockout of GSKIP. Since GSKIP is an inhibitor of GSK3β, an increased activity of GSK3β was expected for the GSKIP KO. Accordingly, similarities to the mouse models for constitutive activation of GSK3α and GSK3β ($GSK3\alpha^{S21A/S21A}$, $GSK3\beta^{S9A/S9A}$) or to the knockout of FRAT/GBP, a negative regulator of GSK3β, were anticipated. However, the $GSK3\alpha^{S21A/S21A}$/$GSK3\beta^{S9A/S9A}$ double knockin mice, in which neither GSK3 isoform can be inactivated by phosphorylation, are viable [229]. Also, a triple knockout of all three FRAT genes resulted in no obvious phenotype, although it had previously been assumed that FRAT is an essential component of Wnt signalling pathways [230]. It is therefore likely that the putative lethality of the GSKIP KO is not solely caused by a lack of GSK3β inhibition but also by other, possibly unknown functions of GSKIP.

5. Outlook

The GSKIP KO mouse model

While a conditional knockout mouse model for GSKIP was established in this thesis, a detailed analysis is still pending. In future experiments, the cause and time point of lethality of the GSKIP knockout will be analysed. This might reveal a role of GSKIP in embryonic development. In order to circumvent embryonic lethality, allow normal development and obtain adult GSKIP$^{-/-}$ mice, an inducible Cre gene will be utilised in the future to express Cre in adult GSKIP$^{flox/flox}$ mice. The initial analysis of the resulting phenotype will focus on the following cell biological aspects: (A) the abundance, localisation and activity of both GSK3β and type II PKA, (B) the phosphorylation status of GSK3β and PKA substrates, (C) potential mechanisms compensating for the loss of GSKIP such as altered expression of other regulatory proteins for GSK3β and AKAPs (e.g. AKAP220 and MAP2D).

Considering the expression levels of GSKIP, GSK3β and PKA as well as the known functions of GSK3β, PKA and AKAPs, it is conceivable that the knockout of GSKIP affects the nervous system or reproductive tissues. In this case, tissue- or cell type-specific expression of Cre could be used to achieve a selective knockout of GSKIP. Given the reduced expression of GSKIP in gliomas, carcinogenesis will be a very interesting aspect to examine in GSKIP$^{-/-}$ mice.

The physiological relevance of the GSKIP-RIIα-GSK3β complex

Ternary complex complex formation of GSKIP, RIIα and GSK3β has so far only been observed *in vitro* (3.5). As a next step it will be attempted to isolate such a complex also from cultured cells or from tissues (e.g. by immunoprecipitation). It will also be important to define the physiological stimuli that trigger the PKA-dependent phsophorylation of GSK3β that is mediated by GSKIP. In addition, the mechanism underlying GSKIP/GSKIPtide-mediated phosphorylation of GSK3β in resting cells remains to be elucidated. For this purpose, an effect of GSKIP/GSKIPtide on the GSK3β-axin interaction or on IPP-2 phosphorylation could be investigated (Fig. 37).

GSK3β scaffolds

The GSK3β-binding sites of AKAP220, MAP2D and SMYD2 identified here using peptide arrays need to be confirmed on the protein level by co-immunoprecipitation and pull-down assays. In such experiments it should also be determined whether GSKIP, AKAP220,

MAP2D and axin compete for GSK3β binding (Fig. 38). Furthermore, the presence of SMYD2 in GSKIP, AKAP220 and axin protein complexes (Fig. 38) [106] suggests an involvement of these complexes in the regulation of SMYD2. Therefore, it could be investigated whether the association of SMYD2 with GSK3β and its scaffolding proteins controls the methylation of specific SMYD2 substrates.

3D protein structures

To date, there is no 3D structure of a full-length AKAP in complex with either the RII D/D domain or with full-length RII subunits of PKA available. GSKIP would be an excellent candidate for such a structural investigation either by NMR or by X-ray crystallography for the following reasons: GSKIP is a small AKAP, it is soluble and it can easily be purified. Initial HSQC experiments performed here have shown that GSKIP binds to the RIIα D/D domain dimer. In combination with a GSKIP-RII structure, the available 3D structure of unbound GSKIP would help to understand conformational changes occurring upon PKA binding. Moreover, parts of GSKIP located outside the RIIBD might be involved in the interaction with RII and could thus clearly be identified.

Similar structural investigations are also conceivable for the GSKIP-GSK3β complex. There are crystal structures of GSK3β in complex with GSK3β-binding peptides derived from axin-1 and FRAT/GBP [103;231] but there is no 3D structure of GSK3β bound to a full-length protein. Again, GSKIP would be a good candidate because of its abovementioned properties. A potential GSKIP-GSK3β 3D structure could provide valuable information on the regulation of GSK3β by scaffolding proteins.

6. Summary

A-kinase anchoring proteins (AKAPs) localise the cAMP-dependent protein kinase A (PKA) to distinct cellular compartments and thereby facilitate access to PKA substrates in close vicinity. In addition, AKAPs bind other signalling proteins, allowing for the integration of cAMP signalling with other signalling pathways in a temporally and spatially controlled manner. GSK3β interaction protein (GSKIP) had been identified in a database screen as a novel AKAP and had been shown to bind regulatory RII subunits of PKA *in vitro*.

In this thesis, the AKAP function of GSKIP was demonstrated in live cells by cAMP agarose pull-down experiments and by fluorescence cross-correlation spectroscopy (FCCS). In addition, it was shown that GSKIP is a ubiquitously expressed, cytosolic AKAP that forms a complex with PKA RIIα and GSK3β *in vitro* as determined by enzyme-linked immunosorbent assays (ELISA). Moreover, GSKIP was found to increase the PKA-dependent phosphorylation of GSK3β serine-9 and thus inhibition of GSK3β.

GSKIP is highly conserved among fungi, invertebrates and vertebrates. In a peptide spot array-based approach, the potential RII- and GSK3β-interaction domains of GSKIP orthologues were tested for RIIα and GSK3β binding, respectively. The interaction with RIIα and thus an AKAP function was only observed in vertebrate orthologues of GSKIP. In contrast, the binding to GSK3β was found for most of the peptides derived from fungal, invertebrate and vertebrate GSKIP proteins.

In order to develop a basis for the elucidation of the physiological function of GSKIP, a mouse model for the conditional knockout of GSKIP was developed during this thesis. Genomic mouse DNA containing the GSKIP coding sequence was used to generate a targeting vector in which exon 2 of the GSKIP gene was flanked by loxP sites (floxed). This allowed a Cre-catalysed removal of exon 2 and thereby a disruption of the gene. The targeting vector was site-specifically integrated into the genome of embryonic stem (ES) cells. Recombinant ES cells were injected into mouse embryos which developed into mice carrying a floxed GSKIP allele. The genetic modification was inherited to filial generations and by breeding to a Cre-expressing mouse strain, the floxed sequence containing exon 2 was removed. The resulting $GSKIP^{+/-}$ mice were viable and fertile. Male and female $GSKIP^{+/-}$ mice were crossed but did not yield $GSKIP^{-/-}$ offspring, implying that a homozygous deletion of GSKIP is embryonically lethal.

In future experiments, a detailed phenotypic analysis of GSKIP knockout mice will be performed with the prospect of gaining insight into the cause of embryonic lethality and into the physiological function of GSKIP.

7. Zusammenfassung

A-Kinase-Ankerproteine (AKAP) binden die cAMP-abhängige Proteinkinase A (PKA) durch direkte Proteininteraktion in spezifischen zellulären Kompartimenten. Dadurch wird die Phosphorylierung nahe gelegener Substrate ermöglicht. Außerdem interagieren AKAP direkt mit weiteren Signalproteinen und können so räumlich und zeitlich verschiedene Signalwege integrieren. In einer in unserer Arbeitsgruppe durchgeführten Datenbanksuche wurde das *GSK3β interaction protein* (GSKIP) als neues AKAP identifiziert. Seine AKAP-Funktion (Interaktion mit regulatorischen RII-Untereinheiten der PKA) wurde *in vitro* nachgewiesen.

In der vorliegenden Arbeit wurde die AKAP-Funktion von GSKIP durch cAMP-Agarose-Präzipitationen und durch Fluoreszenz-Kreuzkorrelations-Spektroskopie erstmals auch in lebenden Zellen nachgewiesen. Es wurde gezeigt, dass GSKIP ein ubiquitär exprimiertes, zytosolisches AKAP ist, das *in vitro* einen Komplex mit der RIIα-Untereinheit der PKA und der GSK3β bildet. Weiterhin wurde festgestellt, dass GSKIP in Zellen zu einer Erhöhung der PKA-abhängigen inhibitorischen Phosphorylierung der GSK3β führt.

GSKIP ist evolutionär konserviert. Die den RII- und GSK3β-Bindedomänen entsprechenden Regionen verschiedener Orthologe von GSKIP wurden als Peptid-Spots synthetisiert und hinsichtlich einer RIIα- bzw. GSK3β-Bindung untersucht. Dabei wurde festgestellt, dass die Interaktion mit GSK3β in GSKIP-Orthologen aus Pilzen, Invertebraten und Vertebraten konserviert ist. Die RIIα-Bindung hingegen wurde nur für Vertebraten gezeigt.

Als Basis für die Aufklärung der physiologischen Funktion von GSKIP wurde in dieser Arbeit ein konditionelles GSKIP-*knockout*-Mausmodell generiert. Genomische DNA aus der Maus, welche die GSKIP-kodierende Sequenz enthält, wurde für die Klonierung eines *Targeting*-Vektors verwendet, in dem das Exon 2 des GSKIP-Gens von loxP-Sequenzen flankiert (gefloxt) wurde. Diese ermöglichten eine von der Cre-Rekombinase katalysierte Inaktivierung des Gens. Der *Targeting*-Vektor wurde sequenzspezifisch in das Genom embryonaler Stamm- (ES)-Zellen integriert. Rekombinante ES-Zellen wurden in Mausembryonen injiziert, aus denen sich Mäuse mit einem gefloxten GSKIP-Allel entwickelten. Diese genetische Modifikation wurde an Folgegenerationen vererbt. Durch das Verpaaren mit einem Cre-Rekombinase exprimierenden Mausstamm wurde die gefloxte Sequenz entfernt. Die resultierenden $GSKIP^{+/-}$-Mäuse waren lebens- und fortpflanzungsfähig. Allerdings brachten $GSKIP^{+/-} \times GSKIP^{+/-}$-Verpaarungen keine $GSKIP^{-/-}$-Nachkommen hervor, was auf eine embryonale Lethalität der homozygoten Gendeletion hindeutet.

Zukünftig soll eine detaillierte Analyse des Phänotyps der GSKIP-*knockout*-Maus erfolgen, um die Ursache der embryonalen Lethalität und die physiologische Funktion von GSKIP aufzuklären.

8. Bibliography

[1] Spindel ER (2005) Second-Messenger Systems and Signal Transduction Mechanisms. In *Endocrinology* (Melmed S & Conn PM, eds), pp. 35-48. Humana Press.

[2] Scott JD & Pawson T (2009) Cell signaling in space and time: where proteins come together and when they're apart. *Science*, **326,** 1220-1224.

[3] Hall RA & Lefkowitz RJ (2002) Regulation of G protein-coupled receptor signaling by scaffold proteins. *Circ. Res.*, **91,** 672-680.

[4] Locasale JW, Shaw AS, & Chakraborty AK (2007) Scaffold proteins confer diverse regulatory properties to protein kinase cascades. *Proc. Natl. Acad. Sci. U. S. A*, **104,** 13307-13312.

[5] Pawson CT & Scott JD (2010) Signal integration through blending, bolstering and bifurcating of intracellular information. *Nat. Struct. Mol. Biol.*, **17,** 653-658.

[6] Beavo JA & Brunton LL (2002) Cyclic nucleotide research -- still expanding after half a century. *Nat. Rev. Mol. Cell Biol.*, **3,** 710-718.

[7] Clapham DE & Neer EJ (1997) G protein beta gamma subunits. *Annu. Rev. Pharmacol. Toxicol.*, **37,** 167-203.

[8] Albert PR & Robillard L (2002) G protein specificity: traffic direction required. *Cell Signal.*, **14,** 407-418.

[9] Cooper DM (2005) Compartmentalization of adenylate cyclase and cAMP signalling. *Biochem. Soc. Trans.*, **33,** 1319-1322.

[10] Sunahara RK & Taussig R (2002) Isoforms of mammalian adenylyl cyclase: multiplicities of signaling. *Mol. Interv.*, **2,** 168-184.

[11] Willoughby D & Cooper DM (2007) Organization and Ca2+ regulation of adenylyl cyclases in cAMP microdomains. *Physiol Rev.*, **87,** 965-1010.

[12] Kamenetsky M, Middelhaufe S, Bank EM, Levin LR, Buck J, & Steegborn C (2006) Molecular details of cAMP generation in mammalian cells: a tale of two systems. *J. Mol. Biol.*, **362,** 623-639.

[13] Insel PA & Ostrom RS (2003) Forskolin as a tool for examining adenylyl cyclase expression, regulation, and G protein signaling. *Cell Mol. Neurobiol.*, **23,** 305-314.

[14] de Rooij J, Rehmann H, van Triest M, Cool RH, Wittinghofer A, & Bos JL (2000) Mechanism of regulation of the Epac family of cAMP-dependent RapGEFs. *J. Biol. Chem.*, **275,** 20829-20836.

[15] Shapiro P (2002) Ras-MAP kinase signaling pathways and control of cell proliferation: relevance to cancer therapy. *Crit Rev. Clin. Lab Sci.*, **39,** 285-330.

[16] Conti M & Beavo J (2007) Biochemistry and physiology of cyclic nucleotide phosphodiesterases: essential components in cyclic nucleotide signaling. *Annu. Rev. Biochem.*, **76,** 481-511.

[17] Houslay MD (2010) Underpinning compartmentalised cAMP signalling through targeted cAMP breakdown. *Trends Biochem. Sci.*, **35,** 91-100.

[18] Omori K & Kotera J (2007) Overview of PDEs and their regulation. *Circ. Res.*, **100,** 309-327.

[19] Kim C, Vigil D, Anand G, & Taylor SS (2006) Structure and dynamics of PKA signaling proteins. *Eur. J. Cell Biol.*, **85,** 651-654.

[20] Taylor SS, Kim C, Cheng CY, Brown SH, Wu J, & Kannan N (2008) Signaling through cAMP and cAMP-dependent protein kinase: diverse strategies for drug design. *Biochim. Biophys. Acta*, **1784,** 16-26.

[21] Pearce LR, Komander D, & Alessi DR (2010) The nuts and bolts of AGC protein kinases. *Nat. Rev. Mol. Cell Biol.*, **11,** 9-22.

[22] Edelman AM, Blumenthal DK, & Krebs EG (1987) Protein serine/threonine kinases. *Annu. Rev. Biochem.*, **56,** 567-613.

[23] Shabb JB (2001) Physiological substrates of cAMP-dependent protein kinase. *Chem. Rev.*, **101,** 2381-2411.

[24] Uhler MD, Carmichael DF, Lee DC, Chrivia JC, Krebs EG, & McKnight GS (1986) Isolation of cDNA clones coding for the catalytic subunit of mouse cAMP-dependent protein kinase. *Proc. Natl. Acad. Sci. U. S. A.*, **83,** 1300-1304.

[25] Uhler MD, Chrivia JC, & McKnight GS (1986) Evidence for a second isoform of the catalytic subunit of cAMP-dependent protein kinase. *J. Biol. Chem.*, **261,** 15360-15363.

[26] Showers MO & Maurer RA (1986) A cloned bovine cDNA encodes an alternate form of the catalytic subunit of cAMP-dependent protein kinase. *J. Biol. Chem.*, **261,** 16288-16291.

[27] Beebe SJ, Oyen O, Sandberg M, Froysa A, Hansson V, & Jahnsen T (1990) Molecular cloning of a tissue-specific protein kinase (C gamma) from human testis--representing a third isoform for the catalytic subunit of cAMP-dependent protein kinase. *Mol. Endocrinol.*, **4,** 465-475.

[28] Carlson CR, Ruppelt A, & Tasken K (2003) A kinase anchoring protein (AKAP) interaction and dimerization of the RIalpha and RIbeta regulatory subunits of protein kinase a in vivo by the yeast two hybrid system. *J. Mol. Biol.*, **327,** 609-618.

[29] Tasken K, Skalhegg BS, Solberg R, Andersson KB, Taylor SS, Lea T, Blomhoff HK, Jahnsen T, & Hansson V (1993) Novel isozymes of cAMP-dependent protein kinase exist in human cells due to formation of RI alpha-RI beta heterodimeric complexes. *J. Biol. Chem.*, **268,** 21276-21283.

[30] Barradeau S, Imaizumi-Scherrer T, Weiss MC, & Faust DM (2002) Intracellular targeting of the type-I alpha regulatory subunit of cAMP-dependent protein kinase. *Trends Cardiovasc. Med.*, **12,** 235-241.

[31] Pidoux G & Tasken K (2010) Specificity and spatial dynamics of protein kinase A signaling organized by A-kinase-anchoring proteins. *J. Mol. Endocrinol.*, **44,** 271-284.

[32] Skroblin P, Grossmann S, Schafer G, Rosenthal W, & Klussmann E (2010) Mechanisms of Protein Kinase A Anchoring. *Int. Rev. Cell Mol. Biol.*, **283C,** 235-330.

[33] Cadd G & McKnight GS (1989) Distinct patterns of cAMP-dependent protein kinase gene expression in mouse brain. *Neuron*, **3,** 71-79.

[34] Scott JD (1991) Cyclic nucleotide-dependent protein kinases. *Pharmacol. Ther.*, **50,** 123-145.

[35] Wong W & Scott JD (2004) AKAP signalling complexes: focal points in space and time. *Nat. Rev. Mol. Cell Biol.*, **5,** 959-970.

[36] Welch EJ, Jones BW, & Scott JD (2010) Networking with AKAPs: context-dependent regulation of anchored enzymes. *Mol. Interv.*, **10,** 86-97.

[37] Skalhegg BS & Tasken K (2000) Specificity in the cAMP/PKA signaling pathway. Differential expression,regulation, and subcellular localization of subunits of PKA. *Front. Biosci.*, **5,** D678-D693.

[38] Nolan MA, Babcock DF, Wennemuth G, Brown W, Burton KA, & McKnight GS (2004) Sperm-specific protein kinase A catalytic subunit Calpha2 orchestrates cAMP signaling for male fertility. *Proc. Natl. Acad. Sci. U. S. A.*, **101,** 13483-13488.

[39] Orstavik S, Reinton N, Frengen E, Langeland BT, Jahnsen T, & Skalhegg BS (2001) Identification of novel splice variants of the human catalytic subunit Cbeta of cAMP-dependent protein kinase. *Eur. J. Biochem.*, **268,** 5066-5073.

[40] Solberg R, Sandberg M, Natarajan V, Torjesen PA, Hansson V, Jahnsen T, & Tasken K (1997) The human gene for the regulatory subunit RI alpha of cyclic adenosine 3', 5'-monophosphate-dependent protein kinase: two distinct promoters provide differential regulation of alternately spliced messenger ribonucleic acids. *Endocrinology*, **138,** 169-181.

[41] Sastri M, Barraclough DM, Carmichael PT, & Taylor SS (2005) A-kinase-interacting protein localizes protein kinase A in the nucleus. *Proc. Natl. Acad. Sci. U. S. A.*, **102,** 349-354.

[42] Gao N, Asamitsu K, Hibi Y, Ueno T, & Okamoto T (2008) AKIP1 enhances NF-kappaB-dependent gene expression by promoting the nuclear retention and phosphorylation of p65. *J. Biol. Chem.*, **283,** 7834-7843.

[43] Gangal M, Clifford T, Deich J, Cheng X, Taylor SS, & Johnson DA (1999) Mobilization of the A-kinase N-myristate through an isoform-specific intermolecular switch. *Proc. Natl. Acad. Sci. U. S. A.*, **96,** 12394-12399.

[44] Breitenlechner C, Engh RA, Huber R, Kinzel V, Bossemeyer D, & Gassel M (2004) The typically disordered N-terminus of PKA can fold as a helix and project the myristoylation site into solution. *Biochemistry*, **43,** 7743-7749.

[45] Tholey A, Pipkorn R, Bossemeyer D, Kinzel V, & Reed J (2001) Influence of myristoylation, phosphorylation, and deamidation on the structural behavior of the N-terminus of the catalytic subunit of cAMP-dependent protein kinase. *Biochemistry*, **40,** 225-231.

[46] Kannan N, Neuwald AF, & Taylor SS (2008) Analogous regulatory sites within the alphaC-beta4 loop regions of ZAP-70 tyrosine kinase and AGC kinases. *Biochim. Biophys. Acta*, **1784,** 27-32.

[47] Theurkauf WE & Vallee RB (1982) Molecular characterization of the cAMP-dependent protein kinase bound to microtubule-associated protein 2. *J. Biol. Chem.*, **257,** 3284-3290.

[48] Lohmann SM, DeCamilli P, Einig I, & Walter U (1984) High-affinity binding of the regulatory subunit (RII) of cAMP-dependent protein kinase to microtubule-associated and other cellular proteins. *Proc. Natl. Acad. Sci. U. S. A*, **81,** 6723-6727.

[49] Kinderman FS, Kim C, von Daake S, Ma YL, Pham BQ, Spraggon G, Xuong NH, Jennings PA, & Taylor SS (2006) A dynamic mechanism for AKAP binding to RII isoforms of cAMP-dependent protein kinase. *Molecular Cell*, **24,** 397-408.

[50] Appert-Collin A, Baisamy L, & Diviani D (2006) Regulation of g protein-coupled receptor signaling by a-kinase anchoring proteins. *J. Recept. Signal. Transduct. Res.*, **26,** 631-646.

[51] Dessauer CW (2009) Adenylyl cyclase-A-kinase anchoring protein complexes: the next dimension in cAMP signaling. *Mol. Pharmacol.*, **76,** 935-941.

[52] Nijholt IM, Dolga AM, Ostroveanu A, Luiten PG, Schmidt M, & Eisel UL (2008) Neuronal AKAP150 coordinates PKA and Epac-mediated PKB/Akt phosphorylation. *Cell Signal.*, **20,** 1715-1724.

[53] Stefan E, Wiesner B, Baillie GS, Mollajew R, Henn V, Lorenz D, Furkert J, Santamaria K, Nedvetsky P, Hundsrucker C, Beyermann M, Krause E, Pohl P, Gall I, MacIntyre AN, Bachmann S, Houslay MD, Rosenthal W, & Klussmann E (2007) Compartmentalization of cAMP-dependent signaling by phosphodiesterase-4D is involved in the regulation of vasopressin-mediated water reabsorption in renal principal cells. *J. Am. Soc. Nephrol.*, **18,** 199-212.

[54] Flynn MP, Maizels ET, Karlsson AB, McAvoy T, Ahn JH, Nairn AC, & Hunzicker-Dunn M (2008) Luteinizing hormone receptor activation in ovarian granulosa cells promotes protein kinase A-dependent dephosphorylation of microtubule-associated protein 2D. *Mol. Endocrinol.*, **22,** 1695-1710.

[55] Schillace RV, Voltz JW, Sim AT, Shenolikar S, & Scott JD (2001) Multiple interactions within the AKAP220 signaling complex contribute to protein phosphatase 1 regulation. *J. Biol. Chem.*, **276,** 12128-12134.

[56] Jivan A, Earnest S, Juang YC, & Cobb MH (2009) Radial spoke protein 3 is a mammalian protein kinase A-anchoring protein that binds ERK1/2. *J. Biol. Chem.*, **284,** 29437-29445.

[57] Tanji C, Yamamoto H, Yorioka N, Kohno N, Kikuchi K, & Kikuchi A (2002) A-kinase anchoring protein AKAP220 binds to glycogen synthase kinase-3beta (GSK-3beta) and mediates protein kinase A-dependent inhibition of GSK-3beta. *J. Biol. Chem.*, **277,** 36955-36961.

[58] Hundsrucker C, Skroblin P, Christian F, Zenn HM, Popara V, Joshi M, Eichhorst J, Wiesner B, Herberg FW, Reif B, Rosenthal W, & Klussmann E (2010) Glycogen synthase kinase 3beta interaction protein functions as an A-kinase anchoring protein. *J. Biol. Chem.*, **285,** 5507-5521.

[59] Hulme JT, Ahn M, Hauschka SD, Scheuer T, & Catterall WA (2002) A novel leucine zipper targets AKAP15 and cyclic AMP-dependent protein kinase to the C terminus of the skeletal muscle Ca2+ channel and modulates its function. *J. Biol. Chem.*, **277,** 4079-4087.

[60] Jarnaess E, Ruppelt A, Stokka AJ, Lygren B, Scott JD, & Tasken K (2008) Dual specificity A-kinase anchoring proteins (AKAPs) contain an additional binding region that enhances targeting of protein kinase A type I. *J. Biol. Chem.*, **283,** 33708-33718.

[61] Lim CJ, Han J, Yousefi N, Ma Y, Amieux PS, McKnight GS, Taylor SS, & Ginsberg MH (2007) Alpha4 integrins are type I cAMP-dependent protein kinase-anchoring proteins. *Nat. Cell Biol.*, **9,** 415-421.

[62] Carr DW, Hausken ZE, Fraser ID, Stofko-Hahn RE, & Scott JD (1992) Association of the type II cAMP-dependent protein kinase with a human thyroid RII-anchoring protein. Cloning and characterization of the RII-binding domain. *J. Biol. Chem.*, **267,** 13376-13382.

[63] Herberg FW, Maleszka A, Eide T, Vossebein L, & Tasken K (2000) Analysis of A-kinase anchoring protein (AKAP) interaction with protein kinase A (PKA) regulatory subunits: PKA isoform specificity in AKAP binding. *J. Mol. Biol.*, **298,** 329-339.

[64] McConnell BK, Popovic Z, Mal N, Lee K, Bautista J, Forudi F, Schwartzman R, Jin JP, Penn M, & Bond M (2009) Disruption of protein kinase A interaction with A-kinase-anchoring proteins in the heart in vivo: effects on cardiac contractility, protein kinase A phosphorylation, and troponin I proteolysis. *J. Biol. Chem.*, **284,** 1583-1592.

[65] Hundsrucker C, Rosenthal W, & Klussmann E (2006) Peptides for disruption of PKA anchoring. *Biochem. Soc. Trans.*, **34,** 472-473.

[66] Hundsrucker C, Krause G, Beyermann M, Prinz A, Zimmermann B, Diekmann O, Lorenz D, Stefan E, Nedvetsky P, Dathe M, Christian F, McSorley T, Krause E, McConnachie G, Herberg FW, Scott JD, Rosenthal W, & Klussmann E (2006) High-affinity AKAP7 delta-protein kinase A interaction yields novel protein kinase A-anchoring disruptor peptides. *Biochemical Journal*, **396,** 297-306.

[67] Hundsrucker C & Klussmann E (2008) Direct AKAP-Mediated Protein-Protein Interactions as Potential Drug Targets. *Handb. Exp. Pharmacol.*, 483-503.

[68] Hundsrucker C (2008) Development of peptidic disruptors for the inhibition of AKAP-PKA interactions and bioinformatics approach to identify new AKAPs. *Dissertation, Free University of Berlin*, 1-166.

[69] Zenn HM (2010) Regulation und Koordination der Proteinkinase A im cAMP-vermittelten Signalweg. *Dissertation, University of Kassel*, 1-129.

[70] Chou HY, Howng SL, Cheng TS, Hsiao YL, Lieu AS, Loh JK, Hwang SL, Lin CC, Hsu CM, Wang C, Lee CI, Lu PJ, Chou CK, Huang CY, & Hong YR (2006) GSKIP is homologous to the Axin GSK3beta interaction domain and functions as a negative regulator of GSK3beta. *Biochemistry*, **45,** 11379-11389.

[71] Doble BW & Woodgett JR (2003) GSK-3: tricks of the trade for a multi-tasking kinase. *J. Cell Sci.*, **116,** 1175-1186.

[72] Ali A, Hoeflich KP, & Woodgett JR (2001) Glycogen synthase kinase-3: properties, functions, and regulation. *Chem. Rev.*, **101,** 2527-2540.

[73] Woodgett JR (1990) Molecular cloning and expression of glycogen synthase kinase-3/factor A. *EMBO J.*, **9,** 2431-2438.

[74] Hoeflich KP, Luo J, Rubie EA, Tsao MS, Jin O, & Woodgett JR (2000) Requirement for glycogen synthase kinase-3beta in cell survival and NF-kappaB activation. *Nature*, **406,** 86-90.

[75] Rayasam GV, Tulasi VK, Sodhi R, Davis JA, & Ray A (2009) Glycogen synthase kinase 3: more than a namesake. *Br. J. Pharmacol.*, **156,** 885-898.

[76] Antos CL, McKinsey TA, Frey N, Kutschke W, McAnally J, Shelton JM, Richardson JA, Hill JA, & Olson EN (2002) Activated glycogen synthase-3 beta suppresses cardiac hypertrophy in vivo. *Proc. Natl. Acad. Sci. U. S. A*, **99,** 907-912.

[77] Forde JE & Dale TC (2007) Glycogen synthase kinase 3: a key regulator of cellular fate. *Cell Mol. Life Sci.*, **64,** 1930-1944.

[78] Force T & Woodgett JR (2009) Unique and overlapping functions of GSK-3 isoforms in cell differentiation and proliferation and cardiovascular development. *J. Biol. Chem.*, **284,** 9643-9647.

[79] Fiol CJ, Mahrenholz AM, Wang Y, Roeske RW, & Roach PJ (1987) Formation of protein kinase recognition sites by covalent modification of the substrate. Molecular mechanism for the synergistic action of casein kinase II and glycogen synthase kinase 3. *J. Biol. Chem.*, **262,** 14042-14048.

[80] Frame S, Cohen P, & Biondi RM (2001) A common phosphate binding site explains the unique substrate specificity of GSK3 and its inactivation by phosphorylation. *Mol. Cell*, **7,** 1321-1327.

[81] Patel S, Doble B, & Woodgett JR (2004) Glycogen synthase kinase-3 in insulin and Wnt signalling: a double-edged sword? *Biochem. Soc. Trans.*, **32,** 803-808.

[82] Fang X, Yu SX, Lu Y, Bast RC, Jr., Woodgett JR, & Mills GB (2000) Phosphorylation and inactivation of glycogen synthase kinase 3 by protein kinase A. *Proc. Natl. Acad. Sci. U. S. A*, **97,** 11960-11965.

[83] Li M, Wang X, Meintzer MK, Laessig T, Birnbaum MJ, & Heidenreich KA (2000) Cyclic AMP promotes neuronal survival by phosphorylation of glycogen synthase kinase 3beta. *Mol. Cell Biol.*, **20,** 9356-9363.

[84] Cross DA, Alessi DR, Cohen P, Andjelkovich M, & Hemmings BA (1995) Inhibition of glycogen synthase kinase-3 by insulin mediated by protein kinase B. *Nature*, **378,** 785-789.

[85] Sutherland C, Leighton IA, & Cohen P (1993) Inactivation of glycogen synthase kinase-3 beta by phosphorylation: new kinase connections in insulin and growth-factor signalling. *Biochem. J.*, **296 (Pt 1),** 15-19.

[86] Stambolic V & Woodgett JR (1994) Mitogen inactivation of glycogen synthase kinase-3 beta in intact cells via serine 9 phosphorylation. *Biochem. J.*, **303 (Pt 3),** 701-704.

[87] Zhao X, Zhuang S, Chen Y, Boss GR, & Pilz RB (2005) Cyclic GMP-dependent protein kinase regulates CCAAT enhancer-binding protein beta functions through inhibition of glycogen synthase kinase-3. *J. Biol. Chem.*, **280,** 32683-32692.

[88] Sakoda H, Gotoh Y, Katagiri H, Kurokawa M, Ono H, Onishi Y, Anai M, Ogihara T, Fujishiro M, Fukushima Y, Abe M, Shojima N, Kikuchi M, Oka Y, Hirai H, & Asano T (2003) Differing roles of Akt and serum- and glucocorticoid-regulated kinase in glucose metabolism, DNA synthesis, and oncogenic activity. *J. Biol. Chem.*, **278,** 25802-25807.

[89] Persad S, Troussard AA, McPhee TR, Mulholland DJ, & Dedhar S (2001) Tumor suppressor PTEN inhibits nuclear accumulation of beta-catenin and T cell/lymphoid enhancer factor 1-mediated transcriptional activation. *J. Cell Biol.*, **153,** 1161-1174.

[90] Fang X, Yu S, Tanyi JL, Lu Y, Woodgett JR, & Mills GB (2002) Convergence of multiple signaling cascades at glycogen synthase kinase 3: Edg receptor-mediated phosphorylation and inactivation by lysophosphatidic acid through a protein kinase C-dependent intracellular pathway. *Mol. Cell Biol.*, **22,** 2099-2110.

[91] Jensen J, Brennesvik EO, Lai YC, & Shepherd PR (2007) GSK-3beta regulation in skeletal muscles by adrenaline and insulin: evidence that PKA and PKB regulate different pools of GSK-3. *Cell Signal.*, **19,** 204-210.

[92] Taurin S, Hogarth K, Sandbo N, Yau DM, & Dulin NO (2007) Gbetagamma-mediated prostacyclin production and cAMP-dependent protein kinase activation by endothelin-1 promotes vascular smooth muscle cell hypertrophy through inhibition of glycogen synthase kinase-3. *J. Biol. Chem.*, **282,** 19518-19525.

[93] Torii K, Nishizawa K, Kawasaki A, Yamashita Y, Katada M, Ito M, Nishimoto I, Terashita K, Aiso S, & Matsuoka M (2008) Anti-apoptotic action of Wnt5a in dermal fibroblasts is mediated by the PKA signaling pathways. *Cell Signal.*, **20,** 1256-1266.

[94] Suzuki A, Ozono K, Kubota T, Kondou H, Tachikawa K, & Michigami T (2008) PTH/cAMP/PKA signaling facilitates canonical Wnt signaling via inactivation of glycogen synthase kinase-3beta in osteoblastic Saos-2 cells. *J. Cell Biochem.*, **104,** 304-317.

[95] Fujino H, West KA, & Regan JW (2002) Phosphorylation of glycogen synthase kinase-3 and stimulation of T-cell factor signaling following activation of EP2 and EP4 prostanoid receptors by prostaglandin E2. *J. Biol. Chem.*, **277,** 2614-2619.

[96] Bayatti N, Zschocke J, & Behl C (2003) Brain region-specific neuroprotective action and signaling of corticotropin-releasing hormone in primary neurons. *Endocrinology*, **144,** 4051-4060.

[97] Juhaszova M, Zorov DB, Kim SH, Pepe S, Fu Q, Fishbein KW, Ziman BD, Wang S, Ytrehus K, Antos CL, Olson EN, & Sollott SJ (2004) Glycogen synthase kinase-3beta mediates convergence of protection signaling to inhibit the mitochondrial permeability transition pore. *J. Clin. Invest*, **113,** 1535-1549.

[98] Yusta B, Estall J, & Drucker DJ (2002) Glucagon-like peptide-2 receptor activation engages bad and glycogen synthase kinase-3 in a protein kinase A-dependent manner and prevents apoptosis following inhibition of phosphatidylinositol 3-kinase. *J. Biol. Chem.*, **277,** 24896-24906.

[99] O'Driscoll C, Wallace D, & Cotter TG (2007) bFGF promotes photoreceptor cell survival in vitro by PKA-mediated inactivation of glycogen synthase kinase 3beta and CREB-dependent Bcl-2 up-regulation. *J. Neurochem.*, **103,** 860-870.

[100] Kleiveland CR, Kassem M, & Lea T (2008) Human mesenchymal stem cell proliferation is regulated by PGE2 through differential activation of cAMP-dependent protein kinase isoforms. *Exp. Cell Res.*, **314,** 1831-1838.

[101] Chien AJ, Conrad WH, & Moon RT (2009) A Wnt survival guide: from flies to human disease. *J. Invest Dermatol.*, **129,** 1614-1627.

[102] Hedgepeth CM, Deardorff MA, Rankin K, & Klein PS (1999) Regulation of glycogen synthase kinase 3beta and downstream Wnt signaling by axin. *Mol. Cell Biol.*, **19,** 7147-7157.

[103] Dajani R, Fraser E, Roe SM, Yeo M, Good VM, Thompson V, Dale TC, & Pearl LH (2003) Structural basis for recruitment of glycogen synthase kinase 3beta to the axin-APC scaffold complex. *EMBO J.*, **22,** 494-501.

[104] Rubinfeld B, Tice DA, & Polakis P (2001) Axin-dependent phosphorylation of the adenomatous polyposis coli protein mediated by casein kinase 1epsilon. *J. Biol. Chem.*, **276,** 39037-39045.

[105] Howng SL, Hwang CC, Hsu CY, Hsu MY, Teng CY, Chou CH, Lee MF, Wu CH, Chiou SJ, Lieu AS, Loh JK, Yang CN, Lin CS, & Hong YR (2010) Involvement of the residues of GSKIP, AxinGID, and FRATtide in their binding with GSK3beta to unravel a novel C-terminal scaffold-binding region. *Mol. Cell Biochem.*, **339,** 23-33.

[106] Ewing RM, Chu P, Elisma F, Li H, Taylor P, Climie S, McBroom-Cerajewski L, Robinson MD, O'Connor L, Li M, Taylor R, Dharsee M, Ho Y, Heilbut A, Moore L, Zhang S, Ornatsky O, Bukhman YV, Ethier M, Sheng Y, Vasilescu J, Abu-Farha M, Lambert JP, Duewel HS, Stewart II, Kuehl B, Hogue K, Colwill K, Gladwish K, Muskat B, Kinach R, Adams SL, Moran MF, Morin GB, Topaloglou T, & Figeys D (2007) Large-scale mapping of human protein-protein interactions by mass spectrometry. *Mol. Syst. Biol.*, **3,** 89.

[107] Pilot-Storck F, Chopin E, Rual JF, Baudot A, Dobrokhotov P, Robinson-Rechavi M, Brun C, Cusick ME, Hill DE, Schaeffer L, Vidal M, & Goillot E (2010) Interactome mapping of the phosphatidylinositol 3-kinase-mammalian target of rapamycin pathway identifies deformed epidermal autoregulatory factor-1 as a new glycogen synthase kinase-3 interactor. *Mol. Cell Proteomics.*, **9,** 1578-1593.

[108] Wu C, Orozco C, Boyer J, Leglise M, Goodale J, Batalov S, Hodge CL, Haase J, Janes J, Huss JW, III, & Su AI (2009) BioGPS: an extensible and customizable portal for querying and organizing gene annotation resources. *Genome Biol.*, **10,** R130.

[109] Su AI, Wiltshire T, Batalov S, Lapp H, Ching KA, Block D, Zhang J, Soden R, Hayakawa M, Kreiman G, Cooke MP, Walker JR, & Hogenesch JB (2004) A gene atlas of the mouse and human protein-encoding transcriptomes. *Proc. Natl. Acad. Sci. U. S. A*, **101,** 6062-6067.

[110] Walker JR, Su AI, Self DW, Hogenesch JB, Lapp H, Maier R, Hoyer D, & Bilbe G (2004) Applications of a rat multiple tissue gene expression data set. *Genome Res.*, **14,** 742-749.

[111] Lattin JE, Schroder K, Su AI, Walker JR, Zhang J, Wiltshire T, Saijo K, Glass CK, Hume DA, Kellie S, & Sweet MJ (2008) Expression analysis of G Protein-Coupled Receptors in mouse macrophages. *Immunome. Res.*, **4,** 5.

[112] Bateman A, Coin L, Durbin R, Finn RD, Hollich V, Griffiths-Jones S, Khanna A, Marshall M, Moxon S, Sonnhammer EL, Studholme DJ, Yeats C, & Eddy SR (2004) The Pfam protein families database. *Nucleic Acids Res.*, **32,** D138-D141.

[113] Hunter S, Apweiler R, Attwood TK, Bairoch A, Bateman A, Binns D, Bork P, Das U, Daugherty L, Duquenne L, Finn RD, Gough J, Haft D, Hulo N, Kahn D, Kelly E, Laugraud A, Letunic I, Lonsdale D, Lopez R, Madera M, Maslen J, McAnulla C, McDowall J, Mistry J, Mitchell A, Mulder N, Natale D, Orengo C, Quinn AF, Selengut JD, Sigrist CJ, Thimma M, Thomas PD, Valentin F, Wilson D, Wu CH, & Yeats C (2009) InterPro: the integrative protein signature database. *Nucleic Acids Res.*, **37,** D211-D215.

[114] Waterston RH, Lindblad-Toh K, Birney E, Rogers J, Abril JF, Agarwal P, Agarwala R, Ainscough R, Alexandersson M, An P, Antonarakis SE, Attwood J, Baertsch R, Bailey J, Barlow K, Beck S, Berry E, Birren B, Bloom T, Bork P, Botcherby M, Bray N, Brent MR, Brown DG, Brown SD, Bult C, Burton J, Butler J, Campbell RD, Carninci P, Cawley S, Chiaromonte F, Chinwalla AT, Church DM, Clamp M, Clee C, Collins FS, Cook LL, Copley RR, Coulson A, Couronne O, Cuff J, Curwen V, Cutts T, Daly M, David R, Davies J, Delehaunty KD, Deri J, Dermitzakis ET, Dewey C, Dickens NJ, Diekhans M, Dodge S, Dubchak I, Dunn DM, Eddy SR, Elnitski L, Emes RD, Eswara P, Eyras E, Felsenfeld A, Fewell GA, Flicek P, Foley K, Frankel WN,

Fulton LA, Fulton RS, Furey TS, Gage D, Gibbs RA, Glusman G, Gnerre S, Goldman N, Goodstadt L, Grafham D, Graves TA, Green ED, Gregory S, Guigo R, Guyer M, Hardison RC, Haussler D, Hayashizaki Y, Hillier LW, Hinrichs A, Hlavina W, Holzer T, Hsu F, Hua A, Hubbard T, Hunt A, Jackson I, Jaffe DB, Johnson LS, Jones M, Jones TA, Joy A, Kamal M, Karlsson EK, Karolchik D, Kasprzyk A, Kawai J, Keibler E, Kells C, Kent WJ, Kirby A, Kolbe DL, Korf I, Kucherlapati RS, Kulbokas EJ, Kulp D, Landers T, Leger JP, Leonard S, Letunic I, Levine R, Li J, Li M, Lloyd C, Lucas S, Ma B, Maglott DR, Mardis ER, Matthews L, Mauceli E, Mayer JH, McCarthy M, McCombie WR, McLaren S, McLay K, McPherson JD, Meldrim J, Meredith B, Mesirov JP, Miller W, Miner TL, Mongin E, Montgomery KT, Morgan M, Mott R, Mullikin JC, Muzny DM, Nash WE, Nelson JO, Nhan MN, Nicol R, Ning Z, Nusbaum C, O'Connor MJ, Okazaki Y, Oliver K, Overton-Larty E, Pachter L, Parra G, Pepin KH, Peterson J, Pevzner P, Plumb R, Pohl CS, Poliakov A, Ponce TC, Ponting CP, Potter S, Quail M, Reymond A, Roe BA, Roskin KM, Rubin EM, Rust AG, Santos R, Sapojnikov V, Schultz B, Schultz J, Schwartz MS, Schwartz S, Scott C, Seaman S, Searle S, Sharpe T, Sheridan A, Shownkeen R, Sims S, Singer JB, Slater G, Smit A, Smith DR, Spencer B, Stabenau A, Stange-Thomann N, Sugnet C, Suyama M, Tesler G, Thompson J, Torrents D, Trevaskis E, Tromp J, Ucla C, Ureta-Vidal A, Vinson JP, Von Niederhausern AC, Wade CM, Wall M, Weber RJ, Weiss RB, Wendl MC, West AP, Wetterstrand K, Wheeler R, Whelan S, Wierzbowski J, Willey D, Williams S, Wilson RK, Winter E, Worley KC, Wyman D, Yang S, Yang SP, Zdobnov EM, Zody MC, & Lander ES (2002) Initial sequencing and comparative analysis of the mouse genome. *Nature*, **420,** 520-562.

[115] Evans MJ & Kaufman MH (1981) Establishment in culture of pluripotential cells from mouse embryos. *Nature*, **292,** 154-156.

[116] Martin GR (1981) Isolation of a pluripotent cell line from early mouse embryos cultured in medium conditioned by teratocarcinoma stem cells. *Proc. Natl. Acad. Sci. U. S. A*, **78,** 7634-7638.

[117] Smithies O, Gregg RG, Boggs SS, Koralewski MA, & Kucherlapati RS (1985) Insertion of DNA sequences into the human chromosomal beta-globin locus by homologous recombination. *Nature*, **317,** 230-234.

[118] Bradley A, Evans M, Kaufman MH, & Robertson E (1984) Formation of germ-line chimaeras from embryo-derived teratocarcinoma cell lines. *Nature*, **309,** 255-256.

[119] Doetschman T, Maeda N, & Smithies O (1988) Targeted mutation of the Hprt gene in mouse embryonic stem cells. *Proc. Natl. Acad. Sci. U. S. A*, **85,** 8583-8587.

[120] Thomas KR & Capecchi MR (1987) Site-directed mutagenesis by gene targeting in mouse embryo-derived stem cells. *Cell*, **51,** 503-512.

[121] Friedel RH, Wurst W, Wefers B, & Kuhn R (2011) Generating conditional knockout mice. *Methods Mol. Biol.*, **693,** 205-231.

[122] Bronson RT (2001) How to study pathologic phenotypes of knockout mice. *Methods Mol. Biol.*, **158,** 155-180.

[123] Kos CH (2004) Cre/loxP system for generating tissue-specific knockout mouse models. *Nutr. Rev.*, **62,** 243-246.

[124] Sauer B & Henderson N (1988) Site-specific DNA recombination in mammalian cells by the Cre recombinase of bacteriophage P1. *Proc. Natl. Acad. Sci. U. S. A*, **85,** 5166-5170.

[125] O'Gorman S, Fox DT, & Wahl GM (1991) Recombinase-mediated gene activation and site-specific integration in mammalian cells. *Science*, **251,** 1351-1355.

[126] Esposito D & Scocca JJ (1997) The integrase family of tyrosine recombinases: evolution of a conserved active site domain. *Nucleic Acids Res.*, **25,** 3605-3614.

[127] Kuhn R & Torres RM (2002) Cre/loxP recombination system and gene targeting. *Methods Mol. Biol.*, **180,** 175-204.

[128] Branda CS & Dymecki SM (2004) Talking about a revolution: The impact of site-specific recombinases on genetic analyses in mice. *Dev. Cell*, **6,** 7-28.

[129] Schmidt A, Wiesner B, Weisshart K, Schulz K, Furkert J, Lamprecht B, Rosenthal W, & Schulein R (2009) Use of Kaede fusions to visualize recycling of G protein-coupled receptors. *Traffic.*, **10,** 2-15.

[130] Henn V, Edemir B, Stefan E, Wiesner B, Lorenz D, Theilig F, Schmitt R, Vossebein L, Tamma G, Beyermann M, Krause E, Herberg FW, Valenti G, Bachmann S, Rosenthal W, & Klussmann E (2004) Identification of a novel A-kinase anchoring protein 18 isoform and evidence for its role in the vasopressin-induced aquaporin-2 shuttle in renal principal cells. *J. Biol. Chem.*, **279,** 26654-26665.

[131] Graham FL, Smiley J, Russell WC, & Nairn R (1977) Characteristics of a human cell line transformed by DNA from human adenovirus type 5. *J. Gen. Virol.*, **36,** 59-74.

[132] Ross RA, Spengler BA, & Biedler JL (1983) Coordinate morphological and biochemical interconversion of human neuroblastoma cells. *J. Natl. Cancer Inst.*, **71,** 741-747.

[133] Hooper M, Hardy K, Handyside A, Hunter S, & Monk M (1987) HPRT-deficient (Lesch-Nyhan) mouse embryos derived from germline colonization by cultured cells. *Nature*, **326,** 292-295.

[134] Niendorf S (2005) Analyse der in vivo Funktion der murinen Ubiquitin-Isopeptidase UBPY. *Dissertation, Free University Berlin*, 1-136.

[135] Farley FW, Soriano P, Steffen LS, & Dymecki SM (2000) Widespread recombinase expression using FLPeR (flipper) mice. *Genesis.*, **28,** 106-110.

[136] Rodriguez CI, Buchholz F, Galloway J, Sequerra R, Kasper J, Ayala R, Stewart AF, & Dymecki SM (2000) High-efficiency deleter mice show that FLPe is an alternative to Cre-loxP. *Nat. Genet.*, **25,** 139-140.

[137] Schwenk F, Baron U, & Rajewsky K (1995) A cre-transgenic mouse strain for the ubiquitous deletion of loxP-flanked gene segments including deletion in germ cells. *Nucleic Acids Res.*, **23,** 5080-5081.

[138] Osoegawa K, Tateno M, Woon PY, Frengen E, Mammoser AG, Catanese JJ, Hayashizaki Y, & de Jong PJ (2000) Bacterial artificial chromosome libraries for mouse sequencing and functional analysis. *Genome Res.*, **10,** 116-128.

[139] Southern EM (1975) Detection of specific sequences among DNA fragments separated by gel electrophoresis. *J. Mol. Biol.*, **98,** 503-517.

[140] Oksche A, Boese G, Horstmeyer A, Furkert J, Beyermann M, Bienert M, & Rosenthal W (2000) Late endosomal/lysosomal targeting and lack of recycling of the ligand-occupied endothelin B receptor. *Mol. Pharmacol.*, **57,** 1104-1113.

[141] Frank R (2002) The SPOT-synthesis technique. Synthetic peptide arrays on membrane supports--principles and applications. *J. Immunol. Methods*, **267,** 13-26.

[142] Kramer A & Schneider-Mergener J (1998) Synthesis and screening of peptide libraries on continuous cellulose membrane supports. *Methods Mol. Biol.*, **87,** 25-39.

[143] Bregman DB, Bhattacharyya N, & Rubin CS (1989) High affinity binding protein for the regulatory subunit of cAMP-dependent protein kinase II-B. Cloning, characterization, and expression of cDNAs for rat brain P150. *J. Biol. Chem.*, **264,** 4648-4656.

[144] Klussmann E, Maric K, Wiesner B, Beyermann M, & Rosenthal W (1999) Protein kinase A anchoring proteins are required for vasopressin-mediated translocation of aquaporin-2 into cell membranes of renal principal cells. *J. Biol. Chem.*, **274,** 4934-4938.

[145] Vaynberg J & Qin J (2006) Weak protein-protein interactions as probed by NMR spectroscopy. *Trends Biotechnol.*, **24,** 22-27.

[146] Piotto M, Saudek V, & Sklenar V (1992) Gradient-tailored excitation for single-quantum NMR spectroscopy of aqueous solutions. *J. Biomol. NMR*, **2,** 661-665.

[147] Johnson BV, Shindo N, Rathjen PD, Rathjen J, & Keough RA (2008) Understanding pluripotency--how embryonic stem cells keep their options open. *Mol. Hum. Reprod.*, **14,** 513-520.

[148] Poueymirou WT, Auerbach W, Frendewey D, Hickey JF, Escaravage JM, Esau L, Dore AT, Stevens S, Adams NC, Dominguez MG, Gale NW, Yancopoulos GD, DeChiara TM, & Valenzuela DM (2007) F0 generation mice fully derived from gene-targeted embryonic stem cells allowing immediate phenotypic analyses. *Nat. Biotechnol.*, **25,** 91-99.

[149] Bacia K & Schwille P (2007) Fluorescence correlation spectroscopy. *Methods Mol. Biol.*, **398,** 73-84.

[150] Hwang LC & Wohland T (2007) Recent advances in fluorescence cross-correlation spectroscopy. *Cell Biochem. Biophys.*, **49,** 1-13.

[151] Bacia K, Kim SA, & Schwille P (2006) Fluorescence cross-correlation spectroscopy in living cells. *Nat. Methods*, **3,** 83-89.

[152] Yokoyama N, Yin D, & Malbon CC (2007) Abundance, complexation, and trafficking of Wnt/beta-catenin signaling elements in response to Wnt3a. *J. Mol. Signal.*, **2,** 11.

[153] Hoshi M, Sato M, Kondo S, Takashima A, Noguchi K, Takahashi M, Ishiguro K, & Imahori K (1995) Different localization of tau protein kinase I/glycogen synthase kinase-3 beta from glycogen synthase kinase-3 alpha in cerebellum mitochondria. *J. Biochem.*, **118,** 683-685.

[154] Lin CC, Chou CH, Howng SL, Hsu CY, Hwang CC, Wang C, Hsu CM, & Hong YR (2009) GSKIP, an inhibitor of GSK3beta, mediates the N-cadherin/beta-catenin pool in the differentiation of SH-SY5Y cells. *J. Cell Biochem.*, **108,** 1325-1336.

[155] Prudovsky I, Tarantini F, Landriscina M, Neivandt D, Soldi R, Kirov A, Small D, Kathir KM, Rajalingam D, & Kumar TK (2008) Secretion without Golgi. *J. Cell Biochem.*, **103,** 1327-1343.

[156] Bendtsen JD, Nielsen H, von HG, & Brunak S (2004) Improved prediction of signal peptides: SignalP 3.0. *J. Mol. Biol.*, **340,** 783-795.

[157] Bendtsen JD, Jensen LJ, Blom N, von HG, & Brunak S (2004) Feature-based prediction of non-classical and leaderless protein secretion. *Protein Eng Des Sel*, **17,** 349-356.

[158] Krogh A, Larsson B, von HG, & Sonnhammer EL (2001) Predicting transmembrane protein topology with a hidden Markov model: application to complete genomes. *J. Mol. Biol.*, **305,** 567-580.

[159] Cokol M, Nair R, & Rost B (2000) Finding nuclear localization signals. *EMBO Rep.*, **1,** 411-415.

[160] la Cour T., Kiemer L, Molgaard A, Gupta R, Skriver K, & Brunak S (2004) Analysis and prediction of leucine-rich nuclear export signals. *Protein Eng Des Sel*, **17,** 527-536.

[161] Guda C & Subramaniam S (2005) pTARGET [corrected] a new method for predicting protein subcellular localization in eukaryotes. *Bioinformatics.*, **21,** 3963-3969.

[162] Briesemeister S, Rahnenfuhrer J, & Kohlbacher O (2010) YLoc--an interpretable web server for predicting subcellular localization. *Nucleic Acids Res.*, **38 Suppl,** W497-W502.

[163] Briesemeister S, Rahnenfuhrer J, & Kohlbacher O (2010) Going from where to why--interpretable prediction of protein subcellular localization. *Bioinformatics.*, **26,** 1232-1238.

[164] Briesemeister S, Blum T, Brady S, Lam Y, Kohlbacher O, & Shatkay H (2009) SherLoc2: a high-accuracy hybrid method for predicting subcellular localization of proteins. *J. Proteome. Res.*, **8,** 5363-5366.

[165] Blum T, Briesemeister S, & Kohlbacher O (2009) MultiLoc2: integrating phylogeny and Gene Ontology terms improves subcellular protein localization prediction. *BMC. Bioinformatics.*, **10,** 274.

[166] Seibel NM, Eljouni J, Nalaskowski MM, & Hampe W (2007) Nuclear localization of enhanced green fluorescent protein homomultimers. *Anal. Biochem.*, **368,** 95-99.

[167] Lester LB, Langeberg LK, & Scott JD (1997) Anchoring of protein kinase A facilitates hormone-mediated insulin secretion. *Proc. Natl. Acad. Sci. U. S. A*, **94,** 14942-14947.

[168] Pan C, Kumar C, Bohl S, Klingmueller U, & Mann M (2009) Comparative proteomic phenotyping of cell lines and primary cells to assess preservation of cell type-specific functions. *Mol. Cell Proteomics.*, **8,** 443-450.

[169] Figeys D (2004) Combining different 'omics' technologies to map and validate protein-protein interactions in humans. *Brief. Funct. Genomic. Proteomic.*, **2,** 357-365.

[170] Tian JM & Schibler U (1991) Tissue-specific expression of the gene encoding hepatocyte nuclear factor 1 may involve hepatocyte nuclear factor 4. *Genes Dev.*, **5,** 2225-2234.

[171] Fraser ID, Tavalin SJ, Lester LB, Langeberg LK, Westphal AM, Dean RA, Marrion NV, & Scott JD (1998) A novel lipid-anchored A-kinase Anchoring Protein facilitates cAMP-responsive membrane events. *EMBO J.*, **17,** 2261-2272.

[172] Henn V, Edemir B, Stefan E, Wiesner B, Lorenz D, Theilig F, Schmitt R, Vossebein L, Tamma G, Beyermann M, Krause E, Herberg FW, Valenti G, Bachmann S, Rosenthal W, & Klussmann E (2004) Identification of a novel A-kinase anchoring protein 18 isoform and evidence for its role in the vasopressin-induced aquaporin-2 shuttle in renal principal cells. *J. Biol. Chem.*, **279,** 26654-26665.

[173] Cardarelli F, Bizzarri R, Serresi M, Albertazzi L, & Beltram F (2009) Probing nuclear localization signal-importin alpha binding equilibria in living cells. *J. Biol. Chem.*, **284,** 36638-36646.

[174] Ota T, Suzuki Y, Nishikawa T, Otsuki T, Sugiyama T, Irie R, Wakamatsu A, Hayashi K, Sato H, Nagai K, Kimura K, Makita H, Sekine M, Obayashi M, Nishi T, Shibahara T, Tanaka T, Ishii S, Yamamoto J, Saito K, Kawai Y, Isono Y, Nakamura Y, Nagahari K, Murakami K, Yasuda T, Iwayanagi T, Wagatsuma M, Shiratori A, Sudo H, Hosoiri T, Kaku Y, Kodaira H, Kondo H, Sugawara M, Takahashi M, Kanda K, Yokoi T, Furuya T, Kikkawa E, Omura Y, Abe K, Kamihara K, Katsuta N, Sato K, Tanikawa M, Yamazaki M, Ninomiya K, Ishibashi T, Yamashita H, Murakawa K, Fujimori K, Tanai H, Kimata M, Watanabe M, Hiraoka S, Chiba Y, Ishida S, Ono Y, Takiguchi S, Watanabe S, Yosida M, Hotuta T, Kusano J, Kanehori K, Takahashi-Fujii A, Hara H, Tanase TO, Nomura Y, Togiya S, Komai F, Hara R, Takeuchi K, Arita M, Imose N, Musashino K, Yuuki H, Oshima A, Sasaki N, Aotsuka S, Yoshikawa Y, Matsunawa H, Ichihara T, Shiohata N, Sano S, Moriya S, Momiyama H, Satoh N, Takami S, Terashima Y, Suzuki O, Nakagawa S, Senoh A, Mizoguchi H, Goto Y, Shimizu F, Wakebe H, Hishigaki H, Watanabe T, Sugiyama A, Takemoto M, Kawakami B, Yamazaki M, Watanabe K, Kumagai A, Itakura S, Fukuzumi Y, Fujimori Y, Komiyama M, Tashiro H, Tanigami A, Fujiwara T, Ono T, Yamada K, Fujii Y, Ozaki K, Hirao M, Ohmori Y, Kawabata A, Hikiji T, Kobatake N, Inagaki H, Ikema Y, Okamoto S, Okitani R, Kawakami T, Noguchi S, Itoh T, Shigeta K, Senba T, Matsumura K, Nakajima Y, Mizuno T, Morinaga M, Sasaki M, Togashi T, Oyama M, Hata H, Watanabe M, Komatsu T, Mizushima-Sugano J, Satoh T, Shirai Y, Takahashi

Y, Nakagawa K, Okumura K, Nagase T, Nomura N, Kikuchi H, Masuho Y, Yamashita R, Nakai K, Yada T, Nakamura Y, Ohara O, Isogai T, & Sugano S (2004) Complete sequencing and characterization of 21,243 full-length human cDNAs. *Nat. Genet.*, **36,** 40-45.

[175] Li S, Armstrong CM, Bertin N, Ge H, Milstein S, Boxem M, Vidalain PO, Han JD, Chesneau A, Hao T, Goldberg DS, Li N, Martinez M, Rual JF, Lamesch P, Xu L, Tewari M, Wong SL, Zhang LV, Berriz GF, Jacotot L, Vaglio P, Reboul J, Hirozane-Kishikawa T, Li Q, Gabel HW, Elewa A, Baumgartner B, Rose DJ, Yu H, Bosak S, Sequerra R, Fraser A, Mango SE, Saxton WM, Strome S, Van Den Heuvel S, Piano F, Vandenhaute J, Sardet C, Gerstein M, Doucette-Stamm L, Gunsalus KC, Harper JW, Cusick ME, Roth FP, Hill DE, & Vidal M (2004) A map of the interactome network of the metazoan C. elegans. *Science*, **303,** 540-543.

[176] Zhang F, Phiel CJ, Spece L, Gurvich N, & Klein PS (2003) Inhibitory phosphorylation of glycogen synthase kinase-3 (GSK-3) in response to lithium. Evidence for autoregulation of GSK-3. *J. Biol. Chem.*, **278,** 33067-33077.

[177] Smalley MJ, Sara E, Paterson H, Naylor S, Cook D, Jayatilake H, Fryer LG, Hutchinson L, Fry MJ, & Dale TC (1999) Interaction of axin and Dvl-2 proteins regulates Dvl-2-stimulated TCF-dependent transcription. *EMBO J.*, **18,** 2823-2835.

[178] McGuffin LJ, Bryson K, & Jones DT (2000) The PSIPRED protein structure prediction server. *Bioinformatics.*, **16,** 404-405.

[179] Sanchez C, Diaz-Nido J, & Avila J (2000) Phosphorylation of microtubule-associated protein 2 (MAP2) and its relevance for the regulation of the neuronal cytoskeleton function. *Prog. Neurobiol.*, **61,** 133-168.

[180] Ferhat L, Ben-Ari Y, & Khrestchatisky M (1994) Complete sequence of rat MAP2d, a novel MAP2 isoform. *C R. Acad. Sci. III*, **317,** 304-309.

[181] Obar RA, Dingus J, Bayley H, & Vallee RB (1989) The RII subunit of cAMP-dependent protein kinase binds to a common amino-terminal domain in microtubule-associated proteins 2A, 2B, and 2C. *Neuron*, **3,** 639-645.

[182] Salvador LM, Flynn MP, Avila J, Reierstad S, Maizels ET, Alam H, Park Y, Scott JD, Carr DW, & Hunzicker-Dunn M (2004) Neuronal microtubule-associated protein 2D is a dual a-kinase anchoring protein expressed in rat ovarian granulosa cells. *J. Biol. Chem.*, **279,** 27621-27632.

[183] Rhodes DR, Kalyana-Sundaram S, Mahavisno V, Varambally R, Yu J, Briggs BB, Barrette TR, Anstet MJ, Kincead-Beal C, Kulkarni P, Varambally S, Ghosh D, & Chinnaiyan AM (2007) Oncomine 3.0: genes, pathways, and networks in a collection of 18,000 cancer gene expression profiles. *Neoplasia.*, **9,** 166-180.

[184] Sun L, Hui AM, Su Q, Vortmeyer A, Kotliarov Y, Pastorino S, Passaniti A, Menon J, Walling J, Bailey R, Rosenblum M, Mikkelsen T, & Fine HA (2006) Neuronal and glioma-derived stem cell factor induces angiogenesis within the brain. *Cancer Cell*, **9,** 287-300.

[185] Liang Y, Diehn M, Watson N, Bollen AW, Aldape KD, Nicholas MK, Lamborn KR, Berger MS, Botstein D, Brown PO, & Israel MA (2005) Gene expression profiling reveals molecularly and clinically distinct subtypes of glioblastoma multiforme. *Proc. Natl. Acad. Sci. U. S. A*, **102,** 5814-5819.

[186] Buchholz M, Braun M, Heidenblut A, Kestler HA, Kloppel G, Schmiegel W, Hahn SA, Luttges J, & Gress TM (2005) Transcriptome analysis of microdissected pancreatic intraepithelial neoplastic lesions. *Oncogene*, **24,** 6626-6636.

[187] Kaiser S, Park YK, Franklin JL, Halberg RB, Yu M, Jessen WJ, Freudenberg J, Chen X, Haigis K, Jegga AG, Kong S, Sakthivel B, Xu H, Reichling T, Azhar M, Boivin GP, Roberts RB, Bissahoyo AC, Gonzales F, Bloom GC, Eschrich S, Carter SL, Aronow JE, Kleimeyer J, Kleimeyer M, Ramaswamy V, Settle SH, Boone B, Levy S, Graff JM, Doetschman T, Groden J, Dove WF, Threadgill DW, Yeatman TJ, Coffey RJ, Jr., & Aronow BJ (2007) Transcriptional recapitulation and subversion of embryonic colon development by mouse colon tumor models and human colon cancer. *Genome Biol.*, **8,** R131.

[188] UniProt Consortium (2011) Ongoing and future developments at the Universal Protein Resource. *Nucleic Acids Res.*, **39,** D214-D219.

[189] LePage DF & Conlon RA (2006) Animal models for disease: knockout, knock-in, and conditional mutant mice. *Methods Mol. Med.*, **129,** 41-67.

[190] Buchholz F, Angrand PO, & Stewart AF (1996) A simple assay to determine the functionality of Cre or FLP recombination targets in genomic manipulation constructs. *Nucleic Acids Res.*, **24,** 3118-3119.

[191] Scarff KL, Ung KS, Sun J, & Bird PI (2003) A retained selection cassette increases reporter gene expression without affecting tissue distribution in SPI3 knockout/GFP knock-in mice. *Genesis.*, **36,** 149-157.

[192] Pham CT, MacIvor DM, Hug BA, Heusel JW, & Ley TJ (1996) Long-range disruption of gene expression by a selectable marker cassette. *Proc. Natl. Acad. Sci. U. S. A*, **93,** 13090-13095.

[193] Yao HB, Shaw PC, Wong CC, & Wan DC (2002) Expression of glycogen synthase kinase-3 isoforms in mouse tissues and their transcription in the brain. *J. Chem. Neuroanat.*, **23,** 291-297.

[194] Lester LB, Coghlan VM, Nauert B, & Scott JD (1996) Cloning and characterization of a novel A-kinase anchoring protein. AKAP 220, association with testicular peroxisomes. *J. Biol. Chem.*, **271,** 9460-9465.

[195] Sarma GN, Kinderman FS, Kim C, von DS, Chen L, Wang BC, & Taylor SS (2010) Structure of D-AKAP2:PKA RI complex: insights into AKAP specificity and selectivity. *Structure.*, **18,** 155-166.

[196] Gold MG, Lygren B, Dokurno P, Hoshi N, McConnachie G, Tasken K, Carlson CR, Scott JD, & Barford D (2006) Molecular basis of AKAP specificity for PKA regulatory subunits. *Molecular Cell*, **24,** 383-395.

[197] Truong K & Ikura M (2001) The use of FRET imaging microscopy to detect protein-protein interactions and protein conformational changes in vivo. *Curr. Opin. Struct. Biol.*, **11,** 573-578.

[198] Selvin PR (1995) Fluorescence resonance energy transfer. *Methods Enzymol.*, **246,** 300-334.

[199] Park H, Pack C, Kinjo M, & Kaang BK (2008) In vivo quantitative analysis of PKA subunit interaction and cAMP level by dual color fluorescence cross correlation spectroscopy. *Mol. Cells*, **26,** 87-92.

[200] Rivard RL, Birger M, Gaston KJ, & Howe AK (2009) AKAP-independent localization of type-II protein kinase A to dynamic actin microspikes. *Cell Motil. Cytoskeleton*, **66,** 693-709.

[201] Seeling JM, Miller JR, Gil R, Moon RT, White R, & Virshup DM (1999) Regulation of beta-catenin signaling by the B56 subunit of protein phosphatase 2A. *Science*, **283,** 2089-2091.

[202] Hsu W, Zeng L, & Costantini F (1999) Identification of a domain of Axin that binds to the serine/threonine protein phosphatase 2A and a self-binding domain. *J. Biol. Chem.*, **274,** 3439-3445.

[203] Cook D, Fry MJ, Hughes K, Sumathipala R, Woodgett JR, & Dale TC (1996) Wingless inactivates glycogen synthase kinase-3 via an intracellular signalling pathway which involves a protein kinase C. *EMBO J.*, **15,** 4526-4536.

[204] Chen G, Bower KA, Ma C, Fang S, Thiele CJ, & Luo J (2004) Glycogen synthase kinase 3beta (GSK3beta) mediates 6-hydroxydopamine-induced neuronal death. *FASEB J.*, **18,** 1162-1164.

[205] Kozlovsky N, Amar S, Belmaker RH, & Agam G (2006) Psychotropic drugs affect Ser9-phosphorylated GSK-3 beta protein levels in rodent frontal cortex. *Int. J. Neuropsychopharmacol.*, **9,** 337-342.

[206] van Amerongen R. & Berns A (2005) Re-evaluating the role of Frat in Wnt-signal transduction. *Cell Cycle*, **4,** 1065-1072.

[207] Luo W & Lin SC (2004) Axin: a master scaffold for multiple signaling pathways. *Neurosignals.*, **13,** 99-113.

[208] Primot A, Baratte B, Gompel M, Borgne A, Liabeuf S, Romette JL, Jho EH, Costantini F, & Meijer L (2000) Purification of GSK-3 by affinity chromatography on immobilized axin. *Protein Expr. Purif.*, **20,** 394-404.

[209] Adamska M, Degnan SM, Green KM, Adamski M, Craigie A, Larroux C, & Degnan BM (2007) Wnt and TGF-beta expression in the sponge Amphimedon queenslandica and the origin of metazoan embryonic patterning. *PLoS. ONE.*, **2,** e1031.

[210] Manuel M (2009) Early evolution of symmetry and polarity in metazoan body plans. *C. R. Biol.*, **332,** 184-209.

[211] Dehmelt L & Halpain S (2005) The MAP2/Tau family of microtubule-associated proteins. *Genome Biol.*, **6,** 204.

[212] Cho JH & Johnson GV (2003) Glycogen synthase kinase 3beta phosphorylates tau at both primed and unprimed sites. Differential impact on microtubule binding. *J. Biol. Chem.*, **278,** 187-193.

[213] Khuchua Z, Wozniak DF, Bardgett ME, Yue Z, McDonald M, Boero J, Hartman RE, Sims H, & Strauss AW (2003) Deletion of the N-terminus of murine map2 by gene targeting disrupts hippocampal ca1 neuron architecture and alters contextual memory. *Neuroscience*, **119,** 101-111.

[214] Iqbal K, Liu F, Gong CX, Alonso AC, & Grundke-Iqbal I (2009) Mechanisms of tau-induced neurodegeneration. *Acta Neuropathol.*, **118,** 53-69.

[215] Huang J, Perez-Burgos L, Placek BJ, Sengupta R, Richter M, Dorsey JA, Kubicek S, Opravil S, Jenuwein T, & Berger SL (2006) Repression of p53 activity by Smyd2-mediated methylation. *Nature*, **444,** 629-632.

[216] Saddic LA, West LE, Aslanian A, Yates JR, III, Rubin SM, Gozani O, & Sage J (2010) Methylation of the retinoblastoma tumor suppressor by SMYD2. *J. Biol. Chem.*, **285,** 37733-37740.

[217] Eom TY & Jope RS (2009) GSK3 beta N-terminus binding to p53 promotes its acetylation. *Mol. Cancer*, **8,** 14.

[218] Felsberg J, Yan PS, Huang TH, Milde U, Schramm J, Wiestler OD, Reifenberger G, Pietsch T, & Waha A (2006) DNA methylation and allelic losses on chromosome arm 14q in oligodendroglial tumours. *Neuropathol. Appl. Neurobiol.*, **32,** 517-524.

[219] Milde T, Pfister S, Korshunov A, Deubzer HE, Oehme I, Ernst A, Starzinski-Powitz A, Seitz A, Lichter P, von DA, & Witt O (2009) Stepwise accumulation of distinct genomic aberrations in a patient with progressively metastasizing ependymoma. *Genes Chromosomes. Cancer*, **48,** 229-238.

[220] Nowicki MO, Dmitrieva N, Stein AM, Cutter JL, Godlewski J, Saeki Y, Nita M, Berens ME, Sander LM, Newton HB, Chiocca EA, & Lawler S (2008) Lithium inhibits invasion of glioma cells; possible involvement of glycogen synthase kinase-3. *Neuro. Oncol.*, **10,** 690-699.

[221] Korur S, Huber RM, Sivasankaran B, Petrich M, Morin P, Jr., Hemmings BA, Merlo A, & Lino MM (2009) GSK3beta regulates differentiation and growth arrest in glioblastoma. *PLoS. ONE.*, **4,** e7443.

[222] Miyashita K, Kawakami K, Nakada M, Mai W, Shakoori A, Fujisawa H, Hayashi Y, Hamada J, & Minamoto T (2009) Potential therapeutic effect of glycogen synthase kinase 3beta inhibition against human glioblastoma. *Clin. Cancer Res.*, **15,** 887-897.

[223] Aguilar-Morante D, Morales-Garcia JA, Sanz-SanCristobal M, Garcia-Cabezas MA, Santos A, & Perez-Castillo A (2010) Inhibition of glioblastoma growth by the thiadiazolidinone compound TDZD-8. *PLoS. ONE.*, **5,** e13879.

[224] Ku BM, Lee YK, Jeong JY, Ryu J, Choi J, Kim JS, Cho YW, Roh GS, Kim HJ, Cho GJ, Choi WS, & Kang SS (2010) Caffeine inhibits cell proliferation and regulates PKA/GSK3beta pathways in U87MG human glioma cells. *Mol. Cells*.

[225] Lu Y, Zhang M, Lim IA, Hall DD, Allen M, Medvedeva Y, McKnight GS, Usachev YM, & Hell JW (2008) AKAP150-anchored PKA activity is important for LTD during its induction phase. *J. Physiol*, **586,** 4155-4164.

[226] Lu Y, Allen M, Halt AR, Weisenhaus M, Dallapiazza RF, Hall DD, Usachev YM, McKnight GS, & Hell JW (2007) Age-dependent requirement of AKAP150-anchored PKA and GluR2-lacking AMPA receptors in LTP. *EMBO J.*, **26,** 4879-4890.

[227] Schnizler K, Shutov LP, Van Kanegan MJ, Merrill MA, Nichols B, McKnight GS, Strack S, Hell JW, & Usachev YM (2008) Protein kinase A anchoring via AKAP150 is essential for TRPV1 modulation by forskolin and prostaglandin E2 in mouse sensory neurons. *J. Neurosci.*, **28,** 4904-4917.

[228] Tingley WG, Pawlikowska L, Zaroff JG, Kim T, Nguyen T, Young SG, Vranizan K, Kwok PY, Whooley MA, & Conklin BR (2007) Gene-trapped mouse embryonic stem cell-derived cardiac myocytes and human genetics implicate AKAP10 in heart rhythm regulation. *Proc. Natl. Acad. Sci. U. S. A.*, **104,** 8461-8466.

[229] McManus EJ, Sakamoto K, Armit LJ, Ronaldson L, Shpiro N, Marquez R, & Alessi DR (2005) Role that phosphorylation of GSK3 plays in insulin and Wnt signalling defined by knockin analysis. *EMBO J.*, **24,** 1571-1583.

[230] van Amerongen R., Nawijn M, Franca-Koh J, Zevenhoven J, van der Gulden H, Jonkers J, & Berns A (2005) Frat is dispensable for canonical Wnt signaling in mammals. *Genes Dev.*, **19,** 425-430.

[231] Bax B, Carter PS, Lewis C, Guy AR, Bridges A, Tanner R, Pettman G, Mannix C, Culbert AA, Brown MJ, Smith DG, & Reith AD (2001) The structure of phosphorylated GSK-3beta complexed with a peptide, FRATtide, that inhibits beta-catenin phosphorylation. *Structure.*, **9,** 1143-1152.

9. Publications

This work was published partially in the publications indicated by *.

Original articles

- Nedvetsky PI, Tabor V, Tamma G, Beulshausen S, Skroblin P, Kirschner A, Mutig K, Boltzen M, Petrucci O, Vossenkämper A, Wiesner B, Bachmann S, Rosenthal W, Klussmann E. Reciprocal regulation of aquaporin-2 abundance and degradation by protein kinase A and p38-MAP kinase. *J Am Soc Nephrol*. 2010 Oct;21(10):1645-56
- Hundsrucker C[$], Skroblin P[$], Christian F, Zenn HM, Popara V, Joshi M, Eichhorst J, Wiesner B, Herberg FW, Reif B, Rosenthal W, Klussmann E. Glycogen synthase kinase 3β interaction protein functions as an A-kinase anchoring protein. *J Biol Chem*. 2010 Feb 19;285(8):5507-21*
  [$]Both authors contributed equally to this manuscript.
- Lehmann K, Müller JP, Schlott B, Skroblin P, Barz D, Norgauer J, Wetzker R. PI3Kgamma controls oxidative bursts in neutrophils via interactions with PKCalpha and p47phox. *Biochem J*. 2009 May 1;419(3):603-10

Book chapter

- Skroblin P, Grossmann S, Schäfer G, Rosenthal W, Klussmann E. Mechanisms of protein kinase A anchoring. *Int Rev Cell Mol Biol*. 2010 283:235-330*

Oral presentations

- Skroblin P, Hundsrucker C, Rosenthal W, Klussmann E. Evolutionary Conservation of protein-protein interaction modules in glycogen synthase kinase 3 β interaction protein (GSKIP). Peptide Arrays as Tools for Study of Protein Interactions, London, United Kingdom, March 16, 2011
- Skroblin P, Hundsrucker C, Christian F, Rosenthal W, Klussmann E. Compartmentalisation of cAMP signalling in the control of aquaporin-2 trafficking. International Epithelial Transport Workshop, Strobl, Austria, June 26, 2010
- Skroblin P, Hundsrucker C, Christian F, Rosenthal W, Klussmann E. Identification of the new AKAP GSKIP in a peptide array-based approach. University of Oslo Institute for Experimental Medical Research Meeting, Berlin, Germany, May 28, 2010
- Skroblin P, Hundsrucker C, Christian F, Zenn HM, Herberg FW, Rosenthal W, Klussmann E. Identification of GSKIP as an AKAP. *Naunyn-Schmiedeberg's Arch Pharamcol*. 2009 379 (Suppl 1): 28. 50th Annual Meeting Deutsche Gesellschaft für Experimentelle und Klinische Pharmakologie und Toxikologie, Mainz, Germany, March 11, 2009

Poster presentations

- Skroblin P, Hundsrucker C, Christian F, Zenn HM, Popara V, Herberg FW, Faelber K, Joshi M, Reif B, Rosenthal W, Klussmann E. GSKIP is an A-kinase anchoring protein. DFG FOR 942 Symposium: Wnt-associated signaling networks in tumor progression and in development, Göttingen, Germany, August 31 – September 1, 2009
- Skroblin P, Hundsrucker C, Christian F, Popara V, Faelber K, Joshi M, Reif B, Rosenthal W, Klussmann E. Glycogen synthase kinase 3β interaction protein (GSKIP) is an A-kinase achoring protein (AKAP). 11th MDC/FMP PhD Retreat, Kremmen, Germany, September 3-5, 2009
- Skroblin P, Hundsrucker C, Knobeloch KP, Christian F, Popara V, Rosenthal W, Klussmann E. Identification of GSKIP as an AKAP - Development of a conditional knockout mouse model. 10th MDC/FMP PhD Retreat, Templin, Germany, September 18-20, 2008

Appendix

A. Oligonucleotide sequences

Genotyping primers

FLP Fw:	CACTGATATTGTAAGTAGTTT
FLP Rev:	CTAGTGCGAAGTAGTGATCAGG
Cre Fw:	TGCCTGCATTACCGGTCGATGC
Cre Rev:	CCATGAGTGAACGAACCTGGTCG
CN129-5'-PCR-loxp-Fw:	AAAAGTTTAAAAAGGTCTGGAAAGC
CN129-5'-PCR-loxp-Rev:	TCTGCAAGAAAGGAGTAACAGATTT
AmpNeo2-Rev:	TAGTGTTGCTTTTAAGACAGGGTTT

Sequencing primers

Neo-end-seq:	AGGACAGCAAGGGGGAGGAT
CN129-3′-Seq-1:	AACAAAAGTGAGCAAACCAA
CN129-3′-Seq-2:	TCCTCCTAATGGGGCCGCTG
CN129-3′-Seq-3:	TGGAGTAACTTTGTAGTGGT
AclI-5′ Seq:	TTGGACTGTGAGGTCCCA
Acl1-3′ Seq:	CAAGAAAGGAGTAACAGA
5′ start seq-kpn:	GACAGGAGGCCAACGATA
5′ end seq-kpn:	CGCTCAAGTGCTCACAAG
3′ start seq-kpn:	CCCACTTTGTAGACTAGG
3′ end seq-xho:	CCTGGCTGTCCTAGAACT

Oligonucleotides for Oligonucleotide cloning

CN129-AclI-Fw:
AAAAAAACGTTGAATTCATAACTTCGTATAGCATACATTATACGAAGTTATAACGTTAAAAA

CN129-AclI-Rev:
TTTTTAACGTTATAACTTCGTATAATGTATGCTATACGAAGTTATGAATTCAACGTTTTTTT

B. Peptide sequences

Soluble peptides

AKAP18d-L314E:	PEDAELVRLSKRLVENAVEKAVQQY
AKAP18d-PP:	PEDAELVRLSKRLPENAPLKAVQQY
GSKIPtide:	SPAYREAFGNALLQRLEALKRDGQS
GSKIPtide-L130P:	SPAYREAFGNALLQRPEALKRDGQS
Ht31:	KGADLIEEAASRIVDAVIEQVKAAG
Ht31-P:	KGADLIEEAASRIPDAPIEQVKAAG

Peptide spots

Drosophila Q9VNV2, 25mers, shift 5, C→S (Fig. 24)

A 1	MGEPKATADPGEEQAFNSEDEANAI	B 1	KIVSSQYDTIDEDSRISALLRNGQE
A 2	ATADPGEEQAFNSEDEANAIINDVK	B 2	QYDTIDEDSRISALLRNGQEQGDDE
A 3	GEEQAFNSEDEANAIINDVKAHVAE	B 3	DEDSRISALLRNGQEQGDDEEEEIF
A 4	FNSEDEANAIINDVKAHVAEISISS	B 4	ISALLRNGQEQGDDEEEEIFETPYA
A 5	EANAIINDVKAHVAEISISSKLASD	B 5	RNGQEQGDDEEEEIFETPYALLDKI
A 6	INDVKAHVAEISISSKLASDATQIY	B 6	QGDDEEEEIFETPYALLDKISPRYV
A 7	AHVAEISISSKLASDATQIYLNIRT	B 7	EEEIFETPYALLDKISPRYVESFGN
A 8	ISISSKLASDATQIYLNIRTIESAT	B 8	ETPYALLDKISPRYVESFGNQLSQQ
A 9	KLASDATQIYLNIRTIESATSSVQV	B 9	LLDKISPRYVESFGNQLSQQLRALQ
A10	ATQIYLNIRTIESATSSVQVSSRGF	B10	SPRYVESFGNQLSQQLRALQQMRTE
A11	LNIRTIESATSSVQVSSRGFKIVSS	B11	ESFGNQLSQQLRALQQMRTEFNEED
A12	IESATSSVQVSSRGFKIVSSQYDTI	B12	QLSQQLRALQQMRTEFNEEDEEEEE
A13	SSVQVSSRGFKIVSSQYDTIDEDSR	B13	LRALQQMRTEFNEEDEEEEEEAEEE
A14	SSRGFKIVSSQYDTIDEDSRISALL	B14	LQQMRTEFNEEDEEEEEEAEEEEKK

Human AKAP220, 25mers, shift 5, C→S (Fig. 25)

A 1	IKKLTKKLKGELAKEFAPATPPSTP	B 7	LSLATEMAASHLDNKIIQEPKVKNP
A 2	KKLKGELAKEFAPATPPSTPHNSSV	B 8	EMAASHLDNKIIQEPKVKNPSLNVQ
A 3	ELAKEFAPATPPSTPHNSSVGSLSE	B 9	HLDNKIIQEPKVKNPSLNVQSQRSV
A 4	FAPATPPSTPHNSSVGSLSENEQNT	B10	IIQEPKVKNPSLNVQSQRSVSPTFL
A 5	PPSTPHNSSVGSLSENEQNTIEKEE	B11	KVKNPSLNVQSQRSVSPTFLNPSDE
A 6	HNSSVGSLSENEQNTIEKEEFMLKL	B12	SLNVQSQRSVSPTFLNPSDENLKTL
A 7	GSLSENEQNTIEKEEFMLKLMRSLS	C 1	SQRSVSPTFLNPSDENLKTLSNFAG
A 8	NEQNTIEKEEFMLKLMRSLSEEVES	C 2	SPTFLNPSDENLKTLSNFAGDLAAE
A 9	IEKEEFMLKLMRSLSEEVESSESGE	C 3	NPSDENLKTLSNFAGDLAAEVITEA
A10	FMLKLMRSLSEEVESSESGELPEVD	C 4	NLKTLSNFAGDLAAEVITEAEKIAK
A11	MRSLSEEVESSESGELPEVDVKSEH	C 5	SNFAGDLAAEVITEAEKIAKVRNSM
A12	EEVESSESGELPEVDVKSEHSGKKV	C 6	DLAAEVITEAEKIAKVRNSMLFKQK
B 1	SESGELPEVDVKSEHSGKKVQFAEA	C 7	VITEAEKIAKVRNSMLFKQKKNSSY
B 2	LPEVDVKSEHSGKKVQFAEALATHI	C 8	EKIAKVRNSMLFKQKKNSSYADGDE
B 3	VKSEHSGKKVQFAEALATHILSLAT	C 9	VRNSMLFKQKKNSSYADGDEDYKVE
B 4	SGKKVQFAEALATHILSLATEMAAS	C10	LFKQKKNSSYADGDEDYKVEEKLDI
B 5	QFAEALATHILSLATEMAASHLDNK	C11	KNSSYADGDEDYKVEEKLDIEAVVH
B 6	LATHILSLATEMAASHLDNKIIQEP	C12	ADGDEDYKVEEKLDIEAVVHPREVD

Rat MAP2D, 25mers, shift 5, C→S (Fig. 26)

A 1	MADERKDEGKAPHWTSASLTEAAAH	E 9	STAITPGTPPSYSSRTPGTPGTPSY
A 2	KDEGKAPHWTSASLTEAAAHPHSPE	E10	PGTPPSYSSRTPGTPGTPSYPRTPG
A 3	APHWTSASLTEAAAHPHSPEMKDQG	F 1	SYSSRTPGTPGTPSYPRTPGTPKSG
A 4	SASLTEAAAHPHSPEMKDQGGSGEG	F 2	TPGTPGTPSYPRTPGTPKSGILVPS
A 5	EAAAHPHSPEMKDQGGSGEGLSRSA	F 3	GTPSYPRTPGTPKSGILVPSEKKVA
A 6	PHSPEMKDQGGSGEGLSRSANGFPY	F 4	PRTPGTPKSGILVPSEKKVAIIRTP
A 7	MKDQGGSGEGLSRSANGFPYREEEE	F 5	TPKSGILVPSEKKVAIIRTPPKSPA
A 8	GSGEGLSRSANGFPYREEEEGAFGE	F 6	ILVPSEKKVAIIRTPPKSPATPKQL
A 9	LSRSANGFPYREEEEGAFGEHGSQG	F 7	EKKVAIIRTPPKSPATPKQLRLINQ
A10	NGFPYREEEEGAFGEHGSQGTYSDT	F 8	IIRTPPKSPATPKQLRLINQPLPDL
B 1	REEEEGAFGEHGSQGTYSDTKENGI	F 9	PKSPATPKQLRLINQPLPDLKNVKS
B 2	GAFGEHGSQGTYSDTKENGINGELT	F10	TPKQLRLINQPLPDLKNVKSKIGST
B 3	HGSQGTYSDTKENGINGELTSADRE	G 1	RLINQPLPDLKNVKSKIGSTDNIKY
B 4	TYSDTKENGINGELTSADRETAEEV	G 2	PLPDLKNVKSKIGSTDNIKYQPKGG
B 5	KENGINGELTSADRETAEEVSARIV	G 3	KNVKSKIGSTDNIKYQPKGGQVRIL
B 6	NGELTSADRETAEEVSARIVQVVTA	G 4	KIGSTDNIKYQPKGGQVRILNKKMD
B 7	SADRETAEEVSARIVQVVTAEAVAV	G 5	DNIKYQPKGGQVRILNKKMDFSKVQ
B 8	TAEEVSARIVQVVTAEAVAVLKGEQ	G 6	QPKGGQVRILNKKMDFSKVQSRSGS
B 9	SARIVQVVTAEAVAVLKGEQEKEAQ	G 7	QVRILNKKMDFSKVQSRSGSKDNIK
B10	QVVTAEAVAVLKGEQEKEAQHKDQP	G 8	NKKMDFSKVQSRSGSKDNIKHSAGG
C 1	EAVAVLKGEQEKEAQHKDQPAALPL	G 9	FSKVQSRSGSKDNIKHSAGGGNVQI
C 2	LKGEQEKEAQHKDQPAALPLAAEET	G10	SRSGSKDNIKHSAGGGNVQIVTKKI
C 3	EKEAQHKDQPAALPLAAEETVNLPP	H 1	KDNIKHSAGGGNVQIVTKKIDLSHV
C 4	HKDQPAALPLAAEETVNLPPSPPPS	H 2	HSAGGGNVQIVTKKIDLSHVTSKSG
C 5	AALPLAAEETVNLPPSPPPSPASEQ	H 3	GNVQIVTKKIDLSHVTSKSGSLKNI
C 6	AAEETVNLPPSPPPSPASEQTAALE	H 4	VTKKIDLSHVTSKSGSLKNIRHRPG
C 7	VNLPPSPPPSPASEQTAALEEATSG	H 5	DLSHVTSKSGSLKNIRHRPGGGRVK
C 8	SPPPSPASEQTAALEEATSGESAQA	H 6	TSKSGSLKNIRHRPGGGRVKIESVK
C 9	PASEQTAALEEATSGESAQAPSAFK	H 7	SLKNIRHRPGGGRVKIESVKLDFKE
C10	TAALEEATSGESAQAPSAFKQAKDK	H 8	RHRPGGGRVKIESVKLDFKEKAQAK
D 1	EATSGESAQAPSAFKQAKDKVTDGI	H 9	GGRVKIESVKLDFKEKAQAKVGSLD
D 2	ESAQAPSAFKQAKDKVTDGITKSPE	H10	IESVKLDFKEKAQAKVGSLDNAHHV
D 3	PSAFKQAKDKVTDGITKSPEKRSSL	I 1	LDFKEKAQAKVGSLDNAHHVPGGGN
D 4	QAKDKVTDGITKSPEKRSSLPRPSS	I 2	KAQAKVGSLDNAHHVPGGGNVKIDS
D 5	VTDGITKSPEKRSSLPRPSSILPPR	I 3	VGSLDNAHHVPGGGNVKIDSQKLNF
D 6	TKSPEKRSSLPRPSSILPPRRGVSG	I 4	NAHHVPGGGNVKIDSQKLNFREHAK
D 7	KRSSLPRPSSILPPRRGVSGDREEN	I 5	PGGGNVKIDSQKLNFREHAKARVDH
D 8	PRPSSILPPRRGVSGDREENSFSLN	I 6	VKIDSQKLNFREHAKARVDHGAEII
D 9	ILPPRRGVSGDREENSFSLNSSISS	I 7	QKLNFREHAKARVDHGAEIITQSPS
D10	RGVSGDREENSFSLNSSISSARRTT	I 8	REHAKARVDHGAEIITQSPSRSSVA
E 1	DREENSFSLNSSISSARRTTRSEPI	I 9	ARVDHGAEIITQSPSRSSVASPRRL
E 2	SFSLNSSISSARRTTRSEPIRRAGK	I10	GAEIITQSPSRSSVASPRRLSNVSS
E 3	SSISSARRTTRSEPIRRAGKSGTST	J 1	TQSPSRSSVASPRRLSNVSSSGSIN
E 4	ARRTTRSEPIRRAGKSGTSTPTTPG	J 2	RSSVASPRRLSNVSSSGSINLLESP
E 5	RSEPIRRAGKSGTSTPTTPGSTAIT	J 3	SPRRLSNVSSSGSINLLESPQLATL
E 6	RRAGKSGTSTPTTPGSTAITPGTPP	J 4	SNVSSSGSINLLESPQLATLAEDVT
E 7	SGTSTPTTPGSTAITPGTPPSYSSR	J 5	SGSINLLESPQLATLAEDVTAALAK
E 8	PTTPGSTAITPGTPPSYSSRTPGTP	J 6	INLLESPQLATLAEDVTAALAKQGL

Human SMYD2, 25mers, shift 5, C→S (Fig. 27)

A 1	MRAEGLGGLERFSSPGKGRGLRALQ	B13	KDLIQSDIAALHHFYSKHLGFPDND
A 2	LGGLERFSSPGKGRGLRALQPFQVG	B14	SDIAALHHFYSKHLGFPDNDSLVVL
A 3	RFSSPGKGRGLRALQPFQVGDLLFS	B15	LHHFYSKHLGFPDNDSLVVLFAQVN
A 4	GKGRGLRALQPFQVGDLLFSSPAYA	B16	SKHLGFPDNDSLVVLFAQVNSNGFT
A 5	LRALQPFQVGDLLFSSPAYAYVLTV	B17	FPDNDSLVVLFAQVNSNGFTIEDEE
A 6	PFQVGDLLFSSPAYAYVLTVNERGN	C 1	SLVVLFAQVNSNGFTIEDEELSHLG
A 7	DLLFSSPAYAYVLTVNERGNHSEYS	C 2	FAQVNSNGFTIEDEELSHLGSAIFP
A 8	SPAYAYVLTVNERGNHSEYSFTRKE	C 3	SNGFTIEDEELSHLGSAIFPDVALM
A 9	YVLTVNERGNHSEYSFTRKEGLSKS	C 4	IEDEELSHLGSAIFPDVALMNHSSS
A10	NERGNHSEYSFTRKEGLSKSGRSKQ	C 5	LSHLGSAIFPDVALMNHSSSPNVIV
A11	HSEYSFTRKEGLSKSGRSKQAFYSN	C 6	SAIFPDVALMNHSSSPNVIVTYKGT
A12	FTRKEGLSKSGRSKQAFYSNVESQK	C 7	DVALMNHSSSPNVIVTYKGTLAEVR
A13	GLSKSGRSKQAFYSNVESQKEDWPM	C 8	NHSSSPNVIVTYKGTLAEVRAVQEI
A14	GRSKQAFYSNVESQKEDWPMHKLES	C 9	PNVIVTYKGTLAEVRAVQEIKPGEE
A15	AFYSNVESQKEDWPMHKLESSPMVV	C10	TYKGTLAEVRAVQEIKPGEEVFTSY
A16	VESQKEDWPMHKLESSPMVVFGENW	C11	LAEVRAVQEIKPGEEVFTSYIDLLY
A17	EDWPMHKLESSPMVVFGENWNPSET	C12	AVQEIKPGEEVFTSYIDLLYPTEDR
B 1	HKLESSPMVVFGENWNPSETVRLTA	C13	KPGEEVFTSYIDLLYPTEDRNDRLR
B 2	SPMVVFGENWNPSETVRLTARILAK	C14	VFTSYIDLLYPTEDRNDRLRDSYFF
B 3	FGENWNPSETVRLTARILAKQKIHP	C15	IDLLYPTEDRNDRLRDSYFFTSESQ
B 4	NPSETVRLTARILAKQKIHPERTPS	C16	PTEDRNDRLRDSYFFTSESQESTTK
B 5	VRLTARILAKQKIHPERTPSEKLLA	C17	NDRLRDSYFFTSESQESTTKDKDKA
B 6	RILAKQKIHPERTPSEKLLAVKEFE	D 1	DSYFFTSESQESTTKDKDKAKVEIR
B 7	QKIHPERTPSEKLLAVKEFESHLDK	D 2	TSESQESTTKDKDKAKVEIRKLSDP
B 8	ERTPSEKLLAVKEFESHLDKLDNEK	D 3	ESTTKDKDKAKVEIRKLSDPPKAEA
B 9	EKLLAVKEFESHLDKLDNEKKDLIQ	D 4	DKDKAKVEIRKLSDPPKAEAIRDMV
B10	VKEFESHLDKLDNEKKDLIQSDIAA	D 5	KVEIRKLSDPPKAEAIRDMVRYARN
B11	SHLDKLDNEKKDLIQSDIAALHHFY	D 6	KLSDPPKAEAIRDMVRYARNVIEEF
B12	LDNEKKDLIQSDIAALHHFYSKHLG	D 7	PKAEAIRDMVRYARNVIEEFRRAKH
D 8	IRDMVRYARNVIEEFRRAKHYKSPS	E 4	WEGALQYGQKIIKPYSKHYPLYSLN
D 9	RYARNVIEEFRRAKHYKSPSELLEI	E 5	QYGQKIIKPYSKHYPLYSLNVASMW
D10	VIEEFRRAKHYKSPSELLEISELSQ	E 6	IIKPYSKHYPLYSLNVASMWLKLGR
D11	RRAKHYKSPSELLEISELSQEKMSS	E 7	SKHYPLYSLNVASMWLKLGRLYMGL
D12	YKSPSELLEISELSQEKMSSVFEDS	E 8	LYSLNVASMWLKLGRLYMGLEHKAA
D13	ELLEISELSQEKMSSVFEDSNVYML	E 9	VASMWLKLGRLYMGLEHKAAGEKAL
D14	SELSQEKMSSVFEDSNVYMLHMMYQ	E10	LKLGRLYMGLEHKAAGEKALKKAIA
D15	EKMSSVFEDSNVYMLHMMYQAMGVS	E11	LYMGLEHKAAGEKALKKAIAIMEVA
D16	VFEDSNVYMLHMMYQAMGVSLYMQD	E12	EHKAAGEKALKKAIAIMEVAHGKDH
D17	NVYMLHMMYQAMGVSLYMQDWEGAL	E13	GEKALKKAIAIMEVAHGKDHPYISE
E 1	HMMYQAMGVSLYMQDWEGALQYGQK	E14	KKAIAIMEVAHGKDHPYISEIKQEI
E 2	AMGVSLYMQDWEGALQYGQKIIKPY	E15	IAIMEVAHGKDHPYISEIKQEIESH
E 3	LYMQDWEGALQYGQKIIKPYSKHYP		

C. NES prediction

For explanations see: http://www.cbs.dtu.dk/services/NetNES/ [160].

```
>GSKIP_HUMAN - NetNES 1.1 prediction
```

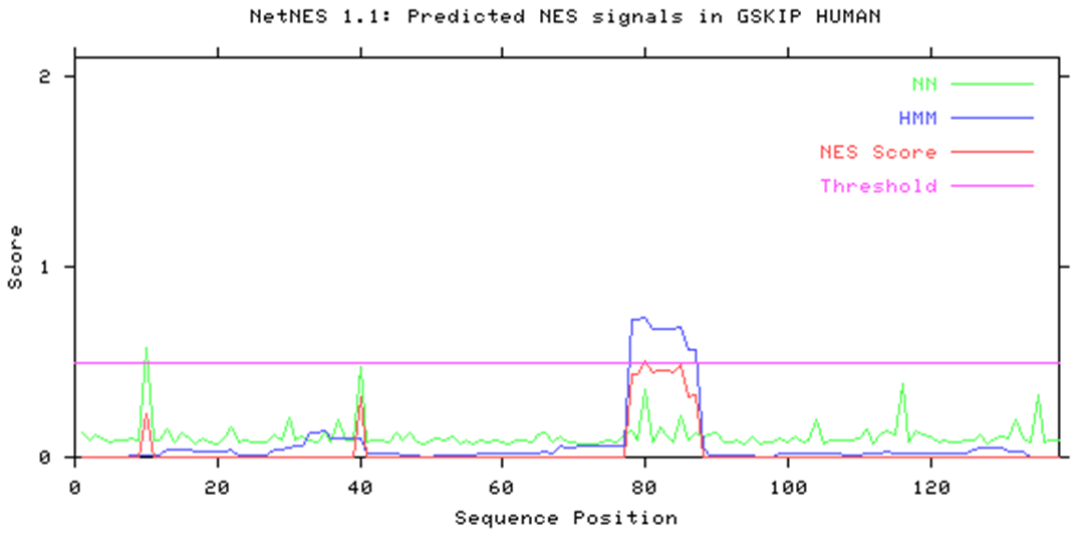

#Seq-Pos-Residue	ANN	HMM	NES	Predicted
GSKIP_HUMAN-1-M	0.127	0.000	0.000	-
GSKIP_HUMAN-2-E	0.094	0.000	0.000	-
GSKIP_HUMAN-3-T	0.120	0.000	0.000	-
GSKIP_HUMAN-4-D	0.102	0.000	0.000	-
GSKIP_HUMAN-5-C	0.083	0.000	0.000	-
GSKIP_HUMAN-6-N	0.092	0.000	0.000	-
GSKIP_HUMAN-7-P	0.091	0.000	0.000	-
GSKIP_HUMAN-8-M	0.097	0.008	0.000	-
GSKIP_HUMAN-9-E	0.085	0.008	0.000	-
GSKIP_HUMAN-10-L	0.572	0.013	0.228	-
GSKIP_HUMAN-11-S	0.091	0.012	0.000	-
GSKIP_HUMAN-12-S	0.089	0.012	0.000	-
GSKIP_HUMAN-13-M	0.145	0.039	0.000	-
GSKIP_HUMAN-14-S	0.077	0.039	0.000	-
GSKIP_HUMAN-15-G	0.133	0.039	0.000	-
GSKIP_HUMAN-16-F	0.097	0.039	0.000	-
GSKIP_HUMAN-17-E	0.073	0.034	0.000	-
GSKIP_HUMAN-18-E	0.102	0.034	0.000	-
GSKIP_HUMAN-19-G	0.084	0.034	0.000	-
GSKIP_HUMAN-20-S	0.071	0.034	0.000	-
GSKIP_HUMAN-21-E	0.109	0.034	0.000	-
GSKIP_HUMAN-22-L	0.157	0.040	0.000	-
GSKIP_HUMAN-23-N	0.079	0.007	0.000	-
GSKIP_HUMAN-24-G	0.088	0.007	0.000	-
GSKIP_HUMAN-25-F	0.076	0.015	0.000	-
GSKIP_HUMAN-26-E	0.075	0.014	0.000	-
GSKIP_HUMAN-27-G	0.081	0.014	0.000	-
GSKIP_HUMAN-28-T	0.115	0.038	0.000	-
GSKIP_HUMAN-29-D	0.088	0.038	0.000	-
GSKIP_HUMAN-30-M	0.208	0.053	0.000	-
GSKIP_HUMAN-31-K	0.093	0.055	0.000	-
GSKIP_HUMAN-32-D	0.105	0.055	0.000	-
GSKIP_HUMAN-33-M	0.087	0.134	0.000	-

GSKIP_HUMAN-34-R	0.077	0.133	0.000	-
GSKIP_HUMAN-35-L	0.132	0.138	0.000	-
GSKIP_HUMAN-36-E	0.077	0.100	0.000	-
GSKIP_HUMAN-37-A	0.202	0.100	0.000	-
GSKIP_HUMAN-38-E	0.094	0.100	0.000	-
GSKIP_HUMAN-39-A	0.091	0.100	0.000	-
GSKIP_HUMAN-40-V	0.475	0.100	0.314	-
GSKIP_HUMAN-41-V	0.083	0.022	0.000	-
GSKIP_HUMAN-42-N	0.093	0.019	0.000	-
GSKIP_HUMAN-43-D	0.094	0.019	0.000	-
GSKIP_HUMAN-44-V	0.082	0.020	0.000	-
GSKIP_HUMAN-45-L	0.124	0.017	0.000	-
GSKIP_HUMAN-46-F	0.087	0.011	0.000	-
GSKIP_HUMAN-47-A	0.125	0.008	0.000	-
GSKIP_HUMAN-48-V	0.078	0.008	0.000	-
GSKIP_HUMAN-49-N	0.074	0.004	0.000	-
GSKIP_HUMAN-50-N	0.093	0.004	0.000	-
GSKIP_HUMAN-51-M	0.096	0.005	0.000	-
GSKIP_HUMAN-52-F	0.088	0.005	0.000	-
GSKIP_HUMAN-53-V	0.107	0.010	0.000	-
GSKIP_HUMAN-54-S	0.070	0.007	0.000	-
GSKIP_HUMAN-55-K	0.093	0.009	0.000	-
GSKIP_HUMAN-56-S	0.067	0.009	0.000	-
GSKIP_HUMAN-57-L	0.092	0.017	0.000	-
GSKIP_HUMAN-58-R	0.084	0.017	0.000	-
GSKIP_HUMAN-59-C	0.091	0.017	0.000	-
GSKIP_HUMAN-60-A	0.076	0.017	0.000	-
GSKIP_HUMAN-61-D	0.071	0.017	0.000	-
GSKIP_HUMAN-62-D	0.088	0.017	0.000	-
GSKIP_HUMAN-63-V	0.090	0.019	0.000	-
GSKIP_HUMAN-64-A	0.083	0.018	0.000	-
GSKIP_HUMAN-65-Y	0.119	0.018	0.000	-
GSKIP_HUMAN-66-I	0.133	0.028	0.000	-
GSKIP_HUMAN-67-N	0.075	0.020	0.000	-
GSKIP_HUMAN-68-V	0.109	0.056	0.000	-
GSKIP_HUMAN-69-E	0.075	0.052	0.000	-
GSKIP_HUMAN-70-T	0.081	0.053	0.000	-
GSKIP_HUMAN-71-K	0.074	0.055	0.000	-
GSKIP_HUMAN-72-E	0.067	0.055	0.000	-
GSKIP_HUMAN-73-R	0.073	0.055	0.000	-
GSKIP_HUMAN-74-N	0.077	0.055	0.000	-
GSKIP_HUMAN-75-R	0.092	0.055	0.000	-
GSKIP_HUMAN-76-Y	0.080	0.055	0.000	-
GSKIP_HUMAN-77-C	0.115	0.055	0.000	-
GSKIP_HUMAN-78-L	0.136	0.719	0.433	-
GSKIP_HUMAN-79-E	0.087	0.719	0.436	-
GSKIP_HUMAN-80-L	0.355	0.729	0.502	Yes
GSKIP_HUMAN-81-T	0.079	0.674	0.445	-
GSKIP_HUMAN-82-E	0.156	0.674	0.460	-
GSKIP_HUMAN-83-A	0.113	0.674	0.460	-
GSKIP_HUMAN-84-G	0.076	0.674	0.448	-
GSKIP_HUMAN-85-L	0.222	0.680	0.480	-
GSKIP_HUMAN-86-K	0.088	0.569	0.316	-
GSKIP_HUMAN-87-V	0.124	0.569	0.325	-
GSKIP_HUMAN-88-V	0.106	0.050	0.000	-
GSKIP_HUMAN-89-G	0.114	0.009	0.000	-
GSKIP_HUMAN-90-Y	0.126	0.009	0.000	-
GSKIP_HUMAN-91-A	0.078	0.009	0.000	-
GSKIP_HUMAN-92-F	0.084	0.009	0.000	-
GSKIP_HUMAN-93-D	0.090	0.009	0.000	-
GSKIP_HUMAN-94-Q	0.074	0.009	0.000	-
GSKIP_HUMAN-95-V	0.109	0.009	0.000	-

```
GSKIP_HUMAN-96-D          0.067   0.004   0.000      -
GSKIP_HUMAN-97-D          0.080   0.004   0.000      -
GSKIP_HUMAN-98-H          0.080   0.004   0.000      -
GSKIP_HUMAN-99-L          0.101   0.024   0.000      -
GSKIP_HUMAN-100-Q         0.075   0.021   0.000      -
GSKIP_HUMAN-101-T         0.110   0.021   0.000      -
GSKIP_HUMAN-102-P         0.079   0.021   0.000      -
GSKIP_HUMAN-103-Y         0.091   0.021   0.000      -
GSKIP_HUMAN-104-H         0.203   0.021   0.000      -
GSKIP_HUMAN-105-E         0.073   0.021   0.000      -
GSKIP_HUMAN-106-T         0.094   0.021   0.000      -
GSKIP_HUMAN-107-V         0.092   0.022   0.000      -
GSKIP_HUMAN-108-Y         0.087   0.006   0.000      -
GSKIP_HUMAN-109-S         0.085   0.006   0.000      -
GSKIP_HUMAN-110-L         0.095   0.011   0.000      -
GSKIP_HUMAN-111-L         0.152   0.021   0.000      -
GSKIP_HUMAN-112-D         0.074   0.020   0.000      -
GSKIP_HUMAN-113-T         0.122   0.021   0.000      -
GSKIP_HUMAN-114-L         0.137   0.029   0.000      -
GSKIP_HUMAN-115-S         0.115   0.023   0.000      -
GSKIP_HUMAN-116-P         0.391   0.023   0.000      -
GSKIP_HUMAN-117-A         0.076   0.023   0.000      -
GSKIP_HUMAN-118-Y         0.139   0.023   0.000      -
GSKIP_HUMAN-119-R         0.120   0.023   0.000      -
GSKIP_HUMAN-120-E         0.113   0.023   0.000      -
GSKIP_HUMAN-121-A         0.083   0.023   0.000      -
GSKIP_HUMAN-122-F         0.086   0.024   0.000      -
GSKIP_HUMAN-123-G         0.076   0.020   0.000      -
GSKIP_HUMAN-124-N         0.080   0.020   0.000      -
GSKIP_HUMAN-125-A         0.087   0.020   0.000      -
GSKIP_HUMAN-126-L         0.089   0.044   0.000      -
GSKIP_HUMAN-127-L         0.115   0.045   0.000      -
GSKIP_HUMAN-128-Q         0.074   0.045   0.000      -
GSKIP_HUMAN-129-R         0.102   0.045   0.000      -
GSKIP_HUMAN-130-L         0.108   0.045   0.000      -
GSKIP_HUMAN-131-E         0.095   0.026   0.000      -
GSKIP_HUMAN-132-A         0.197   0.026   0.000      -
GSKIP_HUMAN-133-L         0.103   0.026   0.000      -
GSKIP_HUMAN-134-K         0.080   0.000   0.000      -
GSKIP_HUMAN-135-R         0.324   0.000   0.000      -
GSKIP_HUMAN-136-D         0.078   0.000   0.000      -
GSKIP_HUMAN-137-G         0.094   0.000   0.000      -
GSKIP_HUMAN-138-Q         0.085   0.000   0.000      -
GSKIP_HUMAN-139-S         0.086   0.000   0.000      -
//
```

D. Targeting vector sequence

In the sequence of the targeting vector pPNT-FRT3-GSKIP, important features are indicated as follows:

loxP **bold**

FRT *italics*

5′/3′ homology underlinded

neo cassette yellow highlighter

(including promoters and polyadenylation signal)

HSV-tk cassette turquoise highlighter

(including promoter)

>pPNT-FRT3-GSKIP - 14515 bp

GCTCGAAATTAACCCTCACTAAAGGGAACAAAAGCTGGAGCTCCACCGCGGTGGCGGCCTAGGCCTCACTGGCCG
TCGAGTTTAAACGGCCGGCCACCAGGTGCGGCCGCGGTACCCTGCTATCCTCTCTGGCTCCTGCTGCTGTCTTTT
CCCCTTGTCAGCATTATCGTTGGCCTCCTGTCCTCATCCCAAGATGGCTGCCAAAAGTGTGCTGTGACTGGACTA
AAAAGACCATGAAAAAGTCCATTGTATGAGAACTGGAGTCAGTCTCTGCCACATCACCTGCTGACTCCACTCAGT
AGGGAAGAGGCATCCGATTCCCCTCAGAAAATGTGGGCGTAACTGGACAAGGGAAAGACGTGGGAAGCAAGCAAG
TCTGATATGGGCAGGACAGAACAATGCTTAAGAGCACTTCCCTGGGCTGGAGAGATGGCTCAGAGGTTAAGAGCA
CTGGCTGCTCTTCCAGAGATCCTGAGTTCAATTCCCAACAACCACATGGCGGCTCACAACCATCTGTAATGAGAT
CTGATGCCTTCTTCTGGTGTGTCTGAAGACATTACAGTGTACCCATATACTTAAATAAAATCTTTAAAAAAAAAA
AAAAGCACTTCCCTATTCTCACAGAGCAGCAAGGGTCAGCTCCCAGCACCCACACGGTCACATGACCACCAAGCT
CAAGTGGTCATACCACCACTCAAGCTCCAGGGGGGCCAATGCCACCTTCTGGCCTCCATAGGCCCCTGGGTACGC
TTGTGCATGTGTGTACACACACGTACAGACACACATCTACACATAACTAAAATAAATCATTATCAAAAGCTTTAA
ATCTTCCACATCGTTCTCAAAGGGATGCATGAAGTTCCCTAGGTATCATCTTTTTGGAGCTGATGGTTACCCAGT
AACCATCTGGTGTCGGACTCTGCCAGCCTGTAAGGCCGTCTTCCTGCCAGTGCTGGACGCCTGCTGACAGCTTTA
TGAACATCTTTTTCATGTAATGGTTATTCTGATGTCTGTAACTGTTCTTTATTACCAAGGTAAAGACATGACACA
CTTGGTGCTTAGGAGCTAAAACCTTCCAGACTTTTCTTTTTTTAATCAGTTCAGGGCCAAGTCAGTGAAAGCACT
TATTCCTAACCACTGGACCAATGGATCAAGCTGAGTTTATAGACTATAGTAAACAGTCACTTCTATAAAACCAAG
CGTATCCCTAAACAGTGTATTAGTTGAGCAGGGGAGACATGTTTAAATGATTGTGTTGCATACAATCATAGTAGA
AGGTGCATCATTGGCTTTGTGCGTTTGCCATTCCTTCACACGAAGGCTTTTGACTCCCAAGTTATCTTAGTTTCA
GCTTCATGGAAGGGGATTTTGAGACCATTGCTCTAACACTTTCATTCTGAGTTTCACACCCAGCCACTCTGCATT
TCAGTCCCTAGTCAGCTCTTCATTCTCCTATTACAGGGCTTCACGCCGCCAGCACTCTTTTACATAGAAAATTCT
AGATTTGCACAGTGATACAGAAATTAGAATTAGATTTTAGGTGCATAACATCATCCATTTTCTTAGATATAGGTG
TGACTTATATTTCTTAAATATTGGTGTGATTTCAAACAAACTGGGTTCTTTTCCACTTCTGTGTGAACTTGACAG
ATAAAAATATTCTGTAAGCCTCAAAAAAAGGTATTTACTCAAGGAAATACATGCTAAGACAATGAGCTTTTGTTC
TTTGCCTCACAGACTGACAAAAGTTTAAAAAGGTCTGGAAAGCTTGTGTTGATGCCCACAGTGCTTCTCTTTGGA
GGAATGTGCACTTTGGAGCTTTGGCTTAGGAATGCAATGGAGTGCGCTCAGTGGGGCTCACTGGGCATCCTAGTA
GGAGCATGGGGACAGGTGCTGAGAGTGAGTTGGACTGTGAGGTCCCAGCTTGAGAGCTTTCAGAGGAGATGTGTA
CGTGGCCTAAAGACCGCGCTCGCTCGGGATACTTTGCTGGAGAACGTTGAATTC**ATAACTTCGTATAGCATACAT**
TATACGAAGTTATAACGTTGCTGCTTTCTGCCCTTGTCCAGTTGCAATGTTTTTCCATTAAAAAAAATCTGTTAC
TCCTTTCTTGCAGAATGGAAACAGACTATAATCCCGTGGAGCTAAGCAGTATGTCTGGATTTGAAGAAGGCTCCG
AGCTCAATGGGTTTGAAGGAGCGGATATGAAGGACATGCAGCTGGAGGCCGAGGCAGTTGTAAACGATGTACTCT
TTGCTGTCAACCACATGTTTGTCTCAAAAAGCATGCCCTGTGCAGATGATGTGGCTTACATCAATGTGGAGACAA
AGGAAAGGAACAGATACTGCCTGGAGCTCACAGAAGCAGGGCTCAGGGTAACTCACTTTTATTTTTAGAAGAAAA
AAAAAAAGCATATCTTTATCATTTTATCAGAAAGGATAAAGAGGAACATTACATACAAATCAGAGATGGGTATCT
TCAAAAAAAAAAAGAAAGAAAGAAAAGAAATATTTTCCCCAAAATTTTGGTTAATAAATTTTTTATCAACACAGA
ATTTGAGGGTGTAAATACATTTCGAAACAGTTGATTCAGTCTGCTGTAATCGTTACCACCCTTCTTTCATTCCTG
TAGCTAATTTTGTCTCCCAGAGTGGGCTCTCTGCAGGGGGTGCCCTTGTAGTTGCTGTGCTGAAAGAGCTCTGCT
CACCTTCCACCTTCCATCCAAGCTAGATGCTTAGACTGGGCTGTGTACCAGGAGCGTGTTGTACAGGCCAGAACC
CACATAAAAGAGGAAAGCGAATACTTTACAGACTTAGCATCTGACTTCCATAGATGTGTCGTGTGTGTGTGTGTG
TGTGTGTGTGTGTGTGTGTGTGTGTGTGTGTGTGCGCGCGTGTACAATATTTTGAATTTTTTGAAGATACTCAGA
GGCTGGGCGTGGTGATAGCAGTCCATTAATCCCAGCACTCAGGAGGCAGAGGCAGGTGGATCTCTGAGATTGAGG
CCAGCCAGGATTGTATAGTGAGACCCACCCTGTATTTTCATTGATTAAAAAGGAAGAAAGGGCTGGGCGTGGTGG
CGCACACCTTTAATCCCAGCACTTGGGATGCAGAGGCAGGTGGATTTCTGAGTTCGAGGCCAGCCTGGTCTACAA

AGTGAGTTCCAGGACAGCCAGGGCTACACAGAGAAACCCTGTCTCGGGAAAAAAAAAAAAAAAAGGAAAAAAGG
AATGCTTAGTGGTAGAGGCCTGGGTTCAGTTCTCAGCAGCAGGCTGGAATGGAGAGGCTTCATCACCAGTATTTT
ATTGCAAGAAGGTAGCTTGGGACAGGAGGTCATGAGTATGTATGGAGCTCAGGGAGGGTGAGGCCTGGAGGGATG
GCTCAGTGGTTAGGAACACGTTTCTCTTGTCCCTGTTGGATTCCCAGCACCCACAGGTCACACACTGCGACTGTG
ACTGCAGCTCAGGAAGTTGTCTCCTCTCCTCTAGCCTCCATGGTTGTCTGCGCTCAAGTGCTCACAAGCACATAT
GTACATAATTTAATTTTTTTAAAAAAGGATAAAAAATGGTTTCAGAGCCAAGCATGGCGGTACCGTCGACGGCCG
C**ATAACTTCGTATAGCATACATTATACGAAGTTAT**C*GAAGTTCCTATTCTCTAGAAAGTATAGGAACTTC*AAGCT
AATTCTACCGGGTAGGGGAGGCGCTTTTCCCAAGGCAGTCTGGAGCATGCGCTTTAGCAGCCCCGCTGGGCACTT
GGCGCTACACAAGTGGCCTCTGGCCTCGCACACATTCCACATCCACCGGTAGGCGCCAACCGGCTCCGTTCTTTG
GTGGCCCCTTCGCGCCACCTTCTACTCCTCCCCTAGTCAGGAAGTTCCCCCCCGCCCCGCAGCTCGCGTCGTGCA
GGACGTGACAAATGGAAGTAGCACGTCTCACTAGTCTCGTGCAGATGGACAGCACCGCTGAGCAATGGAAGCGGG
TAGGCCTTTGGGGCAGCGGCCAATAGCAGCTTTGCTCCTTCGCTTTCTGGGCTCAGAGGCTGGGAAGGGGTGGGT
CCGGGGGCGGGCTCAGGGGCGGGCTCAGGGGCGGGGCGGGCGCCCGAAGGTCCTCCGGAGGCCCGGCATTCTGCA
CGCTTCAAAAGCGCACGTCTGCCGCGCTGTTCTCCTCTTCCTCATCTCCGGGCCTTTCGACCTGCAGCCAATATG
GGATCGGCCATTGAACAAGATGGATTGCACGCAGGTTCTCCGGCCGCTTGGGTGGAGAGGCTATTCGGCTATGAC
TGGGCACAACAGACAATCGGCTGCTCTGATGCCGCCGTGTTCCGGCTGTCAGCGCAGGGGCGCCCGGTTCTTTTT
GTCAAGACCGACCTGTCCGGTGCCCTGAATGAACTGCAGGACGAGGCAGCGCGGCTATCGTGGCTGGCCACGACG
GGCGTTCCTTGCGCAGCTGTGCTCGACGTTGTCACTGAAGCGGGAAGGGACTGGCTGCTATTGGGCGAAGTGCCG
GGGCAGGATCTCCTGTCATCTCACCTTGCTCCTGCCGAGAAAGTATCCATCATGGCTGATGCAATGCGGCGGCTG
CATACGCTTGATCCGGCTACCTGCCCATTCGACCACCAAGCGAAACATCGCATCGAGCGAGCACGTACTCGGATG
GAAGCCGGTCTTGTCGATCAGGATGATCTGGACGAAGAGCATCAGGGGCTCGCGCCAGCCGAACTGTTCGCCAGG
CTCAAGGCGCGCATGCCCGACGGCGAGGATCTCGTCGTGACCCATGGCGATGCCTGCTTGCCGAATATCATGGTG
GAAAATGGCCGCTTTTCTGGATTCATCGACTGTGGCCGGCTGGGTGTGGCGGACCGCTATCAGGACATAGCGTTG
GCTACCCGTGATATTGCTGAAGAGCTTGGCGGCGAATGGGCTGACCGCTTCCTCGTGCTTTACGGTATCGCCGCT
CCCGATTCGCAGCGCATCGCCTTCTATCGCCTTCTTGACGAGTTCTTCTGAGGGGATCAATTCTCTAGAGCTCGC
TGATCAGCCTCGACTGTGCCTTCTAGTTGCCAGCCATCTGTTGTTTGCCCCTCCCCCGTGCCTTCCTTGACCCTG
GAAGGTGCCACTCCCACTGTCCTTTCCTAATAAAATGAGGAAATTGCATCGCATTGTCTGAGTAGGTGTCATTCT
ATTCTGGGGGGTGGGGTGGGGCAGGACAGCAAGGGGGAGGATTGGGAAGACAATAGCAGGCATGCTGGGGATGCG
GTGGGCTCTATGGCTTCTGAGGCGGAAAGAACCAGCTGGGGCTCGATCGAGATCC*GAAGTTCCTATTCTCTAGAA*
*AGTATAGGAACTTC*CCGGGATCCTGCAGGCACGTGGCGCGCCCCCGGGTACCTACCTTTAATCCCTGGGAGGCAG
AAGCAGGTAGCTCTCTGAGTTCAAGGCCAGCCTAGTCTACAAAGTGGGTTTCAGGACAGCCAGGTTACACAGAGA
AACCCTGTCTTAAAAGCAACACTACTACTACTACTACTACTACTACTACTACTAATAATAATAATAATAATAATAATA
ATAATGTTTATTATGTCATTTTTCAAGATTTTAACACTTGAAAAAAGAACAAAAGTGAGCAAACCAAACCTCTTA
AAGAGCAATGGGGGAAGCAAGGCACATTGTGGGTAGTGGTCCTGCGTTCTAAGCTACTTGATAGATTGCTCCCAG
CTGAAATGCATATCATCCGCTGAGAAACGGTGTCACTGCACAAGCCCTTCAGGCAGCCGACCCTTGCCTTGTGTG
CCAGGATGGACGCTGACCACTGCTTACTGCTGCCCTTCTCTCGTAGGTGGTGGGCTATGCTTTTGACCAGGTGGA
GGATCATTTGCAAACCCCCTACCATGAGACAGTCTACTCCTTGTTGGATACTCTCAGCCCTGCCTACCGGGAAGC
ATTCGGAAACGCGCTCCTTCAGAGACTGGAAGCTTTGAAACGAGATGGACAGTCATGACTCATGACTCATCTTCC
TCCTAATGGGGCCGCTGCTGGTATAGAATCTAACATAAGGCTTGACACCCTTGCGTACAGTCACTGTAGAAAGCG
CATCATTCATTGGCTTTGTGTGTTCGCCATTCCTTCACACGCAGGCTTTTGACTCCCAGCGTAATTGAGTTGTCT
TAGTTTCAGCTTCATGGAAGGGGATTTAATTTTGAGACCATTGCTCTGACACTCCCATTCTGAGTTTCACACCCA
GCACTCTGCATTTCAATCCCTAGTCAGCTCTTCATTCTCCTGTTACAGGGCTTCAATGCTGCCAGCACTCTTTTA
CATAGAAAATTCTAGATTTGCACAGTGATACAGAAATTAGAATCACCTAACTTCAGACCTGGATTCAGCCTGCTA
AATCAGGGGTTTACTACTAGCTTGGAGTAACTTTGTAGTGGTTATTTTGTACCTGGCCTTATTGGAAACAAACTG
TCAACTAGTTTCCCCTGCACAAATTCTGAAATGTACTGCTCTGCTTAATCTAGTCACATGACCAAGTGGGCTGGT
GAAGATGGGTTGCTCATCTGTTTCTTAACTAAGATAAAATGGAAGGCAGGGACAGAAATCGTTCTCCATTCCTTG
TTTGCAACAGCCAGCCAGCCTAGAGCGGACAGACCATTCGCAAATGAATGTAACAATTACTCATCTCCATGATGT
CTAAGCACATGAGCAAATAGAGGAACAGGCCCACCTCATCCTCCAGTGTGGATCTCTTCAAAGGAAGAAGATCCT
GGTTTCCTAGGAAACGGTATTTTGGCCTGTGTTGATTCTTACTCTGAATGTTTGTTTACAATGTACAGTATATAT
ATATATATATGCACATATATATTCAGAACGTATTTTTGCTTCAATGCTTACTTTCTATAAAGCAGTGCTTTGGTA
TTCCTACAGCGCCCTTCTTCCCCAGCAGTTGGACAGTGCTCTGTCTCATTGCCACATGAACAGTGTAACATGAGT
GCATTGTATGGTTCGAAACCAAAGGATGAATGAAGCATTCAGAAACTTGATATTTAAAAAAGAGATGCTCTGTAT
TTTATATTTTATTACAGTCCCCGGTGTTTATAAACGTAATAAAGTCCTCCGTGCTGCTGCATGTTTTCCAGTATG
TGACAAACAGAAAGGACCTGGCTCTGTTCTAGTTGTCACCCAGAGCTGCCTCAGCTGCCACCGTCTGCATCTGGG
CACACCTTCATACACTGGTCATCAGCAGATGTTTTTGTCGTTAGTTTGCAAAGGGCATTTTTAGCCTCTGAAGAC
CATGGGAGGAAAGGTGAAGGGTAGAGCCCTTGCCTGTCGTGGGTAAGCACCCAGCCCTGTCCTGAGGATCTAAAC
AGTCTTAAAATGCTTCTGGGGACCAGGCTTGGTAGAGTTCCCTCTGCATTGCCAATGCCACCGAGAGTTCACTGG
GTGTTTGACCCTGGCTTTACAAGACTCTTTTTCTGGTGTGATGTCTGGTTGCCTGCAGTGTGCACAGTGAAGCCC
AGCCTCAGGCTCTCTTTCTGGTGTGATGTCTGGTGTGATGCCTGCAGTGTGCACAGTGAAGCCCAGCCTCAGGCT
CTCTTTCTGGTGTGATTTCTGGTTGCCTGCAGTATGCACAGTGAAGTCCGGCCTCAGGCTCTCTTTCTGGTGTGA
TGTCTGGTTGCCTGCGGTGTGCACAGTGAAGTCCGGCCTCAGGCTCTCTTTCTGGTGTGATTTCTGGTTGCCTGC
AGTGTGCACAGTGAAGTCCGGCCTCAGGCTCTCTTTCTGGTGTGATGTCTGGTTGCCTGCGGTGTGCACAGTGAA

GCCCGGCCTCAGGCTCTCTTTCTGGTGTGATGTCTGGTGTGATGCCTGCAGTGTGCACAGTGAAGCCCTGCCTCA
GGCTCTCTTTCTGGTGTGATGTCTGGTTGCCTGCAGTGTGCACAGTGAAGCCCAGCCTCAGGCTCTCTTTCTGGT
GTGATGTCTGGTGTGATGCCTGCAGTGTGCACAGTGAAGCCCAGCCTCAGGCTCTCTTTCTGGTGTGATTTCTGG
TTGCCTGTGGGGTGCACAGAGAAGCCCGGCCTCAGGCTCTCTTTCTGGTGTGATGTCTGGTTGCCTGCAGTGTGC
ACAGTGAAGCCCGGCCTCAGGTTGAACTTTCTTGTGCTTAATCTCAGGCTAACATTTTAAAAAATGATGTTTGTA
GAGTTTAAATAAAATTATTTACTTGATTTTGAGTTGAGCATAAAGCAGTCATGCTTAAAAACTGAAATGGTTTAT
TTTGTGATAAGTGGCTGATTCAAAGATCTTATCAAAATGTGCCAGCACTTTTTAAATTCAACAATGTTATATTTT
GAGTTGAAGTGAGAGAAGGGAGTTGTTCTTTCCTTTATTACTTAAAACAAAGGGGATCAGTACACACACACACAC
ACACACACACACACACACACACGTGTGAGCACAGGCAGACCTCTATCCTAAGCTAAGCTAGTTTTTAAGATTAAC
CATATAAATTAAACCTTGATTTTACTTCTAAAGAAAAAAAATCCTCTGACTCAAATCAATTTCAAAAGAGTTGTG
CGTGAGCACACACATAGCCTGAGCATTGGGAAGTGAAGAAAGAGCCGAGGCTGTCATCCTCAGCTACAGAGGATA
CGGGAGGTCAGCCCAGGCGAAACCTAAAGTGGGATTACAGCAGTGGGCAGATGAGTTTAGACAACTCACAGGGGA
GGAATAATGAAAGCTATTCAGTGACCACTTGAAAGGGGCTCCAAAATGGAGGAGGAGCACAGAAATACAACGTGA
GAGGTGTTTGACTCTGCTGATAATGTGAGAAAATGTCAACAGTTGGACCATGGCAGGCAAGATGGCTCAGTGAAA
GTACTATCTCCACACCAGACAGCCTGGATGGGAGCTCAGGACCTACGGGGGGGGGGGGGGGGGGGGGCGCCTAT
TTCCACAAGTCTTTTAAAAAGAGTTTTGTTTCTTGTTTTTTGTTTTTTTAGTCAGGGTTTCTCTTGGTAGCCCTG
GCTGTCCTAGAACTCACTCTGTAGATCAGGCTGGTCTCAAACTGGGAGATCCCCCAACCTCTGCCTCTCGAGTCG
AGAAATTCTACCGGGTAGGGGAGGCGCTTTTCCCAAGGCAGTCTGGAGCATGCGCTTTAGCAGCCCCGCTGGGCA
CTTGGCGCTACACAAGTGGCCTCTGGCCTCGCACACATTCCACATCCACCGGTAGGCGCCAACCGGCTCCGTTCT
TTGGTGGCCCCTTCGCGCCACCTTCTACTCCTCCCCTAGTCAGGAAGTTCCCCCCCGCCCCGCAGCTCGCGTCGT
GCAGGACGTGACAAATGGAAGTAGCACGTCTCACTAGTCTCGTGCAGATGGACAGCACCGCTGAGCAATGGAAGC
GGGTAGGCCTTTGGGGCAGCGGCCAATAGCAGCTTTGCTCCTTCGCTTTCTGGGCTCAGAGGCTGGGAAGGGGTG
GGTCCGGGGGCGGGCTCAGGGGCGGGCTCAGGGGCGGGGCGGGCGCCCGAAGGTCCTCCGGAGGCCCGGCATTCT
GCACGCTTCAAAAGCGCACGTCTGCCGCGCTGTTCTCCTCTTCCTCATCTCCGGGCCTTTCGACCTGCAGCGACC
CGCTTAACAGCGTCAACAGCGTGCCGCAGATCTTGGTGGCGTGAAACTCCCGCACCTCTTCGGCCAGCGCCTTGT
AGAAGCGCGTATGGCTTCGTACCCCTGCCATCAACACGCGTCTGCGTTCGACCAGGCTGCGCGTTCTCGCGGCCA
TAACAACCGACGTACGGCGTTGCGCCCTCGCCGGCAACAAAAAGCCACGGAAGTCCGCCTGGAGCAGAAAATGCC
CACGCTACTGCGGGTTTATATAGACGGTCCCCACGGGATGGGGAAAACCACCACCACGCAACTGCTGGTGGCCCT
GGGTTCGCGCGACGATATCGTCTACGTACCCGAGCCGATGACTTACTGGCGGGTGTTGGGGGCTTCCGAGACAAT
CGCGAACATCTACACCACACAACACCGCCTCGACCAGGGTGAGATATCGGCCGGGGACGCGGCGGTGGTAATGAC
AAGCGCCCAGATAACAATGGGCATGCCTTATGCCGTGACCGACGCCGTTCTGGCTCCTCATATCGGGGGGGAGGC
TGGGAGCTCACATGCCCCGCCCCCGGCCCTCACCCTCATCTTCGACCGCCATCCCATCGCCGCCCTCCTGTGCTA
CCCGGCCGCGCGATACCTTATGGGCAGCATGACCCCCCAGGCCGTGCTGGCGTTCGTGGCCCTCATCCCGCCGAC
CTTGCCCGGCACAAACATCGTGTTGGGGGCCCTTCCGGAGGACAGACACATCGACCGCCTGGCCAAACGCCAGCG
CCCCGGCGAGCGGCTTGACCTGGCTATGCTGGCCGCGATTCGCCGCGTTTATGGGCTGCTTGCCAATACGGTGCG
GTATCTGCAGGGCGGCGGGTCGTGGCGGGAGGATTGGGGACAGCTTTCGGGGGCGGCCGTGCCGCCCCAGGGTGC
CGAGCCCCAGAGCAACGCGGGCCCACGACCCCATATCGGGGACACGTTATTTACCCTGTTTCGGGCCCCCGAGTT
GCTGGCCCCCAACGGCGACCTGTATAACGTGTTTGCCTGGGCTTTGGACGTCTTGGCCAAACGCCTCCGTCCCAT
GCATGTCTTTATCCTGGATTACGACCAATCGCCCGCCGGCTGCCGGGACGCCCTGCTGCAACTTACCTCCGGGAT
GGTCCAGACCCACGTCACCACCCCAGGCTCCATACCGACGATCTGCGACCTGGCGCGCACGTTTGCCCGGGAGAT
GGGGGAGGCTAACTGAAACACGGAAGGAGACAATACCGGAAGGAACCCGCGCTATGACGGCAATAAAAAGACAGA
ATAAAACGCACGGGTGTTGGGTCGTTTGTTCATAAACGCGGGGTTCGGTCCCAGGGCTGGCACTCTGTCGATACC
CCACCGAGACCCCATTGGGACCAATACGCCCGCGTTTCTTCCTTTTCCCCACCCCAACCCCCAAGTTCGGGTGAA
GGCCCAGGGCTCGCAGCCAACGTCGGGGCGGCAAGCCCTGCCATAGCCACGGGCCCCGTGGGTTAGGGACGGGGT
CCCCCATGGGGAATGGTTTATGGTTCGTGGGGGTTATTATTTTGGGCGTTGCGTGGGGTCAGGTCCACGACTGGA
CTGAGCAGACAGACCCATGGTTTTTGGATGGCCTGGGCATGGACCGCATGTACTGGCGCGACACGAACACCGGGC
GTCTGTGGCTGCCAAACACCCCCGACCCCCAAAAACCACCGCGCGGATTTCTGGCGCCGCCGGACGAACTAAACC
TGACTACGGCATCTCTGCCCCTTCTTCGCTGGTACGAGGAGCGCTTTTGTTTTGTATTGGTCACCACGGCCGAGT
TTCCGCGGGACCCCGGCCAGGACCTGCAGAAATTGATGATCTATTAAACAATAAAGATGTCCACTAAAATGGAAG
TTTTTCCTGTCATACTTTGTTAAGAAGGGTGAGAACAGAGTACCTACATTTTGAATGGAAGGATTGGAGCTACGG
GGGTGGGGGTGGGGTGGGATTAGATAAATGCCTGCTCTTTACTGAAGGCTCTTTACTATTGCTTTATGATAATGT
TTCATAGTTGGATATCATAATTTAAACAAGCAAAACCAAATTAAGGGCCAGCTCATTCCTCCCACTCATGATCTA
TAGATCTATAGATCTCTCGTGGGATCATTGTTTTTCTCTTGATTCCCACTTTGTGGTTCTAAGTACTGTGGTTTC
CAAATGTGTCAGTTTCATAGCCTGAAGAACGAGATCAGCAGCCTCTGTTCCACATACACTTCATTCTCAGTATTG
TTTTGCCAAGTTCTAATTCCATCAGAAGCTTGGCACTGGCCGTCGTTTTACAACGTCGTGACTGGGAAAACCCTG
GCGTTACCCAACTTAATCGCCTTGCAGCACATCCCCCTTTCGCCAGCTGGCGTAATAGCGAAGAGGCCCGCACCG
ATCGCCCTTCCCAACAGTTGCGCAGCCTGAATGGCGAATGGCGCCTGATGCGGTATTTTCTCCTTACGCATCTGT
GCGGTATTTCACACCGCATATGGTGCACTCTCAGTACAATCTGCTCTGATGCCGCATAGTTAAGCCAGCCCCGAC
ACCCGCCAACACCCGCTGACGCGCCCTGACGGGCTTGTCTGCTCCCGGCATCCGCTTACAGACAAGCTGTGACCG
TCTCCGGGAGCTGCATGTGTCAGAGGTTTTCACCGTCATCACCGAAACGCGCGAGACGAAAGGGCCTCGTGATAC
GCCTATTTTTATAGGTTAATGTCATGATAATAATGGTTTCTTAGACGTCAGGTGGCACTTTTCGGGGAAATGTGC
GCGGAACCCCTATTTGTTTATTTTTCTAAATACATTCAAATATGTATCCGCTCATGAGACAATAACCCTGATAAA

TGCTTCAATAATATTGAAAAAGGAAGAGTATGAGTATTCAACATTTCCGTGTCGCCCTTATTCCCTTTTTTGCGG
CATTTTGCCTTCCTGTTTTTGCTCACCCAGAAACGCTGGTGAAAGTAAAAGATGCTGAAGATCAGTTGGGTGCAC
GAGTGGGTTACATCGAACTGGATCTCAACAGCGGTAAGATCCTTGAGAGTTTTCGCCCCGAAGAACGTTTTCCAA
TGATGAGCACTTTTAAAGTTCTGCTATGTGGCGCGGTATTATCCCGTATTGACGCCGGGCAAGAGCAACTCGGTC
GCCGCATACACTATTCTCAGAATGACTTGGTTGAGTACTCACCAGTCACAGAAAAGCATCTTACGGATGGCATGA
CAGTAAGAGAATTATGCAGTGCTGCCATAACCATGAGTGATAACACTGCGGCCAACTTACTTCTGACAACGATCG
GAGGACCGAAGGAGCTAACCGCTTTTTTGCACAACATGGGGGATCATGTAACTCGCCTTGATCGTTGGGAACCGG
AGCTGAATGAAGCCATACCAAACGACGAGCGTGACACCACGATGCCTGTAGCAATGGCAACAACGTTGCGCAAAC
TATTAACTGGCGAACTACTTACTCTAGCTTCCCGGCAACAATTAATAGACTGGATGGAGGCGGATAAAGTTGCAG
GACCACTTCTGCGCTCGGCCCTTCCGGCTGGCTGGTTTATTGCTGATAAATCTGGAGCCGGTGAGCGTGGGTCTC
GCGGTATCATTGCAGCACTGGGGCCAGATGGTAAGCCCTCCCGTATCGTAGTTATCTACACGACGGGGAGTCAGG
CAACTATGGATGAACGAAATAGACAGATCGCTGAGATAGGTGCCTCACTGATTAAGCATTGGTAACTGTCAGACC
AAGTTTACTCATATATACTTTAGATTGATTTAAAACTTCATTTTTAATTTAAAAGGATCTAGGTGAAGATCCTTT
TTGATAATCTCATGACCAAAATCCCTTAACGTGAGTTTTCGTTCCACTGAGCGTCAGACCCCGTAGAAAAGATCA
AAGGATCTTCTTGAGATCCTTTTTTTCTGCGCGTAATCTGCTGCTTGCAAACAAAAAAACCACCGCTACCAGCGG
TGGTTTGTTTGCCGGATCAAGAGCTACCAACTCTTTTTCCGAAGGTAACTGGCTTCAGCAGAGCGCAGATACCAA
ATACTGTCCTTCTAGTGTAGCCGTAGTTAGGCCACCACTTCAAGAACTCTGTAGCACCGCCTACATACCTCGCTC
TGCTAATCCTGTTACCAGTGGCTGCTGCCAGTGGCGATAAGTCGTGTCTTACCGGGTTGGACTCAAGACGATAGT
TACCGGATAAGGCGCAGCGGTCGGGCTGAACGGGGGGTTCGTGCACACAGCCCAGCTTGGAGCGAACGACCTACA
CCGAACTGAGATACCTACAGCGTGAGCTATGAGAAAGCGCCACGCTTCCCGAAGGGAGAAAGGCGGACAGGTATC
CGGTAAGCGGCAGGGTCGGAACAGGAGAGCGCACGAGGGAGCTTCCAGGGGGAAACGCCTGGTATCTTTATAGTC
CTGTCGGGTTTCGCCACCTCTGACTTGAGCGTCGATTTTTGTGATGCTCGTCAGGGGGGCGGAGCCTATGGAAAA
ACGCCAGCAACGCGGCCTTTTTACGGTTCCTGGCCTTTTGCTGGCCTTTTGCTCACATGTTCTTTCCTGCGTTAT
CCCCTGATTCTGTGGATAACCGTATTACCGCCTTTGAGTGAGCTGATACCGCTCGCCGCAGCCGAACGACCGAGC
GCAGCGAGTCAGTGAGCGAGGAAGCGGAAGAGCGCCCAATACGCAAACCGCCTCTCCCCGCGCGTTGGCCGATTC
ATTAATGCAGCTGGCACGACAGGTTTCCCGACTGGAAAGCGGGCAGTGAGCGCAACGCAATTAATGTGAGTTAGC
TCACTCATTAGGCACCCCAGGCTTTACACTTTATGCTTCCGGCTCGTATGTTGTGTGGAATTGTGAGCGGATAAC
AATTTCACACAGGAAACAGCTATGACCATGATTACGCCAA